UNIVERSITY OF LIVERPOOL

Identification of Ochronosis, its Inhibition by Nitisinone, and the Use of Surgical and Chemical Interventions in Murine Models of Alkaptonuria

Thesis submitted in accordance with the requirements of the University of Liverpool for the degree of Doctor in Philosophy by Craig Mathew Keenan

February 2015

Acknowledgements

First and foremost I would like to offer my sincere thanks and appreciation to my supervisors, Professor Jim Gallagher and Professor Jonathan Jarvis. I would like to place on record my gratitude to them for giving me the opportunity to undertake this PhD project, and providing me with the resources and support to successfully complete my research objectives. I would also like to thank Professor Ranganath who has always been supportive of my work, and whose input has been crucial to the success of my project. I owe a massive debt of gratitude to Brenda Wlodarski who has taught me everything there is to know about histology. Without her help and countless hours of expert teaching I would not have been able to obtain the quality of sections that make up the majority of this thesis. She is an expert histologist and I feel privileged to have learnt from one of the best. Many thanks must go to Jane Dillon for proof reading many abstracts and a large portion of this thesis, and for our constant discussions about The Wire, The Sopranos, and Breaking Bad!! I must also thank Peter Wilson for all his help in the lab, and for proving a worthy opponent both on the football pitch, and in the pub over the last four years – even if he is an Evertonian! I would also like to thank Hazel Sutherland and Andrew Preston for all their help with the AKU mouse model, without it this thesis would have not been possible. Finally I would like to thank Eftychia Psarelli for her help and expertise in deciphering the statistical data.

The greatest thanks must go to my family and friends who have always been supportive of me during my PhD. In particular I would like to thank my Mum and Dad who have always encouraged and supported me during my studies – even though they still don't understand anything about my work! I hope you will both be proud of this thesis. I would also like to thank my brother and sister who have always offered words of encouragement during the last four years. Special thanks must go to my niece Sophia who has provided me with many, many laughs over the last two years – maybe you can follow in my footsteps one day! I would also like to thank Ben Alexander for being the best mate you could ask for. Our time spent going to concerts and having a few (too many) drinks has been a staple of my PhD, so here's to many more great times ahead!!

Alkaptonuria (AKU) is an ultra-rare autosomal recessive disorder resulting from a deficiency of the homogentisate 1,2-dioxygenase (Hgd) enzyme and is characterized by accumulation of homogentisic acid (HGA) in plasma. The disorder has three distinct stages of disease beginning with the excretion of large quantities of HGA in the urine, followed by deposition of HGA as a polymerized pigment in collagenous tissues principally in the cartilages of loaded joints (termed ochronosis), and finally the early onset of severe and devastating osteoarthropathy. There is currently no effective treatment available to AKU patients. Studying the extreme osteoarthritis (OA) phenotype seen in AKU is helping to increase understanding of more common OA, and may help elucidate the mechanisms behind the initiation and progression of OA. Although a murine model of AKU has previously been reported, published studies reported that Hgd-/- mice did not develop ochronosis. The aim of this thesis was to make a comprehensive survey of Hgd-/- mice to identify if ochronosis was present, determine the pathogenesis of the disorder, and to establish whether a potential treatment could prevent pigment deposition in tissues.

Through studying a large number of Hgd-/- mice, of a wide variety of ages, this thesis has provided novel findings in relation to the presence of ochronosis in these mice. Using a modified version of Schmorl's stain, which can specifically identify ochronotic pigment, ochronosis was observed in Hgd-/- mice for the first time. The identification of the earliest stages of ochronosis in Hgd-/- mice provided an opportunity to follow the pathogenesis of the disease throughout their lifespan. Pigmentation was initially identified in the pericellular matrix (PCM) of chondrons in the articular calcified cartilage (ACC), before progressing intracellularly. Examination of aged mice revealed widespread pigmentation throughout all areas of the tibio-femoral joint. Quantification of the pigmented chondrons demonstrated a progressive, linear increase in pigmentation with increasing age. Similar to ochronosis observed in AKU patients, Hgd-/- mice exhibited signs of ochronotic osteoarthropathy which became progressively worse with age. The early identification of ochronosis and its associated osteoarthropathy in Hgd-/- mice is helping to investigate the biochemical and pathological changes associated with AKU in humans.

Following the identification of ochronosis Hgd-/- mice were treated with nitisinone, which had been identified as a possible therapeutic for AKU. Administration of nitisinone throughout the lifespan completely prevented deposition of ochronotic pigment. When given mid-life, nitisinone stopped any further pigment deposition but was unable to reverse the effects of ochronosis which had already taken place. The results showed nitisinone to be an effective treatment against the initiation and progression of AKU.

During the course of investigation to identify ochronotic pigment at the ultrastructural level, high resolution transmission electron microscopy revealed the presence of previously undescribed microanatomical concentric lamellae in the ACC of Hgd-/- and wild type mice. Although the pathogenesis of these structures is still undetermined they may play a role in OA development as they appear to be associated with tidemark advancement and increased cartilage mineralization.

In summary the studies reported in this thesis present novel findings on the identification of pigmentation, and on the initiation, progression and mechanism of ochronosis which leads to ochronotic osteoarthropathy in Hgd-/- mice. The prevention of ochronotic pigmentation, using the drug nitisinone, was also reported for the first time.

ABBREVIATIONS

ACC – Articular calcified cartilage

ACL – Anterior cruciate ligament

AKU – Alkaptonuria

ADAMTS – A disintegrin and metalloproteinase with thrombospondin motifs

BCP – Basic calcium phosphate

BMP – Bone morphogenetic protein

BQA – Benzoquinone acetic acid

BSU – Biological services unit

COMP – Cartilage oligomeric matrix protein

CPPD – Calcium pyrophosphate dehydrate

DMM – Destabilization of the medial meniscus

DNA – Deoxyribonucleic acid

ECM – Extracellular matrix

EDTA – Ethylenediaminetetraacetic acid

EP – Epiphyseal plate

ERT – Enzyme replacement therapy

FGF – Fibroblast growth factor

GAG – Glycosaminoglycan

Gly – Glycine

H&E – Haematoxylin and eosin

HA – Hyaluronan

HAC – Hyaline articular cartilage

HGA – Homogentisic acid

Hgd – Homogentisate 1,2-dioxygenase

HPLC – High performance liquid chromatography

HPPD – 4-hydroxyphenylpyruvate dioxygenase

HT-1 – Hereditary tyrosinemia type 1

IL – Interleukin

ITM – Interterritorial matrix

LFC – Lateral femoral condyle

LM – Lateral meniscus

LTP – Lateral tibial plateau

MAA – Maleylacetoacetic acid

MFC – Medial femoral condyle

MM – Medial meniscus

MMP – Matrix metalloproteinase

MMTL – Medial meniscotibial ligament

MTP – Medial tibial plateau

NFR – Nuclear fast red

OA – Osteoarthritis

OARSI – Osteoarthritis research society international

PBFS – Phosphate buffered formalin solution

PBS – Phosphate buffered saline

PCL – Posterior cruciate ligament

PCM – Pericellular matrix

PCR – Polymerase chain reaction

rER – Rough endoplasmic reticulum

ROS – Reactive oxygen species

SCB – Subchondral bone

SEM – Scanning electron microscopy

TEM – Transmission electron microscopy

TGF – Transforming growth factor

TIMP – Tissue inhibitors of metalloproteinases

TM – Territorial matrix

TNF – Tumour necrosis factor

TP – Tibial plateau

WT – Wild type

Table of Contents

Table of Figures

Tables

1. Introduction

1.1 ALKAPTONURIA

1.1.1 History

Alkaptonuria (AKU) is an ultra-rare autosomal recessive disorder characterised by the deposition of homogentisic acid (HGA) as a polymerized pigment in collagenous tissues (ochronosis). A deficiency in the homogentisate 1,2-dioxygenase (Hgd) enzyme results in an inability to completely metabolise the amino acids tyrosine and phenylalanine, leading to the deposition of HGA as a black pigment, primarily in the cartilages of load-bearing joints (Fig. 1.1). This results in an early onset, devastating osteoarthropathy for which there is currently no effective treatment. AKU is renowned for being the first disease to be described as an 'inborn error of metabolism' by the distinguished English physician, Sir Archibald Garrod [1, 2]. It was also one of the first disorders to conform to the laws of Mendelian inheritance. Although Garrod was the first to describe the features of AKU as one single disorder, several previously published articles documented symptoms consistent with a diagnosis of AKU.

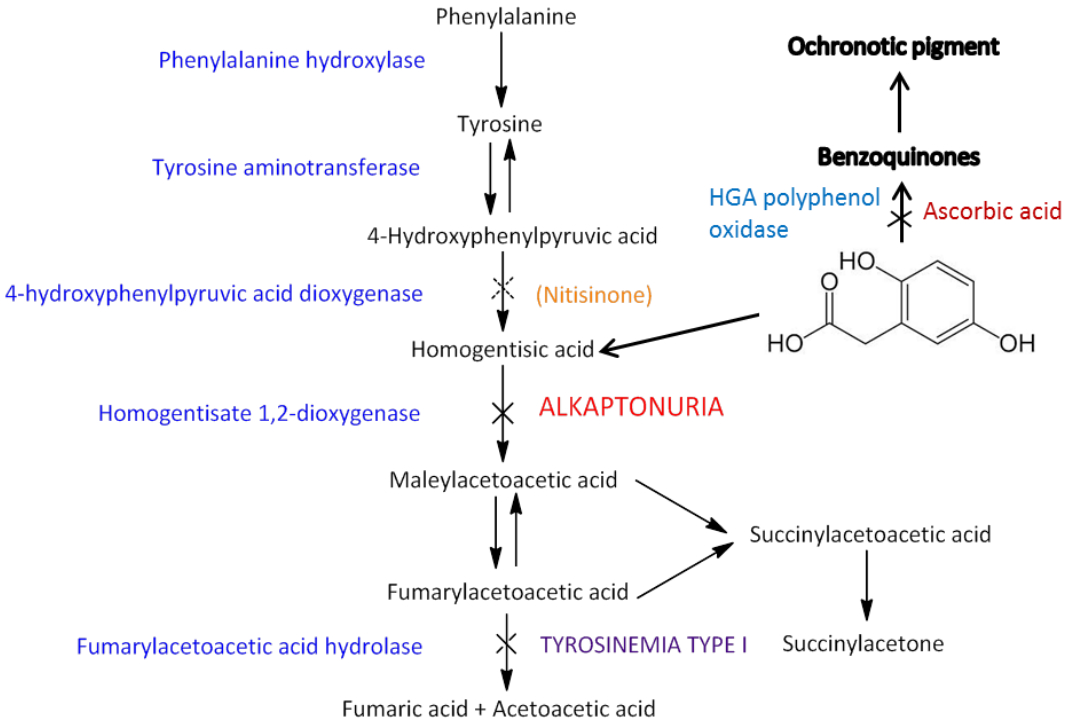

Figure 1.1 – Diagram highlighting the enzyme defect which results in AKU.

The earliest documented case of ochronosis dates back to 1500 B.C. and the Egyptian mummy, *Harwa*. Radiological and biochemical analysis of the intervertebral discs, and the hip and knee joints from the mummy confirmed the diagnosis [3, 4]. Scribonius, writing in 1584, reported that the urine of a school boy was as 'dark as ink' [5]. This was the first time a clinical symptom of AKU had been described in man. In 1859, Boedeker described the reducing abilities of a compound found in the urine of a man presenting with lumbar spine pain and severely reduced mobility. Boedeker observed that the compound was able to reduce alkaline copper solutions, whilst also noting that it absorbed large volumes of atmospheric oxygen in the presence of alkali solutions leading to the compound darkening rapidly. This led Boedeker to name the compound 'alkapton' which was derived from alkali and the Greek word meaning "to absorb greedily". The term ochronosis was first described in 1866 by Virchow [6] following the discovery of black pigmentation in the articular cartilage, intervertebral discs, menisci, and both laryngeal and tracheal cartilage of a 67 year old man who died from congestive heart failure. Although

macroscopically the pigmentation was black, microscopic analysis revealed the colour to be yellowish-brown or 'ochre' leading Virchow to describe the findings as ochronosis. Research by Wolkow and Baumann, published in 1891, detailed the structure and formula of the compound previously termed alkapton. They noted its involvement in AKU and proceeded to name it HGA. Albrecht, writing in 1902, recognized the link between AKU and ochronosis and concluded that long term suffering from AKU resulted in ochronosis. The discovery of ochronotic arthritis was made by Allard and Gross, in 1907, who noted that patients with AKU had very advanced arthritis of both upper and lower limbs. Garrod arguably made the most important contributions to AKU research including identifying the disorder as an 'inborn error of metabolism', and showing there was an association between the amount of tyrosine and phenylalanine consumed and the amount of HGA excreted in individuals with AKU [1, 7]. Garrod presented his work at the Croonian lectures in 1908 were he discussed his work on AKU and demonstrated that AKU, along with several other disorders, followed the laws of Mendelian inheritance [8].

1.1.2 Epidemiology

The incidence of AKU worldwide is estimated to be between 1:250,000 and 1:1,000,000 [9], highlighting its ultra-rare nature. There are however certain countries which are 'hotspots' for AKU and have a much higher prevalence. Slovakia and the Dominican Republic are thought to have an incidence of around 1:19,000 [10, 11]. Recent research carried out in Jordan showed there to be a large number of individuals from the same family, and village suffering from AKU [12, 13]. Although the exact numbers are not known it is thought that Jordan may have the highest frequency of AKU patients in the developed world due to the high number of consanguineous marriages that occur there. A large number of novel mutations of the Hgd gene have been identified in both Slovakia and Jordan [14-16] demonstrating the high prevalence of the disorder in both countries.

1.1.3 Clinical presentations

AKU has several distinct clinical features which are present at different stages throughout life. The earliest and most obvious clinical symptom of AKU is the excretion of HGA in the urine of affected individuals. Upon standing the urine darkens, though this can be quickened by addition of an alkaline solution. The appearance of dark staining of nappies in infants, following the excretion of HGA is the only clinical sign of the disorder in very young patients [17]. Although darkening of the urine can be used as a diagnostic tool for AKU, further analysis of the urine using high performance liquid chromatography (HPLC) [18, 19], or spectrophotometric analysis [9] is usually undertaken to ensure the diagnosis is accurate.

Over a period of time, due to continually high levels of HGA in the body, there is deposition of a dark pigment - resulting from polymerization of HGA - in tissues throughout the body [20]. This process, known as ochronosis, is a hallmark sign of AKU and can help with diagnosis of the disorder. Darkening of the sclera and pinna can be seen from the third decade of life and is the most obvious sign of ochronosis in AKU patients [9]. Ochronosis of the skin is also common in AKU patients [21] however it is also common in people using hydroquinone cream, for conditions such as melasma [22] therefore it is not used on its own as a diagnostic tool for AKU. The tissues most severely affected by pigment deposition, including load-bearing joints such as the knees and hips, are only observed during post-mortem studies or joint replacement surgery. There has been many cases reporting severe pigmentation of the knee and hip joints, along with other joints in AKU patients [23-26]. These tissues show both macroscopic pigmentation which can be easily identified, and microscopic pigmentation which has shown different degrees of ochronosis in the affected tissues. Pigmentation of tendons has also been reported, with both the patellar and Achilles tendons showing discolouration [27]. Recent work by Taylor *et al* [28] has shown there to be an association between collagen fibres and ochronotic pigment in the ligamentous capsule, indicating how these

tissues may become pigmented. Other cartilaginous tissues that have shown signs of ochronosis include the trachea and bronchi [29]. Aside from cartilaginous tissues, post-mortem studies have revealed the involvement of the heart in AKU patients. There have been a number of cases reporting calcification and pigment deposition in the aorta [30-32]. Although AKU is not a fatal condition, the involvement of the cardiac system in the disorder highlights the susceptibility of different tissues with regards to becoming ochronotic. Recently ochronosis has been identified in a mediastinal cyst which was surgically removed from a patient previously diagnosed with AKU [33].

Although darkening of urine and visible signs of ochronosis sometimes present as the initial symptom of AKU, the most common symptom leading to diagnosis is the development of osteoarthritis (OA)-like pain in the joints. Usually detected either clinically or radiographically, the diagnosis of AKU is confirmed by measuring the plasma levels of HGA. Ochronosis in the joints occurs over a sustained period of time leading to destruction of the joint. This is commonly known as ochronotic osteoarthropathy and is the most severe symptom of AKU. The hips and knees often present as the most severely affected joints, however the earliest and most common presentation of the osteoarthropathy is often related to the spine. In a study of 163 cases of AKU involvement of the spine was observed in 159 patients with a significantly lower number presenting with knee and hip pain [34, 35]. In a separate, more recent study of 45 AKU patients a third showed a loss in height highlighting the severity of spinal involvement in the disorder [9]. Ochronotic osteoarthropathy in the knees and hips presents radiographically as severe OA with joint space narrowing, subchondral sclerosis, and joint surface irregularities often observed [26]. With no current therapeutics widely available for AKU patients the use of surgical intervention to remove the affected joint is the primary form of treatment. Although this form of treatment is far from ideal it has provided a library of samples which are helping researchers understand the pathogenesis of the disorder. Association of the cartilaginous matrix and ochronotic pigment has been

consistently observed in surgical samples [36-38] indicating a possible mechanistic pathway for the initiation of pigmentation.

1.1.4 Pathogenesis

The pathogenesis of AKU is still yet to be fully understood. It has only been in recent years that possible mechanisms relating to the deposition of ochronotic pigment have been suggested. Taylor and colleagues first identified the association of pigment with the periodicity of fibrillar collagen, suggesting a possible preferential binding site for ochronotic pigment on collagen fibres [28]. Further work by Taylor showed that pigmentation appeared to initiate in the pericellular matrix (PCM) of chondrons deep in the articular calcified cartilage (ACC) [36]. The authors suggest that this may have resulted from alteration of the composition and organisation of the collagen fibres in the PCM, thus leading to pigment deposition. Chow showed that ochronotic cartilage is more disordered than normal cartilage at the atomic level [39] which appears to support the mechanism proposed by Taylor [36]. Once pigmentation is initiated deep in the ACC it appears then to progress up through the hyaline articular cartilage (HAC) leaving the cartilage in a state of 'blanket' pigmentation. These findings suggest that areas of focal damage initially precede pigment deposition, and then progressively become worse resulting in widespread pigmentation of the tissue. Although significant progress has been made to determine the pathogenesis of AKU further work is needed to determine if other mechanisms result in pigment deposition. The pathogenesis of AKU in Hgd-/- mice is reported in Chapters 3 and 4 of this thesis.

1.1.5 Therapeutic options

The current lack of effective therapeutics for the treatment of AKU is a major problem. Due to the ultra-rare nature of the disorder there has been limited research, particularly from pharmacological companies, with regards to identifying

possible new and effective treatments. Several possible therapies have been identified however they have shown mixed results in man.

1.1.5.1 Ascorbic acid (Vitamin C)

Ascorbic acid was the first compound to be identified as a possible treatment for AKU [40]. Studies incorporating ascorbic acid in the treatment of AKU patients have shown it to inhibit HGA polyphenol oxidase resulting in a reduction in the amount of benzoquinone acetic acid (BQA) synthesized [41], which itself is an intermediary in the formation of ochronotic pigment. However in this study a concentration of 10mM ascorbic acid was used to inhibit the enzyme, something which would be almost impossible to achieve *in vivo*. Forslind, writing in 1988, noted that "ascorbic acid is not effective in the treatment of symptomatic ochronosis" [42]. It has also been suggested that due to ascorbic acid being a co-factor for 4-hydroxyphenylpyruvate dioxygenase (HPPD), treatment with the compound may actually increase the amount of HGA produced. Treatment with ascorbic acid may also contribute to the formation of renal oxalate stones in AKU patients [9]. The overwhelming evidence appeared to show that ascorbic acid was not beneficial in the treatment of AKU.

1.1.5.2 Low protein diet

There has been some research on the incorporation of a low protein diet as a way of reducing the levels of HGA in AKU patients. Similar to the use of ascorbic acid in AKU there is not much evidence suggesting a low protein diet has any future as a treatment option for AKU patients. A study from Mayatepek showed that a low protein diet may actually increase the amount of BQA produced [43], which would lead to an increase in the amount of ochronotic pigment formed. A separate study conducted by Haas and colleagues showed that HGA levels were reduced by a low protein diet, however this only occurred in patients under 12 years of age after which the effect was lost [44]. The authors also noted that compliance with dietary

restriction decreased progressively with age, and that behavioural problems emerged during diet restriction [44]. Similar to ascorbic acid use in AKU patients, the incorporation of a low protein diet did not appear to have a beneficial effect.

1.1.5.3 Enzyme replacement therapy

As AKU results from a single enzyme deficiency the ideal treatment, at least in principle, would be the replacement of the Hgd enzyme thereby ensuring effective metabolism of HGA. In theory this technique should be possible, as long as the recombinant enzyme can be delivered to the liver without issue. Recent studies of enzyme replacement therapy (ERT) in Pompe disease, which itself is an autosomal recessive disorder causing damage to muscle and nerve cells, has shown beneficial effects in both infantile and adult patients [45-47]. This is positive news for AKU patients as it highlights the potential of ERT as a practical treatment for the disorder.

1.1.5.4 Nitisinone

Nitisinone is currently the most effective treatment option for AKU patients. Originally developed as a herbicide [48], it is routinely used for the treatment of hereditary tyrosinemia type 1 (HT-1) [49, 50]. Nitisinone reversibly inhibits 4-HPPD which is responsible for the conversion of hydroxyphenylpyruvate into HGA (Fig. 1.1). Following its effectiveness in treating HT-1 it was proposed as a potential treatment for AKU. Using a murine model of AKU, Suzuki and colleagues demonstrated that nitisinone could effectively reduce plasma HGA levels in a dose-dependent manner [51]. Initials trials of nitisinone in AKU patients demonstrated a significant reduction in plasma HGA levels, falling below the level of detectability in a number of patients in the trial. Patients who received nitisinone for more than one week also reported decreased pain in their affected joints [52]. Although the initial data appeared positive, there were several adverse effects including the passing of kidney stones and the elevation of tyrosine plasma levels. Elevated

tyrosine poses significant risks as it can cause corneal crystal formation and corneal epithelial damage. A larger scale study of nitisinone use in AKU patients provided mixed results due largely in part to the end point chosen [53]. Hip rotation was defined as the parameter to determine the efficacy of nitisinone however the results showed considerable variability in hip rotation in the same patients from visit to visit [53]. It is clear that nitisinone has potential as a possible treatment for AKU as it significantly reduces plasma HGA however whether it can prevent pigmentation in affected individuals is still unclear. The use of nitisinone in Hgd-/- mice is reported in Chapter 5 of this thesis, along with its efficacy on preventing pigment deposition throughout the mouse lifespan.

1.2 HOMOGENTISATE 1,2-DIOXYGENASE – STRUCTURE, FUNCTION, MUTATIONS

AKU results from a deficiency in the Hgd enzyme, specifically a mutation in the gene coding for the enzyme. The normal human Hgd gene is 54,363bp in length and codes for a 1715 nucleotide sequence. This is split into 14 exons which vary in length from 35 to 360bp [54]. The gene encodes a 445-amino acid protein that forms a dimer of two trimers, producing a functional hexamer which can effectively metabolise HGA [55]. Fernandez-Canon and colleagues mapped the Hgd gene to chromosome 3 (3q21-q23), and showed that expression of the gene was restricted to the liver, kidneys, small intestine, colon, and prostate [56]. The crystalline structure of the enzyme was detailed by Titus and colleagues who described the structure as intimately associated 280-residue N-terminal and 140-residue C-terminal domains, surrounding a central β-sandwich structure [57]. The Hgd enzyme is essential in tyrosine catabolism as it converts HGA to maleylacetoacetic acid (MAA), which is then further metabolised and excreted from the body (Fig. 1.1). Loss of function of the enzyme, as seen in AKU, leads to a build-up of HGA as it can no longer be metabolised. To date there are currently 115 known Hgd mutations [58]. Two-thirds of these mutations are missense, with splicing, frameshift, deletion, expansion and stop mutations comprising the rest. The mutations are distributed throughout the entire Hgd gene however there is a

higher prevalence in exons 6, 8, 10, and 13 [58]. There is no correlation with the type of Hgd mutation, the level of HGA in the plasma and urine, and the severity of the disorder.

1.3 HOMOGENTISIC ACID

HGA is a small highly water soluble molecule which upon oxidation, either with the addition of NaOH or in the presence of molecular O_2, forms a highly reactive quinone intermediate known as BQA. This molecule subsequently undergoes polymerization to produce the pigmented polymer deposited in the tissues of AKU patients. During autoxidation HGA produces oxygen radicals, $O_2^{\cdot-}$, $OH^{\cdot}$, and H_2O_2, which are thought to play a role in the development of ochronotic osteoarthropathy [59]. HGA is also found in species of marine bacterium where it has been identified as the primary precursor of melanin synthesis [60]. These bacteria produce a compound known as pyomelanin, through metabolism of HGA, which is also known as alkapton [61, 62].

1.4 CARTILAGE

Cartilage is a flexible connective tissue found throughout the human body. There are three types which are distinguished by their unique composition which relates to their specific function in the body. The three types of cartilage are known as hyaline, elastic, and fibrocartilage. Although compositionally different there are similarities between each type of cartilage. The most distinct properties of cartilage are that it is both avascular and aneural. Cartilage contains only one cell type which is responsible for the production and maintenance of the collagen rich matrix; these cells are known as chondrocytes. Hyaline cartilage is the most predominant cartilage in the body and is found in several tissues of the body including the trachea and on the end of long bones, where it is known as articular cartilage. The matrix of hyaline cartilage consists primarily of type II collagen and chondroitin sulphate. Elastic cartilage is found in the pinna, Eustachian tube, and epiglottis.

Histologically it is similar in appearance to hyaline cartilage containing both type II collagen and chondroitin sulphate however it also contains a significant amount of elastic fibres throughout its matrix. Fibrocartilage is found in several tissues of the body including the intervertebral discs, the pubic symphysis, and the menisci of the knees. Unlike hyaline and elastic cartilage, fibrocartilage contains type I collagen which provides strength and durability, hence it is located in tissues requiring these traits.

1.4.1 Composition of the peri- and extracellular matrix in articular cartilage

The PCM directly surrounds chondrocytes in articular cartilage and is thought to play a role in the biomechanics of joints [63]. The PCM is rich in hyaluronan (HA), a non-sulphated glycosaminoglycan (GAG), fibronectin, and proteoglycans including perlecan, biglycan, and decorin. Type VI collagen is the primary collagen type present in the PCM, however types II and IX are also present but in much smaller amounts. Type X collagen is also found in the PCM of chondrocytes, primarily in hypertrophic cells located in the ACC. The composition of the extracellular matrix (ECM), which compromises the territorial and interterritorial matrices (TM/ITM), in articular cartilage relates directly to its function. Biomechanical loads are constantly applied to joints therefore the tissue must be able to withstand these pressures to function normally, and to prevent any mechanical damage. The main constituent of ECM is water which accounts for between 65-80% of the wet weight of the tissue. The presence of water helps with distribution of load and ensures the cartilage does not become deformed when put under enormous stress. Water helps with the transport and distribution of nutrients in articular cartilage which is an essential process due to the avascular nature of cartilage, whilst also providing a source of lubrication for articulation of the joints. Collagen is the most abundant macromolecule in cartilage, constituting between 10-20% of the wet weight of the tissue. Collagen fibres provide tensile strength to cartilage whilst also providing a binding site for proteoglycans (Fig. 1.2). Type II collagen is the principal fibre type in cartilage, however other collagens including types I, IV, VI, IX, X, and XI are present

but in significantly lower amounts. Proteoglycans, which comprise around 10-15% of the wet weight of the ECM, are heavily glycosylated proteins usually consisting of a central protein unit with one or more covalently attached GAG chain. There are a variety of proteoglycans in the cartilaginous matrix which are essential for normal function. The largest and most abundant proteoglycan is aggrecan which contains more than 100 chondroitin sulphate and keratan sulphate chains (Fig. 1.2). Aggrecan provides cartilage with its osmotic properties, which are critical to resist compressive loads. The smaller proteoglycans include decorin and bigylcan, which interact with collagens type II and IV respectively and help with many processes in cartilage. HA, a nonsulphated GAG, is another key component of the ECM and contributes significantly to cell proliferation and migration. Chondrocytes are the only cell type in cartilage and are responsible for the synthesis of all matrix components as well as regulating matrix turnover [64]. Chondrocytes are not present in large numbers in the ECM, in fact they account for around just 5% of the total volume of the cartilage. They receive nutrients through osmotic diffusion as cartilage is avascular. The concentration of oxygen is remarkably low in cartilage so it is quite surprising that chondrocytes survive in such a harsh environment. Mechanical loading affects the functions of chondrocytes, and can lead to the production of matrix degradation enzymes.

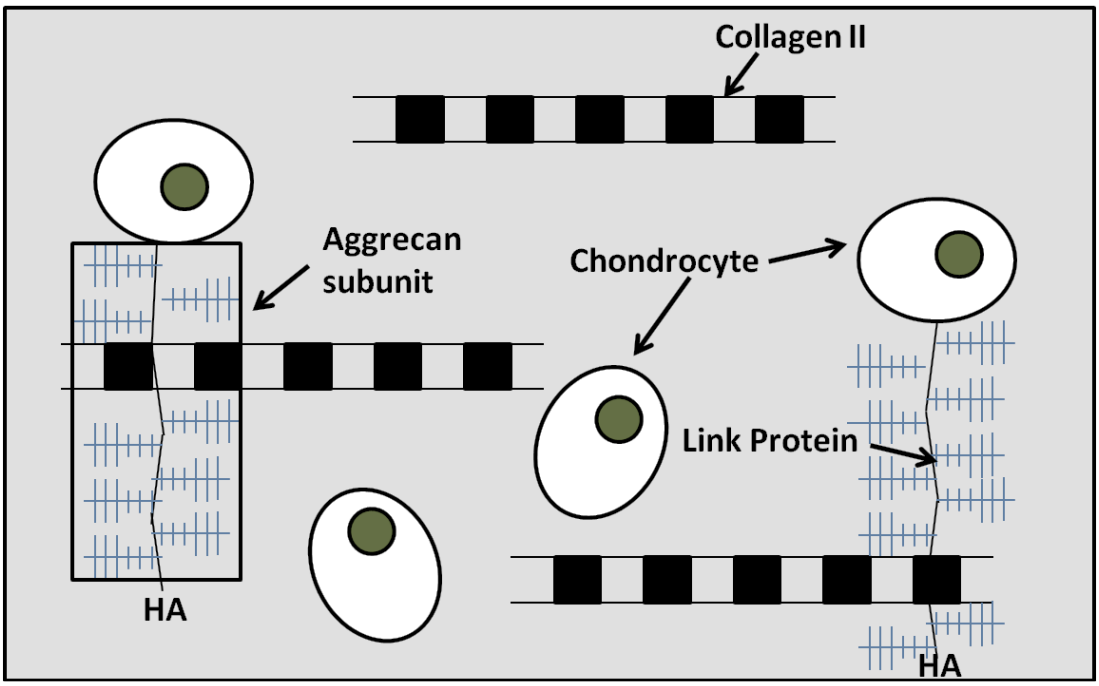

Figure 1.2 – Diagram highlighting the interactions of collagen, chondrocytes, and proteoglycans in the extracellular matrix of articular cartilage. Type II collagen fibres, which provide cartilage with tensile strength, interact with proteoglycan aggregates trapping them within the collagen network. Aggrecan is the largest proteoglycan and is critical to cartilage structure. It interacts with HA to form stable tertiary complexes in the matrix. Non-aggregating proteoglycans including decorin and fibromodulin also interact with collagen fibrils, and play a role in fibrillogenesis. Chondrocytes are the only cell type in cartilage and are responsible for production and maintenance of the matrix, including synthesizing proteoglycan subunits.

1.4.2 Structure of articular cartilage

The structure of articular cartilage, much like the composition of the tissue, is critical to its function in protecting joints from excessive loading. Morphologically there are four zones; the superficial zone is the uppermost layer which is followed by the middle, deep and calcified zones. The superficial, middle, and deep zones form the unmineralized portion of articular cartilage and are collectively known as HAC. The mineralized area is commonly referred to as ACC (Fig. 1.3).

1.4.2.1 Superficial zone

The superficial zone is the thinnest of the four layers of articular cartilage. The chondrocytes located in this zone are flattened and are aligned parallel to the joint surface. They synthesize a protein called lubricin which plays an important role in the articulation of the joints [65]. The chondrocytes also synthesize large amounts of fibrillar collagen which is aligned parallel to the joint surface, and provides the superficial zone with the greatest tensile strength in articular cartilage [66]. Any damage to this zone can lead to alterations of the mechanical properties and be a causative effect in the development of OA.

1.4.2.2 Middle zone

Chondrocytes located in the middle zone are more spherical than chondrocytes in the superficial zone. They are embedded in an extensive ECM which is rich in aggrecan. The collagen fibrils in this zone are much larger in diameter than the superficial zone and are more randomly orientated. The middle zone is effective in transferring the sheer forces from the superficial zone throughout the rest of the zones of cartilage.

1.4.2.3 Deep zone

The chondrocytes in the deep zone are spherical in shape and are aligned perpendicular to the joint surface. Collagen fibrils in the deep zone also lie perpendicular to the joint surface. Cell density is at its lowest in the deep zone yet aggrecan is found at its highest concentration. Similar to the middle zone, the deep zone distributes load and resists compression.

1.4.2.4 Calcified zone

As stated previously, the calcified zone is commonly known as ACC. It is separated from the unmineralized zones by the tidemark which is highly basophilic, and may play a role in the biomechanics of joints [67]. The chondrocytes in ACC express a hypertrophic phenotype and are unique in that they synthesize type X collagen which upon release from the cell calcifies the surrounding matrix [68]. As the chondrocytes in ACC are surrounded by a calcified matrix they show very low metabolic activity. Calcification of the matrix provides important structural integrity which along with the subchondral bone (SCB) is important for the shock absorbance properties of the tissue.

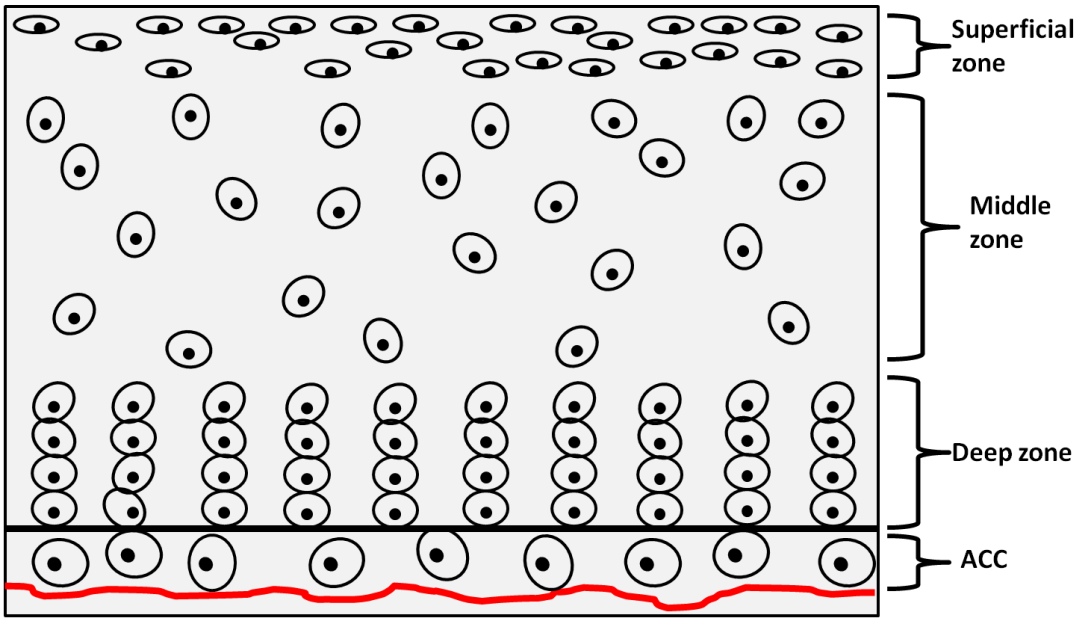

Figure 1.3 – Zones of articular cartilage. Chondrocytes located in the superficial zone are flat, lie parallel to the articular surface, and occupy around 10-20% of the cartilage volume. Chondrocytes located in the middle zone are spherical in shape and occupy around 40-60% of the cartilage volume. Chondrocytes in the deep zone appear spherical in shape, lie perpendicular to the articular surface, and account for around 30-40% of the cartilage volume. Chondrocytes in the calcified zone express a hypertrophic phenotype and help to calcify their surrounding matrix. The tidemark, indicated by the black line, separates HAC and ACC. The red line indicates the SCB plate which separates the ACC from the underlying SCB.

1.4.3 Chondrocytes

Chondrocytes are the only cell type in cartilage and are responsible for maintaining the ECM. Under normal physiological conditions chondrocytes maintain a stable equilibrium between the synthesis and degradation of matrix components. Chondrocytes survive in a low oxygen environment, and rely on osmotic diffusion to receive nutrients as cartilage is avascular. They express different phenotypes depending on what zone they are located in, this allows them to carry out functions specific to that area of cartilage. Chondrocytes are surrounded by the PCM which is rich in type VI collagen and proteoglycans [69] (Fig. 1.4). Type XI collagen, and chondroitin and keratan sulphates, both of which are components of aggrecan, have also been identified in the PCM [70-72]. The chondrocyte and its surrounding PCM form a functional and metabolic unit which is termed the 'chondron' [73]. When cartilage becomes damaged and its matrices disrupted, chondrocytes respond by increasing synthesis of inflammatory cytokines including interleukin-1 (IL-1) and tumour necrosis factor-α (TNF-α). These cytokines increase synthesis of matrix metalloproteinases (MMPs) which breakdown the ECM, this is thought to be a factor in the onset of OA [74, 75](Fig. 1.4).

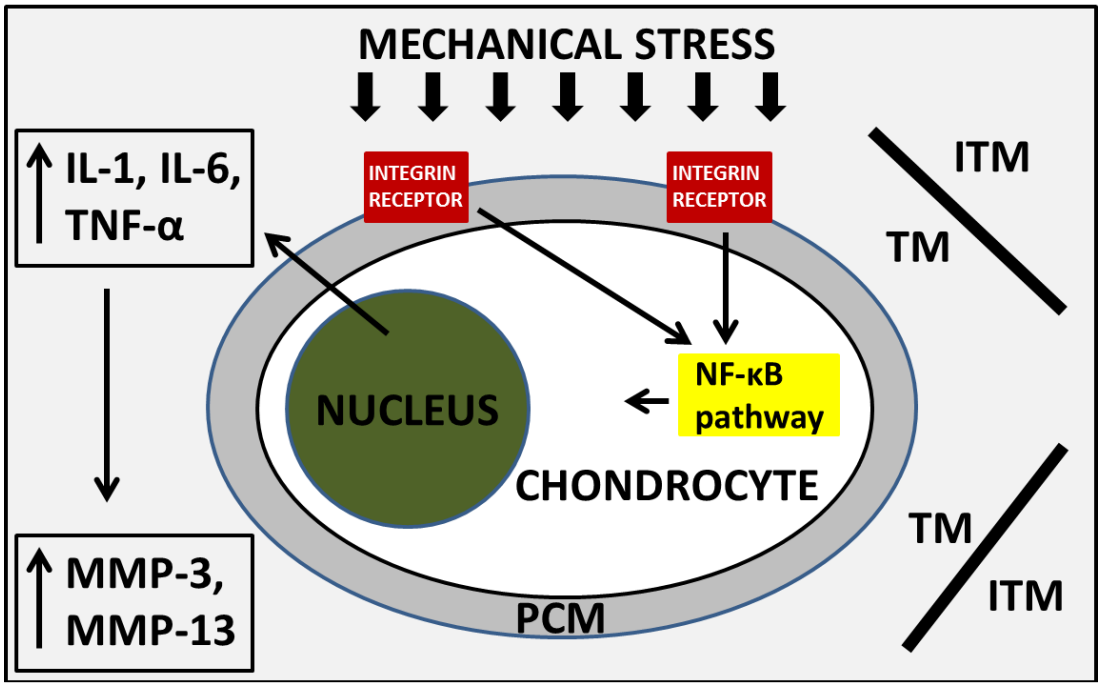

Figure 1.4 – Diagram of chondrocyte structure and function. . Chondrocytes are contained in lacuna which are filled with extracellular fluid, and are surrounded by the PCM which is rich in type VI collagen and aggrecan. The TM and ITM constitute the majority of the cartilage in which the chondrocytes lie. The function of chondrocytes can become altered when they are placed under mechanical stress leading to an increase in synthesis of matrix degradation enzymes. MMPs, amongst others, degrade collagen fibres resulting in severely damaged cartilage and the development of OA.

1.4.4 Collagen

Collagen is the most abundant protein present in the ECM. Collagens consist of three polypeptide chains arranged in a triple helical formation. The domains in the structure form as a result of glycine being used as the third amino acid in a repeating peptide triplet to give Gly-X-Y, where X and Y are often proline and hydroxyproline respectively [76]. Individual collagen fibrils have a distinct periodicity at 67nm which give it an unmistakeable banding pattern. Type II collagen is the primary fibre type in ECM however there are others present throughout each different zone of the matrix. The PCM is rich in type VI collagen, the TM and ITM although both rich in type II collagen also contain types IX and XI,

whilst type X collagen is present extensively throughout ACC. Collagen fibres are fundamental in providing the tensile strength of cartilage and as a result any degradation of collagen can cause significant problems, particularly in weight bearing joints.

1.4.5 Collagen biosynthesis, assembly and supramolecular organisation

The biosynthesis of collagen is a complex multistep process, involving both intracellular and extracellular processes. The first stage involves transcription of the collagen genes producing mRNA. The ribosome-bound mRNA is then translated in the rER into procollagen α chains. Following the formation of procollagen a series of post-translational modifications take place, including hydroxylation of proline and lysine residues. 4-hydroxyproline is essential for intramolecular hydrogen bonds which are critical to ensuring the stability of the triple helices, whilst hydroxylysine residues are involved in the cross-linking of collagen molecules during fibril formation [77]. Other post-translational modifications include trimerization, disulphide bonding, and folding of the procollagen chains into procollagen trimers; the latter requiring enzymes including peptidyl-prolyl *cis-trans*-isomerase for effective formation and folding. Once procollagen molecules have been assembled they are transported to the Golgi complex where they are released into the extracellular space, via secretory vesicles. Following secretion the procollagen trimers are processed, which involves cleavage of the C- and N-propeptides by specific proteases belonging to the ADAMTS and BMP1/Tolloid-like families [78, 79]. The final stage of collagen biosynthesis is the formation of covalent cross-links which help stabilize fibril formation. This process is regulated by a number of different enzymes, including members of the lyase oxidase family which are vital to the cross-linking of the fibrillar collagens, including types I, II and III. Lyase oxidase converts lysine or hydroxylysine residues in the C- and N-telopeptide regions to peptidyl aldehydes which then spontaneously react with several other molecules to form covalent cross-links [80]. One characteristic trait shared by all members of the collagen family is the formation of the triple helix structure. Prior to the assembly of

the triple helix, a glycine residue must be present in every third position of the α-procollagen chains leading to the assembly of a triple helix. For instance, type II collagen is composed of three α1(II)-chains forming a homotrimeric molecule, whilst type VI collagen forms a heterotrimer composed of three different α-chains. Following the synthesis and assembly of collagen fibrils they form supramolecular structures which provide the tensile strength and stability for a range of tissues. There are a number of different collagen families based on their supramolecular organisation, these include fibril-forming collagens, fibril-associated collagens with interrupted triple helices (FACIT), network forming collagens, microfibrillar collagens, transmembrane collagens and basement membrane collagens. Fibril-forming collagens include types I and II, which are the major constituents of bone and articular cartilage respectively. These collagens assemble into supramolecular aggregates with the fibrils defined by their characteristic 67nm banding pattern.

1.5 BONE

1.5.1 Formation, structure, and function

Bone is a highly specialized tissue which has many important functions in the body. Bone is formed by two processes during fetal development; intramembranous, and endochondral ossification. Intramembranous ossification occurs primarily during formation of the flat bones of the skull, and relates to the formation of bone from connective tissue. Endochondral ossification occurs extensively throughout the body, including the long bones of joints, and relates to the formation of bone initially from hyaline cartilage which becomes ossified in two separate areas leading to development of the epiphyseal plate (EP) and articular cartilage. There are two types of bone in the body, cortical and trabecular. Cortical bone is a rigid structure forming the outer layer of bones, whilst trabecular bone which has a much larger surface area than cortical bone is located internally. Bone marrow is located within the trabecular bone and is primarily involved in the formation of the cellular components of blood (haematopoiesis). Bone is almost completely composed of bone matrix which can be split into both organic and inorganic components. Type I

collagen forms the majority of the organic matrix in bone and is initially laid down as osteoid before becoming mineralized. The inorganic matrix is predominantly composed of hydroxyapatite which is also laid down as osteoid before becoming mineralized. The primary function of bone is to provide structural support to the body particularly during movement, including distribution of mechanical loads across joints. Bone also acts as a storage area for minerals including calcium and phosphorus which are vitally important for homeostasis.

1.5.2 Cells

There are three main cell types in bone, each with their own specific and important function. Osteoblasts are crucial to bone formation and mineralization. They also synthesize hormones and produce alkaline phosphatase which itself plays a role in the mineralization of bone. Osteoclasts are large multinucleated cells responsible for the resorption of bone. They are derived from hematopoietic lineage and migrate to the bone surface to begin the process of resorption which they do with a phagocytic-like mechanism, similar to macrophages. Osteocytes are derived from osteoblasts which have become entombed in the matrix they themselves produced. Similar to chondrocytes the space they occupy in the matrix is known as a lacuna. Osteocytes are thought to play a role in regulating bone's response to mechanical loading [81].

1.5.3 Remodelling

Bone is continually altered in response to biomechanical and biochemical stimuli. Constant mechanical loading can cause micro-damage which ultimately needs to be repaired in order for the bone to sustain its function of providing structural support to the body. Remodelling of bone is a critical process which helps maintain bone structure and function. It occurs only if there is a balance between resorption and formation of bone. The process of bone remodelling is mediated by osteoclasts, osteoblasts, and osteocytes which were only recently implicated in the process

[82]. Osteoclastic resorption of bone releases stored calcium into the systemic circulation which then ceases allowing osteoblasts to mineralize the calcium at the site of resorption.

1.5.4 Subchondral bone

Beneath the layer of ACC in long bones lies the SCB which is important to for the stability of joints. The two tissues, although structurally different, are vitally important in helping to distribute the mechanical load placed upon articulating joints. SCB undergoes constant remodelling which can alter the properties of joints and cause severe consequences. SCB is known to be extremely important in the pathogenesis of OA [83, 84], so much so that it has been suggested as a possible therapeutic target for the prevention of OA [85, 86]. It is thought that SCB also plays an important role in the initiation and progression of ochronotic arthropathy in AKU [36].

1.6 OSTEOARTHRITIS

1.6.1 Epidemiology

OA is a progressive joint disease characterized by articular cartilage degeneration, SCB remodelling, and osteophyte formation. OA is the most common form of joint pain in the developed world [87]. There is limited literature on the prevalence and incidence of OA due to the problems of accurately diagnosing the disorder radiographically and clinically. Symptomatic knee OA, which is one of the most common forms of OA, is thought to affect around 10-15% of patients aged 60 and over in the USA [88]. Other frequently affected sites include the spine, hands and hips.

1.6.2 Pathogenesis

There are a variety of factors believed to be involved in the initiation and progression of OA however there is no definite agreement to what is the actual cause. One of the most cited reasons for development of OA is abnormal loading of joints resulting in microtrauma to the cartilage and underlying SCB [89-91]. Abnormal loading of cartilage is thought to alter the function and phenotype of chondrocytes leading to activation and/or upregulation of matrix degrading enzymes. The process of chondrocyte induced degradation of the matrix is known as chondrocytic chondrolysis [92]. Normal physiological loading of joints has been shown to be beneficial, particularly in mice, as it can accelerate bone healing, and reduce the levels of the cartilage degradation enzyme MMP-13 [93, 94]. Ageing has also been linked to OA progression due to the continuous loading of joints (wear and tear) throughout an individual's lifetime. Similar to abnormal loading of joints, the continuous stress placed on joints in ageing individuals can lead to cartilage degradation due in part to accumulation of damaged matrix molecules which are not replaced during matrix turnover. Once the structure and integrity of the matrix becomes compromised it can lead to further degenerative changes. OA was originally thought to involve only cartilage however it is now accepted that the SCB has a role in OA pathogenesis [83, 84, 95]. Remodelling of the SCB has been linked with OA, Radin *et al* have speculated that it leads to altered joint biomechanics resulting in secondary changes in cartilage structure [96]. Severe subchondral sclerosis is observed in OA, whilst there is also evidence that vascularization of the ACC from the SCB is related to the development of OA [97]. Whether changes in the SCB precede cartilage damage, or they are as a result of changes in the cartilage is still up for discussion. Obesity has been linked with the development of OA due in part to the abnormal load placed on joints in obese individuals [98]. There also appears to be metabolic and systemic factors involved in obesity which act both directly and indirectly on chondrocytes leading to an increased risk of developing OA [99]. Adipokines are thought to be one of the major factors linking obesity to OA, in particular leptin which has been identified in OA cartilage. It appears to act as a catabolic factor in cartilage metabolism through induction of MMPs [99]. Other

proinflammatory cytokines including TNF-α and IL-1 are thought to act on chondrocytes and upregulate catabolic processes which are degenerative to the ECM. It is clear that the pathogenesis of OA is linked to a myriad of factors, and while this presents a significant number of targets for potential therapeutic intervention, without a clear understanding of which factors trigger OA initiation it may be a long time before an effective treatment is available.

1.6.3 Relationship between OA and AKU

The pathogenesis of both OA and AKU are still yet to be fully understood. Advances have been made in elucidating the mechanisms behind the initiation and progression of both disorders however more work is needed in this area. Although the exact mechanisms behind both disorders are still unknown, there is little doubt that OA and AKU are very closely linked to one another. Early onset of severe osteoarthropathy is the most devastating consequence that AKU patients suffer. Beginning in the third and fourth decade of life, AKU patients begin to suffer excruciating pain resulting from joint damage caused by deposition of ochronotic pigment. Studies have shown ochronotic joints, obtained at the time of joint replacement surgeries, to be severely osteoarthritic with cartilage erosion visible macroscopically. Microscopic examination of AKU joints has shown further signs of an extreme OA phenotype with complete resorption of the SCB seen in some samples [36]. Similar to OA initiation and progression, both the ACC and SCB appear to play a role in the initiation and progression of ochronotic osteoarthropathy [36, 84, 100] highlighting the close association between the two disorders. Studying the extreme phenotypes of OA seen in AKU may help elucidate mechanisms behind joint destruction and help to identify potential therapeutic targets.

1.7 ANIMAL MODELS OF DISEASE

1.7.1 Importance

Animal experimentation has long been used by the scientific community. Although the use of animals remains controversial, particularly in predicting the effectiveness of treatments in clinical trials [101, 102], they are important research tools in aiding the understanding of disease pathology. Although not every treatment tested in animals is successful in clinical trials, there are examples of treatments which found success after being first trialled in animals. One of the most well-known cases was the development of penicillin as a treatment for bacterial infections. Although initially discovered by Alexander Fleming, it was Howard Florey and Ernst Chain who showed that mice which had been infected with a lethal amount of bacteria, survived when given penicillin [103, 104]. This demonstrated that penicillin was effective against serious bacterial infections and led to the mass production and use of the drug. Although other animals are used, rodents are the primary animal model used to study disease pathogenesis and potential therapeutics, particularly since the development of transgenic mice [105, 106]. Mice share more than 98% of their DNA with humans making them an excellent model to study disease in. Knockout mice, which are engineered to contain defective genes, are the most common type of animal used for research purposes. Disorders including heart disease, diabetes, obesity, Alzheimer's, and arthritis have all been studied in transgenic mice. Without these models of disease it would be difficult to understand the basic mechanisms behind initiation and progression, and to identify potential targets for therapeutic intervention.

1.7.2 AKU animal models

There have been many reports of spontaneous AKU developing in animals including horses, dogs, macaques, chimpanzees, and orang-utans, however ochronosis was rarely documented in these animals [107, 108]. Early attempts to induce AKU in an animal model was undertaken by Moran and colleagues who injected HGA into

rabbits [109]. The animals receiving HGA through intra-articular injections exhibited darkening of the urine and developed joint damage while the animals receiving HGA through intraperitoneal or intravenous routes did not display signs of ochronosis. The first mouse model of AKU was developed in 1994 by Montagutelli and colleagues at the Pasteur Institute in Paris [110]. Although the mice had high circulating levels of HGA, and displayed darkening of their urine the authors did not observe any ochronotic lesions in the joints. They hypothesized this was a result of endogenous production of ascorbic acid by the mice which prevented polymerization of HGA [110]. Ochronosis has since been observed in a second murine model of AKU, originally used to study HT-1 [111]. These mice required nitisinone to survive however when it was removed a very small proportion underwent a spontaneous loss of heterozygosity of Hgd in their liver nodules to become Hgd-/-, effectively making them AKU mice. Severe renal pathology was also observed in the mice making them unsuitable for investigative study. Chapter 3 of this thesis details the use of a novel staining method to identify ochronotic pigmentation, and to document the natural history of the disorder in Hgd-/- mice.

1.7.3 Mouse models of OA

As previously discussed OA is a debilitating condition for which there is currently no effective therapy. The aetiology of the disease also remains unclear making it difficult to identify any possible targets for therapeutic intervention. The use of mouse models to study OA is becoming increasingly wide-spread as they allow for the investigation of pathological changes in OA joints in a relatively short period of time. The anatomy of the mouse knee in particular is ideal for identifying OA changes as the entire tibio-femoral joint can be analysed in a single histological section (Fig. 1.5). Cartilage degradation is localized to the lateral femoral condyle (LFC), medial femoral condyle (MFC), lateral tibial plateau (LTP), and the medial tibial plateau (MTP). Ossification of the lateral and medial menisci (LM & MM) can occur in osteoarthritic joints. Any damage caused to the anterior and/or posterior cruciate ligaments (ACL & PCL) almost inevitably leads to the onset of OA.

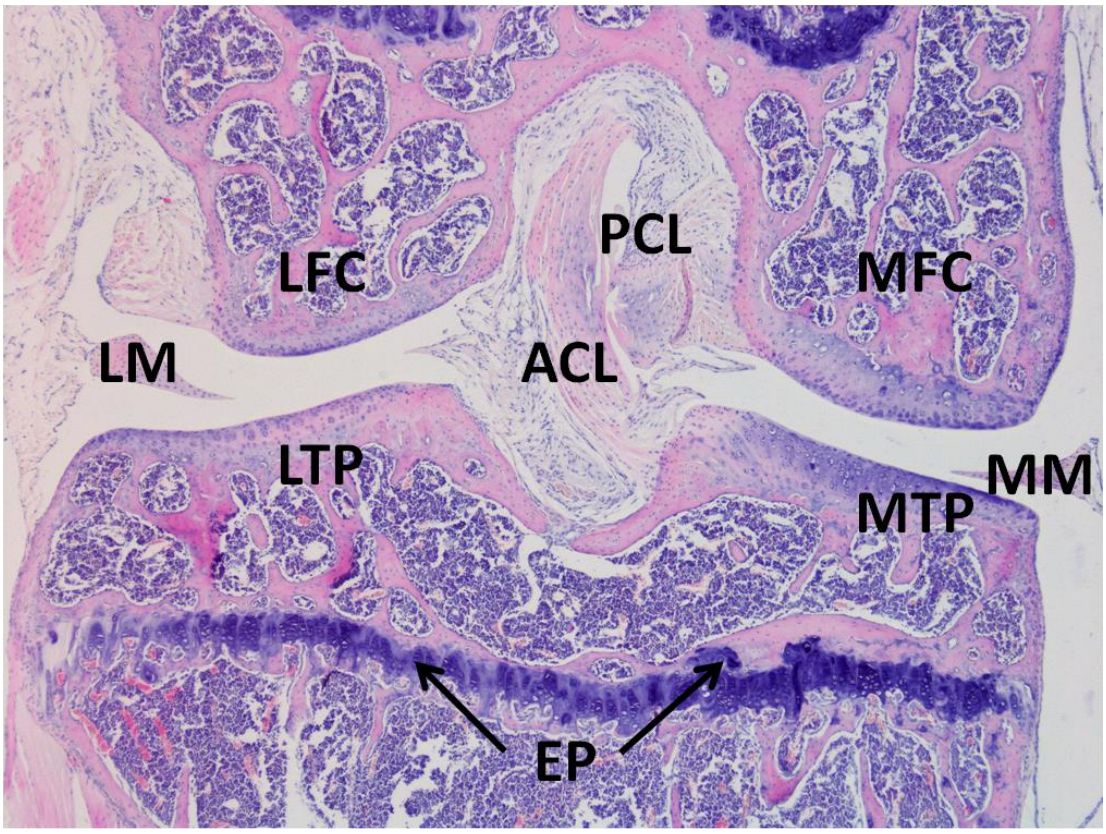

Figure 1.5 – Anatomy of the mouse knee joint. H&E staining of a single coronal section encompassing the entire tibio-femoral joint. The four main areas of the tibio-femoral joint are the; LFC, MFC, LTP, and MTP. These areas are most affected by the onset of OA. The LM and MM provide protection during movement and help disperse weight throughout the joint. Stability in the joint is provided by the ACL and PCL. The EP forms during endochondral ossification.

There are a range of mouse models used to study OA, including C57BL/6 and STR/ort strains [112, 113] which develop spontaneous OA throughout their lifetime. Genetic mouse models of OA are commonly used as they allow researchers to identify the roles of specific genes in the disorder. The production of MMPs, which lead to breakdown of the ECM, is regulated by their endogenous inhibitors, tissue inhibitors of metalloproteinases (TIMP). TIMP-3 null mice exhibit mild cartilage degradation, and show elevated levels of aggrecan and type II collagen cleavage products in the articular cartilage [114]. Mice overexpressing MMP-13 have been shown to have increased cartilage degradation at an early age [115]. The mice also

show high levels of type X collagen expression in HAC suggesting that the chondrocytes in these areas are expressing a different, and abnormal phenotype. Mice deficient for fibroblast growth factor (FGF) receptor-3 have also been shown to develop early onset OA [116].

Surgical induction of OA in mice is also routinely used as it allows for rapid development of moderate to severe OA. Kamekura *et al* described four surgical models of OA in mice including complete transection of the ACL and MM [117]. Different stages of OA were reported for all four models including cartilage degradation and SCB erosion. Glasson and colleagues introduced another surgical model of OA in mice known as destabilization of the medial meniscus (DMM) [118]. DMM is now the preferred method of inducing OA in mice as changes in the joint can be classified into mild, moderate, and severe depending on the time course of the experiment. The DMM model also showed more severe histological changes in the cartilage than the models developed by Kamekura [118].

Although treatment options for OA are currently limited, the availability of mouse models with different stages of OA is important for the testing of any potential treatments. Recently mice with surgically induced OA, resulting from ACL transection, showed no cartilage degradation due to inhibition of transforming growth factor (TGF) β1 by an anti-TGF-β1 antibody. Not only did this show that TGF-β1 appeared to be involved in the pathological changes related to OA, but also that mouse models of OA are important and help develop understanding of the pathogenesis of the disorder, as well as providing a model on which to try new and potentially effective therapeutics.

1.8 AIMS OF THE STUDY

Although progress has been made in understanding the mechanisms behind the initiation and progression of AKU, research is limited to samples obtained from joint replacement surgeries, which usually show advanced ochronosis. Without an established animal model of AKU there is little opportunity to study the progression of the disease, and therefore understand its pathogenesis. It also prevents the testing of any potential therapeutics of which there are currently none widely available to treat AKU. The main aims of this thesis were therefore to try and identify if Hgd-/- mice became pigmented and exhibited signs of ochronotic osteoarthropathy, and to test the efficacy of a potential therapy in preventing deposition of ochronotic pigment.

2. Materials and Methods

2.1 ETHICAL APPROVAL

2.1.1 Mouse tissue

All mouse tissue used in this project was obtained under ethical approval from the Home Office in accordance with their UK guidelines. Under the Animals (Scientific Procedures) Act 1986, a project license granted to Professor Jonathan Jarvis and a personal license (PIL. 40/9710) granted to Craig Keenan allowed for the completion of experiments, Schedule 1 humane killing of mice and use of their tissue for analysis.

2.2 MOUSE HUSBANDRY

All mice were housed and maintained within the University of Liverpool's Biological Services Unit (BSU) in accordance with Home Office UK guidelines. They had full access to drinking water and food, and were kept in a hygienic environment. Cleaning of cages and changes of bedding was carried out on a daily basis.

2.3 MOUSE BREEDING, GENOTYPING AND TREATMENTS

2.3.1 Breeding

2.3.1.1 BALB/c Hgd-/-

Four Hgd-/- (AKU) mouse breeding pairs on a BALB/c background strain were obtained from Dr. X Montagutelli (Pasteur Institute, France) and a colony was established at the University of Liverpool, UK. Control wild type (WT) BALB/c J mice were purchased from Charles River Laboratories, UK.

2.3.1.2 BL/6 Hgd-/-

HgdFah (Hgd+/-, Fah-/-) mice on a BL/6 background strain were crossed with WT BL/6 mice and their offspring genotyped. Any resulting Hgd+/-, Fah+/- were interbred to eventually yield Hgd-/-, Fah+/+ (AKU) mice on the BL/6 background.

2.3.2 Genotyping

2.3.2.1 Hgd

Genomic DNA was extracted from tail tips using DNeasy Blood and Tissue kits (Qiagen, UK), and the Hgd gene typed as previously described [119] with slight modifications. Primer sequences were:

- forward primer 5'-CATTTTCACCGTGCTGACTG-3'
- reverse primer 5'-TTTAGTCGCTGCATCACCTG-3'

A 25µl PCR reaction mix contained 12.5µl of HotStarTaq Mastermix (Qiagen, UK), 1µl of each 100mM primer stock, 2µl of DNA sample and 8.5µl of water. PCR conditions were: 15min at 95°C + 30 cycles (30s at 94°C, 30s at 52°C, 1min at 72°C) + 7min at 72°C. A 1.5µl aliquot of product was digested at 37°C with 0.3µl of HpyCH4III, 1.5µl of New England BioLabs Buffer 4 and 11.7µl of water, for at least 2hrs. Samples were electrophoresed for 30min at 200V on a 3% agarose gel containing SybrSafe (Invitrogen, UK). WT samples produced 170bp and 120bp digest bands, and mutant samples a nondigested 290bp band.

2.3.2.2 Fah

Genomic DNA was extracted from tail tips using DNeasy Blood and Tissue kits (Qiagen, UK), and the Fah gene typed as follows. Primer sequences were:

- forward primer 5'- GGATTGGGAAGACAATAGCAGGC-3'
- reverse primer 5'-TTGCCTCTGAACATAATGCCAAC-3'
- WT primer 5'-TGAGAGGAGGGTACTGGCAGCTAC-3'

A 25µl PCR reaction mix contained 12.5µl of HotStarTaq Mastermix (Qiagen, UK), 0.25µl of mutant primer, 0.5µl of reverse primer, 0.5µl of WT primer, 2µl of DNA sample and 9.25µl of water. PCR conditions were: 15min at 95°C + 30 cycles (30s at 94°C, 30s at 52°C, 1min at 72°C) + 7min at 72°C. Samples were electrophoresed for 30min at 200V on a 3% agarose gel containing SybrSafe (Invitrogen, UK). WT samples produced a 250bp band, and mutant samples a 145bp band.

2.3.3 Treatments

2.3.3.1 Nitisinone – whole life

A cohort of 16 BALB/c Hgd-/- mice (eight male, eight female) were provided with an ad libitum supply of water containing 4mg/l of nitisinone (Shanghai Elittes Organics, China) from 8 to 67 weeks of age. The control group of 16 BALB/c Hgd-/- mice (nine male, seven female) had no drug in their drinking water from 11 to 70 weeks of age. Plasma was taken immediately prior to treatment, and then sampled regularly by tail bleed over the mouse lifetime.

2.3.3.2 Nitisinone – mid-life

A cohort of 8 BALB/c Hgd-/- mice (four male, four female) were provided with filtered water from 8 to 34 weeks of age. They were then provided with an ad libitum supply of water containing 4mg/l of nitisinone from 35 to 80 weeks of age. The control group of 8 BALB/c Hgd-/- mice (four male, four female) had no drug in their drinking water from 8 to 80 weeks of age. Plasma was taken immediately prior to treatment, and then sampled regularly by tail bleed over the mouse lifetime.

2.3.3.3 HGA supplementation

A cohort of 10 BL/6 Hgd-/- mice (five male, five female) were provided with an ad libitum supply of water containing 5mM of HGA from 8 to 74 weeks of age. The control group of 10 BL/6 Hgd-/- mice (five male, five female) had no HGA in their drinking water from 8 to 72 weeks of age. Plasma was taken immediately prior to treatment, and then sampled regularly by tail bleed over the mouse lifetime.

2.4 MURINE SURGERY

2.4.1 Regulation of surgical procedure

Before surgery was performed approval was required from the Home Office to allow the procedure to be carried out. Both the project license and personal license were amended to include the surgical procedure(s) once it had been approved by the Home Office under the Animals (Scientific Procedures) Act 1986.

2.4.2 Surgical preparation

2.4.2.1 Suiting up and scrubbing of surgeons

All surgical procedures were carried in collaboration with Dr. Hazel Sutherland who has extensive experience of performing animal surgery. Upon entering the BSU surgical scrubs, gloves, a mop cap and a facemask were required to be put on before carrying out any preparation work. Scrubbing with a disinfectant and dressing in sterile gowns and gloves were required before surgery was performed.

2.4.2.2 Instrument preparation

All instruments were washed, wrapped and sterilised in a large oven prior to being used in surgery. A range of different sizes of surgical scissors and fine forceps were sterilised to ensure enough instruments were available to complete the surgery.

2.4.2.3 Anaesthesia

Prior to surgery the mice were anaesthetised. Inhalation anaesthetics were used as it allowed for a constant plane of anaesthesia to be maintained during surgery compared with injectable anaesthetics. The mice were anaesthetised using a combination of Isoflurane, NO_2, and O_2. The level of anaesthesia required by the mice varied which was usually due to weight differences between them. Mice weighing more than 30g tended to take longer to become fully anaesthetised and typically required a higher amount of Isoflurane (1.5-2.0%). Levels of NO_2 and O_2 were always maintained at 1.5% regardless of the weight of the mice. The amount of Isoflurane administered never went above 2.0% as this can cause terminal anaesthesia. During surgery, the mice were kept anaesthetised with the same level of Isoflurane required to initially anaesthetise them. The body temperature of the mice was also closely monitored; if a drop in temperature was recorded a heat mat was introduced to help maintain body temperature at 37^{o}C.

2.4.2.4 Site of surgery preparation

Once anaesthetised, the mice were prepped for surgery. Baytril (Enrofloxacin), an antibiotic, was administered subcutaneously at a dose of 5mg/kg (diluted in distilled water). Temgesic (Buprenorphine), an analgesic, was administered intramuscularly into the rectus femoris muscle at a dose of 0.1mg/kg (diluted in distilled water). The area of interest was then shaved and sterilised with iodine.

2.4.3 Destabilization of the medial meniscus

2.4.3.1 General information

DMM is a procedure introduced by by Dr S Glasson *et al* [118] to induce a mild to moderate form of OA in mice. The procedure requires the transection of the medial meniscotibial ligament (MMTL) to free the MM from the tibial plateau (TP). This prevents the meniscus from distributing the body's weight load causing increased mechanical stress and a higher risk of injury. The procedure was followed from the original publication and adapted where necessary.

2.4.3.2 DMM procedure

Using surgical scissors the skin of the left hind limb was incised over the patella and patella ligament to expose the knee joint. Micro surgical scissors were then used to make a small incision medial to the patella ligament, and small amounts of fat removed with blunt dissection. This was frequently followed by bleeding which was stemmed with a cotton bud, while saline was used to keep the joint moist. Identification of the MMTL proved to be difficult in BALB/c Hgd-/- mice as the ligament seemed to be almost translucent. As the MM was easier to identify it was used as a guide to determine where the MMTL attached on both the MM and the TP. Once definitively identified the MMTL was transected using micro surgical scissors. The ability to push the MM in and out of the joint cavity was used as confirmation the MMTL had been transected and the surgery had been successful. The incision in the patella ligament was sutured with a running stitch using 7.0 proline and the skin sutured with a subcutaneous stitch using 6.0 proline. The mice were then immediately transferred to the post-operative recovery room.

2.4.4 Post-operative recovery

Immediately following surgery the mice were placed in a heated room where a temperature of 25^{o}C was maintained to aid their recovery. A second dose of temgesic was administered to help with pain relief. Once the mice had been returned to the BSU they were examined on a daily basis to ensure the surgical wound was healing properly. The general health of the mice was also checked as surgery can often cause a delayed adverse reaction. Restricted movement, weight loss and lack of grooming are known signs of abnormality and were therefore checked. If none of these were apparent upon examination of the mice they were classed as healthy.

2.4.5 Humane killing of animals using schedule 1 procedures

2.4.5.1 General information

All mice were humanely killed using Schedule 1 procedures in accordance with Home Office UK guidelines under the Animals (Scientific Procedures) Act 1986.

2.4.5.2 Overdose of an anaesthetic

Mice were euthanized by a lethal dose of pentoject (sodium pentobarbitone 20% w/v) prompting a rapid loss of consciousness. Pentoject was administered intraperitoneally to minimise any distress.

2.4.5.3 Concussion of the brain and dislocation of the neck

Concussion was caused by striking the cranium of the mice against the edge of the worktop with sufficient force to cause immediate loss of consciousness and/or death. After loss of consciousness was induced, death was confirmed by neck dislocation.

2.4.6 Dissection and harvesting of tissue

2.4.6.1 General information

Once death had been confirmed the mice were dissected either immediately in the BSU or later in the same day in the histology laboratory. It was imperative to collect the tissue on the day of death to prevent autolysis and necrosis. Tissues collected were fixed in either 10% phosphate buffered formalin solution (PBFS) for histological analysis, or 2.5% glutaraldehyde for ultrastructural analysis.

2.4.6.2 Harvesting of tissue

2.4.6.2.1 Hind limb

The skin was removed from the hind limbs exposing the full anatomy of the joint. The majority of the muscle was dissected away and the joint was dissected out by severing close to the femoral head which allowed for removal of the whole hind limb. The tibia was then severed just above the ankle to leave an intact knee joint. After washing in phosphate buffered saline (PBS) the limbs were fixed for analysis.

2.4.6.2.2 Heart

An incision was made into the skin of the mice to allow visualisation of the thoracic cavity which was subsequently opened by cutting through the sternum with surgical scissors. The heart was pried away from its surrounding connective tissue and was removed with its major vessels intact. The heart was washed with PBS to remove excess blood before fixation.

2.4.6.2.3 Liver and Kidneys

The liver was dissected out of the abdominal cavity ensuring none of the lobes were damaged. Once removed, the liver was washed in PBS and small sections of each

lobe were taken to allow for easy fixation and analysis. The kidneys were exposed after removal of the liver. They were dissected out of the abdominal cavity, washed in PBS and sectioned in half to allow for easy fixation and analysis.

2.4.7 Fixation of carcass

After the tissue(s) had been harvested the viscera (guts) were removed and discarded. The carcass was fixed in 150ml of PBFS to ensure adequate fixation. The fixing solution was changed after 24hrs and again if it altered colour as this indicated the solution had become acidic.

2.5 HISTOLOGY

2.5.1 Reagents

Haematoxylin, eosin, potassium ferricyanide, ferric chloride, and nuclear fast red (NFR) were purchased from VWR, UK. Ethylenediaminetetraacetic acid (EDTA), chromic potassium sulphate, bovine gelatine and DPX microscopy mountant were purchased from Sigma, UK. Premium frosted glass slides and 50mm cover slips were purchased from VWR, UK.

2.5.2 Fixation of tissues

2.5.2.1 General information

Fixation is a chemical process which prevents biological tissue from undergoing autolysis and necrosis. Fixation stops any ongoing biochemical reactions leaving the tissue in a life-like state. Tissues harvested were fixed in 10% PBFS solution.

2.5.2.2 Preparation of fixative

PBFS (2.5L) was made up as follows: -

- 250ml of Formaldehyde (37% w/v)
- 250ml of PBS (10x)
- 2000ml distilled water
- Mixed well
- pH adjusted to 7.2–7.4, if required a small amount of HCl (1M) was added

2.5.2.3 Fixation procedure

Once harvested the tissues were immediately placed in PBFS to prevent autolysis. The amount of fixative used was generally 15-20 times greater than the tissue volume. Fixation was carried out at room temperature for 24hrs.

2.5.3 Decalcification of mineralized tissue

2.5.3.1 General information

Decalcification is the process of removing calcium from mineralized tissue. Decalcification was performed using 12% EDTA, a chelating agent that binds calcium thus allowing the tissue to decalcify.

2.5.3.2 Preparation of decalcifying solution

Mineralised tissues were decalcified using 12% EDTA. EDTA (2.5L) was made up as follows: -

- 300g of EDTA
- 2000ml distilled water
- A few drops of phenol red indicator were added and solution mixed
- pH needed to be maintained at 8 to dissolve EDTA (NaOH pellets)

- Once dissolved pH was adjusted to 7.2–7.4 using concentrated HCl
- Solution was made up to a final volume of 2500ml

2.5.3.3 Decalcification procedure

Following fixation, mineralized tissues were placed into EDTA for an initial period of 24hrs. The EDTA solution was then changed and tissues were left to decalcify for a further 6 days (7 days total). Decalcification was complete when tissues were flexible and soft enough to bend.

2.5.4 Processing of tissue

Following decalcification tissues were removed from EDTA and washed several times with PBS. Tissues were processed first through increasing grades of ethanol (70% (15mins), 90% (30mins), and 100% (x4) (1hr)) to dehydrate the tissue. Once dehydrated, tissues were cleared using two changes of xylene (45 minutes in each) before being passed through two changes of paraffin wax (1hr in each) to complete the processing. Processing was performed using a Leica TP1020 tissue processor (Leica, Germany).

2.5.5 Embedding of tissue

Following processing, tissues were placed into heated metallic moulds, submerged in molten paraffin wax and embedded in an orientation which allowed for sectioning of the area of interest. Knee joints from all mice were embedded in the coronal plane to enable simultaneous evaluation of the medial and lateral tibio-femoral joint as recommended by the Osteoarthritis Research Society International (OARSI) histopathology initiative [120]. A plastic chuck was placed on top of the mould to allow sectioning of the block. Tissue blocks were cooled to solidify and then removed from their metallic mould.

2.5.6 Sectioning of tissue

Tissue blocks were cut to remove excess wax, and shaped to have a trapezoid cutting surface. Blocks were initially trimmed at 10µm until the tissue could be seen coming through the block. Sections were then taken every 5µm before being mounted on subbed slides and placed in an incubator at 50^{o}C overnight. Sections from the knee joints of all mice were taken every 5µm from posterior to anterior until the whole joint had been sectioned. Blocks were sectioned using a Leica RM2245 semi-automated microtome (Leica, Germany).

2.5.7 Subbing of slides

2.5.7.1 General information

Microscope slides were subbed with a gelatine solution to help sections adhere to the slide.

2.5.7.2 Subbing solution

- 400ml distilled water
- 0.8g type B bovine gelatine
- Gelatine dissolved in distilled water with heat – NOT EXCEEDING 50^{o}C
- 0.08g chromic potassium sulphate added when gelatine dissolved

2.5.7.3 Subbing procedure

- Slides rinsed in 100% ethanol for 30 seconds
- Left to dry for 5 minutes
- Slides then immersed in subbing solution for 30 seconds
- Dried overnight at room temperature – cover slides to prevent dust building up

2.5.8 Staining of tissue

2.5.8.1 Haematoxylin and eosin

Haematoxylin and eosin (H&E) is the standard dye used in histology to show the gross anatomy of tissues. Haematoxylin stains cell nuclei dark blue whereas eosin stains proteins pink, therefore muscle fibres and connective tissue stain varying shades of pink. There are a number of different haematoxylins which can be used in combination with eosin for staining, each having their own advantages and disadvantages. For the purposes of this research Ehrlich's haematoxylin was used as it has the ability to show the cartilaginous elements of tissue as blue/purple, due to the staining of GAGs, in contrast to the pink of collagenous tissue [121].

2.5.8.1.1 Stock solutions

- Ehrlich's haematoxylin (ripened)
- Eosin (1%)
- Concentrated HCl

2.5.8.1.2 Staining procedure

- Slides were deparaffinised in two changes of xylene - 5 minutes in each
- Hydrated through ethanol (100%, 100%, 70%, 70% - 2 minutes in each) to water
- Stained in haematoxylin for 2-3 minutes
- Washed in running warm water for 3 minutes
- Dipped in 1% HCl for 10-15 seconds to remove residual haematoxylin
- Washed vigorously in running cold water for 5 minutes
- Counterstained in eosin for 1-2 minutes
- Dipped in running cold tap water for 10 seconds to remove residual eosin
- Dehydrated through ethanol (70%, 70%, 100%, 100% - 2 minutes in each)
- Cleared in two changes of xylene - 3 minutes in each
- Mounted with DPX and left to dry

2.5.8.2 Schmorl's stain

Schmorl's stain is generally used to test for the presence of late lipofuscins and melanin in cells. These compounds reduce ferricyanide to ferrocyanide, producing varying shades of blue with a positive result. As Schmorl's stain is used to stain melanin it was theorised it could, in principal, be used to stain for ochronotic pigment as both compounds are thought to have similar structures and are derived from the tyrosine catabolic pathway. By modifying the procedure to include a longer incubation time, Schmorl's stain has been shown to identify the presence of ochronotic pigmentation in murine and human tissues [122].

2.5.8.2.1 Incubating solution

- 1% Ferric chloride – 37.5ml
- 1% Potassium ferricyanide – 5ml
- Distilled water – 7.5ml

2.5.8.2.2 Staining procedure

- Slides were deparaffinised in two changes of xylene - 5 minutes in each
- Hydrated through ethanol (100%, 100%, 70%, 70% - 2 minutes in each) to water
- Immersed in Schmorl's stain for up to 15 minutes
- Washed well in running cold water to remove any residual ferricyanide
- Treated with 1% acetic acid for 5 minutes to prevent over-staining
- Counterstained in NFR for 3-5 minutes
- Washed in running cold water to remove any residual NFR
- Dehydrated through ethanol (70%, 70%, 100%, 100% - 2 minutes in each)
- Cleared in two changes of xylene - 3 minutes in each
- Mounted with DPX and left to dry
-

2.5.9 Quantification of pigmented chondrons in the tibio-femoral joint

The first whole section that encompassed the entire tibio-femoral joint (MTP, MFC, LTP, & LFC) was selected as representative of each mouse for quantification analysis. From these sections, pigmented chondrons present in the articular cartilage and entheses of the femoral condyles and articular cartilage of the TP were quantified (Fig. 2.1).

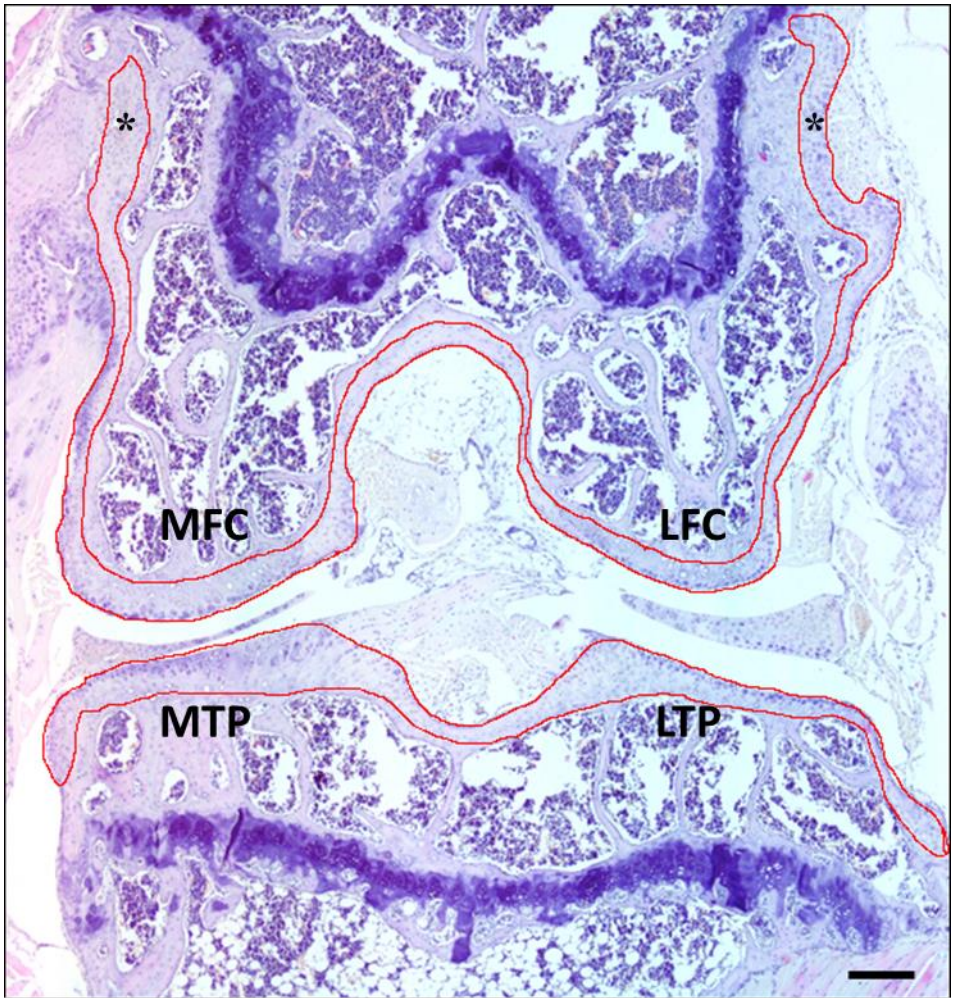

Figure 2.1 – Areas of quantification in the tibio-femoral joint of Hgd-/- mice. The red lines on the image highlight the areas where pigmented chondrons were quantified in the tibio-femoral joint (* = entheses). Bar = 50µm.

2.5.10 Light microscopy analysis

Analysis of all tissues used for histology was performed using light microscopy. Two different microscopes were used in this thesis, one being a Nikon Eclipse C*i* microscope fitted with a Ds-Fi2 camera and the other a Zeiss Axio Imager 2 microscope. The Zeiss Axio Imager 2 was used strictly for acquiring panoramic images. NIS Br elements was used for image analysis with the Nikon Eclipse microscope.

2.6 STATISTICAL ANALYSIS

An independent samples t-test was used to identify any significant differences between the number of pigmented chondrons in both the control and treated groups in the mid-life nitisinone study. A two-tailed, two-sample, unequal variance t-test was used to determine any significant differences in plasma HGA concentrations of nitisinone-treated mice. A Wilcoxon signed-rank test was used to identify any significant differences between the severity of OA in experimental and control limbs in the DMM study. A retrospective power calculation was performed on both the 8 weeks and 12 weeks post-op groups in the DMM study. This was used to determine the required sample size in any future studies. All statistical analysis was performed using Stata 13 (StataCorp. 2013. Stata Statistical Software: Release 13. College Station, TX: StataCorp LP.) and JMP9 (JMP®, Version *9*. SAS Institute Inc., Cary, NC, 1989-2007).

2.7 TRANSMISSION ELECTRON MICRSCOPY

2.7.1 Reagents

Glutaraldehyde, chloroform and acetone were purchased from Sigma, UK. Osmium tetroxide, uranyl acetate, and Agar 100 resin were purchased from Agar Scientific, UK. Superfrosted microscope slides were purchased from Thermo-Scientific, UK. Paraformaldehyde, propylene oxide and 100 mesh hexagonal copper grids were

purchased from TAAB, UK. Lead citrate was made from a solution of lead nitrate and sodium citrate. Pioloform was purchased from SCI-CHEM, USA.

2.7.2 Preparation of tissue

Tissues selected for transmission electron microscopy (TEM) analysis were micro-dissected to give pieces less than $1mm^3$. Once dissected into manageable sizes the samples underwent fixation and decalcification.

2.7.3 Fixation of tissue

Tissues were fixed in 4% paraformaldehyde with 2.5% glutaraldehyde in 0.1M sodium cacodylate (pH 7.4) or 10% PBFS for 24hrs at room temperature.

2.7.4 Decalcification of tissue

Following fixation, mineralised tissues were placed into EDTA for an initial period of 24hrs. The EDTA solution was then changed and tissues were left to decalcify for a further 6 days (7 days total). Decalcification was complete when tissues were flexible and soft enough to bend.

2.7.5 Processing of tissue

Following decalcification tissues were washed several times with distilled water then post-fixed in freshly made 1% osmium tetroxide for 3hrs at room temperature. Samples were then washed several times with distilled water before being bloc stained in 1% aqueous uranyl acetate for 24hrs at room temperature. Following treatment with uranyl acetate samples were dehydrated through ethanol (30%, 50%, 70%, 90% and 100% (x 4) – each for 10 minutes) on ice, and cleared with propylene oxide for 10 minutes. Samples were then infiltrated with Agar 100 resin.

2.7.6 Resin infiltration

Dilutions of resin were made up in propylene oxide. The infiltration of samples with resin was as follows: -

- 30% resin for 24hrs at room temperature
- 50% resin for 2hrs at room temperature
- 75% resin for 1hr at room temperature
- 100% resin for 24hrs at room temperature
- 100% resin for 1hr at room temperature

Samples were then embedded in a resin mould using fresh 100% resin and placed in an oven at 60^{o}C for 3 days to polymerize.

2.7.7 Sectioning of tissue

Blocks were initially trimmed using a glass knife until the section was at the surface. A small square (300nm x 300nm x 150nm) was then trimmed to isolate the region of interest on the tissue. 70nm sections were cut using a Diatome diamond knife. Blocks were sectioned using a Leica EM UC6 ultramicrotome (Leica, Germany).

2.7.8 Preparation of grids

Plastic coated copper grids were used for the mounting of sections. Large quantities of 100 mesh hexagonal copper grids were cleaned with 100% ethanol and acetone then left to dry. A 0.3% solution of Pioloform diluted in chloroform was prepared fresh to coat the grids. Superfrosted microscope slides were polished with chamois leather and wiped clean with lint free tissue before being dipped into the pioloform solution for 3-4 seconds. The slides were removed with care to ensure the pioloform film had no horizontal lines present and were air dried for 20-30 seconds. Once dry a razor blade was used to cut around the edges of the film which was then separated free by breathing on both sides of the slide. The slide was slowly lowered vertically into a container filled with distilled water to remove the film from either

side of the slide. The grids were then placed shiny side up on the film and collected on a clean slide by placing the slide at a 90^{o} angle and dropping it straight down completely submerging the film. Slides were dried for 24hrs in a condenser.

2.7.9 Post staining of sections

Post staining of sections was performed using lead citrate and uranyl acetate (5% by weight in 50% ethanol and 50% distilled water). Both reagents were spun down to reduce precipitation before use. Grids were placed section side down into uranyl acetate for 5 minutes then washed in three changes of distilled water for 20 seconds in each. Grids were then placed section side down in lead citrate for 5 minutes and again washed with three changes of distilled water for 20 seconds in each. Grids were left to dry on filter paper for 24hrs.

2.7.10 TEM analysis

TEM was performed using an FEI 1210kV Tecnai G2 Spirit BioTWIN electron microscope, and all images were captured using an SIS Megaview III camera.

3. Natural history of ochronosis in murine models of alkaptonuria

3.1 INTRODUCTION

The first objective of this thesis was to document the natural history of ochronosis in Hgd-/- mice. The murine model of AKU was created by Montagutelli and colleagues at the Pasteur Institute, Paris [110]. Eight week old mice, from an inbred stock carrying seven recessive mutations (agouti (*a*), brown (tyrosinase related protein or *Tyrp1*), albino (tyrosinase or *Tyr*), dilute (myosinVa or *Myo5a*), short ear (bone morphogenetic protein 5 or *Bmp5*), pink-eyed dilution (*p*), and piebald (endothelin receptor type B or *Ednrb*)) [123, 124], were given a single injection of ethylnitrosourea (250mg/kg) intraperitoneally to induce mutagenesis. These mice were subsequently mated with 129/Sv-T/+ mice and independent micro-pedigrees were achieved by systematic sibling mating for more than 10 generations. The AKU mutation (Hgd-/-) was then backcrossed onto BALB/cByj (albino) and C57/BL/6J (pigmented) backgrounds. Diagnosis of AKU in the mice was confirmed by darkening of the urine when pipetted onto filter paper infused with 0.5M sodium hydroxide. Although these mice excreted high levels of HGA in their urine, histological studies showed no signs of ochronosis in any of the tissues examined (knee, hip, ankle, spine, liver, kidneys and tail) [110].

A second murine model of AKU was discovered by Manning and colleagues in mice originally containing the tyrosinemia type 1 mutation (FAH-/-) [125]. These mice were used to study HT1 but became ochronotic when crossed with AKU heterozygote's (FAH-/-, Hgd+/-). Nitisinone was administered to the mice to prevent HT1, however when removed a very small proportion underwent a spontaneous loss of heterozygosity of Hgd in their liver nodules to become Hgd-/-, effectively making them AKU mice. Although ochronosis was observed in the knees and kidneys of these mice [111], it is not considered a suitable model of AKU as ochronosis is caused by a spontaneous mutation and is also associated with severe renal pathology, therefore these mice were not used in this study.

Montagutelli hypothesised that ochronosis was not observed in his histological studies of the Hgd-/- mice due to endogenous production of ascorbic acid which is a known antioxidant [110]. It has also been suggested that superior renal function in mice prevents the build-up of HGA in plasma, due to high levels of urinary excretion [110]. Recent research by Tinti *et al* [122] has shown that the use of Schmorl's stain can identify the presence of ochronotic pigmentation in tissues at very low levels. Schmorl's stain is routinely used to identify melanins. Ochronotic pigment and melanin are believed to be similar structures (cross-linked polymers) and both are products of the tyrosine catabolic pathway, which is why it can be used for the staining of ochronotic pigment. Using a modified Schmorl's stain, as a novel method to detect ochronosis, the aim of this work was to identify the presence of ochronotic pigmentation in Hgd-/- mice and to document its natural history. The following Chapter shows the results from these studies in BALB/c and BL/6 mice.

3.2 DESIGN OF STUDY

Twenty nine BALB/c Hgd-/- mice and twenty five BL/6 Hgd-/- mice, covering a wide range of ages from 6.5 – 71.7 weeks, were culled and their left knee analysed histologically. Once sections had been prepared, they were stained with Schmorl's stain to identify if ochronotic pigmentation was present, and H&E to identify any histological changes including signs of osteoarthropathy.

3.3 RESULTS

3.3.1 Histological detection of ochronotic pigment in BALB/c Hgd-/- mice

BALB/c mice were obtained from Dr X. Montagutelli and a colony set up at the University of Liverpool as described in Chapter two. Once weaned, the mice were culled at different time points ranging from 6.5 to 65.7 weeks and their knee joints analysed histologically. The left knee was used for the experimental studies and was sectioned posterior to anterior in each animal.

3.3.1.1 BALB/c Hgd-/- 132.1 (♀), 132.2 (♀), 132.3 (♀) – 6.5 weeks

The earliest time point looked at for this study was 6.5 weeks. It was central to the study to look at a wide range of ages to help identify if pigmentation was present, when it initiated and how it progressed. Initial observations from staining of the knee joints from all three mice at 6.5 weeks of age showed a complete absence of pigmented chondrocytes through the whole joint. This was consistent throughout the HAC and ACC of the femur and tibia (Fig. 3.1).

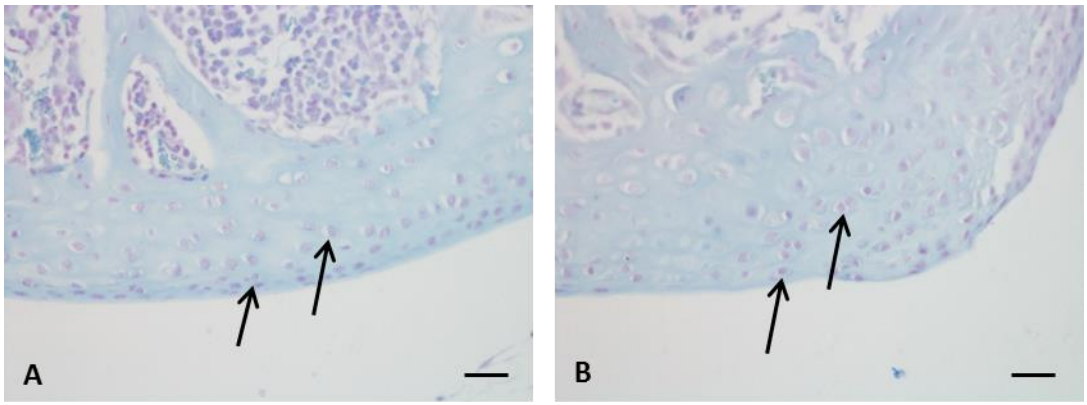

Figure 3.1 - Ochronotic pigmentation was not detectable in a 6.5 week old BALB/c Hgd-/- mouse. Schmorl's staining of BALB/c Hgd-/- 132.2 (♀) showed no signs of pigmentation in the HAC or ACC of the (**A**) LFC and (**B**) MFC. Bar = 20µm.

Three BALB/c Hgd-/- mice (129.2 (♂), 131.1 (♂), 131.2 (♂)) aged 7.8 weeks showed no pigmented chondrons with Schmorl's staining. No images are shown as they are identical to the mice aged 6.5 weeks above.

3.3.1.2 BALB/c Hgd-/- 93.2 (♂), 94.1 (♀) – 15.7 weeks

The third time point analysed was 15.7 weeks with two mice, one male and one female, being culled at this age. Schmorl's staining identified ochronotic pigment deposited in the PCM of a small number of chondrocytes in both the femur and tibia of both mice. This was the first time pigmentation of chondrocytes or their matrices had been seen in Hgd-/- mice. The pigmented chondrons were localized to the ACC (Fig. 3.2).

Figure 3.2 – Initial appearance of pigmentation in a 15.7 week old BALB/c Hgd-/- mouse. Schmorl's staining of BALB/c Hgd-/- 94.1 (♀) showed the appearance of a 'halo' around a small number of chondrocytes in the ACC of the MFC. Bar = 10µm.

The identification of PCM pigmentation around individual chondrocytes in the ACC was significant as it showed that Hgd-/- mice do become pigmented and display symptoms of ochronosis, contrary to early published data [110]. Identification of the pigment also showed that Schmorl's stain was an effective method of identifying ochronosis in mice as it is in humans.

There did appear to be an increase in the number of hypertrophic chondrocytes (Fig. 3.2), from around eight to twenty, when compared to the mice of 6.5 (Fig. 3.1) and 7.8 weeks of age. Chondrocyte hypertrophy occurs naturally during endochondral ossification allowing for calcification of the matrix, leading to the formation of bone in developing mouse embryos. Increased calcification is characteristic of joints which are developing OA. It is possible that the increased chondrocyte hypertrophy seen in BALB/c Hgd-/- 94.1 (15.7 weeks) is related to the early initiation of OA, a known side effect from ochronosis, however it is likely to be due to chondroptosis and active turnover of the cartilage and its matrix by the chondrocytes. Two males aged 19.6 weeks (data not shown) displayed an increase in the number of pigmented chondrocytes compared to those from mice aged 15.7 weeks (Fig. 3.18).

3.3.1.3 BALB/c Hgd-/- 106.1 (♀), 106.2 (♀), 106.3 (♀) – 23.5 weeks

Having identified pigmentation of the PCM in mice at 15.7 weeks of age, the next objective was to see how pigmentation of chondrocytes progressed throughout the tibio-femoral joint. Ochronosis is thought to become progressively more severe with age in humans, ultimately leading to the destruction of load bearing joints.

It was apparent straightaway that all of the mice had a significant increase in the number of pigmented chondrocytes in comparison to younger mice which had been examined (Fig. 3.18). All three mice showed pericellular pigmentation but also, and

more importantly, cellular pigmentation (Fig. 3.3). The progression of pigmentation to the cell itself is characteristic of ochronotic chondrons in humans.

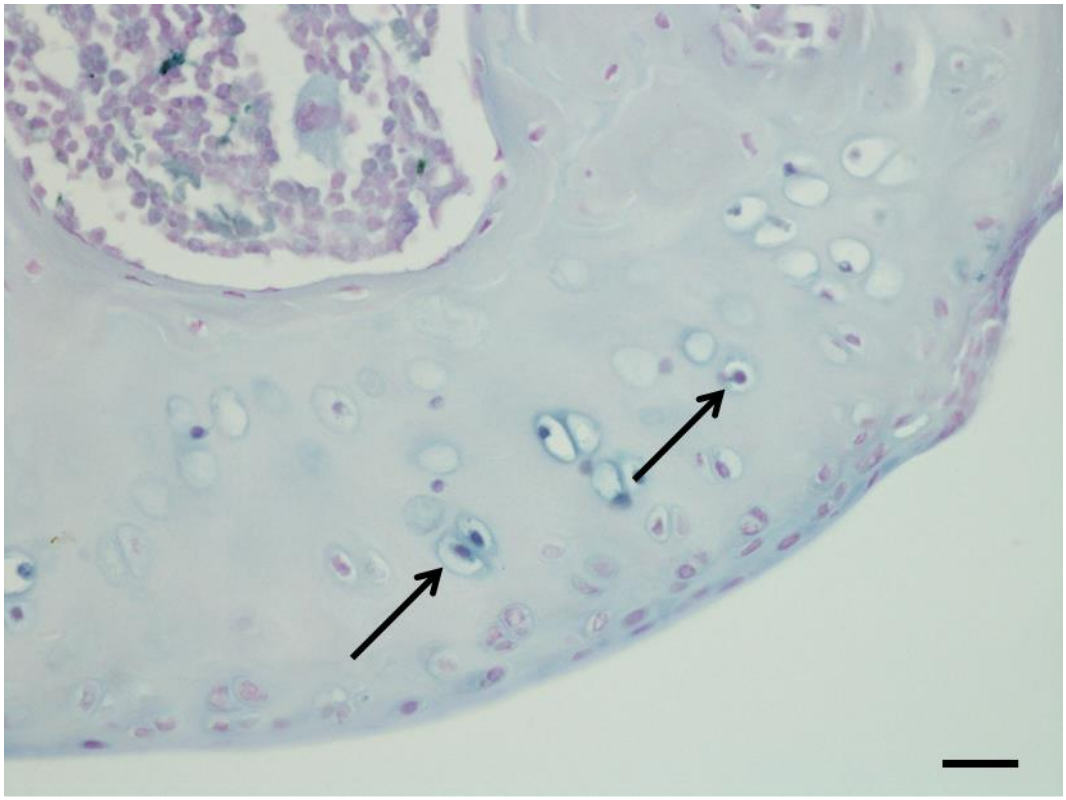

Figure 3.3 – Advancement of pigmentation to cellular compartment of chondrons in a 23.5 week old BALB/c Hgd-/- mouse. Schmorl's staining of BALB/c Hgd-/- 106.1 (♀) showed the spread of pigmentation from the PCM to the cell itself (arrows). This observation was consistent with the progression of ochronosis in human tissue samples. Bar = 20µm.

Analysis of two females aged 25.2 weeks (data not shown), showed slightly lower numbers of pigmented chondrons, 37 and 32 respectively, to those seen in BALB/c Hgd-/- 106.1, 106.2 and 106.3 who were 23.5 weeks (76, 53 and 33 respectively) (Fig. 3.18).

3.3.1.4 BALB/c Hgd-/- 99.1 (♂), 99.2 (♂) – 27.4 weeks

BALB/c Hgd-/- 99.1 (♂) and 99.2 (♂) (27.4 weeks) both showed pigmented chondrons in the ACC as expected, with some accompanying signs of osteoarthropathy (Fig. 3.4).

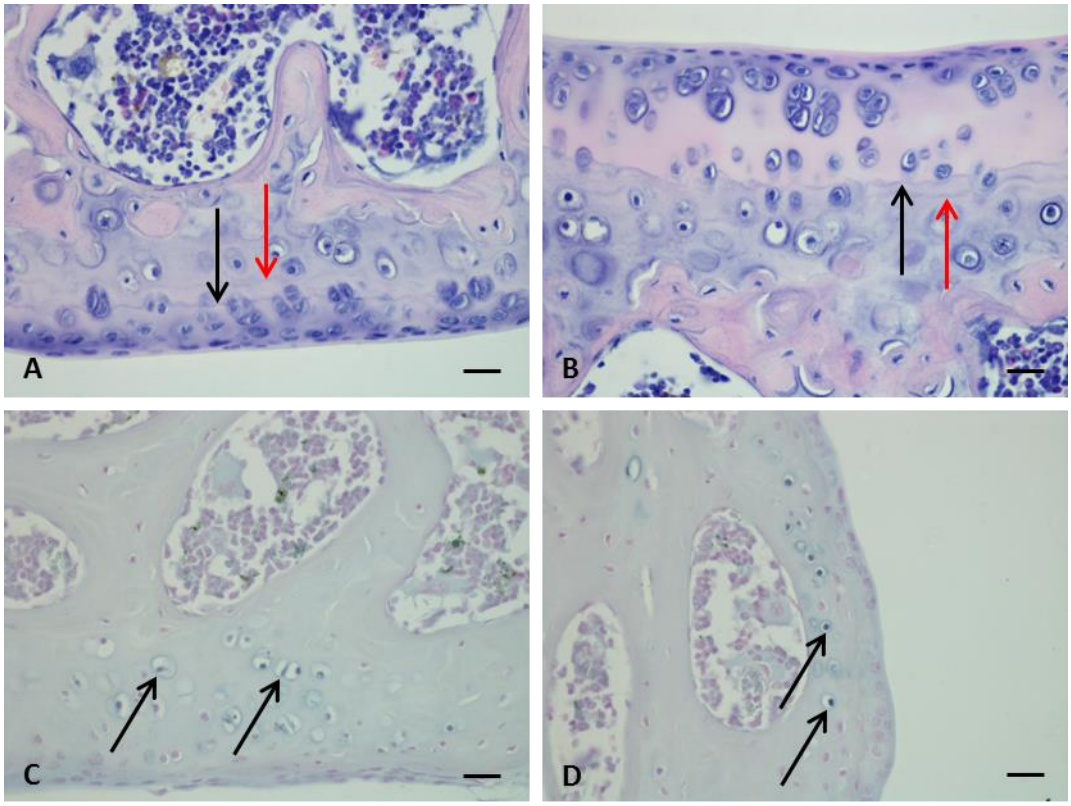

Figure 3.4 – Ochronotic pigmentation in a 27.4 week old BALB/c Hgd-/- mouse with accompanying early signs of osteoarthropathy. H&E staining revealed duplicate tidemarks located in the LFC (**A**) and the LTP (**B**, red arrows) of BALB/c Hgd-/- 99.1 (♂). Schmorl's staining showed pigmented chondrons in the LFC (**C**) showed varying degrees of staining. Pigmentation was present in clusters of chondrons in the LFC (**C**) and in individual chondrons in the MFC (**D**). Bar = 20µm.

The numbers of pigmented chondrons present in BALB/c Hgd-/- 99.1 (♂) and 99.2 (♂) was consistent with the numbers seen in BALB/c 106.1 (♀), 106.2 (♀), 106.3 (♀) (23.5 weeks) and BALB/c Hgd-/- 86.1 (♀) and 86.2 (♀) (25.2 weeks) (Fig. 3.18). With

only a four week age difference between the three sets of mice and with them all being still relatively young, it is not surprising that the amount of pigmented chondrons are fairly similar and quite low. This most likely indicates that although the mice have AKU, it is still at an early stage and has not yet manifested into the severe ochronotic osteoarthropathy which is seen in the third and fourth decades of life in humans. Certain chondrons appeared to be more ochronotic than surrounding cells (Fig. 3.4 (**C** & **D**)). This is an interesting observation as these chondrons clearly appear to be significantly more damaged than some of their neighbours, but with no obvious reason as to why this is the case. The presence of duplicate tidemarks in the LFC (Fig. 3.4 (**A**)) and LTP (Fig. 3.4 (**B**)) along with an increasing number of hypertrophic chondrocytes in the ACC are signs of osteoarthritic changes. Tidemark duplication is an recognised sign of OA [126] and is associated with increased mineralization of the cartilage. The identification of tidemark duplication in BALB/c Hgd-/- mice is significant as the early onset of OA is a well-known side effect resulting from AKU.

3.3.1.5 BALB/c Hgd-/- 92.1 (♂), 92.2 (♂) – 30.9 weeks

BALB/c Hgd-/- 92.1 (♂) and 92.2 (♂) displayed similar traits to the previous mice. Both showed chondron pigmentation in the ACC and duplication of the tidemark in the femoral and tibial condyles. BALB/c Hgd-/- 92.2 (♂) also showed signs of SCB remodelling and projection of the SCB into the articular cartilage (Fig. 3.5).

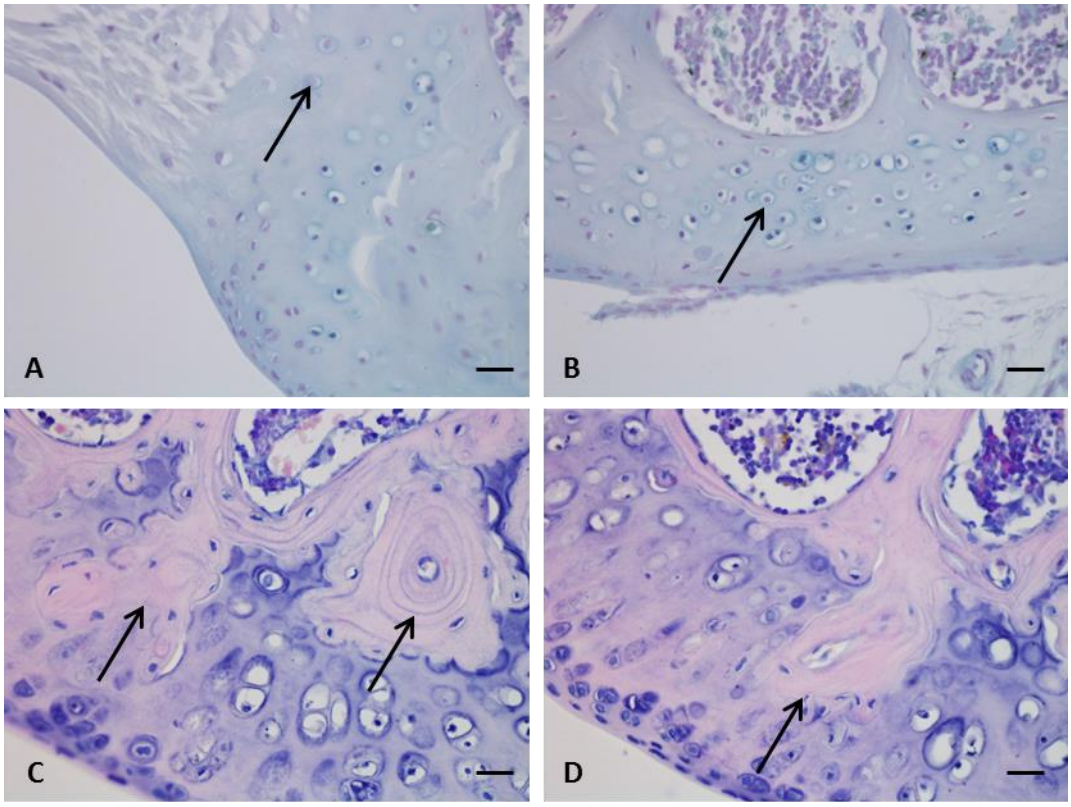

Figure 3.5 – Ochronotic pigmentation in 30.9 week old BALB/c Hgd-/- mice with signs of subchondral bone remodelling and projection of the subchondral bone into the articular calcified cartilage. Schmorl's staining of BALB/c Hgd-/- 92.1 (♂) showed pigmented chondrons in the LFC (**A** & **B**). Some chondrons appeared to be fully pigmented while others (arrowed) showed only pericellular pigmentation. H&E staining revealed SCB remodelling in the MFC of BALB/c Hgd-/- 92.2 (♂) (**C,** right arrow). Vascularisation of the ACC in the MFC was also observed (**C**, left arrow & **D**). Bar = 20µm.

The number of pigmented chondrons present in BALB/c Hgd-/- 92.1 (♂) and 92.2 (♂) (30.9 weeks) was slightly increased compared to the younger mice examined (Fig. 3.18). Both mice showed different stages of chondron pigmentation within the same region, with some cells showing only peri-cellular pigmentation while other cells were fully pyknotic. BALB/c Hgd-/- 92.2 displayed signs of SCB remodelling in the MFC. Projection of SCB into the ACC and its subsequent vascularisation was also observed in the same condyle. Both remodelling of the SCB and vascularisation of

the ACC are indications of OA, as is the presence of duplicate tidemarks which were also observed in both mice.

Two males, BALB/c Hgd-/- 91.1 (♂) and BALB/c Hgd-/- 91.2 (♂), aged 34.4 weeks (data not shown) displayed similar results to BALB/c Hgd-/- 92.1 (♂) and 92.2(♂) (30.9 weeks). The number of pigmented chondrons throughout the tibio-femoral joint was comparable with that seen in BALB/c Hgd-/- 92.1 and 92.2 (Fig. 3.18), as was the progression of chondron pigmentation in the ACC. While no damage or degradation to the surface of the articular cartilage was seen, there was tidemark duplication and some SCB remodelling present in both mice. The amount of pigmentation and the osteoarthritic changes in the cartilage were consistent with what had previously been seen in Hgd-/- mice of similar ages.

3.3.1.6 BALB/c Hgd-/- 86.3 (♀) – 40.4 weeks

BALB/c Hgd-/- 86.3 (♀) was the first mouse to show large scale pigmentation across the whole tibio-femoral joint. There was a significant increase in the total amount of pigmented chondrons in the femur and tibia (Fig. 3.18), many of which were severely ochronotic (Fig. 3.6).

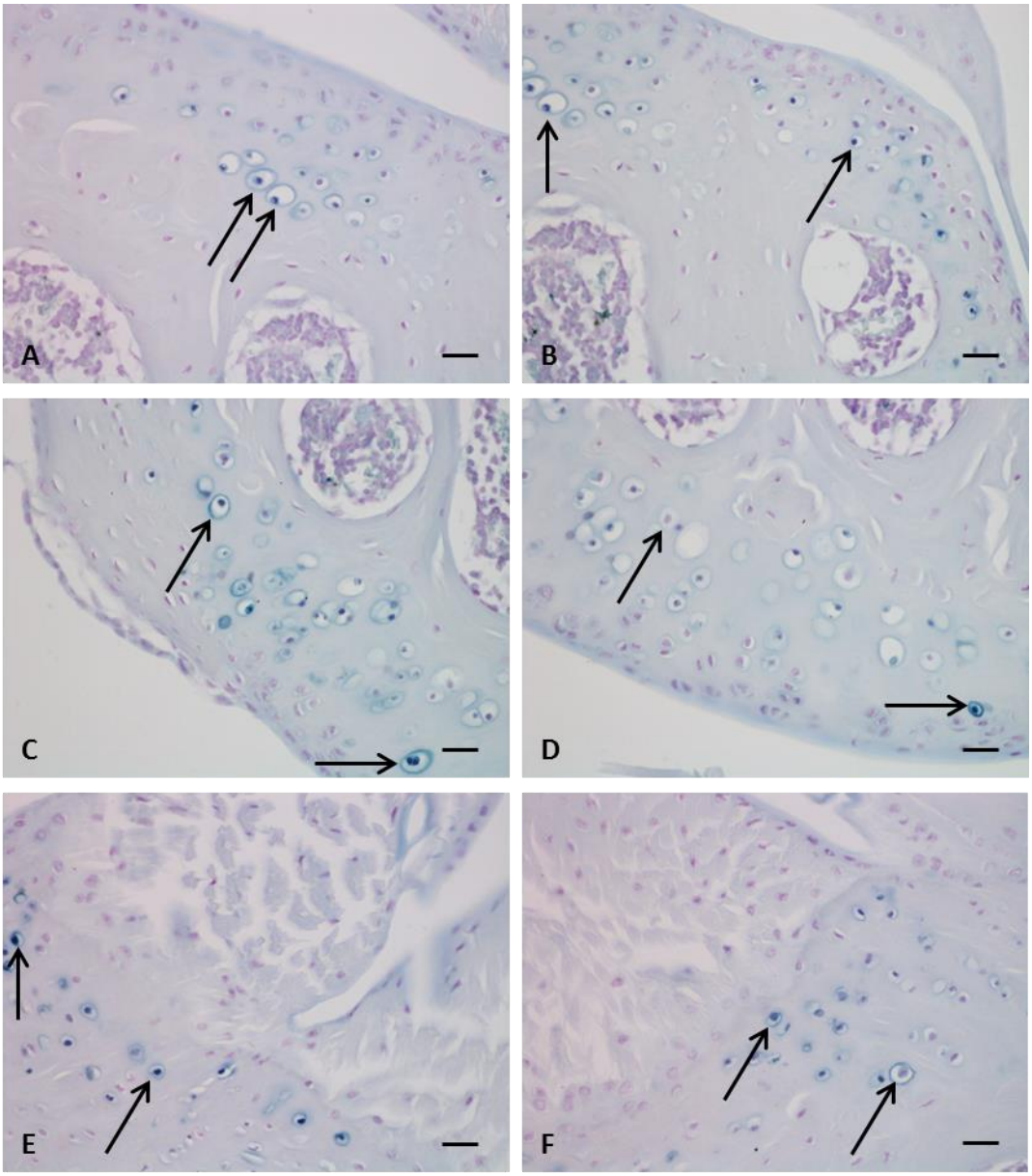

Figure 3.6 – Extensive ochronotic pigmentation in a 40.4 week old BALB/c Hgd-/- mouse. Schmorl's staining of BALB/c Hgd-/- 86.3 (♀) highlighted large numbers of pigmented chondrons in the MTP (**A** & **B**), the MFC (**C** & **D**) and the intercondylar area of the tibia (**E** & **F**). Hypertrophic pyknotic chondrons were distributed throughout the MTP (**A** & **B**, arrowed). A binucleated pyknotic chondron (**C**, right arrow) was present in the MFC as were peri-pigmented and fully pyknotic chondrons (**D**, arrowed). Significant amounts of pigmented chondrons were also present (**E** & **F**, arrowed), for the first time, in the intercondylar area of the tibia. All sections stained with Schmorl's. Bar = 20µm.

BALB/c Hgd-/- 86.3 (♀) (40.4 weeks) represented a significant milestone in the natural history study of the Hgd-/- mice as it was the first mouse to show large scale pigmentation across the whole tibio-femoral joint, as well as a new site of pigmentation; the insertion of the ACL and PCL into the MTP (intercondylar area). Some hypertrophic chondrons showed only pericellular pigmentation (Fig. 3.6 (**D**), left arrow), in areas which were occupied largely with heavily pigmented chondrons. A single binucleated cell was situated in the MFC (Fig. 3.6 (**C**), right arrow), a feature previously unseen until now. Pigmentation was observed for the first time at the intercondylar area of the MTP. There were large numbers of pigmented chondrons located at this site, which is an area of considerable stress in the tibio-femoral joint.

3.3.1.7 BALB/c Hgd-/- 55.1 (♂) – 47.4 weeks

BALB/c Hgd-/- 55.1 (♂) showed widespread pigmentation throughout the tibio-femoral joint. Pigmentation was also located, for the first time, in the fibrocartilaginous entheses of the femoral condyles. Again, like previous mice, there was a mix of unpigmented, peri-pigmented and fully pigmented chondrons in close proximity to one another. There was also pigmentation in the intercondylar area of the tibia (Fig. 3.7).

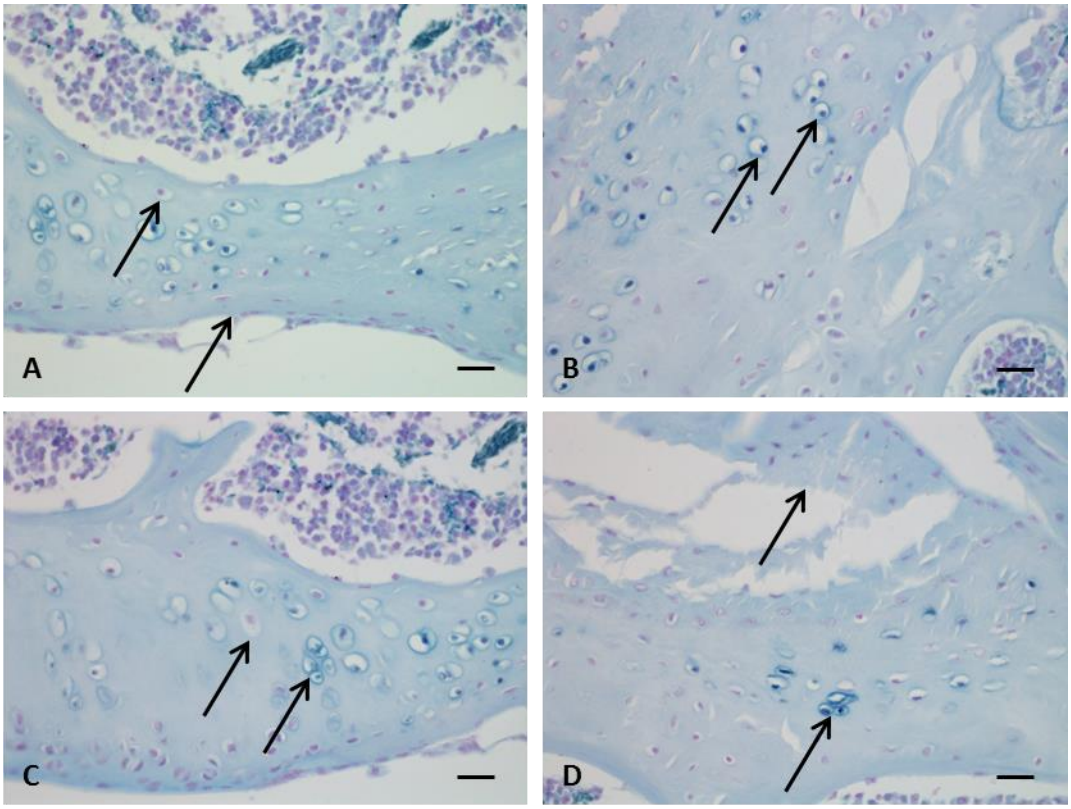

Figure 3.7 – Extensive ochronotic pigmentation in a 47.4 week old BALB/c Hgd-/- mouse. Peri-pigmented chondrons (**A** & **C**, left arrow) were present in areas heavily populated by pyknotic chondrons. Slight fibrillations on the articular surface of the MFC could be seen (**A**, right arrow). Large numbers of pigmented pyknotic chondrons were present in the fibrocartilaginous entheses of both femoral condyles (MFC shown) (**B**, arrowed). The intercondylar area contained pigmented chondrons in small numbers (**D**, right arrow). All sections stained with Schmorl's. Bar = 20µm.

3.3.1.8 BALB/c Hgd-/- 54.3 (♀) – 49.6 weeks

BALB/c Hgd-/- 54.3 (♀) (49.6 weeks) was heavily pigmented throughout the tibio-femoral joint. Ochronotic chondrons were located in all areas of the joint with areas of high stress particularly pigmented. Severe degradation and damage to the cartilage was observed, for the first time in the Hgd-/- mice. The MTP showed complete loss of the articular surface while there was erosion of the HAC and the

presence of vertical clefts extending from the HAC to ACC. Near complete loss of the articular surface on the MFC was also observed. Chondrons in differing stages of pigmentation were visible in close proximity to one another throughout ACC (Fig. 3.8). Large numbers of pigmented chondrons were located at the intercondylar area of the TP (Fig 3.9).

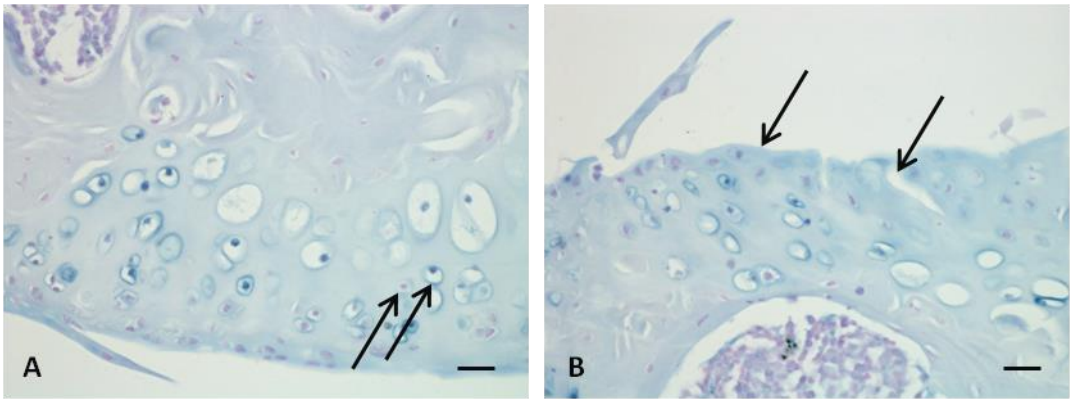

Figure 3.8 – Hyaline articular cartilage damage and degradation in a 49.6 week old BALB/c Hgd-/- mouse. A peri-pigmented and a heavily pigmented chondron were located only microns apart from each other in the MFC (**A**, arrowed). Complete loss of the articular surface (**B**, left arrow), and the presence of a vertical cleft running through the MTP (**B**, right arrow) illustrated the severity of OA in the mouse. All sections stained with Schmorl's. Bar = 20µm.

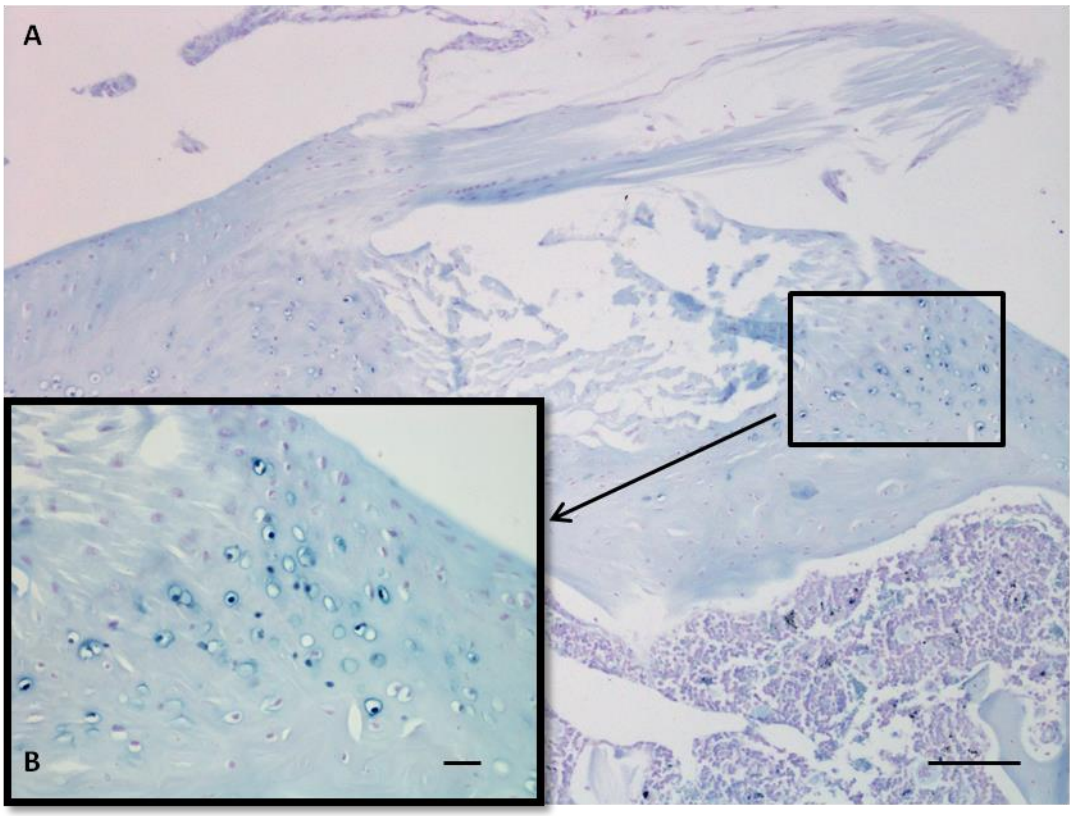

Figure 3.9 – Large numbers of pigmented chondrons located at the insertion of ligaments into the tibial plateau of a 49.6 week old BALB/c Hgd-/- mouse. An overview of the TP (**A**) showed a significant amount of pigmentation running across the area of ACL and PCL insertion into the TP. Bar = 100µm. Inset: (**B**) Large numbers of pigmented chondrons were located at the insertion site of the ligament(s). Section stained with Schmorl's. Bar = 20µm.

3.3.1.9 BALB/c Hgd-/- 61.3 (♀), 61.4 (♀) – 60 weeks

BALB/c Hgd-/- 61.3 (♀), and 61.4 (♀) (60 weeks) were both heavily pigmented (Figs. 3.18 & 3.19). The number of pigmented chondrons was significantly higher than that seen in BALB/c 54.3 Hgd-/- (♀, 49.6 weeks) (Fig. 3.18). Ochronotic pigmentation was widespread in all areas of the tibio-femoral joint including the fibrocartilaginous entheses of the femoral condyles and the intercondylar area of the femur and tibia.

Both mice had osteophytes present on the medial side of the femur and tibia which were heavily pigmented. A single heavily pigmented chondron was observed in the tibial growth plate of both BALB/c Hgd-/- 61.3 (♀) and BALB/c 61.4 (♀), this was something which had not been previously seen in any of the Hgd-/- mice (Figs. 3.10 & 3.11).

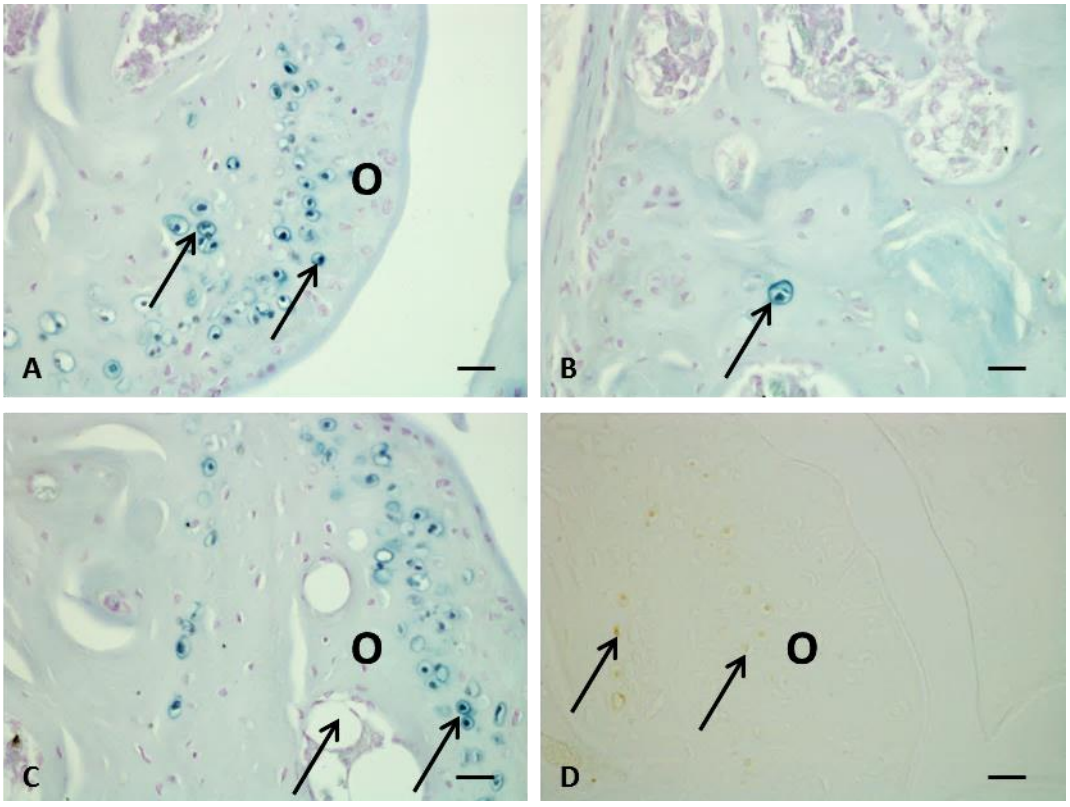

Figure 3.10 – Osteophyte formation and growth plate pigmentation in a 60 week old BALB/c Hgd-/- mouse. A heavily pigmented osteophyte was located on the MFC (**A**, right arrow). Heavily pigmented isogenous groups of chondrons were present close to the formation of the osteophyte (**O**) (**A**, left arrow). A single pigmented pyknotic chondron was present in the tibial growth plate (**B**, arrowed). A heavily pigmented osteophyte was also located on the MTP (**C**, right arrow), surrounded by empty marrow space (**C**, left arrow). An unstained serial section of the MTP shows ochre coloured chondrons (**D**, arrowed). All images taken from BALB/c Hgd-/- 61.3 (♀). **A**, **B** & **C** stained with Schmorl's, **D** unstained. Bar = 20μm.

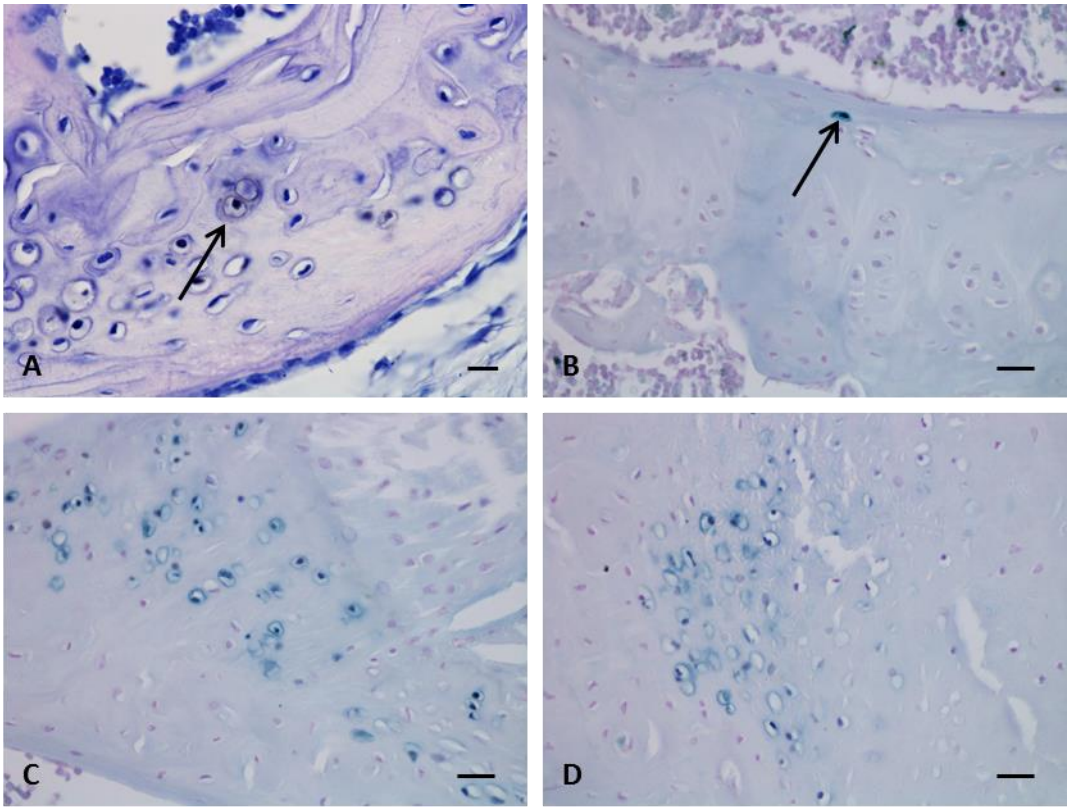

Figure 3.11 – Joint pathology in a 60 week old BALB/c Hgd-/- mouse. Staining with H&E showed the presence of an ochre coloured chondron close to the SCB interface in the LFC (**A**, arrowed). Bar = 10µm. A single pigmented chondron was present in the growth plate of the tibia (**B**, arrowed). Large numbers of pigmented chondrons were present in (**C**) the intercondylar area of the TP and (**D**) the fibrocartilaginous enthesis of the MFC. All images taken from BALB/c Hgd-/- 61.4 (♀). **B**, **C** & **D** stained with Schmorl's. Bar = 20 µm.

Both mice exhibited extensive pigmentation throughout the tibio-femoral joint and showed significant signs of OA including osteophyte formation, tidemark duplication, fibrillations of the articular surface and large amounts of hypertrophic chondrons in the ACC. The pathology identified in both mice was consistent with the progression of ochronosis in humans.

3.3.1.10 BALB/c Hgd-/- 59.2 (♀), 59.3 (♀) – 61.3 weeks

BALB/c Hgd-/- 59.2 (♀) and BALB/c 59.3 (♀) (61.3 weeks) both contained large amounts of pigmentation with the former containing the highest amount of pigmented chondrons observed in the study (Fig. 3.18). Osteophyte formation, degradation of cartilage and tidemark duplication was observed in both mice (Fig. 3.12) which was consistent with previous data. Large numbers of pigmented chondrons were located in the intercondylar area of both the femur and tibia (Fig. 3.13).

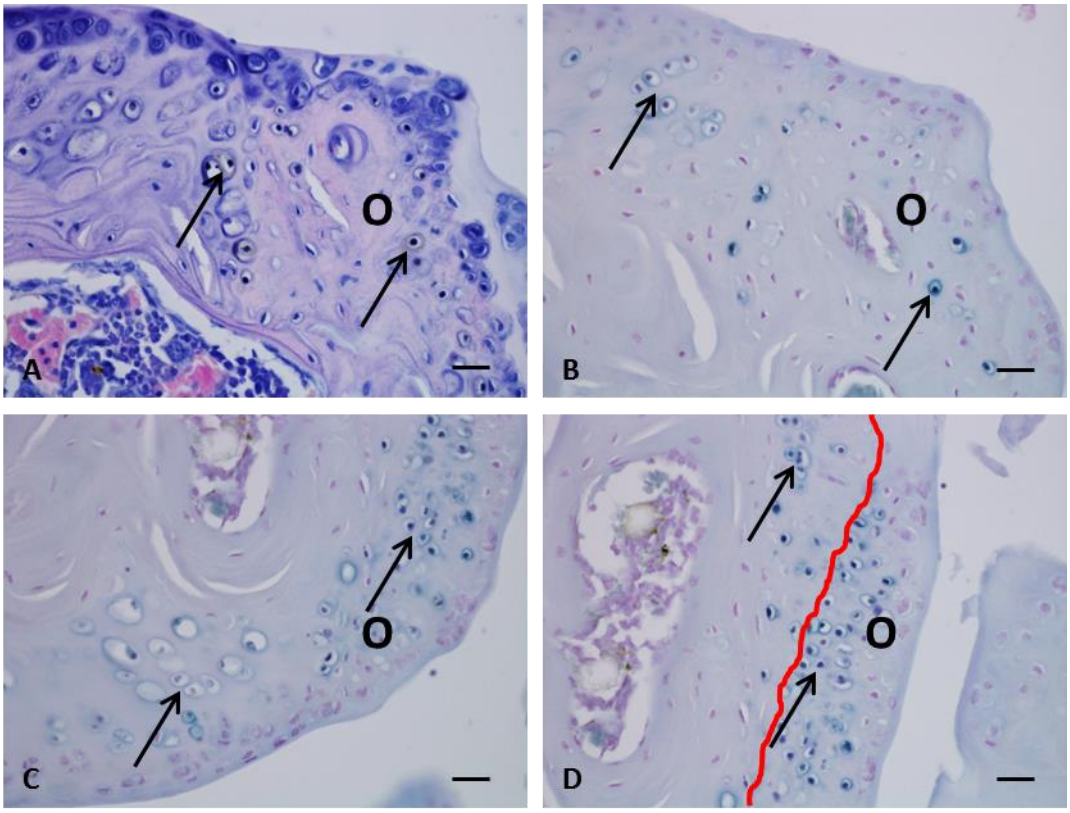

Figure 3.12 – Osteophyte formation and pigmentation in a 61.3 week old BALB/c Hgd-/- mouse. Staining with H&E displayed ochre coloured peri-cellular pigmentation in chondrons in the ACC, and in an osteophyte on the MTP (**A**, arrowed). A near serial section stained with Schmorl's showed isogenous groups of hypertrophic chondrons in the ACC (**B**, left arrow). Large groups of hypertrophic pyknotic chondrons (**C** & **D**, left arrow) and a heavily pigmented osteophyte (**C** & **D**, right arrow) were present on the MFC. All images taken from BALB/c Hgd-/- 59.2 (♀). **B**, **C** & **D** stained with Schmorl's. Bar = 20 µm.

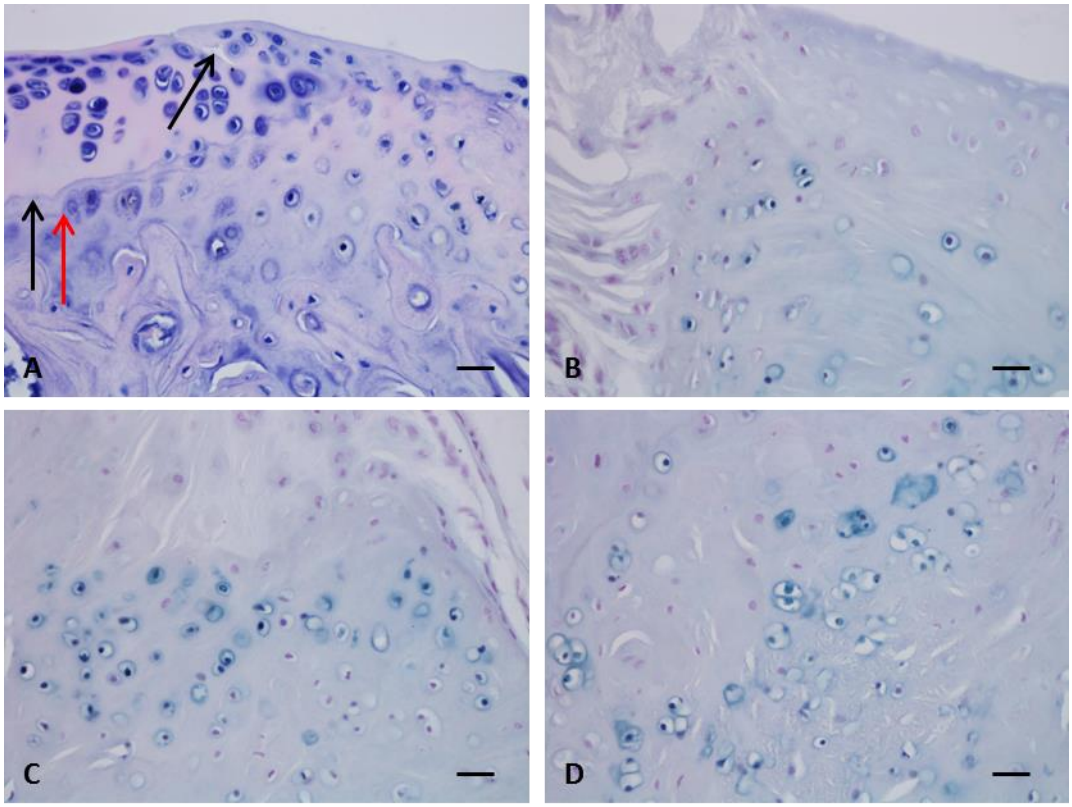

Figure 3.13 – Cartilage damage and areas of substantial pigmentation in a 61.3 week old BALB/c Hgd-/- mouse. Staining with H&E showed the presence of a cleft in HAC (**A**, right arrow) and duplicate tidemarks (**A**, red arrow) in the MTP. Areas of extensive pigmentation were seen in the intercondylar area of the MTP (**B**) and the fibrocartilaginous entheses of the femoral condyles (MFC shown) (**C** & **D**). All images taken from BALB/c Hgd-/- 59.2 (♀). **B**, **C** & **D** stained with Schmorl's. Bar = 20 µm.

3.3.1.11 BALB/c Hgd-/- 50.3 (♀) – 65.7 weeks

The final mouse analysed as part of the BALB/c Hgd-/- natural history study was BALB/c Hgd-/- 50.3 (♀). At 65.7 weeks of age, BALB/c 50.3 was over four weeks older than the previous set of mice examined. Large numbers of pigmented chondrons were observed throughout the joint (Figs. 3.14 & 3.15). However, small numbers of unpigmented and peri-pigmented chondrons were still present in close proximity to the pyknotic chondrons. Again, identical to that seen in younger mice, there were substantial numbers of pigmented chondrons in the intercondylar area

of the femur and tibia and in the fibrocartilaginous entheses of the femur. Three heavily pigmented pyknotic chondrons were located in the growth plate of the tibia, an occurrence which had only previous seen in BALB/c Hgd-/- 61.3 (♀) and 61.4 (♀), where they were also located in the tibial growth plate. Tidemark duplication could be seen in the femur and tibia while minor fibrillations of the articular surface were present on the lateral aspects of the joints (Fig. 3.16).

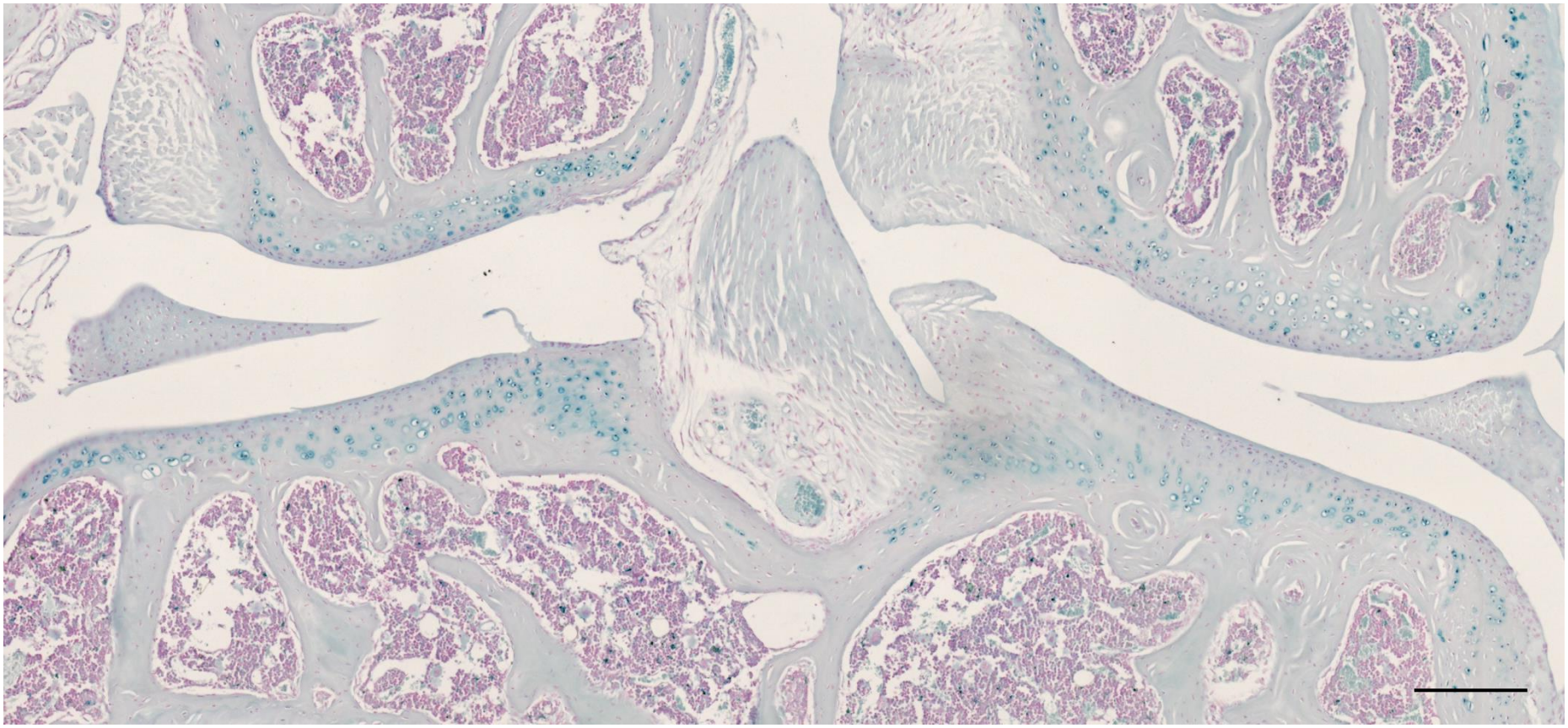

Figure 3.14 – Extensive ochronotic pigmentation in a 65.7 week old BALB/c Hgd-/- mouse. A panoramic image of BALB/c Hgd-/- 50.3 (♀) tibio-femoral joint showing the extent of pigmentation. The number of heavily pigmented pyknotic (blue) chondrons in contrast to normal unstained chondrons was substantial. Section stained with Schmorl's. Bar = 50 µm.

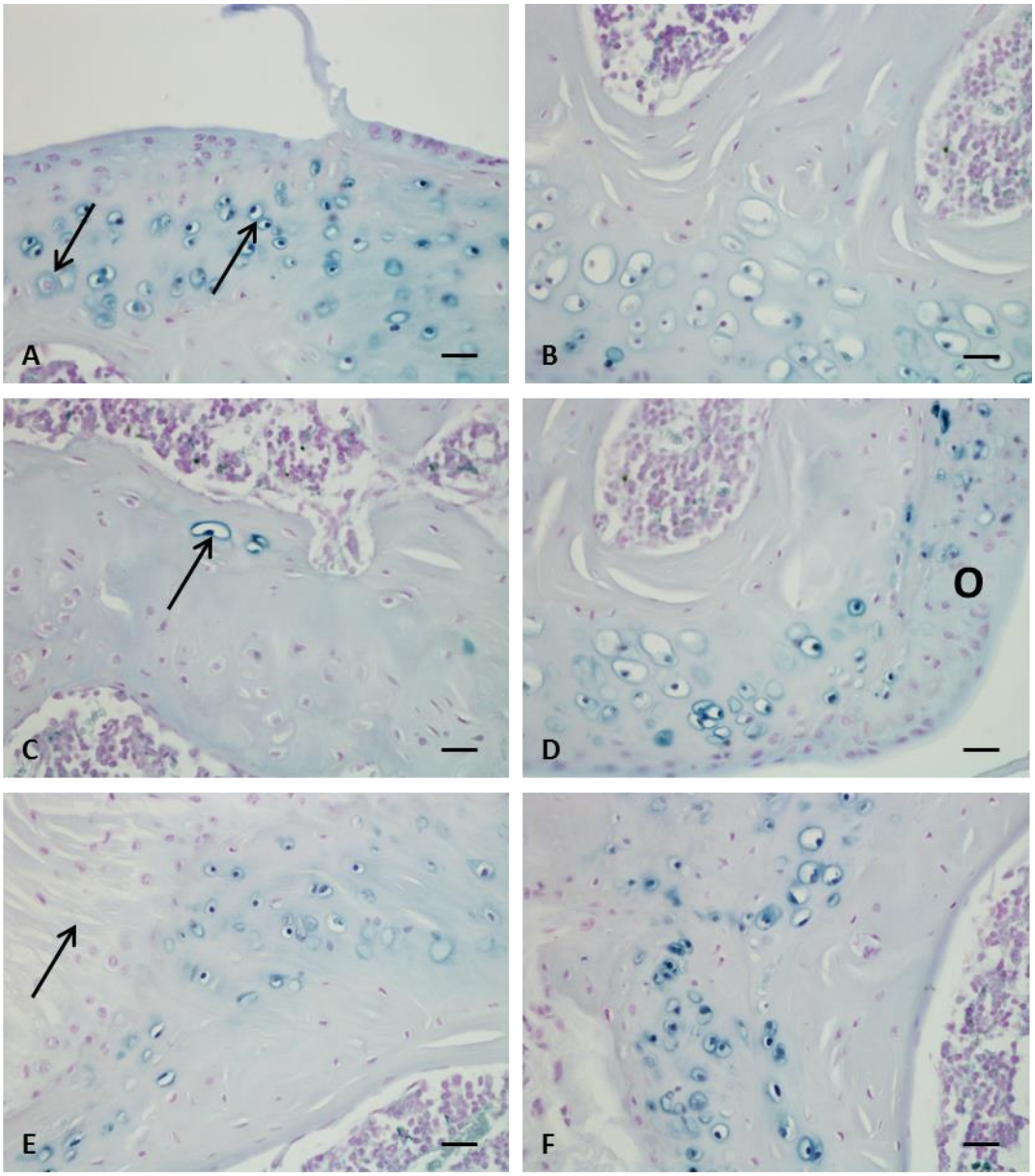

Figure 3.15 – Pathology of ochronosis in a 65.7 week old BALB/c Hgd-/- mouse. Different stages of chondron pigmentation, pericellular (**A**, left arrow) and pyknotic (**A**, right arrow), was seen in close proximity to each other in the LTP. Large numbers of hypertrophic chondrons (**B**) were located in the MFC. Three pyknotic chondrons were present in the tibial growth plate (**C**, arrowed), a rare event in AKU mice. Substantial numbers of pigmented chondrons were present at the intercondylar area of the tibia (ligamentous fibres arrowed) (**E**) and the fibrocartilaginous enthesis of the LFC (**F**). All sections stained with Schmorl's. Bar = 20 µm.

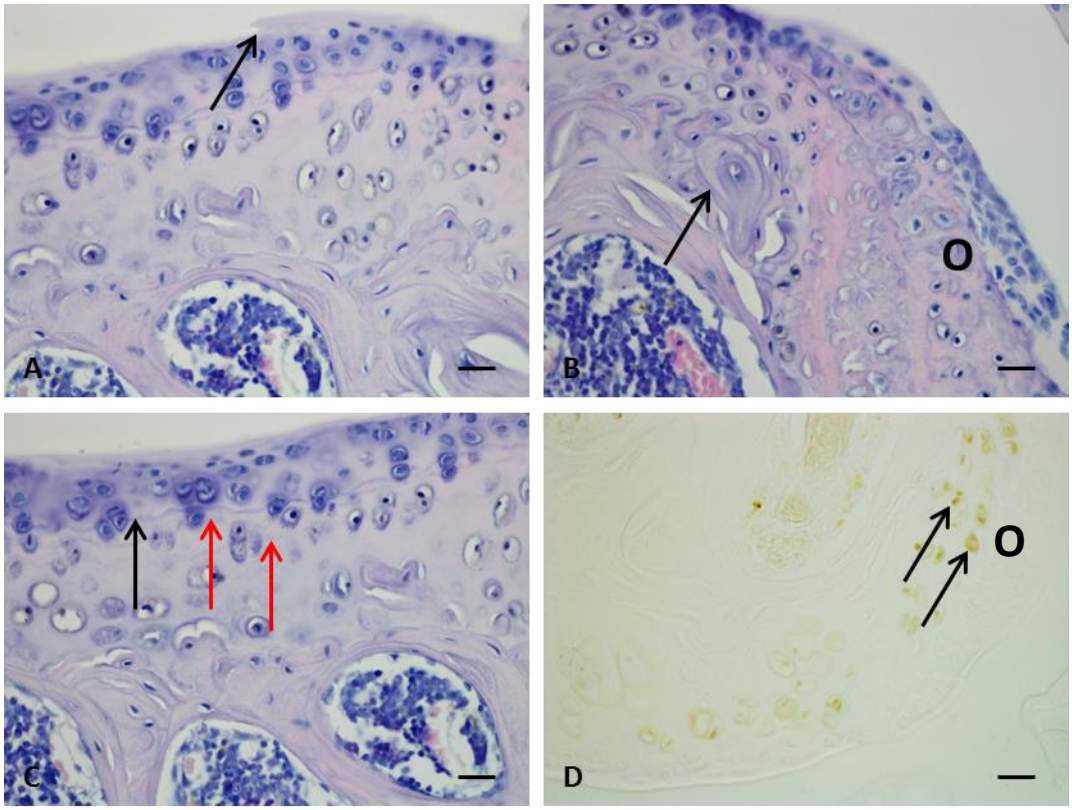

Figure 3.16 – Cartilage degradation in a 65.7 week old BALB/c Hgd-/- mouse. Minor fibrillations to the articular surface of the LTP were observed (**A**, arrowed). The articular surface had been lost in some places along the LTP, but was intact in other areas. A small osteophyte (**O**) appeared to be located on the MTP, as did small amounts of SCB remodelling (**B**, arrowed). Numerous duplicate tidemarks were seen throughout the joint; here three tidemarks can be seen in the LTP (**C**, arrowed, (red arrows indicate duplicate tidemarks)). An unstained section of the MFC highlighted the actual colour of ochronotic chondrons (**D**). A binucleated (**D**, left arrow) and a pyknotic (**D**, right arrow) chondron have been highlighted in the image. **A**, **B** & **C** stained with H&E, **D** unstained. Bar = 20 µm.

3.3.1.12 BALB/c WT (♂) – 21.7, 43.5 and 69.1 weeks

BALB/c WT mice were culled at three different time points and stained with Schmorl's stain to provide a control in the natural history study. All WT mice analysed showed no pigmentation of chondrons and no osteoarthritic changes as expected (Fig. 3.17).

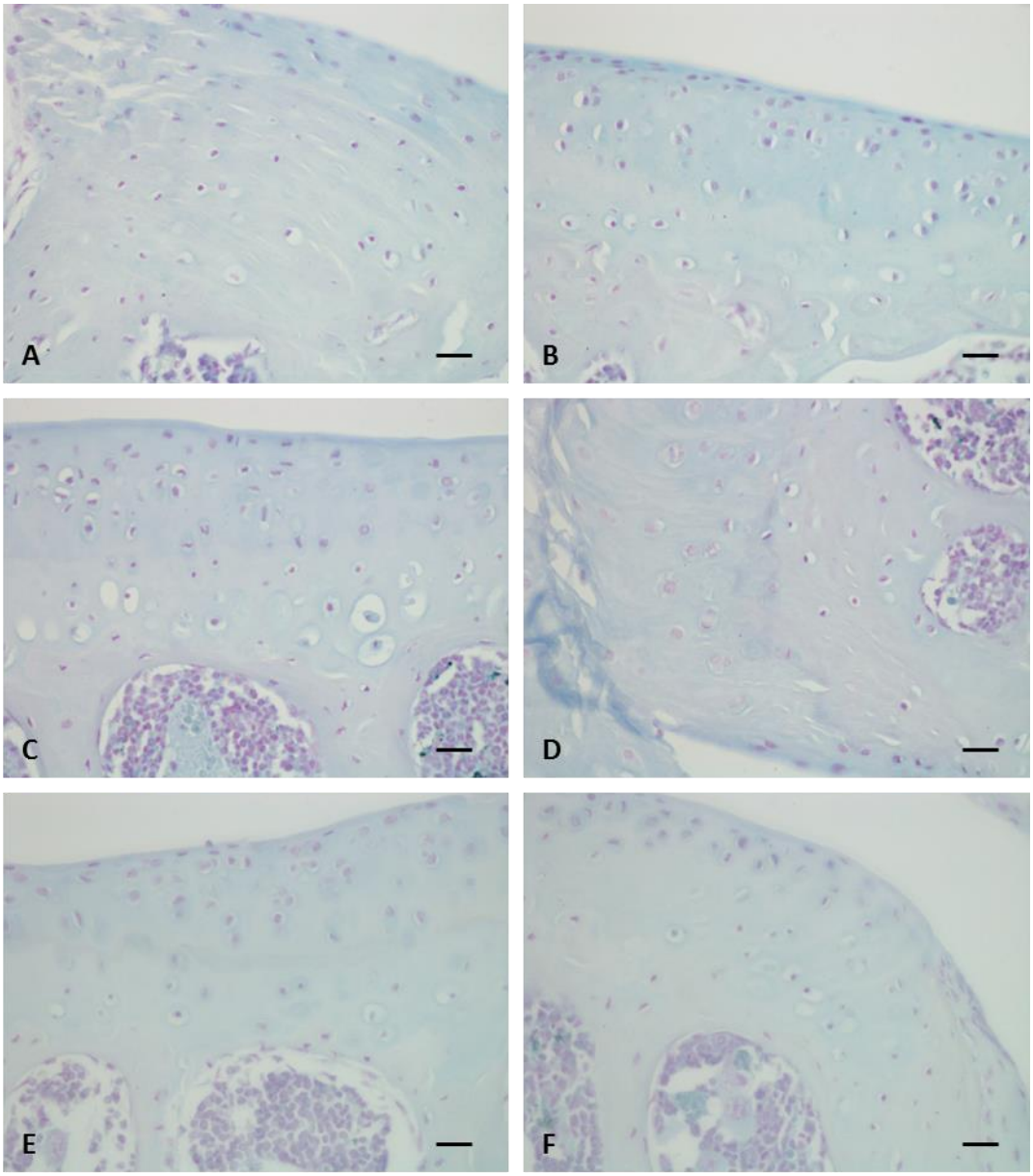

Figure 3.17 – Absence of ochronotic pigmentation in BALB/c wild type mice. Images of 21.7 week old (**A** & **B**), 43.5 week old (**C** & **D**) and 69.1 week old (**E** & **F**) BALB/c WT, all showed no ochronotic chondrons throughout the tibio-femoral joint. All sections stained with Schmorl's. Bar = 20 µm.

3.3.2 Quantification of pigmented chondrons in BALB/c Hgd-/- mice

The number of pigmented chondrons in each mouse involved in the natural history study was quantified. When the data was collated a clear pattern showing a progressive, linear increase in the amount of pigmentation with increasing age was observed (Fig. 3.18).

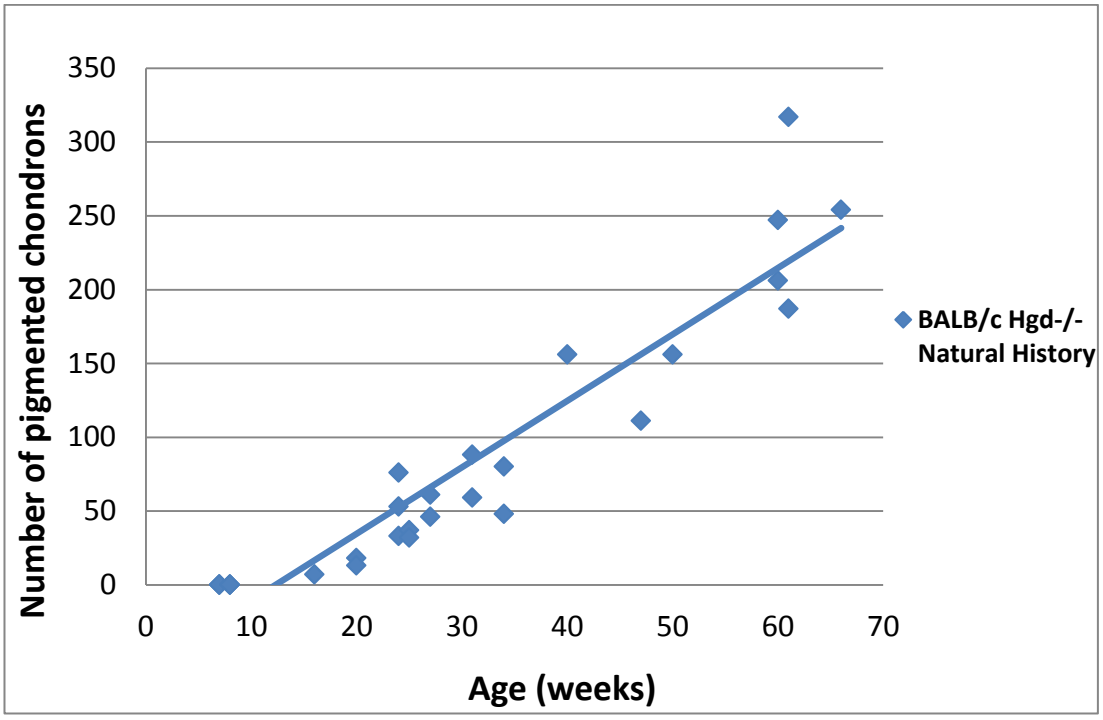

Figure 3.18 – The effect of age on the number of pigmented chondrons observed in BALB/c Hgd-/- mice. Scatter chart demonstrating the linear increase seen in the total number of pigmented chondrons with increasing age in BALB/c Hgd-/- mice. Quantification of pigmented chondrons was performed on a single section from each mouse; this does not represent the total cell number in each mouse.

3.3.2.1 Inter-observer variability in BALB/c Hgd-/- mice

Quantification of pigmented chondrons in BALB/c Hgd-/- mice was performed by a second individual to assess the reliability of the method for scoring pigmented chondrons.

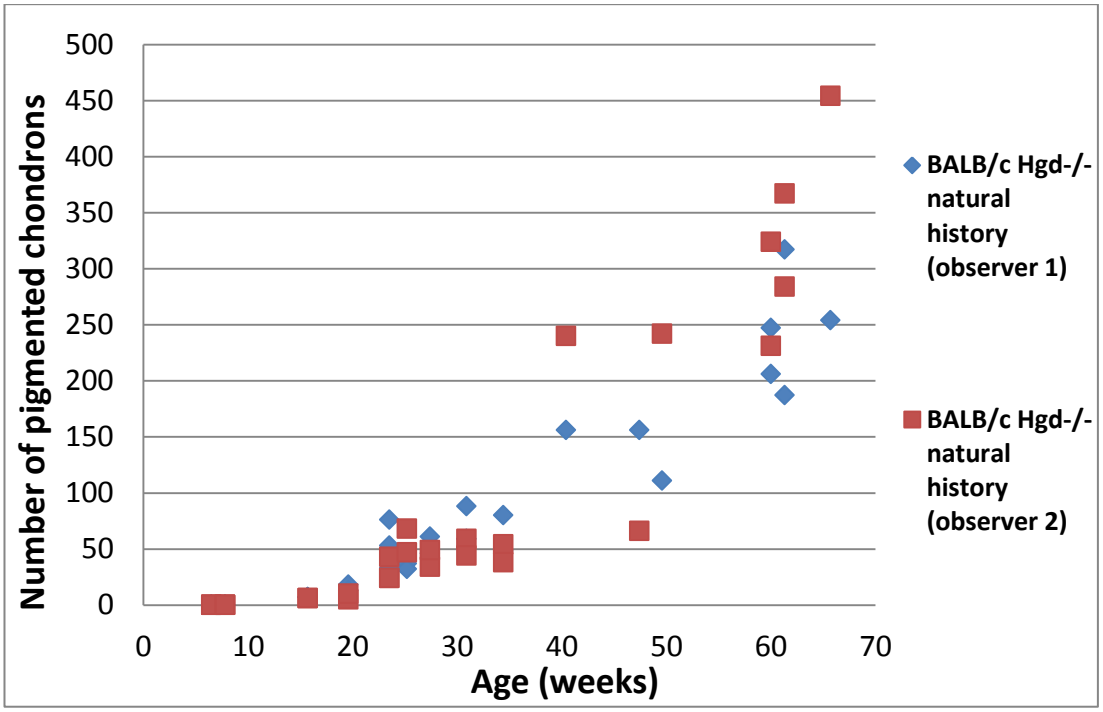

Figure 3.19 – Inter-observer variability in the number of pigmented chondrons in BALB/c Hgd-/- mice. Scatter chart demonstrating the variability in the number of pigmented chondrons in BALB/c Hgd-/- mice when counted by two different individuals.

To determine whether or not there was a significant difference between the two counts the intra-class correlation coefficient (ICC) was calculated to quantify the agreement between measurements. The ICC was 0.86 and was significantly different from 0 ($p<0.001$). The closer the ICC is to 1 signifies that the difference between paired measurements is small in comparison to the difference between subjects.

The pigmented chondron counts from the two individuals show that while inter-observer variability was seen the difference between the counts was not significant, indicating the method for scoring pigmented chondrons was reliable.

The data obtained from the natural history study showed BALB/c Hgd-/- mice developed ochronosis in their knee joints, which is one of the primary sites of ochronosis in AKU patients. The pathology seen in AKU mice was analogous with ochronosis in humans, starting with the initial pericellular pigmentation of chondrons. The observation of early ochronosis in BALB/c Hgd-/- mice was an important finding as it showed that AKU, though presenting in humans as a painful syndrome in mid-life, is the result of a lifelong pathological process. Furthermore, as AKU is associated with the onset of early OA, we can use the model to identify the initiating events in OA by studying the role of SCB and ACC as both play an important role in the pathology of AKU and OA.

3.3.3 Histological detection of ochronotic pigment in BL/6 Hgd-/- mice

HgdFah (Hgd+/-, Fah-/-) mice on a BL/6 background strain were crossed with WT BL/6 mice to yield Hgd-/-, Fah+/+ (AKU) mice on the BL/6 background. Once weaned, the mice were culled at different time points ranging from 6.1 to 46.5 weeks and their knee joints analysed histologically. The left knee was used for the experimental studies and was sectioned posterior to anterior in each animal.

3.3.3.1 BL/6 Hgd-/- 166.2 (♂), 166.3 (♂), 167.3 (♀), 167.4 (♀) – 6.1 weeks

The earliest time point analysed in BL/6 Hgd-/- mice was 6.1 weeks, which was slightly earlier than the first time point examined in BALB/c Hgd-/- mice. Schmorl's staining of the mice showed no pigmented chondrons throughout the tibio-femoral joints of all four mice. H&E staining showed no cartilage degradation or other signs of osteoarthritic nature (Fig. 3.20).

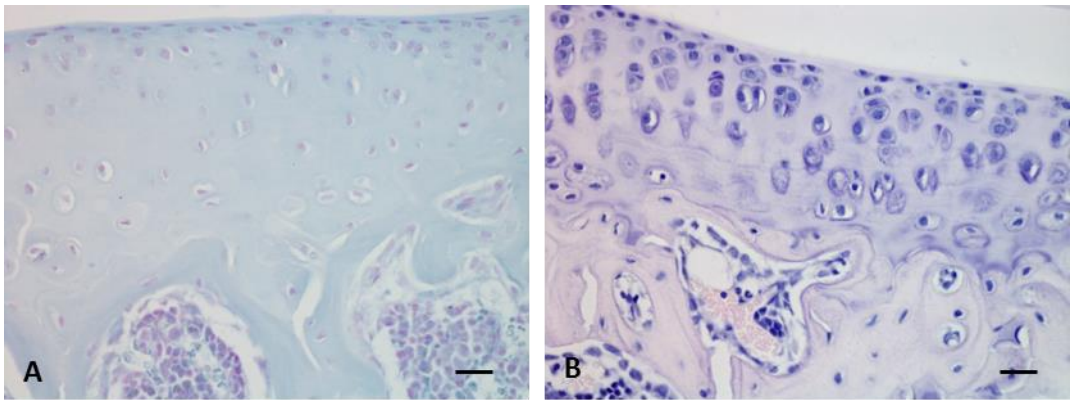

Figure 3.20 – Ochronotic pigment is not detectable in a 6.1 week old BL/6 Hgd-/- mouse. Schmorl's staining of the LTP showed no pigmentation of the cells or their surrounding matrices (**A**). H&E staining of the MTP indicated the cartilage was in excellent condition as no fibrillations or clefts in the articular surface were observed (**B**). Images taken from BL/6 Hgd-/- 167.4 (♀). Bar = 20 µm.

3.3.3.2 BL/6 Hgd-/- 161.1 (♂), 161.2 (♂), 162.1 (♀), 162.2 (♀) – 10.4 weeks

Of the four BL/6 mice analysed at 10.4 weeks of age, BL/6 Hgd-/- 162.2 (♀) displayed early signs of ochronosis. A very small number of pigmented chondrons were observed in the ACC of the LFC and in the intercondylar area of the TP (Fig. 3.21). A number of chondrons appeared heavily pigmented and pyknotic which is somewhat surprising as these chondrons are typically associated with late or end-stage ochronosis. The cartilage of all the mice looked healthy with no obvious damage to the articular surface.

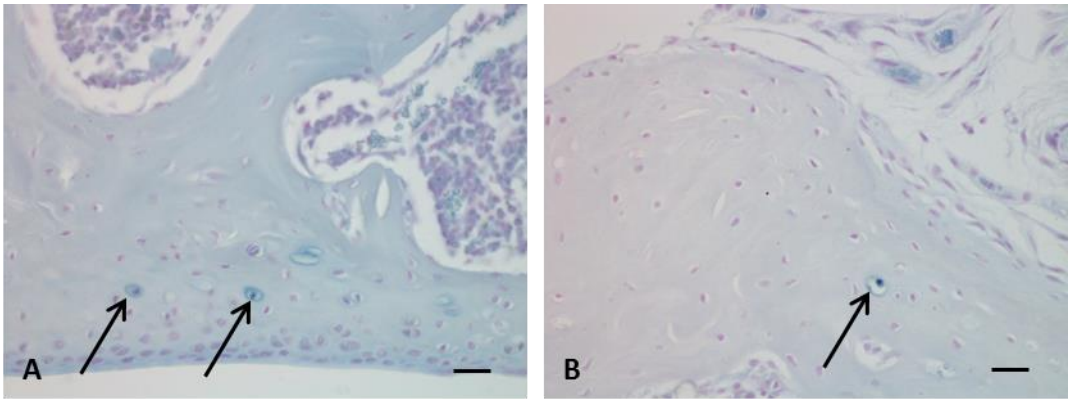

Figure 3.21 – Earliest identification of ochronotic chondrons in a 10.4 week old BL/6 Hgd-/- mice. Schmorl's staining of the LFC of BL/6 Hgd-/- 162.2 (♀) revealed two heavily pigmented pyknotic chondrons (**A**, arrowed). The chondrons were slightly hypertrophic as opposed to most chondrons surrounding them. A single pigmented chondron was located in the intercondylar area of the TP (**B**, arrowed). Bar = 20 μm.

The appearance of heavily pigmented chondrons in BL/6 Hgd-/- 162.2 (♀) marked the earliest identification of ochronotic chondrons in both BL/6 and BALB/c Hgd-/- strains of Hgd-/- mice. BL/6 Hgd-/- 98.4 (♂), 99.3 (♀) (16.1 weeks), which were the next mice in the study, showed comparable numbers of pigmented chondrons to the mice at 10.4 weeks (Fig. 3.40) therefore no images from them are shown.

3.3.3.3 BL/6 Hgd-/- 71.2 (♂), 72.1 (♀) – 27.8 weeks

The next two mice analysed, BL/6 Hgd-/- 71.2 (♂) and 72.1 (♀) (27.8 weeks), were 11 to 12 weeks older than the previous mice examined. As expected, from all the BALB/c and BL/6 Hgd-/- data seen so far, there was an increase in the number of pigmented chondrons located throughout the tibio-femoral joint (Fig. 3.40). The majority of pigmented chondrons, in both mice, were localised to the medial aspect of the joint and were heavily pigmented. All of the pigmented chondrons were hypertrophic, particularly the ones which were severely ochronotic. There was no obvious damage or degradation to the articular surface of the cartilage, however there was some duplication of the tidemarks in both the MFC and MTP (Fig. 3.22).

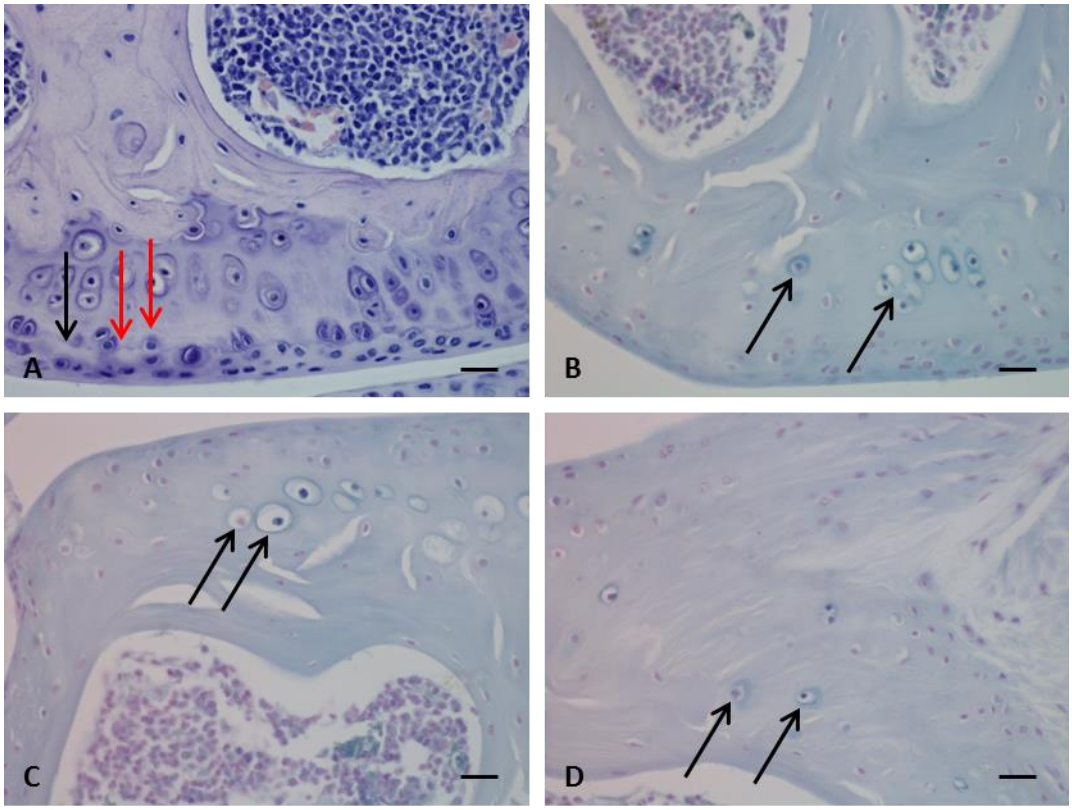

Figure 3.22 – Ochronosis and tidemark duplication in a 27.8 week old BL/6 Hgd-/- mouse. H&E staining of the MFC showed tidemark duplication at the mineralisation front (**A**, red arrows). An isogenous group of heavily pigmented chondrons (**B**, right arrow) was located in the MFC adjacent to a single pigmented, pyknotic chondron (**B**, left arrow). A peri-pigmented chondron (**C**, left arrow) neighbouring a heavily pigmented chondron (**C**, right arrow) was seen in the MTP. Small numbers of pigmented chondrons were located in the intercondylar area of the tibia (**D**, arrowed). All images are taken from the right knee of BL/6 Hgd-/- 72.1 (♀). **B**, **C** & **D** stained with Schmorl's. Bar = 20 µm.

3.3.3.4 BL/6 Hgd-/- 101.3 (♂), 102.3 (♀) – 29.1 weeks

BL/6 Hgd-/- 101.3 (♂) and 102.3 (♀) (29.1 weeks) both showed a large increase in the number of pigmented chondrons present in the tibio-femoral joint, compared to all previous BL/6 Hgd-/- mice (Fig. 3.40). Pigmented chondrons were localised to the ACC and intercondylar areas of the femur and tibia with the medial aspect of the joint containing the most, this was consistent with previous data. Again the

majority of the chondrons were heavily pigmented but there was a noticeable increase in the amount of peri-pigmented chondrons throughout the joint. There was one particular chondron present in BL/6 Hgd-/- 101.3 (♂) which showed intense peri-pigmentation and cellular pigmentation (Fig. 3.23 (**D**)). Staining such as this had not been observed in any of the BL/6 mice examined so far, and was rarely seen in the BALB/c natural history study. Tidemark duplication was observed throughout the joint, the most prominent example being present in the MFC of BL/6 Hgd-/- 101.3 (♂) (Fig. 3.23 (**A**)). The replication of the mineralisation front has been seen in the majority of mice in both strains, and always appears before any cartilage damage. There did appear to be some possible cartilage damage on the LTP of BL/6 Hgd-/- 101.3 (♂), identified by the large clustering of chondrons near the articular surface (Fig. 3.23 (**B**)). The quality of the articular surface appears to have been degraded with small lesions visible. The clustering of the chondrons may be a response to increased mechanical stimuli in the damaged area as an attempt to prevent further degradation of the cartilage.

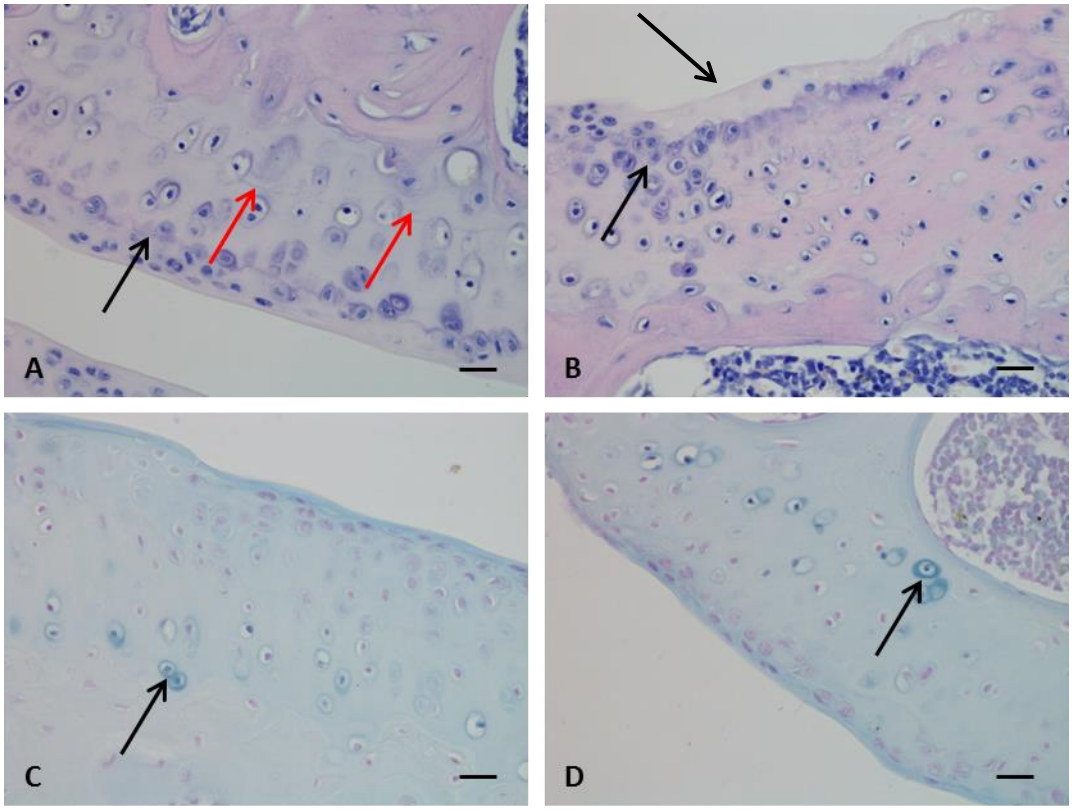

Figure 3.23 – Ochronosis and tidemark duplication in a 29.1 week old BL/6 Hgd-/- mouse. H&E staining of the MFC showed tidemark duplication at the mineralisation front (**A**, red arrows). Clusters of chondrons were present at the articular surface of the LTP (**B**, left arrow). There appeared to be some minor lesions in the cartilage where the clustering was located (B, right arrow). A range of chondrons in different stages of pigmentation were present in the LTP. Two chondrons showing end stage pigmentation have been highlighted (**C**, arrowed). A heavily pigmented chondron residing in the deep layer of the MFC, surrounded by unpigmented and peri-pigmented chondrons is highlighted (**D**, arrowed). **A** & **B** stained with H&E, **C** & **D** stained with Schmorl's. Bar = 20 µm.

It was interesting to note that the number of pigmented chondrons in the tibio-femoral joint of both BL/6 Hgd-/- 101.3 (♂) and 102.3 (♀) (29.1 weeks) was around three times as much as BL/6 Hgd-/- 71.2 (♂) and 72.1 (♀) (27.8 weeks) which were only 1.5 weeks younger (Fig. 3.40). This was a substantial increase for such a short space of time, and is close to 12 weeks earlier than similar numbers were observed

in the BALB/c Hgd-/- mice. These are interesting results as they suggest BL/6 Hgd-/- mice have an earlier onset of severe ochronosis in the tibio-femoral joint, while also suggesting there is a rapid change in the composition or organisation of the cartilage matrix allowing for increased deposition of ochronotic pigment in a short space of time.

3.3.3.5 BL/6 98.3 (♂), 99.4 (♀) – 31.7 weeks

BL/6 Hgd-/- 98.3 (♂) and 99.4 (♀) (31.7 weeks) contained high numbers of ochronotic chondrons, similar to those seen previously in BL/6 Hgd-/- mice aged 29.1 weeks. The pigmented chondrons were fairly evenly distributed throughout the femur and tibia, but like all mice examined the majority of pigmented chondrons were localised to the ACC. There was an increasing number of ochronotic chondrons situated at the intercondylar area of the tibia, an area of high stress where the ACL and PCL attach, but this was only a small proportion compared to the amount present in the ACC. Chondrons in all different stages of pigmentation were scattered throughout the joint. Non-pigmented chondrons were primarily located in the HAC, although small numbers were also present in the ACC. Peri-pigmented and fully pyknotic chondrons were distributed throughout the ACC; pyknotic chondrons were present in higher numbers than peri-pigmented chondrons. Staining of the PCM was visible in an H&E section of the MFC in BL/6 Hgd-/- 99.4 (♀) (Fig. 3.24 (**C**)), suggesting there were large deposits of ochronotic pigment in the matrix of this particular chondron as Schmorl's stain was not required to identify it. There also appeared to be subchondral sclerosis in the LFC of BL/6 Hgd-/- 99.4 (♀) and vascularisation of the ACC (Fig 3.24 (**A**)). This is strikingly similar to BALB/c Hgd-/- 92.2 (♂) which showed subchondral sclerosis and projection of the bone into ACC at 30.9 weeks of age. There is evidence that advancement of the tidemark and the resultant vascularisation of the ACC are associated with OA in humans [97].

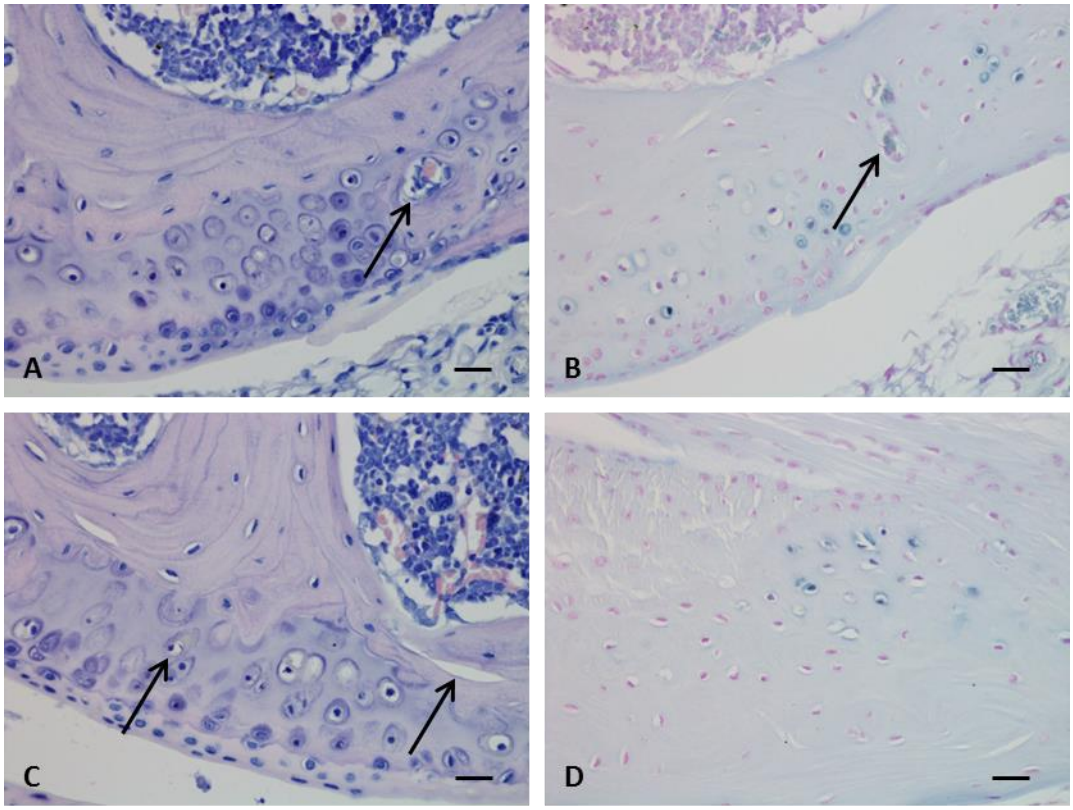

Figure 3.24 – Vascularisation of the articular calcified cartilage in a 31.7 week old BL/6 Hgd-/- mouse. H&E staining of the LFC of BL/6 Hgd-/- 99.4 (♀) highlighted vascularisation of the ACC (**A**, arrowed). A near serial section of the LFC stained with Schmorl's shows the vascularised area surrounded by pigmented chondrons (**B**, arrowed). An area of the MFC which appeared to show resorption of the SCB (**C**, right arrow) and the presence of ochronotic pigment in the PCM of a pyknotic chondron (**C**, left arrow). Schmorl's staining of the intercondylar area of the tibia showed pigmented chondrons present (**D**). All images taken from BL/6 Hgd-/- 99.4 (♀). **A** & **C** stained with H&E, **B** & **D** stained with Schmorl's. Bar = 20 µm.

3.3.3.6 BL/6 Hgd-/- 94.1 (♂), 95.1 (♀) – 37.8 weeks

Pigmentation in both BL/6 Hgd-/- 94.1 (♂) and 95.1 (♀) (37.8 weeks) was at a level relatively comparable to the previous two ages examined in the BL/6 study (Fig. 3.40). BL/6 Hgd-/- 95.1 showed a slight increase in the total amount of pigmented chondrons throughout the tibio-femoral joint while BL/6 Hgd-/- 94.1 showed a very small decrease. Most of the pigmented chondrons in the mice were heavily ochronotic and hypertrophic (Fig. 3.25 (**C** & **D**)). A single pigmented chondron in the deep zone of the ACC displayed interesting properties as it appeared some of the cellular components were pigmented while the nucleus remained unpigmented (Fig. 3.25 (**B**)). This is interesting as it appears to shows the nucleus of the cell is the last region to pigment. Several signs of OA were evident in the mice in the form of ACC vascularisation (Fig 3.25 (**A**)), tidemark duplication (Fig 3.25 (**B**)), SCB remodelling and resorption (Fig. 3.25 (**C**)) as well as initial osteophyte formation (not shown). No damage to the surface of the cartilage was apparent suggesting that the initiation of OA may begin at the SCB/ACC interface and progress up through the cartilage just as ochronosis does in both mice and humans.

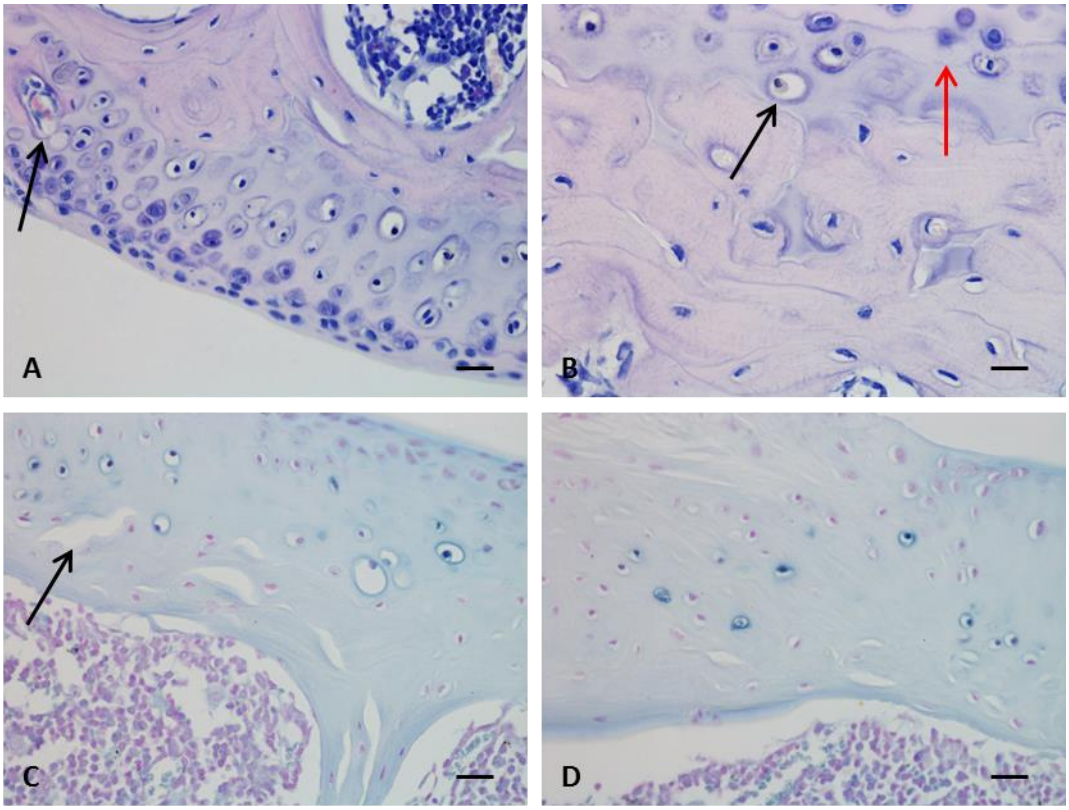

Figure 3.25 – Vascularisation of the articular calcified cartilage and subchondral bone remodelling and resorption in a 37.8 week old BL/6 Hgd-/- mouse. H&E staining of the MFC of BL/6 Hgd-/- 95.1 (♀) showed vascularisation of the ACC (**A**, arrowed). A single pyknotic chondron, in the deep zone of ACC in the MTP, displayed pigmentation of some cellular compartments but not the nucleus (**B**, left arrow). Tidemark duplication was also present in the MTP (**B**, red arrow) (Bar = 10 µm). Schmorl's staining showed pigmented chondrons located at areas of subchondral remodelling and resorption in the MTP (**C**, arrowed). Numerous pigmented chondrons were located at the intercondylar area of the TP (**D**), which is consistent with both BL/6 and BALB/c Hgd-/- mice of increasing age. **A** & **B** stained with H&E, **C** & **D** stained with Schmorl's. Bar = 20 µm.

3.3.3.7 BL/6 Hgd-/- 82.1 (♂), 83.1 (♀) – 41.3 weeks

The number of pigmented chondrons in BL/6 Hgd-/- 82.1 (♂) and 83.1 (♀) (41.3 weeks) was similar to the previous four to six BL/6 mice examined (Fig. 3.40). There was an increased number of pigmented chondrons located at the intercondylar area of the femur and tibia (Fig. 3.26 (**D**)). Non-pigmented chondrons were distributed sparsely throughout the joint signifying how advanced and severe ochronosis in the mice had become. There was some interesting osteoarthritic pathology observed in BL/6 Hgd-/- 82.1 (♂), most noticeably the formation of a meniscal ossicle in the LM (Fig. 3.26 (**A**)). Meniscal ossification is common in mice but very rare in humans [127, 128]. Although it is seen in mice that develop OA, the formation of meniscal ossicle's is a normal phenomenon associated with ageing. Subchondral remodelling was observed across the tibio-femoral joint of both mice. The MTP was the most extensively remodelled area (Fig. 3.26 (**B**)) which may relate to it having the greatest mechanical stresses in the knee joint. Tidemark duplication was located in the articular cartilages of both mice but was most prominent in the MTP.

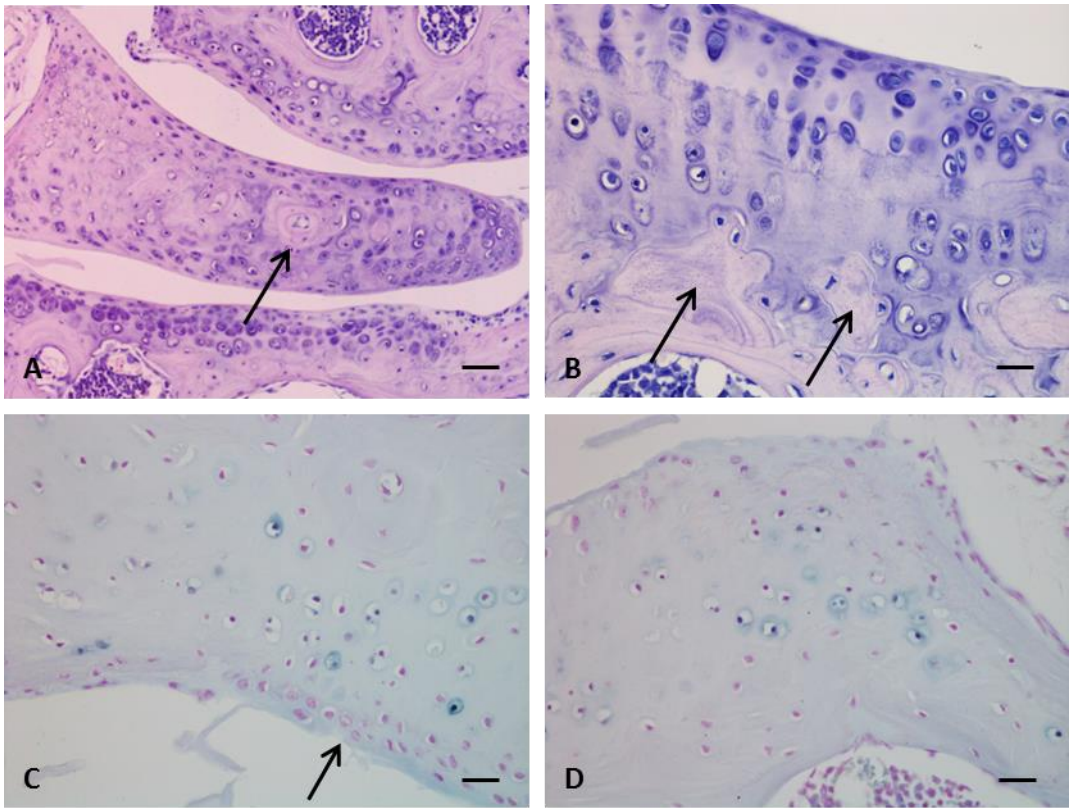

Figure 3.26 – Meniscal ossification, subchondral bone remodelling and ochronosis in a 41.3 week old BL/6 Hgd-/- mouse. H&E staining of the LM of BL/6 Hgd-/- 82.1 (♂) showed formation of cortical bone in the centre of the meniscus surrounded by cartilage (**A**, arrowed). This feature is known as meniscal ossification. Subchondral remodelling and the subsequent deposition of new bone were present in the MTP of BL/6 Hgd-/- 82.1 (**B**, arrowed). Minor fibrillations on the articular surface of the MFC were observed (**C**, arrowed). An increase in the number of pigmented chondrons at the intercondylar area of the tibia was also identified (**D**). All images taken from BL/6 82.1 (♂). **A** & **B** stained with H&E, **C** & **D** stained with Schmorl's. Bar = 20 µm.

3.3.3.8 BL/6 Hgd-/- 66.3 (♀), 67.1 (♂) – 46.5 weeks

BL/6 Hgd-/- 66.3 (♀) displayed a particularly large increase in the number of pigmented chondrons present throughout its tibio-femoral joint compared previous BL/6 mice (Fig. 3.40). BL/6 Hgd-/- 67.1 (♂) showed numbers of pigmented chondrons comparable with the previous four to six BL/6 Hgd-/- mice analysed. The detection of pigmented chondrons in the entheses of the femur (Fig. 3.27 (**D**)), while being the first time seen in BL/6 Hgd-/- mice, was routinely seen in BALB/c Hgd-/- mice of similar ages. BL/6 Hgd-/- 66.3 (♀) showed significant amounts of bone remodelling in the MTP, an area which had dense amounts of pigmentation present (Fig 3.27 (**B**)). Remodelling of SCB appeared in both the femur and tibia of both mice suggesting an osteoarthritic phenotype in the joints of the mice, although there was no obvious damage or degradation to the articular cartilage. H&E staining of the MFC of BL/6 Hgd-/- 66.3 (♀) showed a peri-pigmented chondron located at the boundary of the ACC and SCB (Fig. 3.27 (**A**), left arrow). Pigmentation in humans is believed to start at this boundary and progress up throughout the cartilage; the identification of peri-pigmented chondrons at the SCB/ACC interface in Hgd-/- mice indicates the process of pigmentation initiation and progression is very similar between the two species.

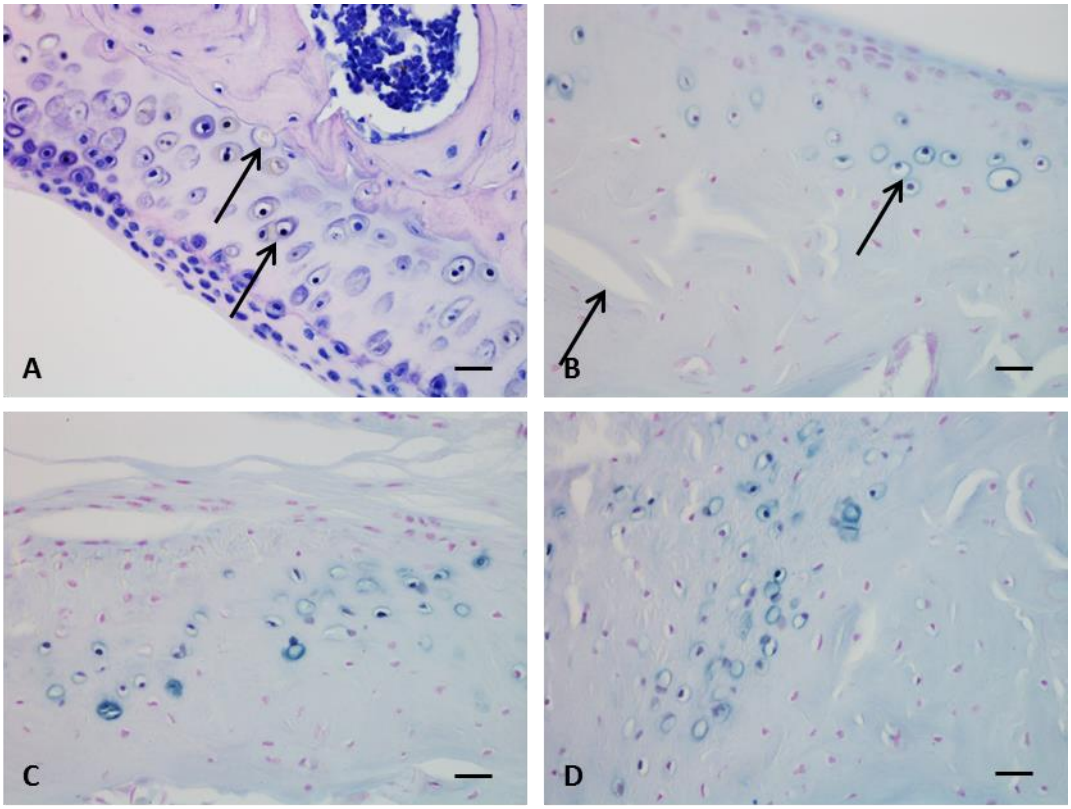

Figure 3.27 – Ochronosis and osteoarthritic pathology in a 46.5 week old BL/6 Hgd-/- mouse. H&E staining of the MFC of BL/6 Hgd-/- 66.3 (♀) depicted a pigmented chondron adjacent to the SCB (**A**, left arrow); the zone where it is thought pigmentation initiates. Two chondrons appeared to be separated by an area of pigmented PCM (**A**, right arrow). Ochronotic chondrons located in the MTP were heavily pigmented (**B**, right arrow). Large areas of SCB remodelling were also present in the MTP (**B**, left arrow). Significant numbers of pigmented chondrons were located at (**C**) the intercondylar area of the tibia and (**D**) the fibrocartilaginous entheses of the femur. All images taken from BL/6 82.1 (♀). **B**, **C** & **D** stained with Schmorl's. Bar = 20 µm.

3.3.3.9 BL/6 Hgd-/- 62.3 (♀) – 62.6 weeks

BL/6 Hgd-/- 62.3 (♀) was heavily pigmented throughout the tibio-femoral joint (Fig 3.28). Large numbers of pigmented chondrons were located in the entheses of the femur (Fig. 3.28 (**C**)) and the intercondylar area of the tibia (Fig. 3.28 (**D**)); both are areas which are known to be associated with high mechanical stress. Clusters of non-pigmented chondrons were located in the ACC (Fig. 3.28 (**A**)). The fact that these clusters were surrounded by groups of severely ochronotic chondrons is interesting and shows that although most of the cartilage has become ochronotic there are still some small areas which are unaffected. Angiogenesis and vascularisation of the ACC (Fig. 3.28 (**B**)) were observed in the MFC. Although fewer pigmented chondrons were present in the area of angiogenesis, that it did occur in the ACC, indicated the cartilage was osteoarthritic.

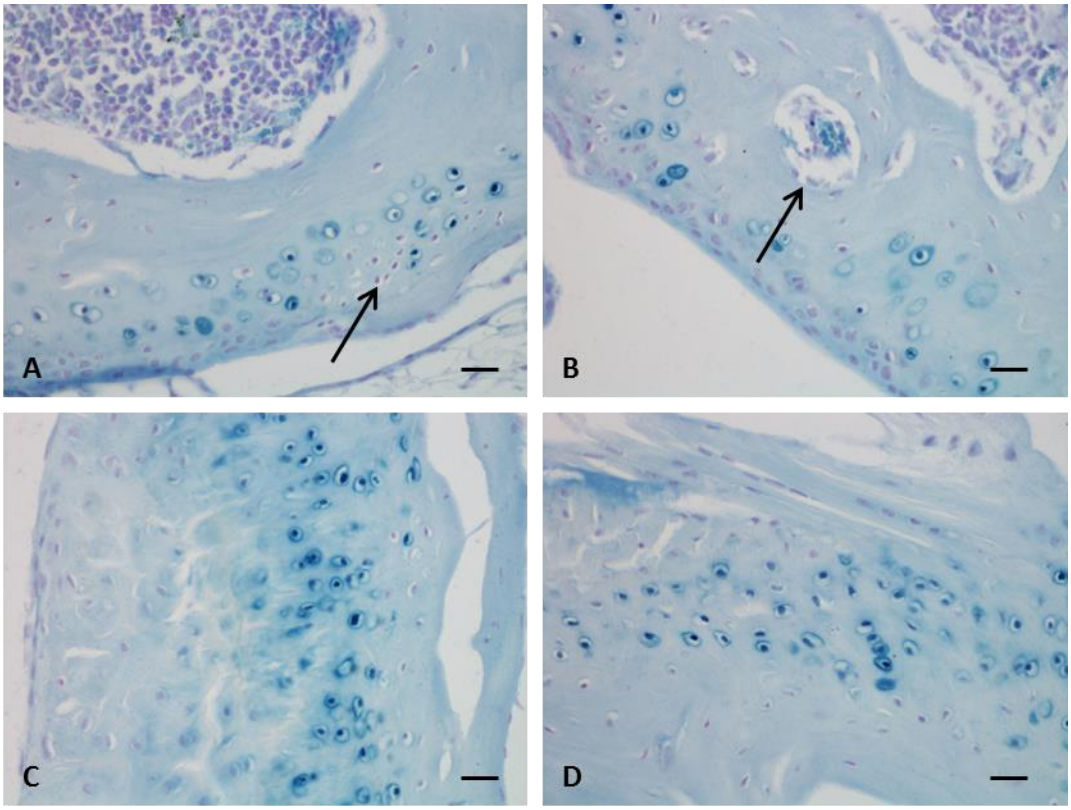

Figure 3.28 – Severe ochronosis and angiogenesis in a 62.6 week old BL/6 Hgd-/- mouse. A cluster of non-pigmented chondrons in the LFC surrounded by severely ochronotic chondrons (**A**, arrowed). Vascularisation of the MFC highlighted the OA changes in the joint of BL/6 Hgd-/- 62.3 (**B**, arrowed). Large numbers of heavily pigmented chondrons were located in (**C**) the fibrocartilaginous entheses of the femur (LFC shown) and (**D**) the intercondylar area of the tibia. All sections stained with Schmorl's. Bar = 20 µm.

Along with angiogenesis (Fig. 3.29 (**A**)), signs of SCB remodelling were present extensively throughout the tibio-femoral joint. In the MFC there were clear signs of bone formation and resorption in the SCB plate (Fig. 3.29 (**B**)), again indicating the joint was osteoarthritic.

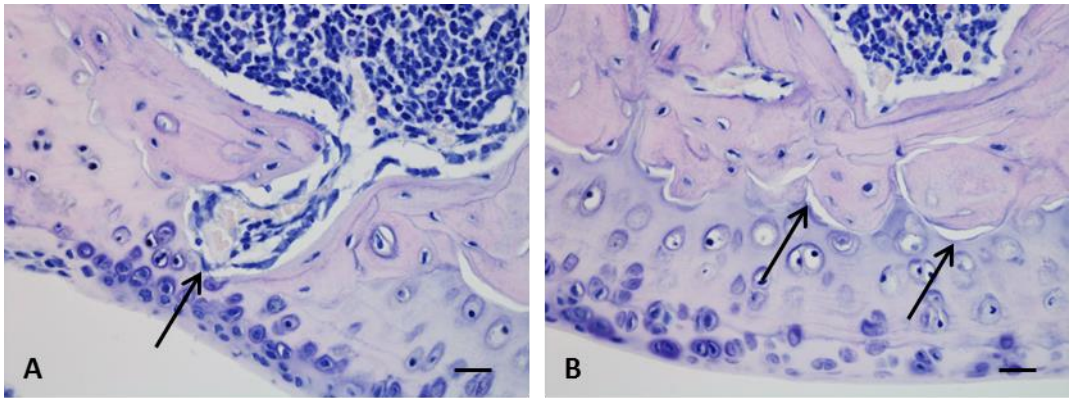

Figure 3.29 – Angiogenesis and subchondral bone remodelling in a 62.6 week old BL/6 Hgd-/- mouse. Angiogenesis in ACC of the MFC (**A**, arrowed); adjacent new areas of bone formation are present. SCB remodelling, shown in the MFC (**B**, arrowed), was present extensively throughout the knee joint. All sections taken from BL/6 Hgd-/- 62.3 and stained with H&E. Bar = 20 µm.

Cartilage damage was located on the LTP of BL/6 Hgd-/- 62.3. Large numbers of chondrocytes in the HAC appeared to be undergoing cellular division (Fig. 3.30, left arrows) in response to what looked like damage to the articular surface and the HAC. The articular surface was no longer attached to the LTP as evident by the lack of chondroblasts in the cartilage; only fully matured chondrons which were situated in the transitional and deep zones of the cartilage could be identified. Fibrocartilage was also located on the LTP (Fig. 3.30, right arrow) which suggested the HAC had been severely damaged, leading to scarring and attempted repair of the injured area. Fibrocartilage has completely different properties and structure to the HAC and its formation in the joint will have only exacerbated the osteoarthritic symptoms seen in the mouse. Meniscal ossification was observed in the LM of BL/6 Hgd-/- 62.3. Staining with Schmorl's stain showed the cartilage of the meniscus was heavily pigmented (Fig. 3.31).

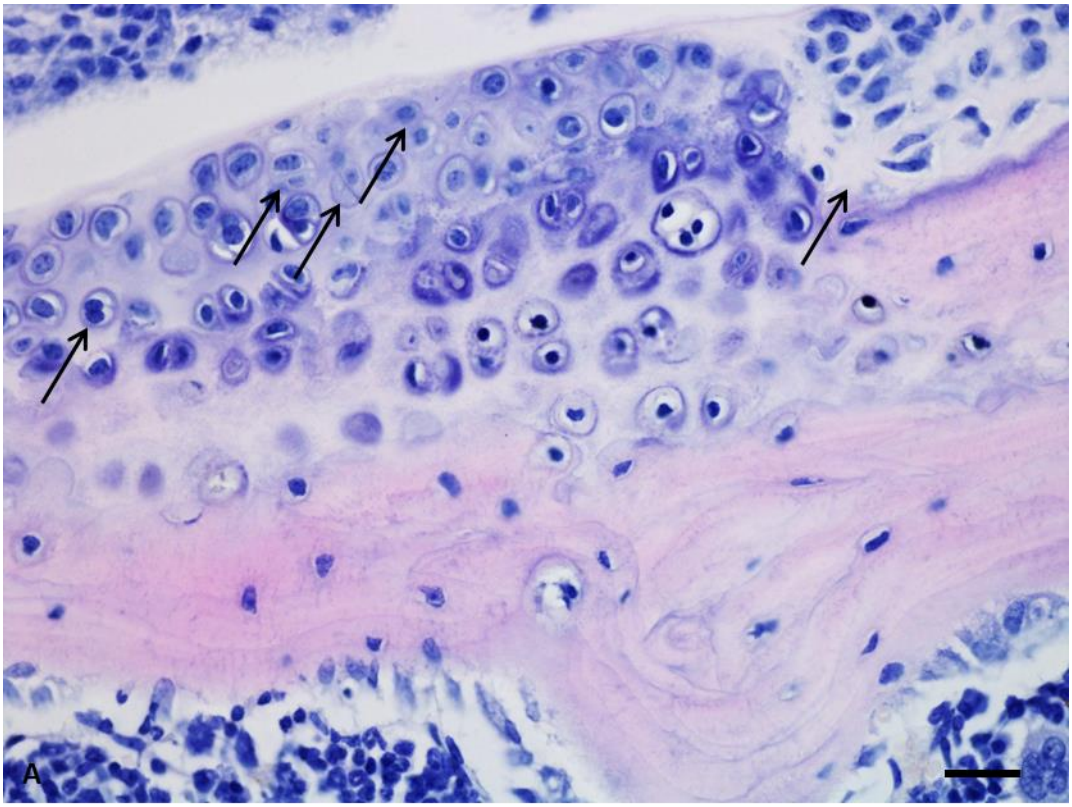

Figure 3.30 – Chondrocyte proliferation and articular cartilage damage in a 62.6 week old BL/6 Hgd-/- mouse. H&E staining of the LTP of BL/6 Hgd-/- 62.3 (♀) showed large amounts of cell division (left arrows) in the HAC. Some of the HAC appeared to have been damage and replaced by fibrocartilaginous tissue (right arrow). Bar = 20 µm.

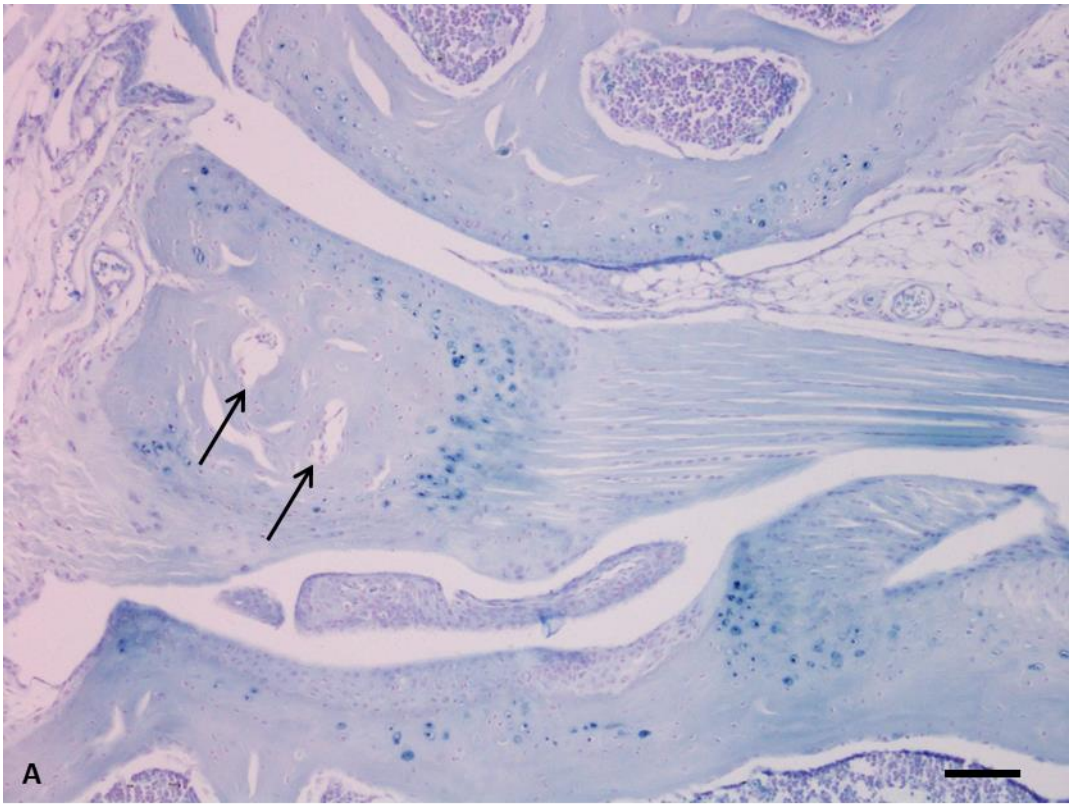

Figure 3.31 – Meniscal ossification in a 62.6 week old BL/6 Hgd-/- mouse. Schmorl's staining of the LM of BL/6 Hgd-/- 62.3 showed the presence of pigmented chondrons in the cartilage of the meniscus. Bar = 100 µm.

3.3.3.10 BL/6 Hgd-/- 49.2 (♀) – 68.3 weeks

BL/6 Hgd-/- 49.2 (♀) (68.3 weeks) displayed a reduction in the amount of pigmented chondrons located throughout the tibio-femoral joint in comparison with BL/6 Hgd-/- mice of similar ages (Fig. 3.40). Although it was quite a significant reduction it was noted as an anomaly as no other mouse showed such a large reduction in the numbers of pigmented chondrons. The most densely populated area of pigmentation was the intercondylar area of the tibia (Fig. 3.32 (**B**)). Two chondrons in the ACC (Fig. 3.32 (**A**)) demonstrated the differences that can occur in chondrons in close proximity to one another. One chondron (left) was only lightly pigmented while the chondron adjacent to it was heavily pigmented and pyknotic.

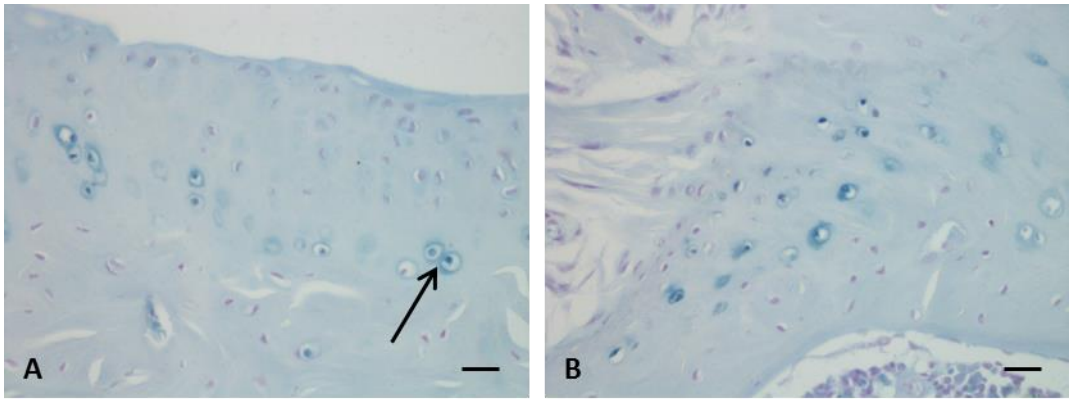

Figure 3.32 – Ochronotic pigmentation in a 68.3 week old BL/6 Hgd-/- mouse. Two chondrons in close proximity in the MTP; one was lightly pigmented (left) yet the other was heavily pigmented and pyknotic (right) (**A**, arrowed). Large numbers of pigmented chondrons were located in the intercondylar area of the tibia (**B**). All sections taken from BL/6 Hgd-/- 49.2 and stained with Schmorl's. Bar = 20 μm.

Fibrillations were observed on the articular surface of the MFC (Fig. 3.33) of BL/6 Hgd-/- 49.2. Parts of the HAC had also been eroded to the point where the ACC was nearly exposed. Heavily pigmented chondrons were situated close to the damaged surface (Fig. 3.34) but it did not appear the damage had caused a proliferation in the number of pigmented chondrons.

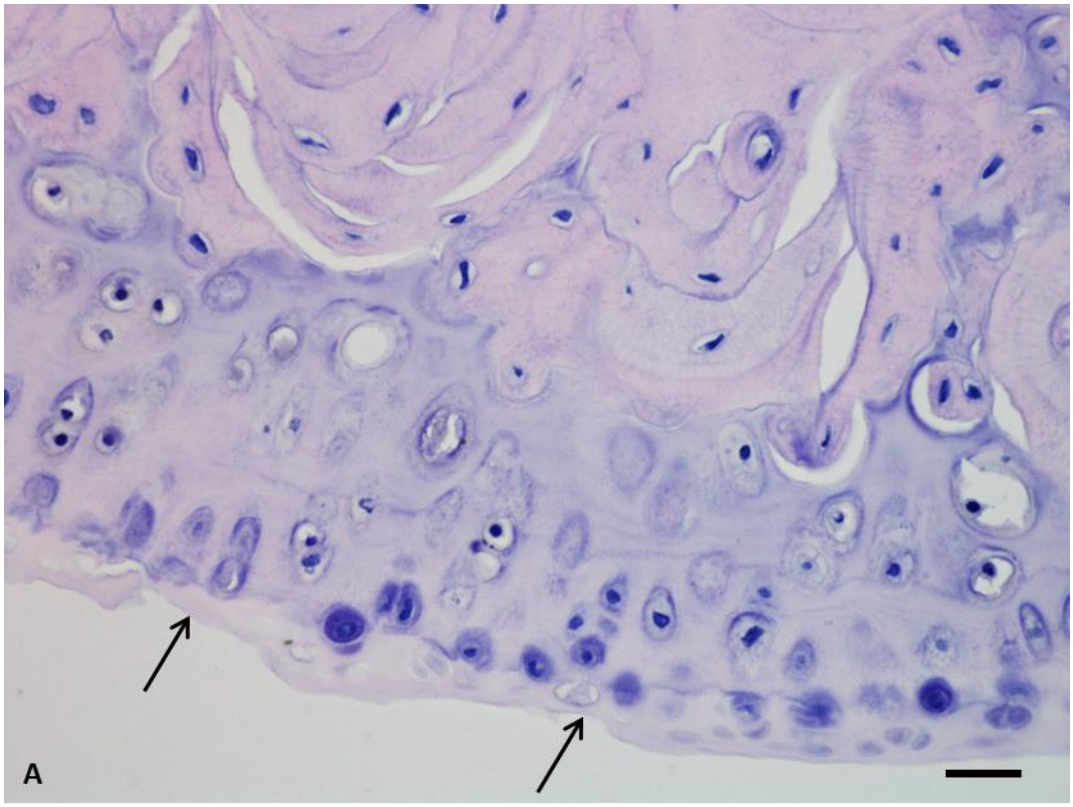

Figure 3.33 – Fibrillations and erosion of the articular surface in a 68.3 week old BL/6 Hgd-/- mouse. H&E staining of the MFC from BL/6 Hgd-/- 49.2 displayed fibrillations and erosion of the articular surface (arrowed). Bar = 20 µm.

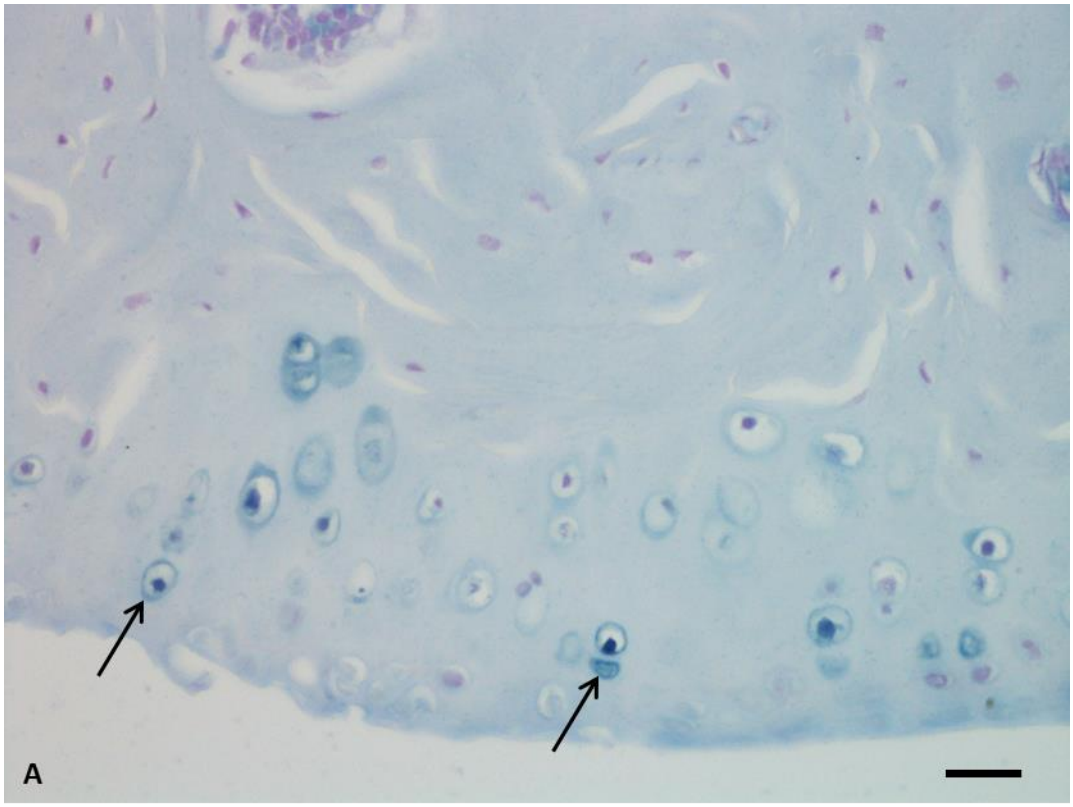

Figure 3.34 – Fibrillations and erosion of the articular surface in a 68.3 week old BL/6 Hgd-/- mouse (II). Schmorl's staining of a near serial section of Fig. 3.33 showed pigmented chondrons (arrowed) located near the damaged surface of the cartilage. Bar = 20 µm.

3.3.3.11 BL/6 Hgd-/- 35.1 (♂) – 71.7 weeks

BL/6 Hgd-/- 35.1 (♂) displayed levels of pigmentation consistent with that of mice of similar ages (Fig. 3.40). There were very few peri-pigmented or non-pigmented chondrons in the joint, showing the severity of ochronosis in the mouse. Dense areas of pigmentation were located throughout the tibio-femoral joint (Fig. 3.35).

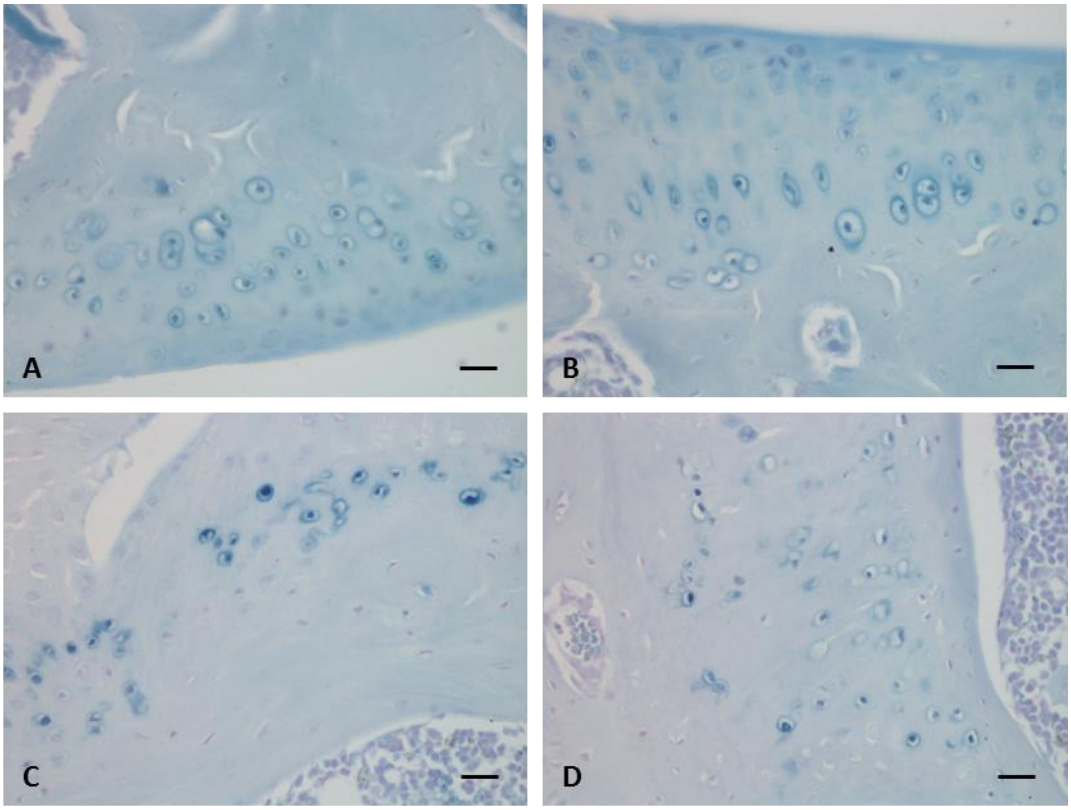

Figure 3.35 – Extensive ochronotic pigmentation in a 71.7 week old BL/6 Hgd-/- mouse. Schmorl's staining revealed large amounts of pigmented chondrons present in the MFC (**A**), MTP (**B**), intercondylar area of the TP (**C**), and fibrocartilaginous enthesis of the LFC (**D**). All sections taken from BL/6 Hgd-/-35.1 and stained with Schmorl's. Bar = 20 µm.

A small area of HAC had eroded exposing the underlying ACC in the joint (Fig. 3.36). Minor fibrillations were also present on the articular cartilage near the damaged area, resulting in the loss of the articular surface and the associated chondroblasts. Although no pigmented chondrons were located directly at the damaged HAC-ACC boundary, they were located in the ACC underneath the injured area (Fig. 3.37). Angiogenesis was also present in the MFC, leading to the vascularisation of the ACC (Fig. 3.38).

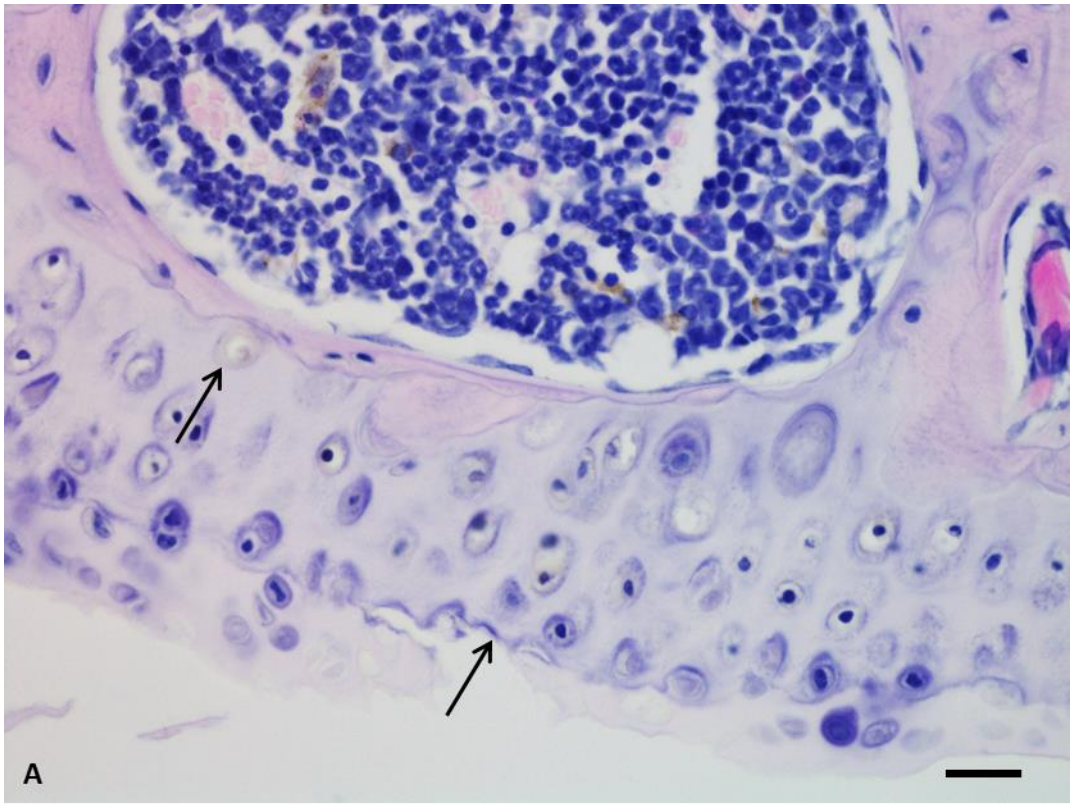

Figure 3.36 – Articular cartilage erosion and signs of pigment initiation in a 71.7 week old BL/6 Hgd-/- mouse. H&E staining of the MFC from BL/6 Hgd-/- 35.1 showed erosion of the HAC to the underlying ACC (right arrow). A fully pigmented chondron located at the boundary of the ACC and SCB (left arrow) - the site where pigmentation is hypothesised to initiate. Bar = 20 µm.

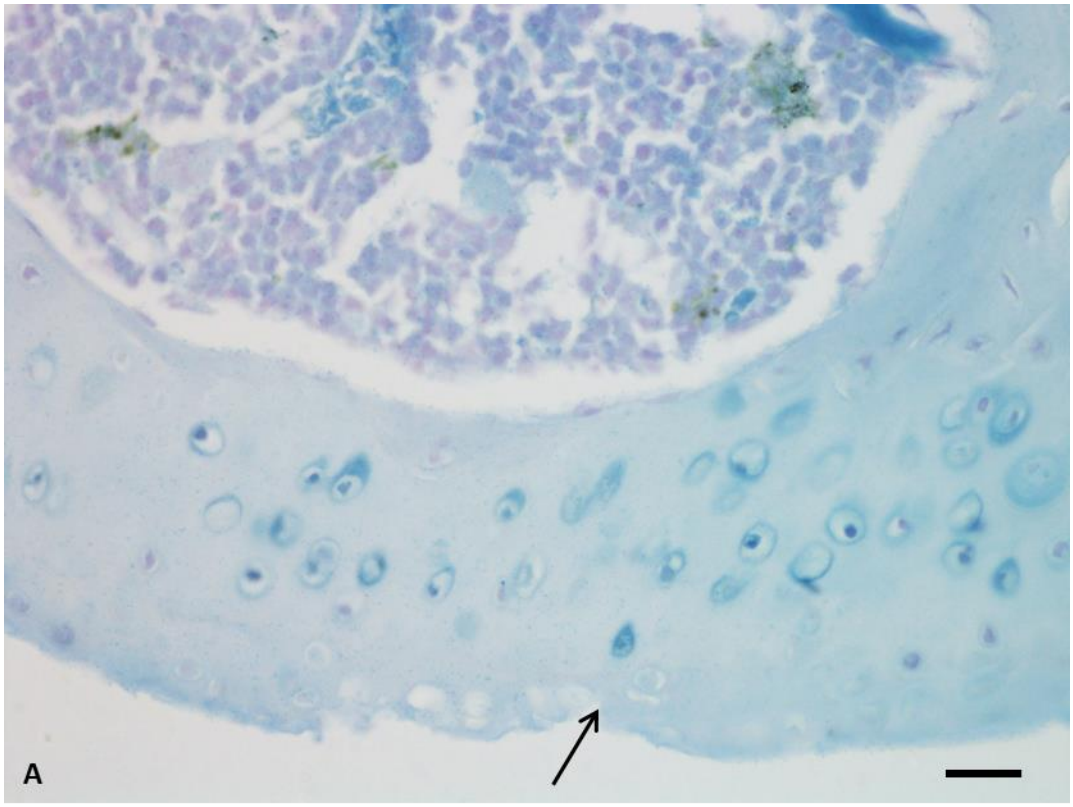

Figure 3.37 – Articular cartilage loss and pigmentation in a 71.7 week old BL/6 Hgd-/- mouse. Schmorl's staining of a near serial section of Fig. 3.36 (BL/6 Hgd-/- 35.1) showed the location of pigmented chondrons in relation to the injured area. Bar = 20 µm.

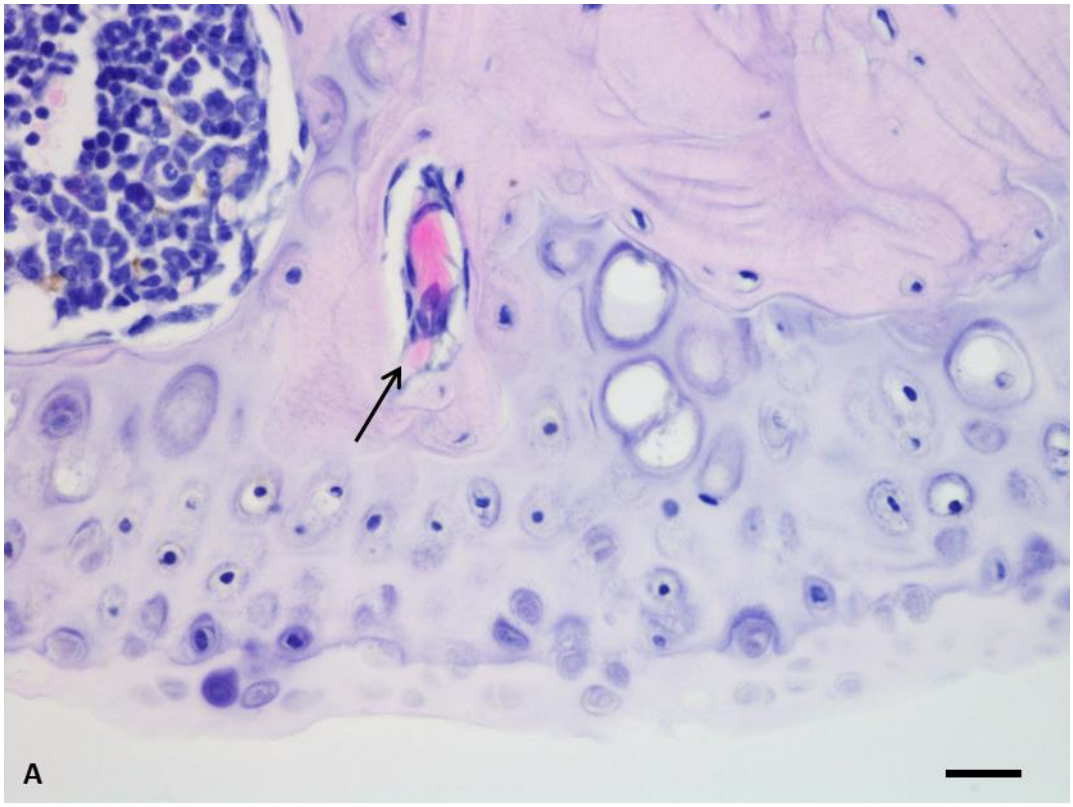

Figure 3.38 – Vascularisation of the articular calcified cartilage in a 71.7 week old BL/6 Hgd-/- mouse. H&E staining of the MFC from BL/6 Hgd-/- 35.1 showed vascularisation of the ACC. Bar = 20 µm.

3.3.3.12 BL/6 WT (♂) – 69.1 weeks

A BL/6 WT was culled at 69.1 weeks and stained with Schmorl's to provide a control in the natural history study. The WT analysed showed no pigmentation or osteoarthritic changes as expected (Fig. 3.39).

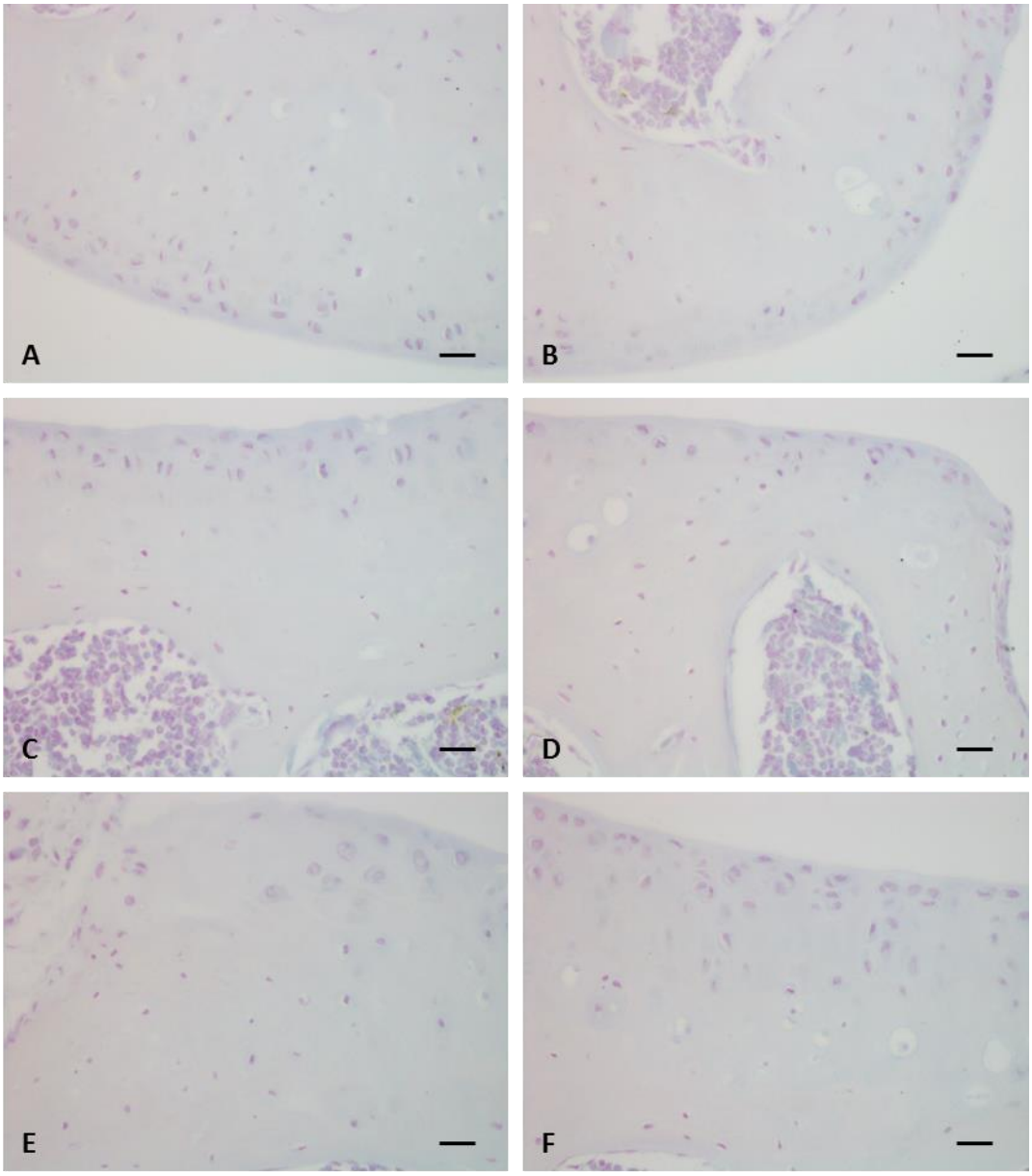

Figure 3.39 – Absence of ochronotic pigmentation in a BL/6 wild type mouse. Images of the MFC (**A** & **B**), the LTP (**C**), and the MTP (**D**, **E** & **F**) from a BL/6 WT showed no pigmented chondrons throughout the tibio-femoral joint. All sections stained with Schmorl's. Bar = 20 µm.

3.3.4 Quantification of pigmented chondrons in BL/6 Hgd-/- mice

The number of pigmented chondrons in each mouse involved in the natural history study was quantified. When the data was collated there was a clear pattern showing a progressive, linear increase in the amount of pigmentation with increasing age (Fig. 3.40).

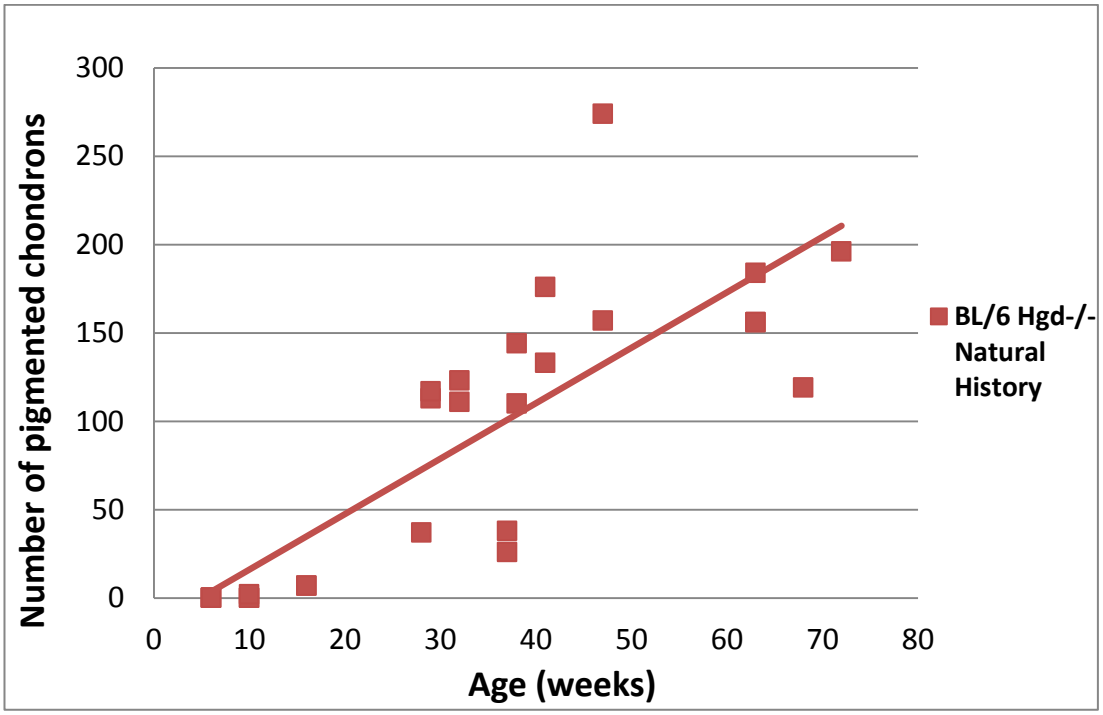

Figure 3.40 – The effect of age on the number of pigmented chondrons in BL/6 Hgd-/- mice. Scatter chart showing the effects of increasing age on pigmentation levels in BL/6 Hgd-/- mice. Quantification of pigmented chondrons was performed on a single section from each mouse; this does not represent the total cell number in each mouse.

3.3.5 Difference between BALB/c and BL/6 pigmented chondron levels

A comparison of pigmented chondron counts between BALB/c Hgd-/- and BL/6 Hgd-/- mice show small areas of intra- and inter- strain variability but the overall pattern is one of a linear increase in pigmentation with increasing age in Hgd-/- mice (Fig. 3.41).

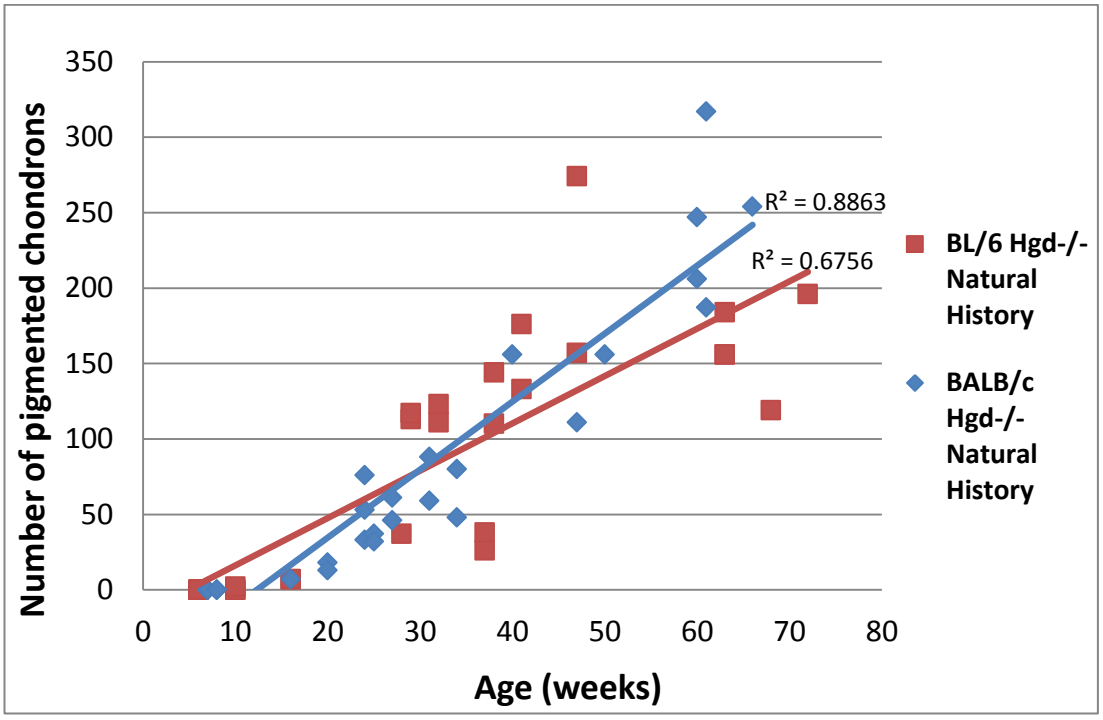

Figure 3.41 – A comparison of the number of pigmented chondrons between BALB/c and BL/6 Hgd-/- mice. Quantification of pigmented chondrons was performed on a single section from each mouse; this does not represent the total cell number in each section.

Although not easily visible on the above chart (Fig. 3.41) BL/6 Hgd-/- mice did develop ochronosis at an earlier time point than the BALB/c Hgd-/- mice. This is shown in Figs. 3.2 and 3.20, both of which correspond to the earliest observation of pigmented chondrons in BALB/c and BL/6 Hgd-/- mice. Pigmentation was first observed in BALB/c Hgd-/- mice at 15.7 weeks (Fig. 3.2), while BL/6 Hgd-/- mice first became pigmented at 10.4 weeks (Fig. 3.21). The pathology seen in the BL/6 Hgd-/-

mice was very similar with ochronosis in humans, starting with the initial peri-cellular pigmentation of chondrons. The very early ochronosis and subsequent progression observed in the BL/6 Hgd-/- mice was an important finding as it was consistent with the findings in the BALB/c Hgd-/- and also with what is thought to occur in ochronosis in humans.

3.4 DISCUSSION

This Chapter presents the first original data on the natural history of ochronosis in murine models of AKU. Montagutelli *et al* [110] first described the Hgd-/- mouse model but failed to find any ochronotic lesions or signs of phenotypic AKU which is consistently seen in humans. Although the mice showed elevated levels of urinary HGA excretion [51, 110], which was synonymous with human ochronosis, it was suggested that endogenous production of ascorbic acid protected tissues from becoming pigmented [110]. A second murine model of ochronosis was developed inadvertently by Manning *et al* [125] who was using FAH-/- mice to study HT-1. After being crossed with Hgd heterozygote's, a small number of these mice contained a double knockout, FAH-/-, Hgd-/-, which in effect made then AKU mice. Even though the mice displayed ochronosis in their tissues [111] the model was not considered suitable as it was produced by a spontaneous mutation occurring in a small minority of the mice.

In this Chapter it has been shown that mice with the Hgd-/- mutation become ochronotic. This is the first study which has detailed the natural history of ochronosis in Hgd-/- mice throughout their entire lifespan. Data collected in this chapter revealed that ochronosis began at a very early age and increased with age, becoming more and more severe with time. Hgd-/- mice also developed OA alongside ochronosis, which is similar to the AKU phenotype in humans. The identification of ochronosis in the tibio-femoral joint also dispels the notion that endogenous production of ascorbic acid acts as a protective agent to prevent pigmentation. The discovery of ochronosis in the Hgd-/- mice is significant as it provides a robust model to evaluate new novel therapies for the treatment of AKU while also providing a new model of experimental OA.

3.4.1 BALB/c Hgd-/- mice

Using Schmorl's stain pigmentation was first identified in BALB/c Hgd-/- mice at 15.7 weeks. Both mice examined at this age, BALB/c Hgd-/- 93.2 (♂) and 94.1 (♀), displayed pericellular pigmentation of chondrons located in the ACC, which is consistent with the initiation of pigmentation in humans [36]. It has been hypothesised that the PCM undergoes a change in its composition and organisation, resulting in the disordering of collagen in the matrix thus allowing for deposition of ochronotic pigment [36, 39]. Ultrastructural studies by Taylor *et al* [28] have shown that collagen fibres in areas of pigmentation are structurally abnormal compared to regular fibres yet show periodic binding of ochronotic shards along the fibres themselves. One of the main aims of the study was to discover when pigmentation initiated, so therapeutic intervention could be administered at the correct time point. The finding of peri-pigmented chondrons at such an early age was vitally important as it showed pigment deposition began very early on in life and not after years of exposure to high HGA, when clinical symptoms become observable.

By 23.5 weeks pigmentation was located intracellularly as well as extracellularly in the chondrons. The number of pigmented chondrons in the ACC of the tibio-femoral joint had also increased linearly with age. The progression of pigmentation to the intracellular compartment of the chondron was probably due to the initial transformation of its pericellular environment. Changes in the composition of the PCM are known to alter the biomechanical and micro environmental properties of the chondron [63, 129]. These changes are significant in terms of cell regulation and most likely allow for intracellular HGA deposition when altered.

Pigmentation continued to increase linearly with age throughout the study but never reached a stage of blanket coverage like that seen in end stage ochronosis in humans [36]. Pigmentation in the mice was localised to chondrons in the ACC. Territorial and interterritorial matrices did not become pigmented. Macroscopic

observation of the tibio-femoral joints did not show any darkening of the cartilage, again a feature associated with ochronosis in humans. The absence of these features in Hgd-/- mice may be associated with a number of factors, one being the short murine lifespan. There is no rational data available on comparable ages between mice and humans but it is reasonable to suggest that a mouse living to a maximum of 70 weeks would not have the same gross accumulation of pigment characteristically seen in humans with AKU. Mice also experience reduced joint loading as they are quadrupedal by nature. Mechanical loading of the tibio-femoral joint can lead to micro trauma in humans [130] and it has been hypothesised that the ECM, while normally resistant to the deposition of pigment, undergoes biomechanical and biochemical changes following mechanically induced damage leading to the accumulation of pigment [36]. It is likely mice experience reduced joint loading due to them being quadrupedal, therefore they are unlikely to suffer a similar magnitude of loading, and micro trauma which may explain the absence of blanket pigmentation in the articular cartilage. The process of articular cartilage matrix remodelling is controlled by a number of molecules including bone morphogenetic proteins (BMPs), fibroblast growth factors (FGFs), TGF-β, and Wnts. These regulate the expression of proteases, most notably MMP-13 [131, 132] and ADAMTS-5 [133, 134], which are responsible for the degradation of the cartilage matrix. Cleavage of aggrecan, collagens, GAGs, and cartilage oligomeric matrix protein (COMP) among others, by MMP-13 and ADAMTS-5, causes changes in the composition of matrix which is a major factor in OA pathogenesis, therefore regulation of these proteases is significant to prevent matrix degradation [135-139]. Increased mechanical stresses applied to joints are thought to upregulate the expression of certain proteases causing degradation of the matrix. As previously stated it is thought the ECM undergoes changes resulting in the accumulation of pigment, highlighting the apparent link between mechanical loading and pigmentation. If mice do experience reduced mechanical loading it is possible the expression of key proteases, involved in cartilage degradation, is not as high as in humans reducing the amount of matrix degradation. This may have prevented the accumulation of pigment throughout the entire articular cartilage preventing blanket pigmentation.

Large numbers of pigmented chondrons were located in the fibrocartilaginous entheses of the femur and the intercondylar area of the femur and tibia, more so in the tibia, in Hgd-/- mice from around 40 weeks of age. Deposition of ochronotic pigment in these areas was probably as a result of the high stress placed upon the region where it attaches to the bone. The function of both ligaments is to distribute stress forced upon the joint by mechanical loading, yet these compressive forces can cause damage to the ligaments when they become excessive [140]. This stress is known to cause compositional changes of the ligamentous ECM, leading to cartilage-related molecules including chondroitin 6 sulphate, aggrecan and type II collagen becoming prominent in the ECM of the entheses, similar to the ECM of the articular cartilage [140, 141]. With the composition of both these matrices being similar it is likely that the entheses responds in a similar way to abnormal loading conditions resulting in deposition of ochronotic pigment. The entheses at both areas are heavily loaded, especially the tibial attachments, which may explain why significant amounts of pigmented chondrons are present at these sites.

Interestingly, pigmented chondrons were also located in the EP in two aged mice. BALB/c Hgd-/- 61.3 (♀) and 61.4 (♀), who were both 60 weeks of age, each contained a single pigmented chondron located in the EP of the tibia (Figs. 3.10 & 3.11). Chondrons located in the EP are involved in endochondral ossification therefore they express a number of different phenotypes and synthesize a number of different collagens and proteoglycans. There is scarce literature regarding the EP in aged mice, nearly all papers focus on its involvement in endochondral ossification, however Chambers *et al* reported that the EP remains open in aged mice and the embedded chondrocytes remain viable and actively synthesize type II collagen and aggrecan [142]. It is possible that pigment deposition in these two chondrocytes is related to the presence of collagen, as collagen fibres are thought to be a primary binding site for ochronotic pigment [28]. However if collagen is a binding site, it is still unclear why only one cell, in each of the mice, became pigmented as all cells in the EP actively synthesize collagen. This may be evidence

that other factors which alter cellular activity are required for the initiation and progression of pigmentation.

Pigmentation in the mice was consistently associated with hypertrophic chondrons. From initial identification of pigmentation, in the PCM of hypertrophic chondrons at 15.9 weeks of age (Fig. 3.2) to the heavily pyknotic chondrons consistent with severe ochronosis, pigmented chondrons were always in some state of hypertrophy. As the number of pigmented chondrons increased so did the number of hypertrophic chondrons, highlighting their association. Chondrocyte hypertrophy is an essential process in endochondral ossification, whereby cartilage is replaced by bone in the development of the skeletal system. Hypertrophic chondrons in the growth plate of developing bone secrete alkaline phosphatase in order to calcify the surrounding matrix leading to bone formation. Although chondron hypertrophy is crucial in endochondral ossification, its role in mature cartilage is unclear [143]. It has been suggested that the initiation of OA is linked with chondron hypertrophy and the resulting increased calcification of the matrix [144] but it has yet to be proved conclusively. Markers of hypertrophy, including type X collagen and MMP-13, are known to be induced in human and murine OA cartilage [117, 145] suggesting increased hypertrophy does play a role in the degradation of the cartilage. The secretion of alkaline phosphatase from large numbers of hypertrophic chondrons in the ACC may be involved in the pathogenesis of OA [146]. As alkaline phosphatase release is involved in calcification, it is possible its secretion led to thinning of the HAC and thickening of the ACC and SCB by increased calcification of the matrix. Indeed, subchondral remodelling and sclerosis was seen in many of the mice from 30 weeks onwards along with other signs of OA, including tidemark duplication, osteophyte formation and thinning of the HAC and ACC. These findings are similar to what is seen in human ochronosis. The identification of large numbers of hypertrophic chondrons in the Hgd-/- mice suggests that calcification and ossification in the ACC may be an important step in the initiation of OA.

Along with the identification of hypertrophic chondrons, other signs of OA including tidemark duplication, osteophyte formation, HAC damage, subchondral remodelling and sclerosis and vascularisation of the ACC were observed in all of the BALB/c Hgd-/- mice from 30 weeks onwards. The tidemark, first described by Fawns and Landells in 1953 [147], denotes the mineralization front separating the HAC and ACC. Tidemark duplication has long been thought to be involved in the initiation and progression of OA [148, 149] as it suggests increased mineralisation of the cartilage in the joint. The identification of duplicate tidemarks in the large majority of Hgd-/- mice in this study suggested early changes consistent with the initiation of OA were present in the tibio-femoral joint. The fact the changes were present in relatively young mice seemed to imply that ochronosis is linked with the initiation of early OA. Cartilage damage and degradation was also associated with tidemark duplication in a number of the mice. Most of the damage was limited to minor fibrillations along the articular surface, however some of the mice showed significant loss of articular cartilage along with the presence of deep vertical clefts running through HAC (Figs. 3.8 & 3.13). Lesions were most severe in the MTP which is consistent with previous observations in mice [150]. Cartilage erosion is a hallmark of human ochronotic and OA tissue [37, 151] so it was not surprising to see it in the murine model of AKU. Although it was not as severe in the animal model, the identification of cartilage degradation highlighted the correlation between ochronosis and OA in the tibio-femoral joint of the Hgd-/- mice. Osteophytes, which are another characteristic sign of OA [152], were identified in a number of aged mice. All of the osteophytes were heavily pigmented which again highlighted the relationship between ochronosis and OA. Interestingly, osteophytes are noticeably absent from human ochronotic tissue [153, 154]. This is surprising as osteophytes are a common feature of OA and most features of OA have been observed in AKU tissue, usually in a far more advanced state than in non-AKU OA samples. It is likely that the osteophytes in the mice were induced by TGF-β as they originated from the periosteum, not the growth plate [152]. Osteophytes are known to limit the movement of OA knees [155], which may have contributed to the absence of blanket pigmentation in the Hgd-/- mice. Increased mechanical stress from loading of the joint is thought to be one of the mechanisms responsible

for pigment deposition [36]. Therefore if the joint is unable to move freely when osteophytes are present it may limit the amount of pigment deposited in the cartilage due to the reduced amount of load placed on the joint. SCB remodelling and vascularisation of ACC was observed in a number of the mice from 30 weeks of age, most noticeably in BALB/c Hgd-/- 92.1 (♂) (Fig. 3.6). A significant amount of SCB remodelling was located in the MFC of BALB/c Hgd-/- 92.1 (♂) along with vascular invasion of ACC. The involvement of SCB in the initiation and progression of OA was first suggested by Radin and colleagues some 30 years ago [96], however it is still unclear what it's true role is in the pathogenesis of OA. Remodelling of the SCB is initiated at areas of focal damage due to excessive loading [95], while vascular invasion of cartilage is known to be related to OA [156]. With pigment deposition thought to be related to changes in matrix composition, it may be the case that increased stiffness of the cartilage resulting from pigmentation leads to SCB changes due to the abnormal distribution of stress across the joint. As vascularisation of the ACC is associated with OA it is reasonable to assume that abnormal and excessive loading can induce vascular invasion of the cartilage which further damages the SCB and ACC and may factor in the deposition of pigment.

3.4.2 BL/6 Hgd-/- mice

BL/6 Hgd-/- 162.2 (♀) was the first mouse of this strain to show signs of pigmentation (Fig. 3.21). At 10.4 weeks of age it was considerably younger than BALB/c Hgd-/- 93.2 (♂) and 94.1 (♀) who were aged 15.7 weeks when the first signs of pigmentation were spotted in the BALB/c strain. Although BL/6 Hgd-/- 162.2 (♀) was the only one of a group of four mice at 10.4 weeks of age to display any pigmentation it was significant as it showed BL/6 Hgd-/- mice pigment earlier than BALB/c Hgd-/- mice. What was also interesting was that the chondrons that were pigmented appeared heavily pigmented and pyknotic which is symptomatic of chondrons in the final stages of pigmentation, so to see these types of chondrons in the initialization of pigmentation was somewhat surprising. The appearance of pigmented chondrons at an earlier age in BL/6 Hgd-/- mice than BALB/c Hgd-/- mice

may be due to the presence of melanin in the BL/6 Hgd-/- strain. Both ochronotic pigment and melanin are products of tyrosine catabolism, in fact pyomelanin, a type of melanin produced by microbes, is exactly the same pigment that is found in AKU [157, 158]. As melanin and ochronotic pigment are thought to be structurally related it is possible that higher natural levels of melanin in the BL/6 Hgd-/- strain lead to an increase in the amount of ochronotic pigment produced which accounts for the earlier deposition of pigment in the chondrons of the BL/6 Hgd-/- mice.

Similar to BALB/c Hgd-/- mice, pigmentation in BL/6 Hgd-/- mice continued to increase with age and was always localized to the ACC, intercondylar areas of the femur and tibia and the entheses of the femur. A stage of blanket pigmentation was never observed in the BL/6 Hgd-/- mice, which was identical to BALB/c Hgd-/- mice. This differed greatly from ochronosis in humans where blanket pigmentation of the tissues is routinely seen. The increase in the number of pigmented chondrons with age correlates with what is seen in the BALB/c Hgd-/- strain and probably results from the same mechanism; compositional changes in the PCM of the chondrons and its surrounding matrices which allow for pigment deposition. The fact that heavily pigmented chondrons were present in the early stages of pigmentation in the BL/6 Hgd-/- mice is peculiar as they are usually associated with the later stages of ochronosis. It may be that the BL/6 Hgd-/- mice have larger scale disruption of their matrices and the collagens that reside in them, predominantly collagen types II, VI, and X, which allows for increased levels of the pigment to become deposited in these areas in a shorter time span. However, other unknown factors may also play a part in this process.

Pigmentation in BL/6 Hgd-/- mice was always associated with hypertrophic chondrons; again this was analogous with what was seen in BALB/c Hgd-/- mice. Although there were large numbers of pigmented chondrons in BL/6 Hgd-/- mice there appeared to be less very hypertrophic chondrons than in BALB/c Hgd-/- mice. Stoop and colleagues observed something similar when comparing the OA changes

in both strains [159] and concluded it was no more than strain to strain differences between the mice.

Osteoarthritic changes were observed in a large number of the BL/6 Hgd-/- mice throughout their whole life span. BL/6 Hgd-/- 35.1 (♂) showed significant signs of OA including erosion of the HAC on the MFC (Figs. 3.36 & 3.37), and vascularisation of the ACC (Fig. 3.38). The loss of HAC in Hgd-/- mice is likely to be due to degradation of type II collagen fibres, most prominently by MMP-13, as these fibres make up a large proportion of the HAC matrix. This is known to occur in OA and is also associated with calcification of the matrix [160]. Tidemark duplication was also present in the majority of the mice from 27 weeks onwards. As previously discussed, tidemark duplication is thought to be a marker of OA initiation as it suggests increased mineralisation occurring in the joint. Large numbers of hypertrophic chondrons were located in the ACC when multiple tidemarks were identified, suggesting that calcification is increased in OA. Clustering of chondrocytes towards the articular surface was observed in a number of mice (Figs. 3.25 & 3.31), all of which had signs of OA present. Chondrocyte clustering is a known feature of OA pathogenesis [161], however its actual role in the disease is relatively unknown. At least in the results detailed in this chapter it seemed to occur in response to damage caused to the articular surface of the cartilage. The repopulation of these damaged areas with increased amounts of chondrocytes may have been an attempt to increase matrix synthesis in order to reduce the amount of cartilage degradation at that site. Vascularisation of the ACC was seen in a number of mice alongside remodelling of SCB. Significant osteoclastic resorption of the ACC had taken place in BL/6 Hgd-/- 62.3 (♀) (Fig. 3.28) which resulted in vascular invasion of the calcified cartilage protruding up close to the HAC. Vascularisation was present in mice of a wide age range, some of which had clear signs of OA while others didn't. This shows that vascular invasion of the ACC and remodelling of SCB appear to both be initiating and late stage features of OA. Meniscal ossification was observed in two BL/6 Hgd-/- mice and was localised to the lateral menisci in both. Ossification of the meniscus is a common occurrence in mice and other rodents

[127], however it has been shown that overgrown calcified menisci can contribute to the formation of OA in mice [162]. The LM in BL/6 Hgd-/- 62.3 (♀) was extremely large and ossified whilst also containing a substantial number of pigmented chondrons. It has been suggested that meniscal calcification can alter the biomechanics of the tibio-femoral joint and contribute to OA lesions [163], and that SCB adapts and changes in response to the altered mechanical load placed upon the joint when calcification of the meniscus occurs [164]. Both BL/6 Hgd-/- mice which had ossification of the menisci showed phenotypic changes consistent with OA, therefore it is possible meniscal ossification contributed to the progression of OA in these animals. However as previously reported in this thesis, meniscal ossification is commonly seen with ageing so the formation of them in these two animals may be nothing more than a sign of ageing.

Although signs of OA were present in both BALB/c and BL/6 strains of Hgd-/- mice it is not clear if these were as a result of the mice having ochronosis or whether they developed spontaneously. OA does develop spontaneously in both BALB/c and BL/6 mice so it is possible the onset of OA in Hgd-/- mice was spontaneous and not related to the progression of ochronosis in the mice. Scoring of the OA changes in both Hgd-/- and WT mice throughout their lifetime, would provide a better understanding of whether the development of OA was spontaneous or directly resulted from the development of ochronosis in Hgd-/- mice.

3.4.3 Summary

The identification of ochronotic osteoarthropathy in the Hgd-/- mice is a significant step forward in our understanding of the pathogenesis of AKU. From the results discussed it appears that initiation of pigmentation in the mice, which is associated with focal changes in chondrocytes and their surrounding matrices, is similar with the human disorder thus demonstrating the appeal of using the Hgd-/- mice to study the natural history of AKU. Both strains of mice showed signs consistent with ochronotic osteoarthropathy progressing throughout their lifespan. Once pigmentation was initiated it progressed with age which then led to the appearance of osteoarthritic changes in the tibio-femoral joint. Again these features were very similar to those observed in ochronosis in humans. One feature that is still not understood in ochronosis, in both humans and mice, is how HGA becomes situated at the site(s) of deposition. As cartilage is avascular there are no blood vessels directly supplying the chondrons, therefore there must be another route that pigment is transferred to the tissue. One route may be through diffusion of HGA from the synovial fluid to the cartilage, however with calcium present in the ACC it may be difficult for the pigment to penetrate through. Another route may be through the SCB vascular system. Pigmentation has been shown to initiate in chondrons deep in the ACC, in both humans and mice, therefore HGA may accumulate in blood vessels in the SCB and diffuse through to the ACC before becoming deposited in chondrons. The discovery of ochronosis in the Hgd-/- mice is important as it provides a robust model to evaluate new novel therapies for the treatment of AKU while also providing a new model of experimental OA.

4. Initiation, distribution and localization of ochronotic pigmentation in Hgd-/- mice

4.1 INTRODUCTION

Following the identification of ochronotic pigmentation and associated osteoarthropathy in Hgd-/- mice (Chapter 3), further analysis was undertaken to try and identify the mechanism of pigment deposition. Until recently the mechanism behind HGA polymer deposition in the collagenous tissues of AKU patients was unknown [20, 35, 41]. Following work by Taylor *et al* [28] which suggested the presence of a preferential binding site(s) for ochronotic pigment on collagen fibres, the same authors proposed a mechanism for the initiation of ochronotic arthropathy in AKU patients [36]. They suggested that the initiation of pigmentation followed focal changes in the matrices of the ACC, thus allowing ochronotic pigment to bind to collagen fibres. The authors also describe the progression of pigmentation from its initiation in the ACC to its blanket distribution throughout the entire articular cartilage.

Chapter 3 of this thesis describes in detail the natural history of ochronosis in BALB/c and BL/6 Hgd-/- mice. Previous to this, little was known about the pathogenesis of ochronosis in Hgd-/- mice [51, 110]. This Chapter proposes a partial mechanism for the initiation and progression of ochronosis in a murine model of AKU. Following apparent changes in the composition and/or organisation of the matrices in the ACC of Hgd-/- mice, ochronotic pigment became deposited in the PCM. Cellular material then became pigmented resulting in widespread pigmentation of the ACC. Although the HAC appears to be unaffected by ochronosis in Hgd-/- mice, the data presented in this chapter shows the initiation and progression of pigmentation, in mice, to be almost identical to the mechanism proposed by Taylor [36].

Although ochronosis is most severe in articulating joints, other tissues in the body can become pigmented. There have been many cases in which pigmentation has been found in aortic valves [31, 165-167], the sclera of the eye [168, 169] and the

ear, including the earwax [170, 171] of AKU patients. For this thesis, large scale analysis was limited to the knee joint as this becomes severely ochronotic in humans. However, several other joints including the femoral head, the calcaneus and the humerus epicondyle (elbow joint), from a BALB/c Hgd-/- mouse aged 65.7 weeks, were examined in order to establish whether ochronosis was present in other articulating joints in Hgd-/- mice as it is in AKU patients. This Chapter details the distribution of ochronotic pigment in these tissues, highlighting the practicality of the Hgd-/- mice as a model of ochronosis.

4.2 DESIGN OF STUDY

Tissue samples from the knee joints of BALB/c and BL/6 Hgd-/- mice were stained with H&E and Schmorl's stain in order to investigate the initiation and progression of ochronotic osteoarthropathy.

Several other articulating joints, as noted in the introduction, were also stained with H&E and Schmorl's stain to determine if pigmentation was located in these areas.

4.3 RESULTS

4.3.1 A proposed mechanism for the initiation of ochronosis in Hgd-/- mice

Pigmentation was first identified in BALB/c Hgd-/- mice at 15.7 weeks of age and at 10.4 weeks of age in BL/6 Hgd-/- mice (Chapter 3). Upon closer examination of the BALB/c Hgd-/- mouse, pigmentation was localised to the PCM of two chondrons in the ACC both of which appeared healthy (Fig. 4.1). No cellular staining was present indicating a change must have occurred in the PCM leading to deposition of ochronotic pigment. Peri-cellular staining of these two chondrons represented the initiation of pigmentation in BALB/c Hgd-/- mice, and was consistent with the proposed mechanism of ochronosis in AKU patients [36].

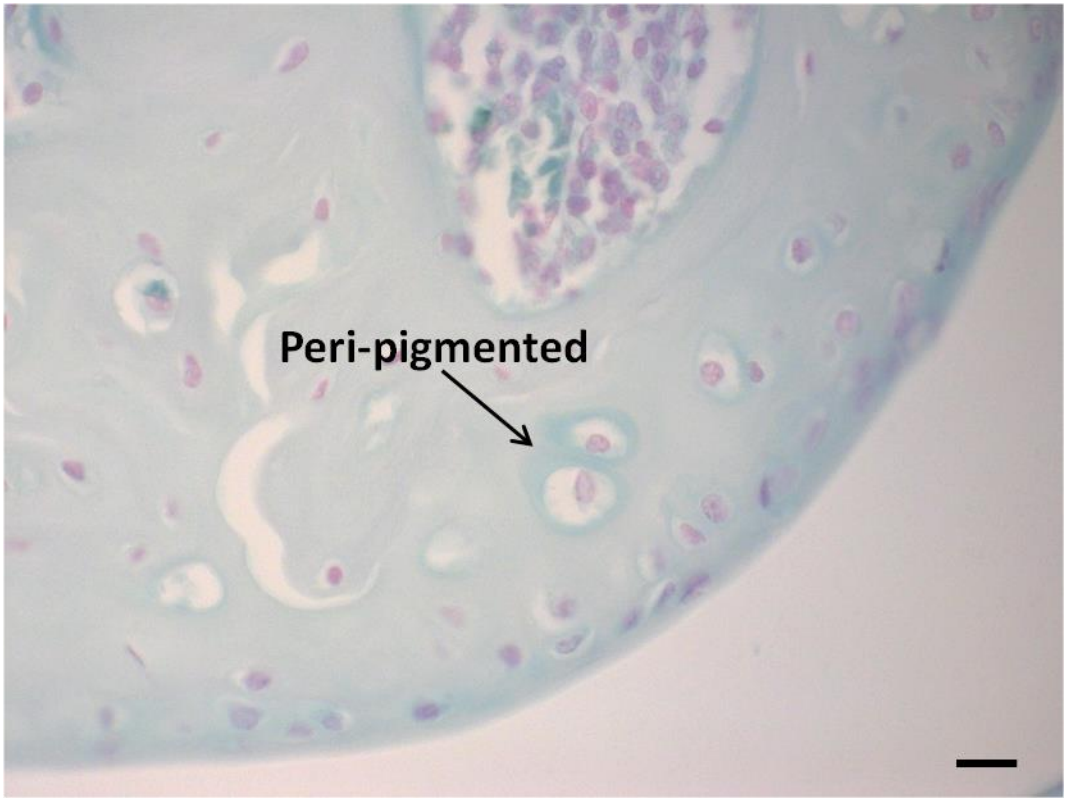

Figure 4.1 – Initiation of ochronotic pigmentation in the pericellular matrix. Two chondrons showed pericellular pigmentation in ACC of the MFC of a 15.7 week old BALB/c Hgd-/- mouse; the first stage of pigmentation in ochronotic chondrons. Section taken from BALB/c Hgd-/- 94.1 & stained with Schmorl's. Bar = 10µm.

In Hgd-/- mice of advancing age there was an increased amount of pigmentation, as detailed in the Chapter 3. In these mice, pigmentation of chondrons had progressed intracellularly (Fig. 4.2). This was probably due to the increasing amounts of HGA being deposited in the chondrons following the initial change in their pericellular environment. Although the number of pigmented chondrons increased, non-pigmented cells were still visible in the ACC. This demonstrated the individuality between chondrons, as although a large percentage of them were pigmented, some appeared to have been completely unaffected or were in the very early stages of pigmentation. Again, this progression of pigmentation was consistent with that previously observed in AKU tissue samples [36].

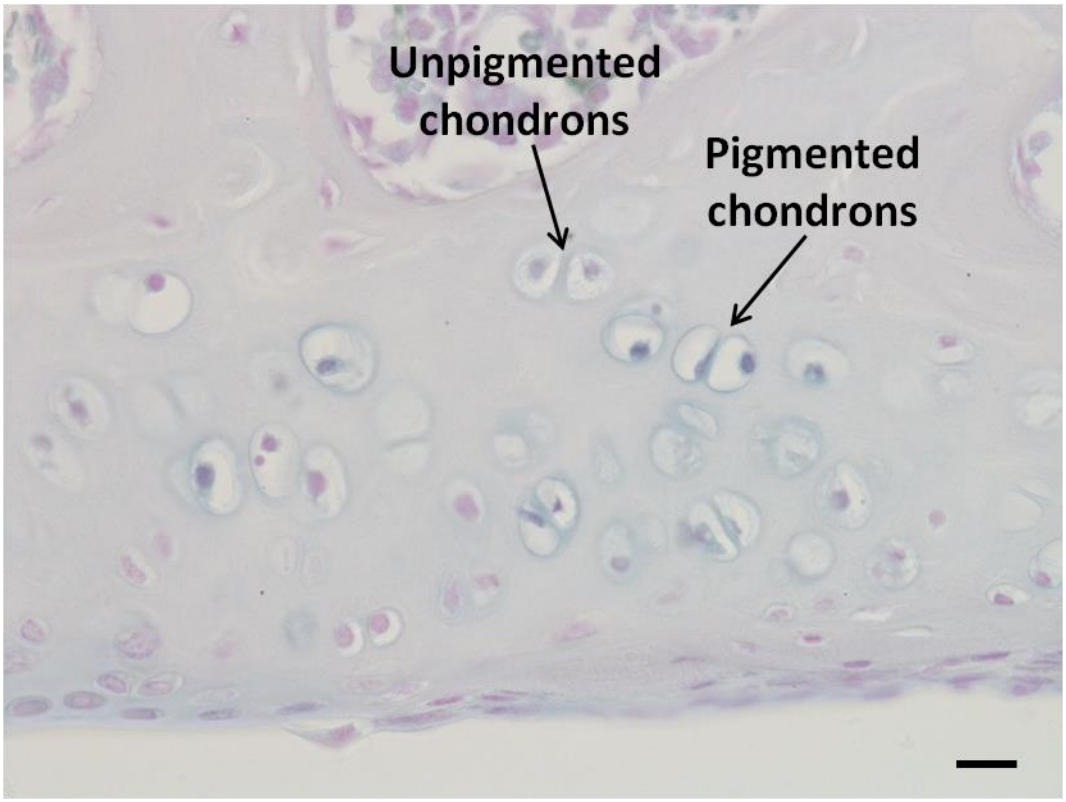

Figure 4.2 – Intracellular progression of ochronotic pigmentation. Pigmented chondrons in ACC of the MFC of a 27.4 week old mouse in which pigmentation had progressed intracellularly. Non-pigmented chondrons were still located in the cartilage; two are located adjacent to the highlighted pigmented chondrons. Section taken from BALB/c Hgd-/- 99.1 & stained with Schmorl's. Bar = 10µm.

The final stage of pigmentation involved chondrons becoming pyknotic and heavily pigmented both intra- and extracellularly. Staining of these chondrons was very intense indicating a large amount of pigment was deposited in the cell (Fig. 4.3). Most of the chondrons in the ACC displayed this phenotype, however a small number were still in the early stages of pigmentation. This is shown best in a section of the LTP from BALB/c Hgd-/- 50.3, aged 65.7 weeks, where the complete staging of chondron pigmentation can be observed (Fig. 4.4).

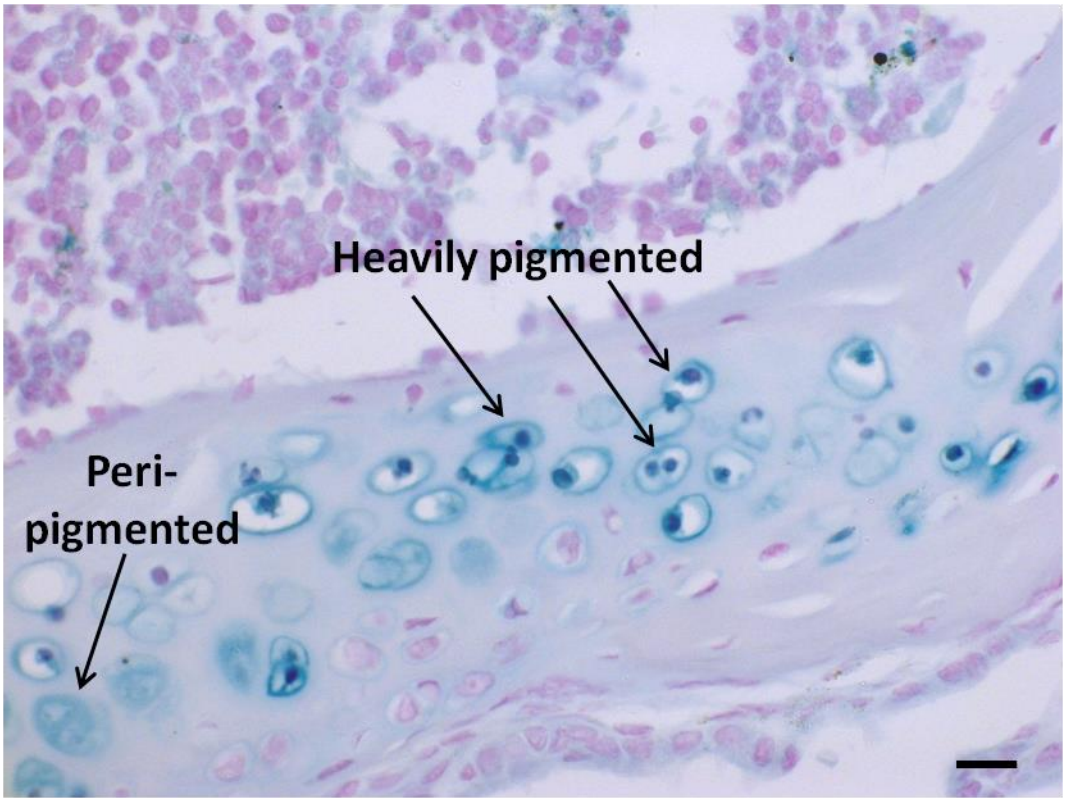

Figure 4.3 – End stage pigmentation of ochronotic chondrons. Heavily pigmented chondrons located throughout the ACC of the LFC of a 65.7 weeks old mouse. Although most chondrons were pyknotic, some chondrons in the early stages of pigmentation were observed. Section taken from BALB/c Hgd-/- 50.3 & stained with Schmorl's. Bar = 10µm.

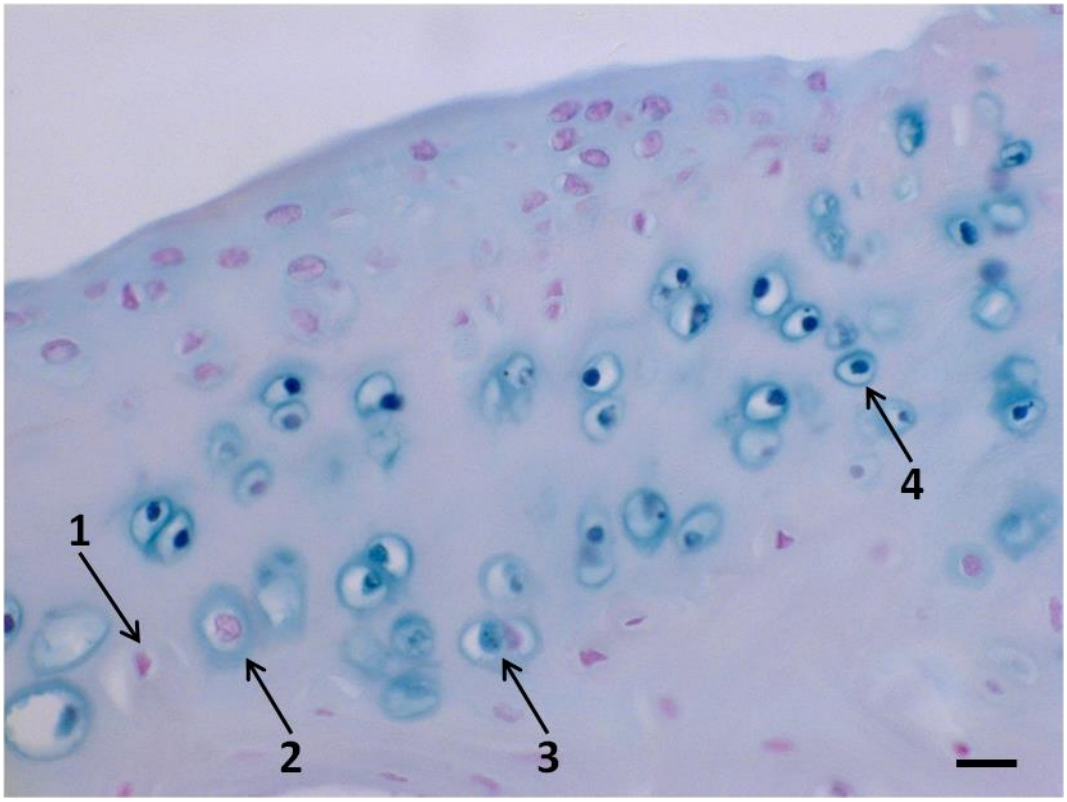

Figure 4.4 – Stages of pigmentation in the lateral tibial plateau of a 65.7 week old BALB/c Hgd-/- mice. (1) Healthy chondron with no staining, (2) healthy chondron with staining of the PCM, (3) chondron with both intracellular and extracellular staining, and (4) a heavily pigmented pyknotic chondron. Section taken from BALB/c Hgd-/- 50.3 & stained with Schmorl's. Bar = 10µm.

When pigmentation was first identified in BL/6 Hgd-/- mice at 10.4 weeks, the pigmented chondrons showed heavy staining of their nuclear material as well as PCM staining (Fig. 4.5). This was unusual as it appeared not to follow the same pattern of pigmentation as BALB/c Hgd-/- mice. However in a BL/6 Hgd-/- mice aged 41.3 weeks (BL/6 Hgd-/- 82.1) the same staging of chondrons was visible (Fig. 4.6), indicating that the mechanism of pigmentation was similar in both strains of mice.

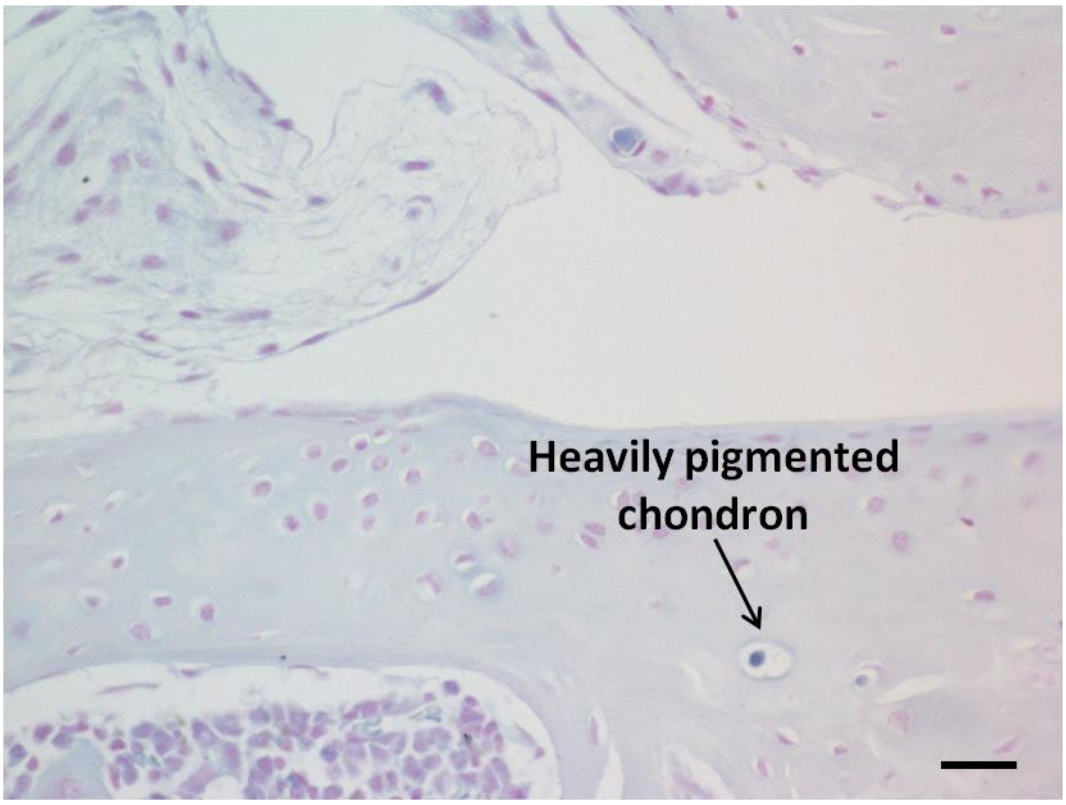

Figure 4.5 – A heavily stained chondron in the lateral tibial plateau of a 10.4 week old BL/6 Hgd-/- mouse. A chondron in the LTP of a 10.4 weeks old BL/6 mouse displaying heavy nuclear staining. Section taken from BL/6 Hgd-/- 162.2 & stained with Schmorl's. Bar = 20µm.

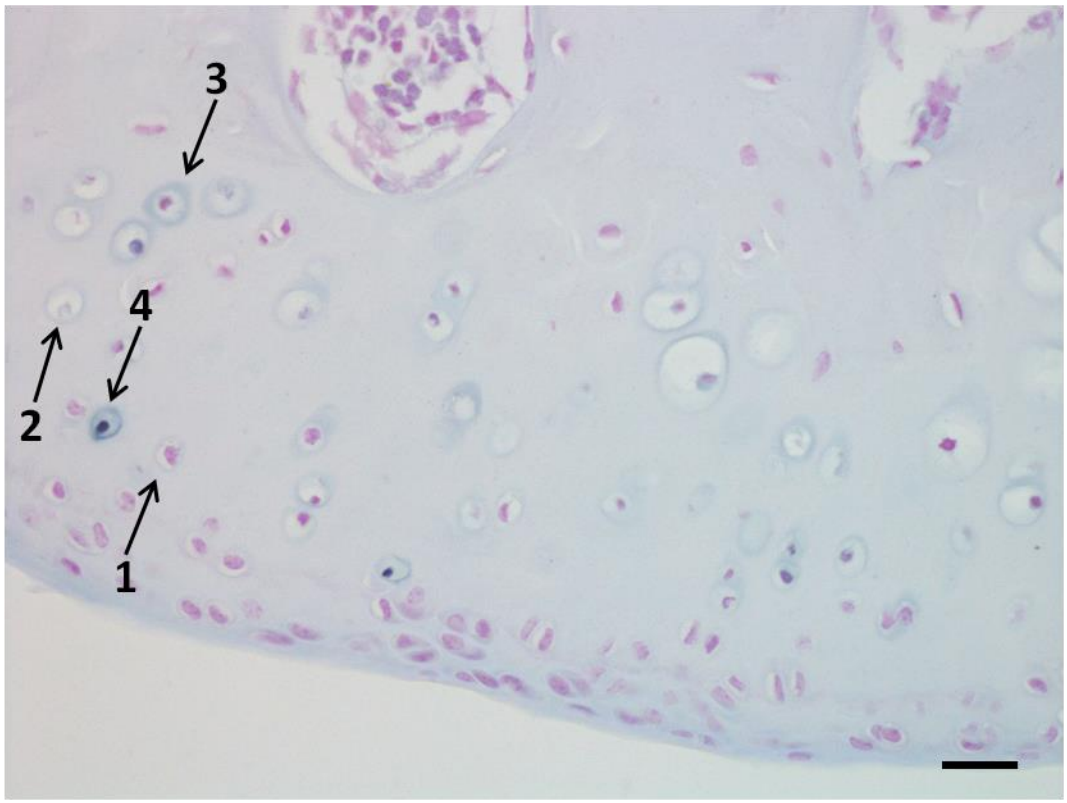

Figure 4.6 – Stages of pigmentation in the medial femoral condyle of BL/6 Hgd-/- 82.1, a 41.3 week old Hgd-/- mouse. (1) Healthy chondron with no staining, (2) healthy chondron with staining of the PCM, (3) a lightly pigmented chondron, and (4) a heavily pigmented pyknotic chondron. Section taken from BL/6 Hgd-/- 82.1 & stained with Schmorl's. Bar = 20µm.

The identification of a possible mechanism for pigment initiation and the ability to show each stage of pigmentation in chondrons in Hgd-/- mice is an important step for AKU research. The initiation of pigmentation appeared to follow a change in the composition and/or organisation of the PCM which is consistent with human data. Once deposition of ochronotic pigment begins it undoubtedly has a detrimental effect on the health of the chondrocyte, leading to an increase in pigment deposition. The entire chondron then becomes pigmented rendering it inactive and leaving the chondrocyte unable to participate in cartilage/matrix turnover. This, in all probability contributes to degradation of the matrix and the osteoarthropathy associated with AKU.

4.3.2 Quantitative analysis of the proposed pigmentation pathway

As previously stated in this Chapter, a pathway for the stages of pigmentation seen in Hgd-/- mice has been proposed. Although the total numbers of pigmented chondrons in BALB/c and BL/6 Hgd-/- mice were quantified for the natural history studies (Chapter 3), these counts did not show the amount of each type of chondrocyte (1-non-pigmented, 2-PCM staining, 3-lightly pigmented chondron and 4-heavily pigmented chondron) at each individual time point. Sections from the natural history studies (Chapter 3) were re-counted to determine the percentage of each type of chondrocyte at each time point in BALB/c and BL/6 Hgd-/- mice (Fig. 4.7)

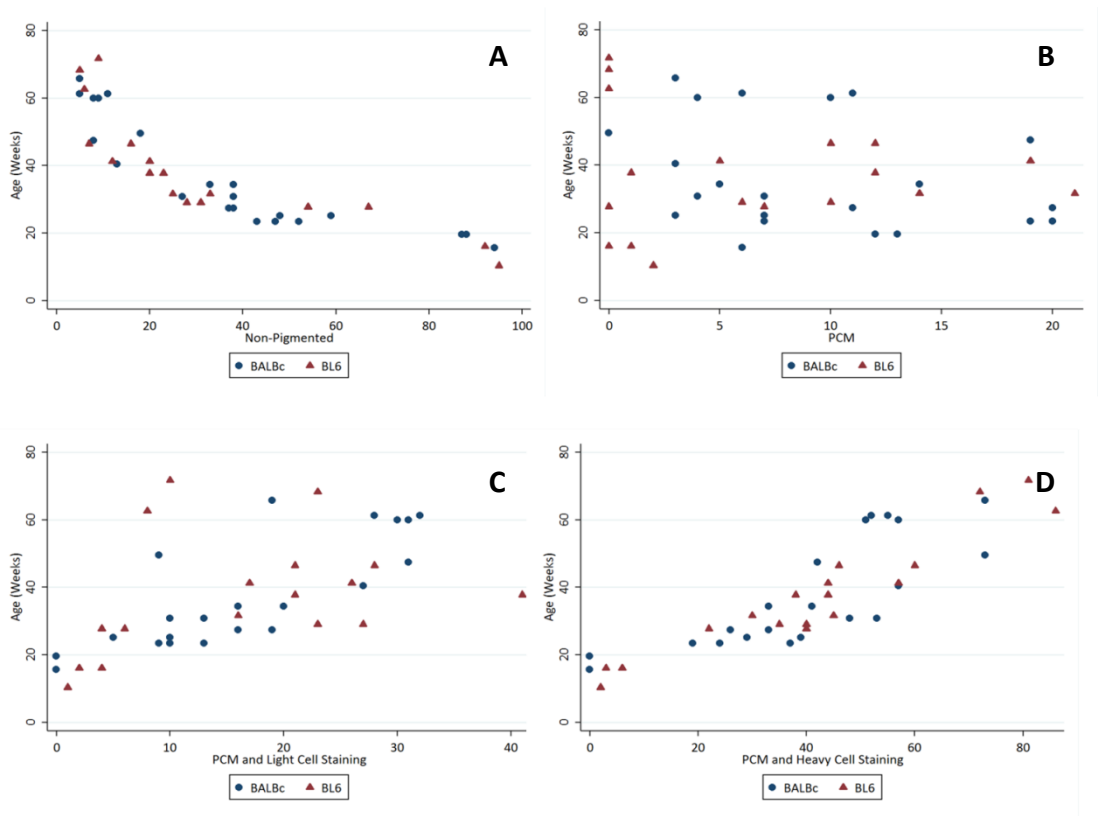

Figure 4.7 – The percentage of each type of chondrocyte in BALB/c and BL/6 Hgd-/- mice. The percentage of each type of chondrocyte, (A) non-pigmented, (B) PCM staining, (C) lightly pigmented chondron(s) and (D) heavily pigmented chondron(s), was plotted against the age of the Hgd-/- mice to provide a visual representation of their association.

It is clear from the charts in Fig. 4.7 that the number of non-pigmented chondrons decreases significantly with age (Fig. 4.7 (**A**)). This was an expected outcome as it had been previously shown in Chapter 3 that aged Hgd-/- mice are populated with large numbers of heavily pigmented chondrons, something which is clearly shown in Fig. 4.7 (**D**). There appeared to be slightly more variability in the amount of PCM stained and lightly stained chondrons with age, however this was not surprising as both these types of chondrons were present in Hgd-/- mice throughout the majority of their lifetime.

Univariate regression analysis was performed to determine if there was any statistical significance between the association of different chondron types in both strains of Hgd-/- mice (Table. 4.1).

	BALBc (n=23)				**BL6 (n=18)**		
	Estimate	95% CI	p-value		Estimate	95% CI	p-value
Non-Pigmented	**-1.55**	**(-1.94, -1.15)**	**<0.001**		**-1.51**	**(-2.04, -0.98)**	**<0.001**
PCM	-0.09	(-0.25, 0.07)	0.238		-0.04	(-0.25, 0.18)	0.725
PCM and LCS	**0.54**	**(0.37, 0.71)**	**<0.001**		0.21	(-0.11, 0.53)	0.188
PCM and HCS	**1.10**	**(0.75, 1.45)**	**<0.001**		**1.33**	**(1.09, 1.58)**	**<0.001**

Table 4.1 – Univariate regression analysis showing the significance of the association between the four different chondron types in BALB/c and BL/6 Hgd-/- mice.

As seen in Table. 4.1, there was a statistically significant association ($p<0.001$) between the percentage of non-pigmented, lightly stained and heavily stained chondrocytes with age in BALB/c Hgd-/- mice. Aged BALB/c Hgd-/- mice were associated with a lower percentage of non-pigmented chondrocytes, and a higher percentage of lightly stained and heavily stained chondrons. BL/6 Hgd-/- mice

showed a statistically significant association between the percentage of non-pigmented and heavily stained chondrocytes with age. Aged BL/6 Hgd-/- mice were associated with a lower percentage of non-pigmented chondrocytes and a higher percentage of heavily stained chondrons, similar to that seen in aged BALB/c Hgd-/- mice.

4.3.3 Distribution of ochronotic pigment in the articulating joints of an aged BALB/c Hgd-/- mouse

Ochronosis is not limited to the knee joint in humans. It has been found in many different tissues, all of which have showed varying degrees of severity. Although large scale analysis of Hgd-/- mice was confined to the knee joint, the femoral head, calcaneus, and the lateral epicondyle of the humerus from a 65.7 week old BALB/c Hgd-/- (ID: BALB/c Hgd-/- 50.3) mouse were all examined to identify if pigmentation, like in humans, was located in other load bearing joints.

4.3.3.1 Femoral head

Schmorl's staining revealed widespread pigmentation throughout the entire femoral head (Fig. 4.8). Heavily pigmented and lightly pigmented chondrons were easily identifiable (Fig. 4.9) indicating the pattern of pigmentation was similar to that seen in the knee joints of the mice. There appeared to be some significant cartilage damage along the surface of the femoral head (Fig. 4.8) which is consistent with that seen in the knee joint of aged Hgd-/- mice.

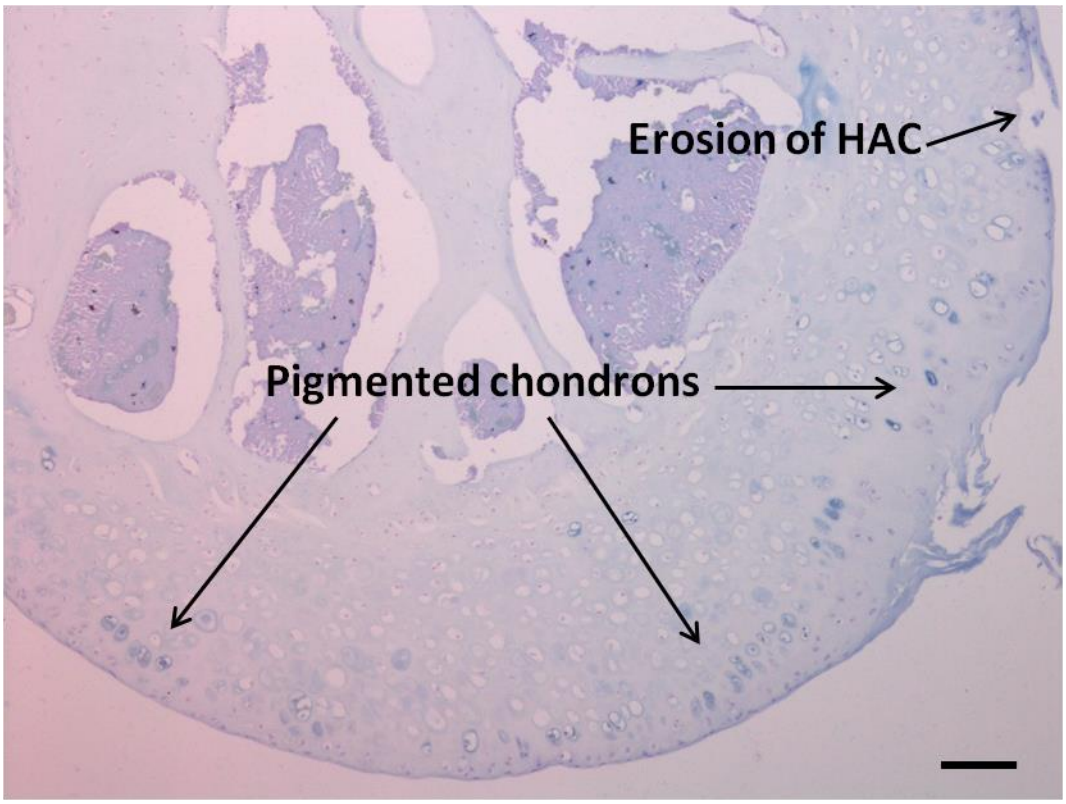

Figure 4.8 – Pigmentation and cartilage damage in the femoral head of a 65.7 week old BALB/c Hgd-/- mouse. Widespread pigmentation and severe cartilage erosion of cartilage was observed in the femoral head. Section taken from BALB/c Hgd-/- 50.3 & stained with Schmorl's. Bar = 10µm.

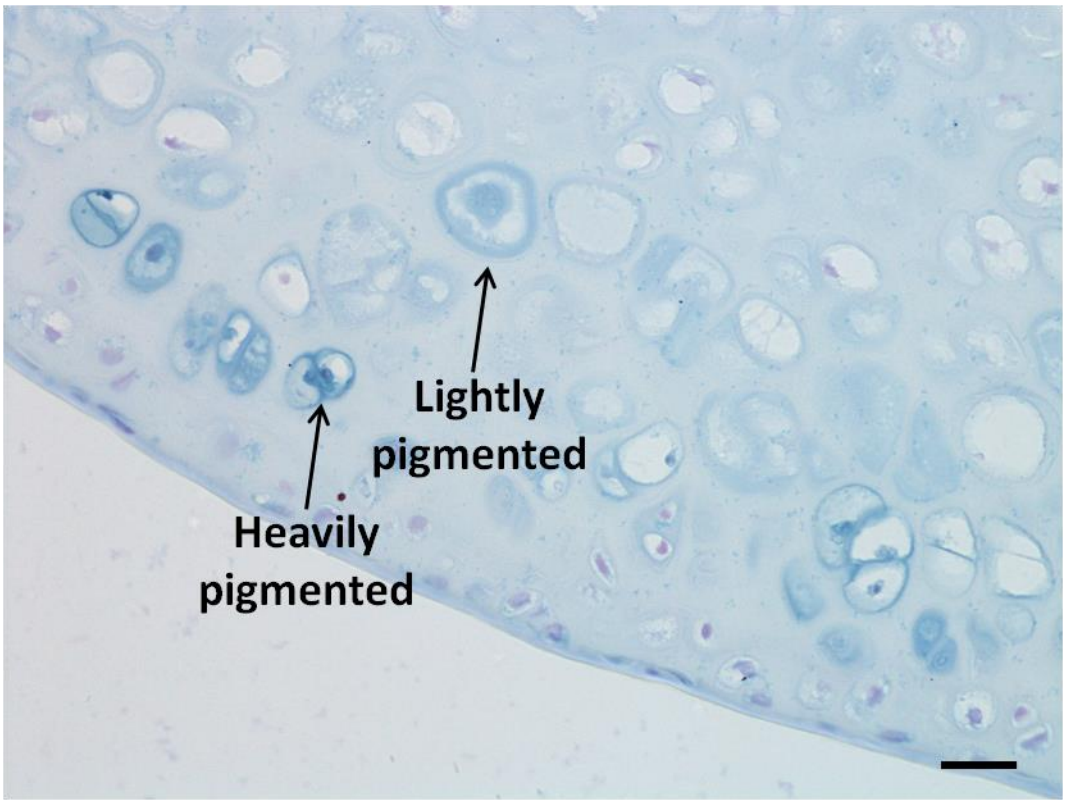

Figure 4.9 – Different stages of pigmentation in the femoral head of a 65.7 week old BALB/c Hgd-/- mouse. Both heavy and lightly stained chondrons were located in close proximity to one another. Section taken from BALB/c Hgd-/- 50.3 & stained with Schmorl's. Bar = 20µm.

4.3.3.2 Calcaneus

Large numbers of pigmented chondrons were clustered at the site of insertion of the Achilles tendon (Fig. 4.10). This area is subject to significant loading over time which may have had an effect on the amount of pigmentation at this area. Most of the chondrons located in the calcaneus were heavily pigmented and hypertrophic, both consistent with the data obtained from the tibio-femoral joint of aged Hgd-/- mice.

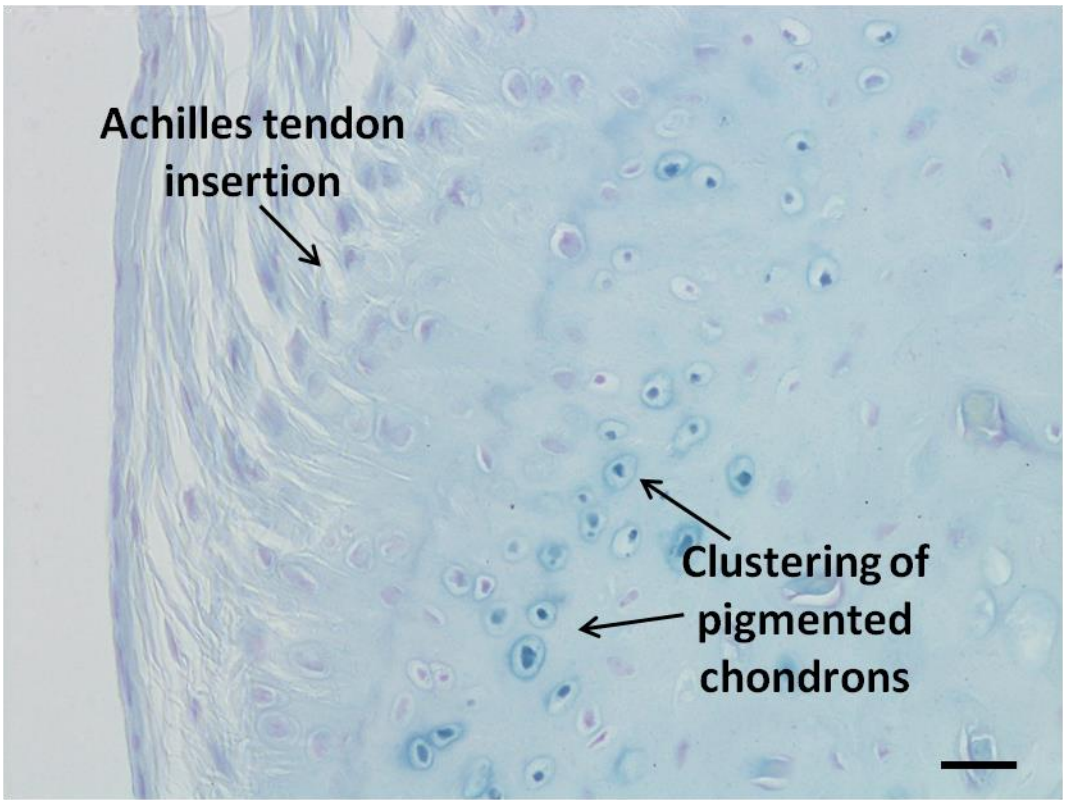

Figure 4.10 – Clustering of pigmented chondrons in the calcaneus of a 65.7 week old BALB/c Hgd-/- mouse. Large numbers of heavily pigmented chondrons were located adjacent to the insertion of the Achilles tendon in the calcaneus. Section taken from BALB/c Hgd-/- 50.3 & stained with Schmorl's. Bar = 20µm.

4.3.3.3 Humerus epicondyles

Significant amounts of pigmentation were located at the lateral epicondyle and radius of the humerus (Fig. 4.11). Heavily pigmented chondrons were scattered throughout the ACC of this area (Fig. 4.12) which was consistent with the location of pigmented chondrons in the tibio-femoral joint of the mice. Again, this area is heavily loaded in mice which may account for the high proportion of pigmented chondrons located in this area.

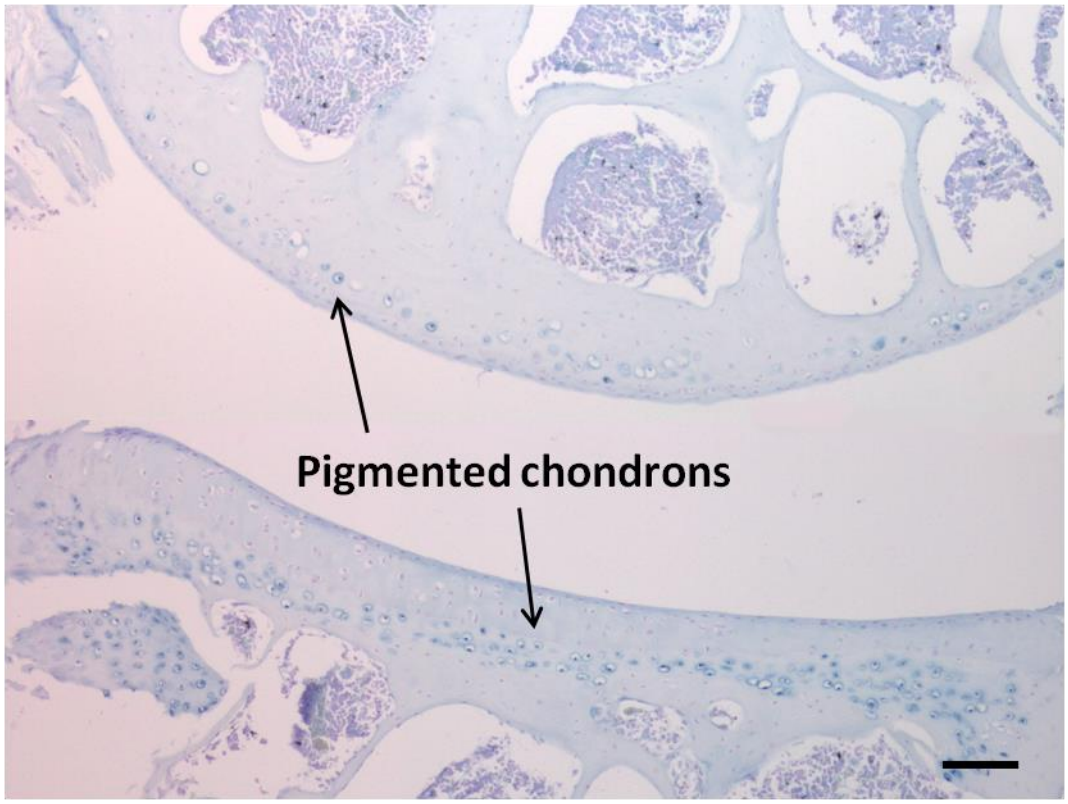

Figure 4.11 – Dense pigmentation in the lateral epicondyle of the humerus and the radius from a 65.7 week old BALB/c Hgd-/- mouse. Large numbers of heavily pigmented chondrons were spread throughout the joint, similar to that observed in the tibio-femoral joint. Section taken from BALB/c Hgd-/- 50.3 & stained with Schmorl's. Bar = 10µm.

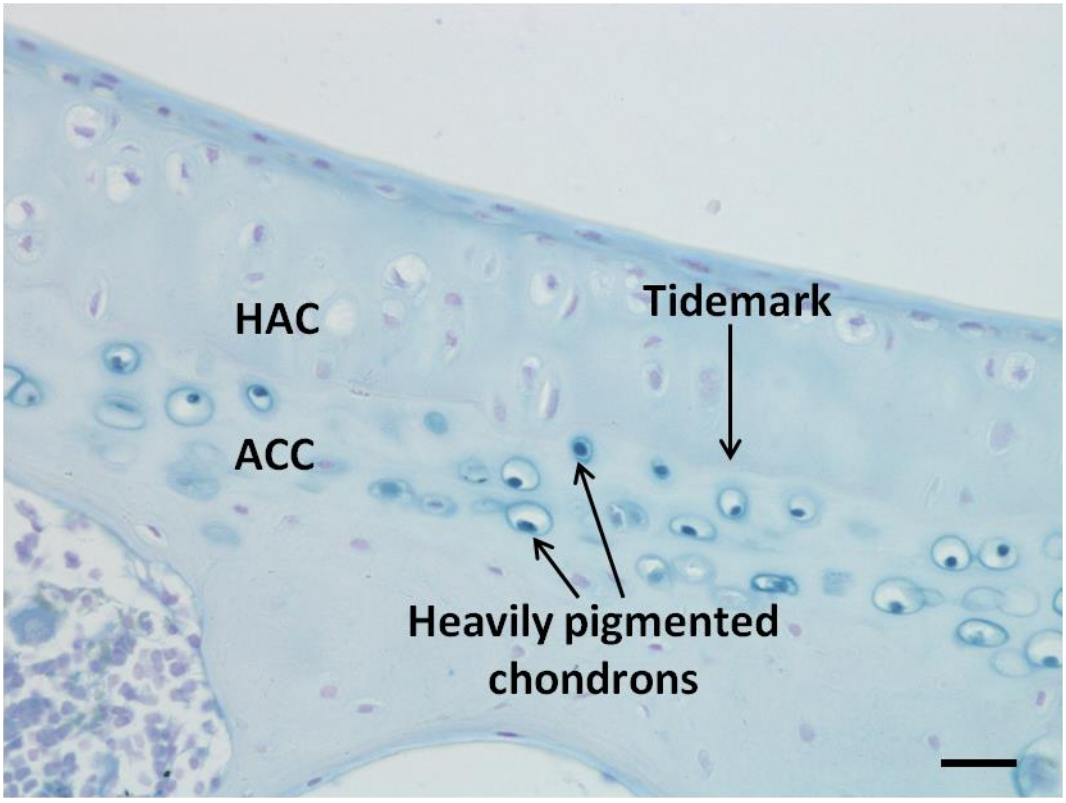

Figure 4.12 – Localisation of pigmentation to articular calcified cartilage in the radius of a 65.7 week old BALB/c Hgd-/- mouse. Pigmented chondrons where all located within the ACC, identical to that observed in the tibio-femoral joint. Section taken from BALB/c Hgd-/- 50.3 & stained with Schmorl's. Bar = 20µm.

The identification of pigmented chondrons in all three joints examined was encouraging as it highlighted the validity of the Hgd-/- mice as a model of ochronosis in humans. The amount of pigmented chondrons, and the phenotype they displayed was consistent with previous observations in the tibio-femoral joints of aged BALB/c Hgd-/- and BL/6 Hgd-/- mice. Although no young mice were examined it is expected they would show the same age related pattern of increasing pigmentation as seen in the tibio-femoral joint (Chapter 3).

4.3.4 Localization of ochronotic pigment to articular calcified cartilage

Microscopic analysis of human AKU samples has shown in severe cases that pigmentation, although initiating in the ACC, progresses throughout both the ACC and HAC. From the murine studies it was clear that pigmentation initiated in, and was localised to areas of calcified cartilage only. Calcified cartilaginous areas of articular cartilage, fibrocartilage, meniscus, and osteophytes, all became pigmented in the tibio-femoral joint of both strains of Hgd-/- mice. In the following photomicrograph (Fig. 4.13), the tidemark has been highlighted which separates the HAC and ACC, making it easy to identify that pigmentation was localised to the ACC in the femoral condyles and TP.

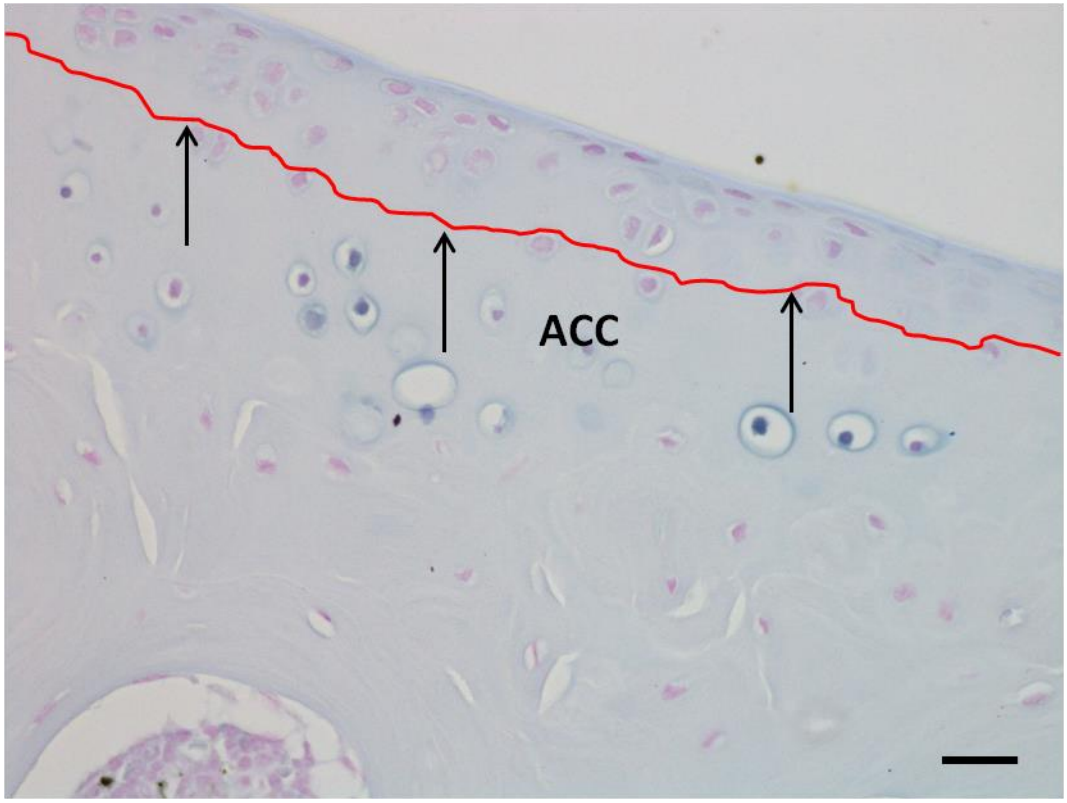

Figure 4.13 – Localisation of pigmentation to the articular calcified cartilage in the medial tibial plateau of a 31.7 week old BL/6 Hgd-/- mouse. Arrows indicating the tidemark highlight the localisation of pigmented chondrons to the ACC. Section taken from BL/6 Hgd-/- 99.4 & stained with Schmorl's. Bar = 20µm.

Dense areas of pigmented chondrons were located in the calcified fibrocartilage of entheses attached to the femoral condyles (Fig. 4.14). These areas are exposed to significant amounts of mechanical loading which may account for the large quantity of pigmentation seen in them.

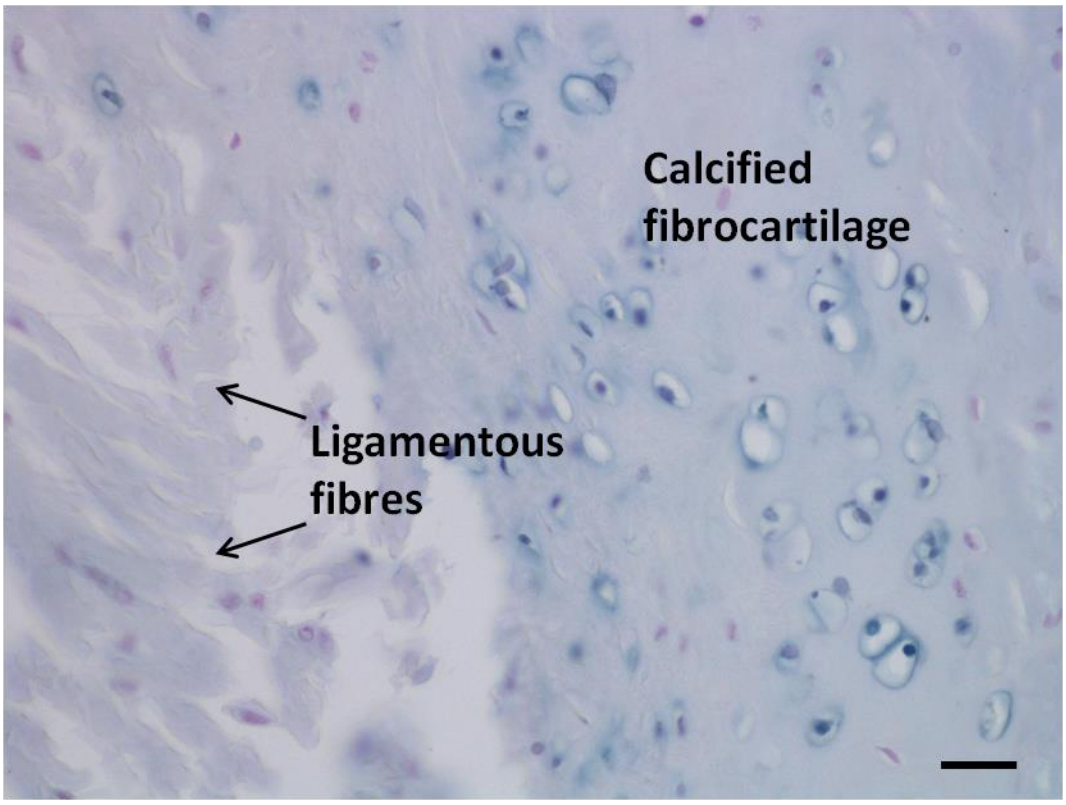

Figure 4.14 – Pigmentation in the enthesis of a 61.3 week old BALB/c Hgd-/- mouse. Pigmented chondrons were seen in the calcified area of the fibrocartilage. Section taken from BALB/c Hgd-/- 59.2 & stained with Schmorl's. Bar = 20µm.

Ossification of the menisci was observed in several of the Hgd-/- mice, in each case pigmented chondrons were identified in the calcified cartilage of the meniscus. The formation of bone in the meniscus of mice is not an uncommon occurrence [127], however it is in humans [128, 172]. Although meniscal ossicle's were observed in mice with OA changes, their formation is a normal phenomenon associated with

ageing. The following photomicrograph, from the LM of a 60 week old BALB/c Hgd-/- mouse, shows pigmented chondrons in calcified cartilage surrounding an area of ossification (Fig. 4.15). Osteophyte formation was also common in Hgd-/- mice. Pigmented chondrons were present in every osteophyte and located in the calcified cartilage surrounding the new bone which had formed (Fig. 4.16).

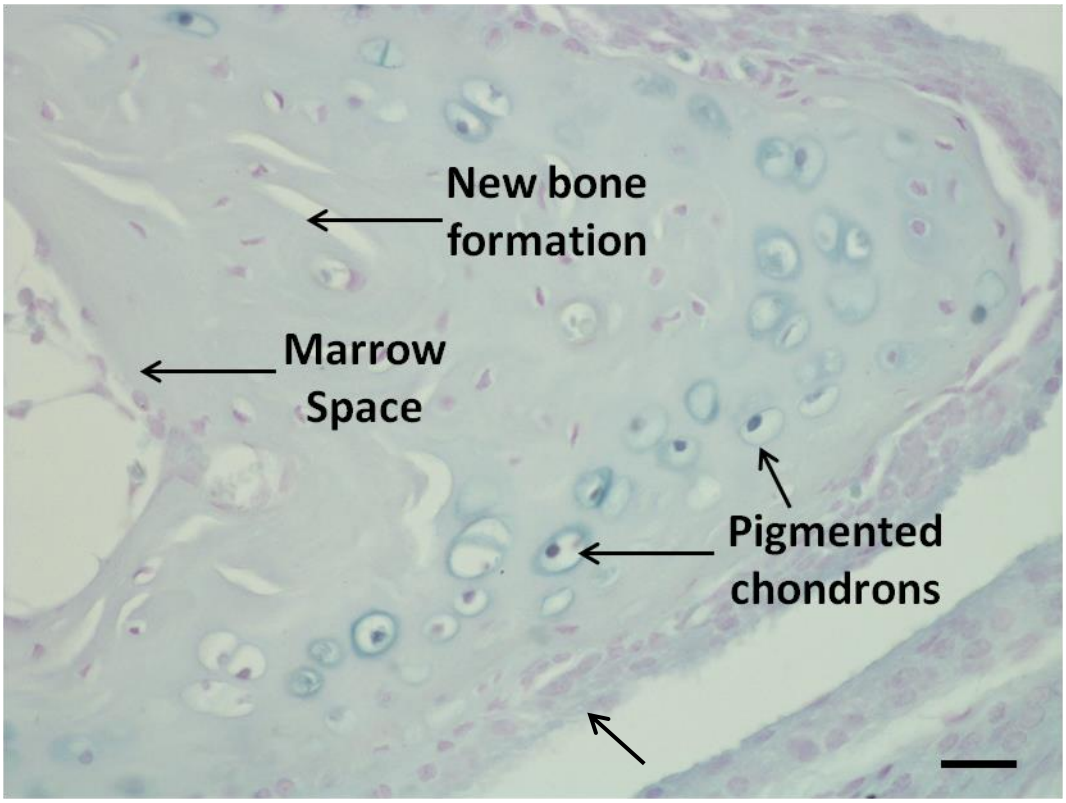

Figure 4.15 – Pigmentation of the lateral meniscus in a 60 week old BALB/c Hgd-/- mouse. Pigmented chondrons, both heavily and lightly stained, were located adjacent to the formation of new cortical bone in the meniscus. A thin layer of uncalcified cartilage (bottom arrow) contained no pigmented chondrons. Section taken from BALB/c Hgd-/- 61.3 & stained with Schmorl's. Bar = 20µm.

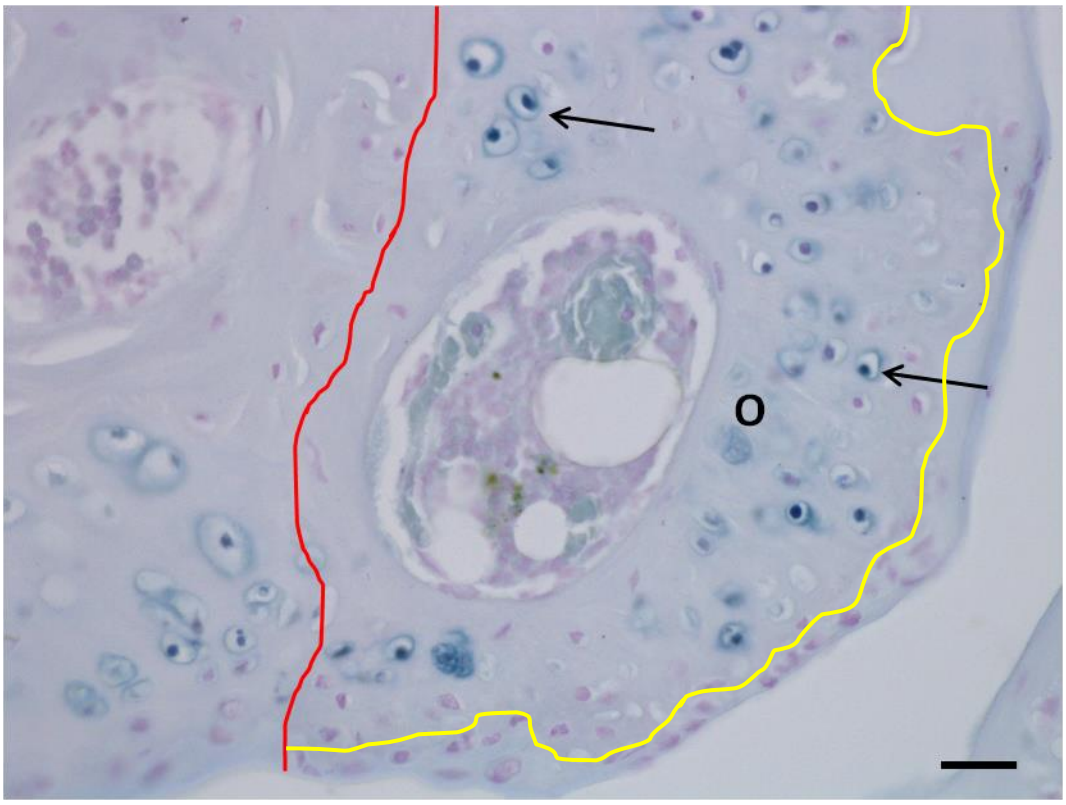

Figure 4.16 – Pigmented chondrons in the calcified cartilage of an osteophyte. The formation of the osteophyte (**O**), denoted by the red line, is associated with osteoarthropathy. All pigmented chondrons (arrowed) in the osteophyte were localised to the calcified cartilage. This is highlighted by the yellow line which is representative of the tidemark separating uncalcified and calcified cartilage. Section taken from BALB/c Hgd-/- 61.4 (60 weeks) & stained with Schmorl's. Bar = 20μm.

The localization of pigmentation to calcified cartilage is an interesting observation as it differs slightly from that seen in human ochronotic samples where pigmentation is seen in both the ACC and HAC. Little is known about the exact structure of ochronotic pigment or how it becomes deposited in chondrons and cartilage however this finding appears to show that the initial key interactions take place in calcified cartilage.

4.5 DISCUSSION

The results detailed in this Chapter reveal interesting pathological features of Hgd-/- mice, most of which show similarities to the pathogenesis of AKU in humans. Taylor and colleagues [36] have previously proposed a mechanism for the initiation and progression of ochronotic osteoarthropathy in humans involving the ACC and SCB. They state that pigmentation initiates following a change in the matrices of the ACC which alters their composition and/or organisation thus facilitating deposition of ochronotic pigment, initially in the PCM before progressing intracellularly. It is vitally important that the mechanism of pigment deposition is identified as it will provide a greater understanding of the pathogenesis of AKU and could lead to the identification of new therapeutic targets. Following on from the natural history study of ochronotic osteoarthropathy in Hgd-/- mice, in Chapter 3 of this thesis, further data analysis of the histological samples obtained revealed details about the staging of chondron pigmentation in Hgd-/- mice.

The first identifiable sign of pigmentation in BALB/c Hgd-/- mice was the presence of pericellular staining in a 15.7 week old mouse (Fig. 4.1). Consistent with the human data reported by Taylor *et al* [36], pigmentation appeared to initiate in the PCM of individual chondrons specifically located in the ACC. Pigmentation then progressed intracellularly (Fig. 4.2) before the cells became pyknotic (Fig. 4.3). This process appears to be very similar to the process of pigmentation in humans suggesting that the pathogenesis of ochronosis in the two species may be closely related. The appearance of pigmentation in the PCM, the first stage of ochronotic osteoarthropathy, is likely linked to an initial change in the composition and/or organisation of the matrix in this area (Fig. 4.17). It is possible this is linked to repetitive and abnormal loading of the articulating joints which has also been linked with the development of OA [173]. Abnormal loading can cause chondrocytes to express catabolic phenotypes resulting in expression and upregulation of matrix degrading proteases which may further increase pigment deposition. The PCM of chondrons is rich in molecules including HA [174], large and small proteoglycans

including perlecan [175], biglycan [176], decorin [177], and types VI [69], IX [178], and X [179] collagen. These molecules are vitally important to cellular activity and any alteration to them, and subsequently the PCM may render the chondrons susceptible to pigment deposition (Fig. 4.16). It has been shown that the PCM of chondrons in disease states has drastically different mechanical properties to the PCM of normal chondrons [180] which is almost certainly a factor in AKU and pigment deposition. As initial pigment deposition takes place in the PCM it is possible a change occurs in this area which leads to the deposition of pigment. It may be that the mechanical properties of the PCM become altered prior to or following initial pigment deposition, resulting in abnormal strain distribution across the tibio-femoral joint and thus leading to further damage and increased pigment deposition (Fig. 4.16). However it is still not known what the initiating factor(s) are that lead to deposition of ochronotic pigment in the PCM. Using a selection of different techniques to isolate chondrons it may be possible to determine if altered mechanical properties of the PCM play a role in pigment deposition. Low-speed homogenisation [181] and enzymatic isolation [182] can be used to characterize chondrons however both have limitations with regards to the amount, and structure of the chondrons isolated. Alexopoulos and colleagues have developed a novel method to mechanically isolate chondrons using what they term a 'microaspirator' [180]. Using this technique the Young's modulus of isolated chondrons can be determined and any change in the mechanical properties of the chondron identified. This technique would be useful to determine if the PCM of ochronotic chondrons from Hgd-/- mice differs from the PCM of chondrons isolated from WT mice. Any variations observed in the Young's modulus between ochronotic and normal chondrons would then appear to show that the PCM of ochronotic chondrons becomes altered resulting in deposition of pigment. Taylor and colleagues have shown there is less extractable proteoglycans in ochronotic cartilage, compared to normal and OA cartilage, which further highlights the apparent association between altered mechanical properties and pigment deposition [183]. Collagens present in the PCM are the most probable deposition site for pigment; evidence for this has been presented by Taylor *et al* [28]. Cleavage of proteoglycans in the PCM may precede pigment deposition as once they are

cleaved binding sites on collagen fibres become uncovered, exposing a site where the pigment polymer can bind. Whether these biomechanical and biochemical changes are specific to AKU tissues is still unknown. It is possible that these changes occur in non-AKU (normal) tissues and HGA is simply a marker of tissue damage. Preliminary studies have shown that incubating normal cartilage in a solution of HGA leads to areas of focal pigmentation in the tissue [184]. Further work is required to validate the initial findings however they appear to suggest that molecules such as HGA may be able to identify areas of tissue damage. This would explain why some chondrons are pigmented, yet others in very close proximity are non-pigmented.

The quantitative analysis shown in Fig. 4.7 supports the proposed staging of pigmentation in BALB/c and BL/6 Hgd-/- mice. The decrease in the number of non-pigmented chondrons as the mice aged is consistent with the hypothesis that increased amounts of pigment are deposited with age. The fact that non-pigmented chondrons are present even in the oldest BALB/c and BL/6 Hgd-/- mice appears to show that a change must occur in the PCM of individual chondrons in order for them to become pigmented. Staining of the PCM of chondrons was identified as the first sign of pigment deposition in Hgd-/- mice. The appearance of PCM stained chondrons throughout the lifetime of Hgd-/- mice suggests that pigmentation initiates in individual chondrons at different time points, and continues throughout life. The gradual increase of light and heavily stained chondrons with age was expected as it was shown in the natural history study of Hgd-/- mice that pigmentation increases with age. With increasing amounts of ochronotic pigment becoming deposited in the tibio-femoral joint over time, the appearance of more heavily stained chondrons is not surprising. This is consistent with the proposed pigmentation pathway, both in Hgd-/- mice and in humans. The data obtained from the quantitive analysis of the proposed pigmentation pathway supports the differing stages of chondron staining and shows that pigmentation does initiate extracellularly before progressing into the cell.

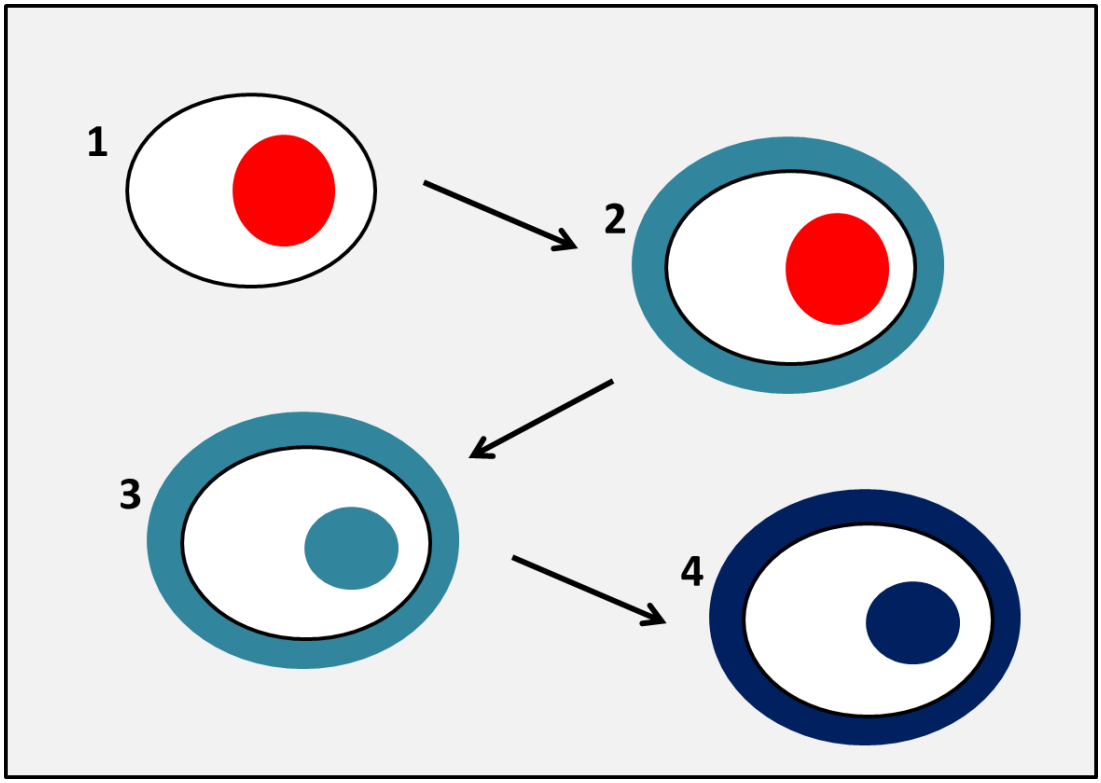

Figure 4.17 – Diagram of the stages of pigmentation in Hgd-/- mice. Although the exact mechanism of pigmentation is still unknown, certain key factors appear to play important roles. Mechanical loading is involved in the development of OA and appears to be implicated in the initiation and progression of ochronotic osteoarthropathy. Changes in the PCM following abnormal loading seems to result in healthy chondrons (1) becoming susceptible to pigment deposition which initiates in the PCM (2). Alterations in strain distribution resulting from changing PCM mechanical properties likely leads to an increase in the amount of pigment deposited in the cells (3). Changes in chondrocyte function and activity also appear to play a role in pigment deposition and may ultimately result in them becoming heavily pigmented (4).

Mechanical and oxidative damage are key factors in cartilage and chondron breakdown, and have been linked with OA initiation and progression [185-189]. The early onset of OA is linked with AKU in humans [190] and results from this thesis have also shown it to be present in the murine model of AKU. There appears to be a role for both mechanical and oxidative damage in the pigmentation process. It is possible that mechanical damage, through abnormal load distribution, is involved in the initiation and progression of pigmentation. Data from Taylor *et al* [36] has shown that presence of pigment stiffens the cartilaginous matrix altering its biomechanical properties. Damage resulting from abnormal load distribution may result in the tissue becoming susceptible to pigmentation. As seen from the figures (Figs. 4.1, 4.2, 4.3 & 4.4) once pigmentation is initiated it triggers a cascade of downstream events leading to accumulation of pigment and the formation of OA. Oxidative damage may also be involved in the proliferation of pigmentation. Both HGA and its quinone intermediate, BQA, have previously been shown to induce DNA damage through the formation of reactive oxygen species (ROS) [59, 191]. ROS also leads to senescence in chondrocytes [192]. It is possible increased formation of HGA/BQA causes damage to the DNA of healthy chondrons through generation of ROS, rendering them senescent and susceptible to pigmentation. The depletion of anti-oxidants by both HGA and BQA can result in damage to macromolecules in cartilage [193]. The resulting structural alterations of the cartilaginous matrix make this another possible mechanism of pigment deposition. The close association of AKU and OA, and the possible roles of mechanical and oxidative damage underline the importance of these processes to the initiation and progression of ochronotic osteoarthropathy.

Although the staging of chondrons in BL/6 Hgd-/- mice did not appear to initially follow the pattern observed in BALB/c Hgd-/- mice (Fig. 4.5), sections from older mice showed the chondrons did appear in all four stages of pigmentation (Fig. 4.6). It is possible that heavy staining of chondrons in young mice is linked to the apparent association between ochronotic pigment, also known as pyomelanin [158], and melanin. BL/6 mice have a considerable amount more melanin than

BALB/c (albino) mice therefore, as ochronotic pigment and melanin are believed to be structurally related, it is possible they have an increased amount of ochronotic pigment forming leading to earlier detection and increased amounts of deposition in BL/6 Hgd-/- mice.

The identification of pigmentation in the femoral head (Fig. 4.8), calcaneus (Fig. 4.10), and humerus epicondyles (Fig. 4.11) in Hgd-/- mice was a significant discovery as it highlighted the practicality of the Hgd-/- mice as a model of human AKU. The femoral head in particular is a site of severe ochronotic osteoarthropathy in humans [30, 194] so it is of great importance that Hgd-/- mice showed signs of ochronotic osteoarthropathy in this joint. Pigmented chondrons in the femoral head, similar to those in the tibio-femoral joint, were localized to the ACC and appeared to show the same initiation and progression process (Fig. 4.9). Macroscopically no pigment was observed however this is consistent with all ochronotic joints in Hgd-/- mice. All three joints were heavily pigmented which is consistent with the finding that pigmentation increases with age. Although none of these joints were looked at in younger Hgd-/- mice previous results obtained from the tibio-femoral joint of younger mice suggest that they would be sparsely pigmented and the number of pigmented chondrons would increase linearly with age. Mechanical damage resulting from persistent heavy loading of all the joints is likely to have contributed to pigmentation, as is the case in the tibio-femoral joint. As expected all pigmented chondrons identified were hypertrophic and located to the ACC, consistent with data already obtained from Hgd-/- mice. The majority of pigmented chondrons in the calcaneus and humerus epicondyles were heavily stained indicating they were in the final stages of pigmentation. There were some lightly stained chondrons in the femoral head (Fig. 4.9) which is consistent with the appearance of some chondrons in the tibio-femoral joint of old Hgd-/- mice. Although the three different joints were only examined in one aged BALB/c Hgd-/- mouse, the data collected provides important information on the pathogenesis of ochronosis in the murine model of AKU.

One interesting pathological feature of ochronosis in Hgd-/- mice was the localization of pigmented chondrons to the ACC (Figs. 4.12, 4.13, 4.14 & 4.16). Calcified cartilage has been less extensively studied than hyaline cartilage and bone due to their significant involvement in OA however in the case of AKU it is of critical importance. It is still unclear as to why pigmentation initiates in the ACC, rather than in the HAC. There must be a close association between molecules present in the ACC and ochronotic pigment, as in both humans [36] and mice pigmentation initiates in this region. Little is known about the complete mineral content of the ACC [195], however studies have shown that the major mineral component by weight is hydroxyapatite [196, 197], similar to the SCB. It is unlikely that ochronotic pigment binds to hydroxyapatite as no pigmentation was located in the bone matrix, of which a significant amount is hydroxyapatite. Chondrocytes located in the ACC exhibit a hypertrophic phenotype while those in HAC do not. It is possible this is linked to the initiation of pigmentation in the ACC as hypertrophic chondrocytes are known to express factors which actively degrade components of the matrix. Alteration of the PCM and its mechanical properties may result in initial pigment deposition leading to further disruption of matrix mechanical properties and in turn, proliferation of pigment deposition in affected chondrons.

The most probable binding sites for pigment in the ACC are collagen [28]. Type VI collagen is the primary collagen in the PCM of chondrons [198, 199] therefore these fibre types are likely to be one of the principal binding sites for ochronotic pigment. Type VI collagen is also found in calcified fibrocartilage, particularly in the menisci and intervertebral discs [200]. Pigmentation is present in the menisci of Hgd-/- mice (Chapter 3) and although the intervertebral discs have not been examined in the Hgd-/- mice, they are a primary site of pigmentation in AKU patients. With large numbers of pigmented chondrons observed in the calcified fibrocartilage of the entheses it is possible that type VI collagen is a preferential binding site for ochronotic pigment. Type II and type X collagen are found in the ACC [195, 201], whilst type II is also the major component of the HAC [160, 195]. Therefore it's possible both are alternative binding sites for ochronotic pigment. Type X collagen

is expressed by hypertrophic chondrons [179, 202] and is found in their PCM [203], along with small amounts of HA [204]. All of the pigmented chondrons in the ACC expressed a hypertrophic phenotype. With pigmentation thought to initiate in the PCM of ochronotic chondrons in both humans [36] and Hgd-/- mice (Chapters 3 & 4) it is possible that type X collagen, along with type VI, is a primary binding site for ochronotic pigment. In humans it is likely that the pigment also binds to type II collagen, GAGs and other molecules as blanket pigmentation of the entire articular cartilage is often observed. However as this stage is never reached in Hgd-/- mice binding of pigment is most probably reserved to the collagens located in the PCM of hypertrophic chondrons in the ACC.

The data discussed in this Chapter further highlights the strength of the murine model of AKU to replicate the pathogenesis seen in human AKU patients. The proposal of a mechanism which is identical to the one seen in humans, the discovery of pigmentation in several different articulating joints, and the localization of pigmentation to the ACC suggests that the murine model of ochronotic osteoarthropathy is an excellent model for AKU research.

5. Testing the efficacy of nitisinone in treating ochronotic osteoarthropathy in Hgd-/- mice

5.1 INTRODUCTION

This Chapter investigated the effects of the compound nitisinone on the initiation and progression of ochronotic osteoarthropathy in alkaptonuric mice. Treatment options for AKU are currently restricted to pain relief and eventually joint replacement surgery(s) leaving patients with persistent and excruciating pain for extended periods of time. Following the identification of ochronotic osteoarthropathy in Hgd-/- mice (Chapter 3) there is now a model which can be used to test the efficacy of different therapies for the treatment of AKU. Nitisinone acts on the tyrosine catabolic pathway (Fig. 1.1) and has been a major success in alleviating the fatal effects of HT-1 [49]. By inhibiting the HPPD enzyme, nitisinone not only prevents the formation of toxic products key to the development of HT-1 but also the formation of HGA. As a result nitisinone was previously trialled as a treatment for AKU patients [52, 53]. The three year trial undertaken at the National Institute of Health [53] provided disappointing results, primarily due to the end-point chosen. Hip rotation was selected as the parameter to determine the efficacy of nitisinone however, the results showed there to be significant variability in the range of motion in the same patients from visit to visit. The data collected from this trial highlighted the need for a whole of life study to determine the benefits and detrimental effects of treating AKU patients with nitisinone for long periods of time. This Chapter details several studies undertaken in which the aims were to identify the effects of nitisinone on pigment deposition and plasma HGA levels throughout the lifespan of Hgd-/- mice. Until now there has been no previous evidence offered to show that nitisinone does inhibit ochronotic pigmentation. The results detailed in this Chapter show nitisinone is able to completely prevent pigmentation when given throughout life, stop further deposition of ochronotic pigment when given mid-life and reduce lifetime levels of plasma HGA, with little or no side-effects. These results reveal that early-stage treatment of AKU with nitisinone can be effective in preventing deposition of ochronotic pigment and the severe osteoarthropathies associated with AKU.

5.2 DESIGN OF STUDY

In both the lifetime and mid-life treated groups the dosage of nitisinone provided in the drinking water of the mice was 4 mg/l. This dosage was selected from HPLC studies which showed this to be the lowest dose which had an effect on HGA levels.

Once the *in vivo* portion of the study was completed, the left knee was dissected out from each mouse and serial sections were stained with H&E and Schmorl's stain to highlight differences in pigmented chondron numbers, and joint changes.

5.3 RESULTS

5.3.1 Lifetime treatment with nitisinone

A cohort of 16 BALB/c Hgd-/- mice (eight male, eight female) were provided with an ad libitum supply of water containing 4mg/l of nitisinone from 8 to 67 weeks of age. The control group of 16 BALB/c Hgd-/- mice (nine male, seven female) had no drug in their drinking water from birth until 71 weeks of age. Plasma was taken immediately prior to treatment, and then sampled regularly by tail bleed over the lifespan of the mice.

5.3.1.1 Treated group

Of the sixteen mice treated with nitisinone, seven were kept in the study until the end of their lives and six were culled halfway through the study. Three mice were discovered to be deceased upon inspection of their cages. All three were male, aged 37 weeks (2) and 53 weeks (1) respectively. The deaths of these mice were not considered to be a consequence of nitisinone administration as death rates similar to these are often observed in long term animal studies. These mice were kept out of the study as they had started to undergo tissue necrosis before fixation therefore the results obtained from them could not be seen as consistent with the other mice in the study. Histology was performed on the mice culled halfway through the study. None of the six mice showed any pigmentation of chondrons and articular cartilage when examined under light microscopy. This was the first observation in alkaptonuric mice that nitisinone may be effective in preventing ochronosis.

The following results are from a selection of the mice treated with nitisinone over their lifetime. Some mice have been excluded as the results seen in all BALB/c Hgd-/- mice were identical.

5.3.1.1.1 BALB/c Hgd-/- 24.4 (♂) – 67 weeks

No pigmentation of chondrons or their surrounding matrices was identified throughout the knee joint of BALB/c Hgd-/- 24.4 (♂).

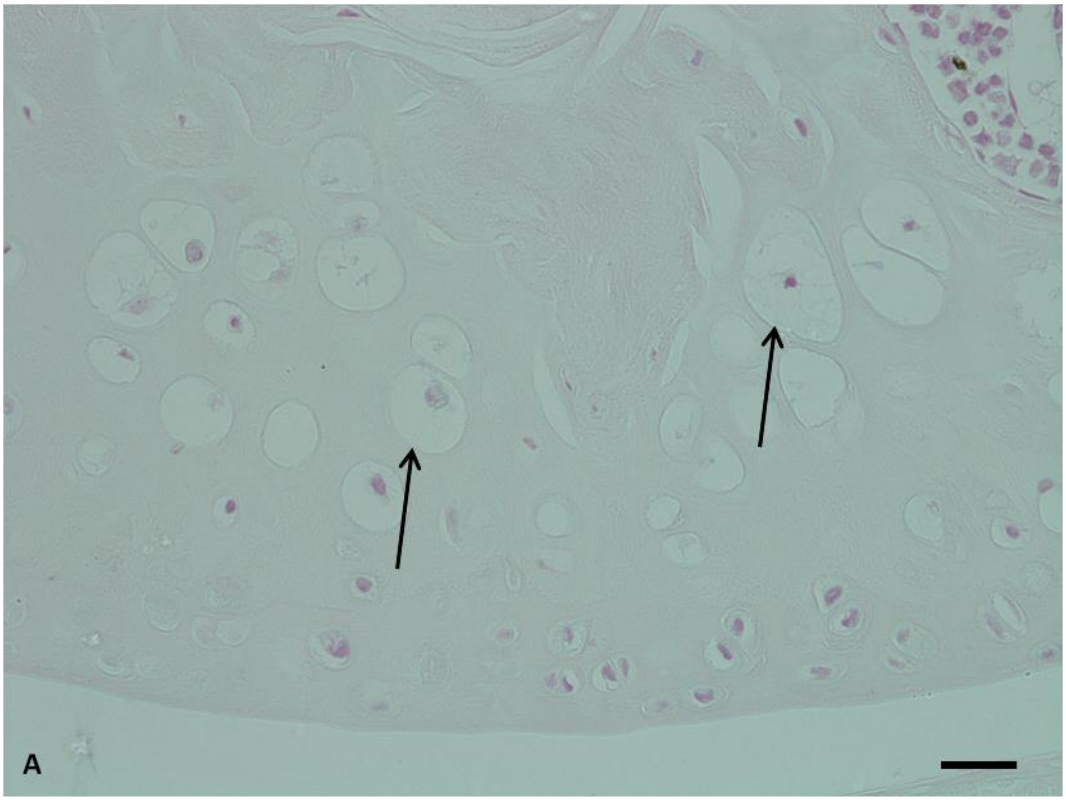

Figure 5.1 – Ochronotic pigment was not detectable in the medial femoral condyle of BALB/c 24.4, a 67 week old Hgd-/- mouse treated with nitisinone. Schmorl's staining did not reveal any chondrocytic (arrowed) or matrix pigmentation in ACC of the MFC. Bar = 20µm.

Figure 5.1 highlighted the effect of nitisinone when given for whole of life. No pigmented chondrons were located in the MFC or in any other area of the joint. Pigmented chondrons are usually localised to the ACC in Hgd-/- mice, however treatment with nitisinone prevented any chondrons from becoming pigmented.

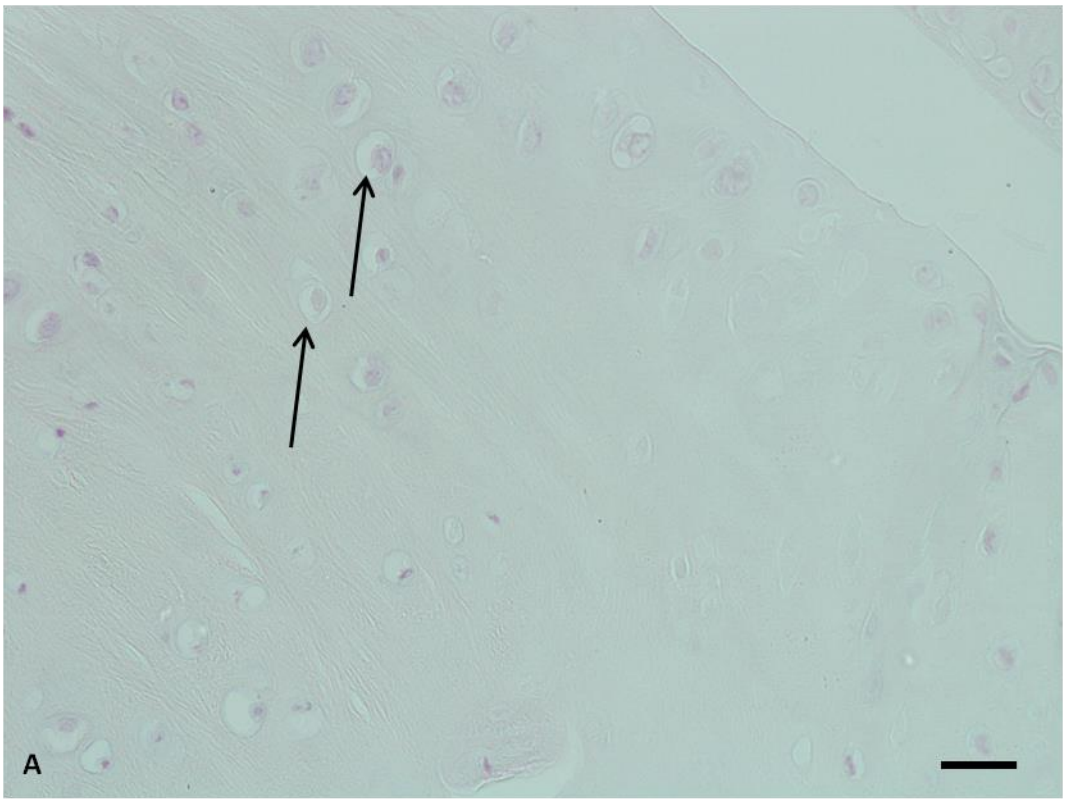

Figure 5.2 – Ochronotic pigmentation was not detectable in the intercondylar area of BALB/c 24.4, a 67 week old Hgd-/- mouse treated with nitisinone. Schmorl's staining did not reveal any pigmentation in the intercondylar area of the tibia (arrowed). This area becomes heavily pigmented in Hgd-/- mice. Bar = 20µm.

Figure 5.2 showed absence of pigmentation from the intercondylar area of the tibia in BALB/c Hgd-/- 24.4. This area becomes heavily pigmented in aged Hgd-/- mice, characterised by the dark blue staining of chondrons, yet is completely free of pigmentation when nitisinone is administered. There was no cartilage degeneration seen, although an osteophyte was present on the MTP.

5.3.1.1.2 BALB/c Hgd-/- 25.3 (♀) – 67 weeks

Pigmentation was absent from the knee joint of BALB/c Hgd-/- 25.3 (♀). Chondrons in all areas of the joint including the LFC (Fig. 5.3) and LTP (Fig. 5.4) were not pigmented and the articular cartilage showed no signs of damage or degeneration.

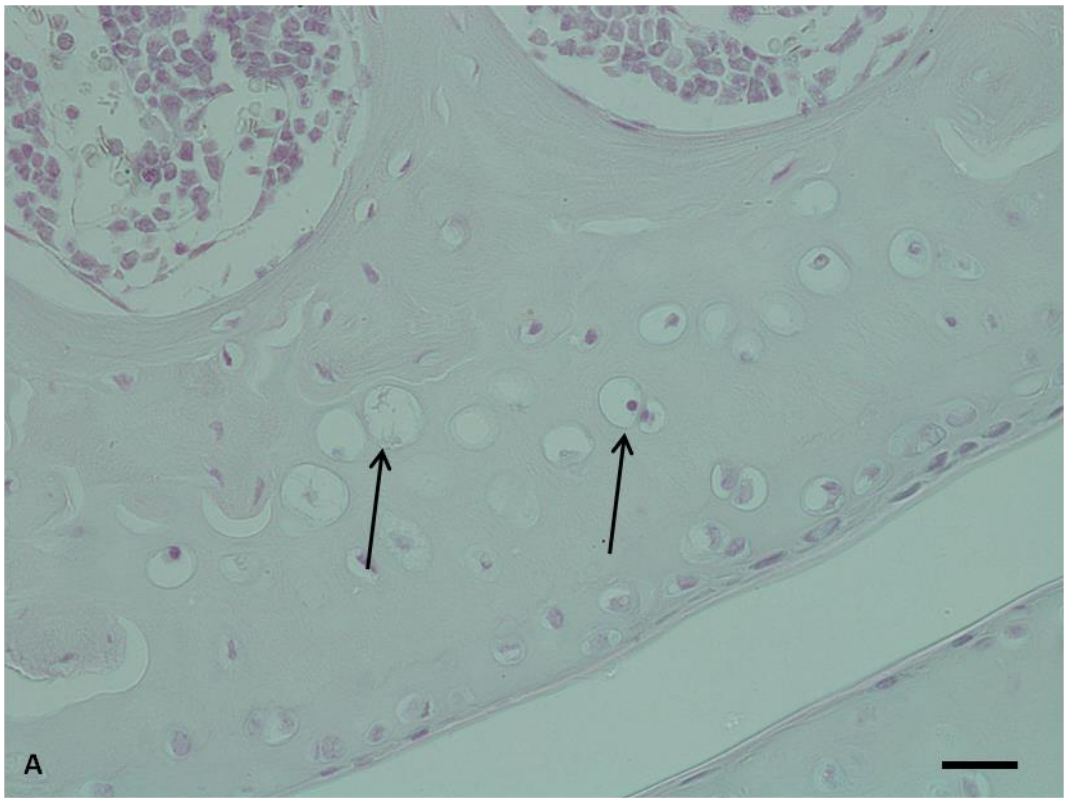

Figure 5.3 - Ochronotic pigmentation was not detectable in the lateral femoral condyle of BALB/c 25.3, a 67 week old Hgd-/- mouse treated with nitisinone. Schmorl's staining did not reveal any pigmented chondrons in the LFC of BALB/c Hgd-/- 25.3 (arrowed). Bar = 20µm.

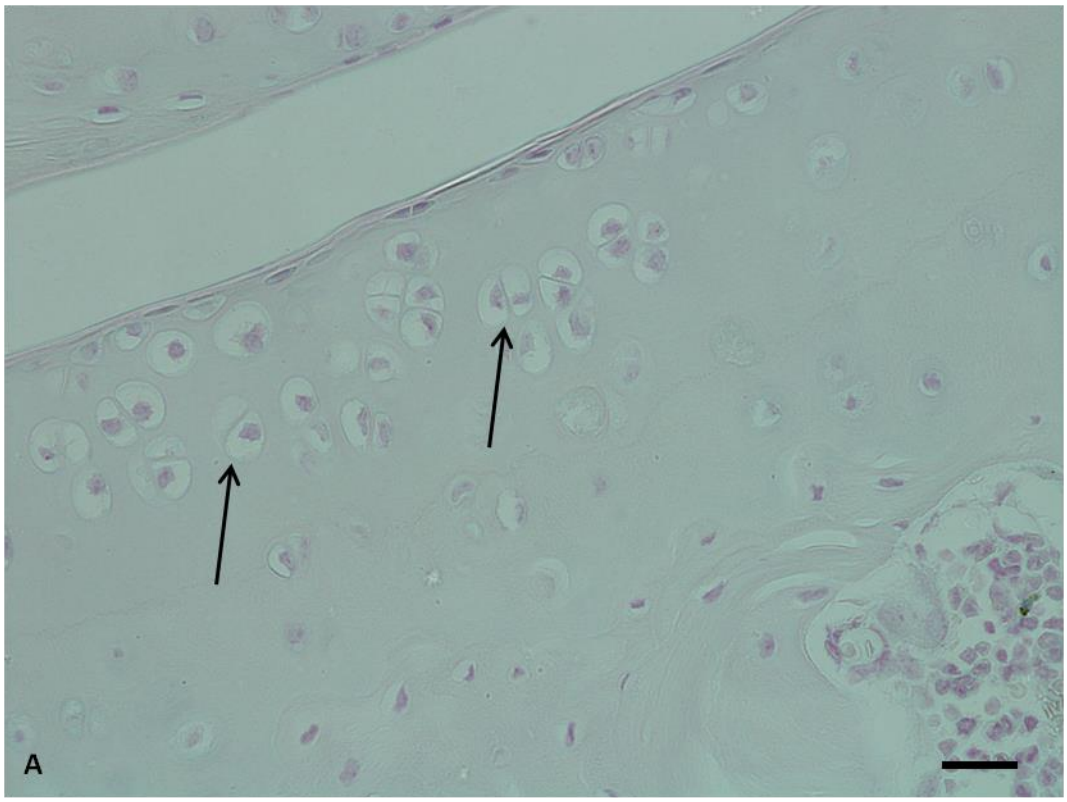

Figure 5.4 - Ochronotic pigmentation was not detectable in the lateral tibial plateau of BALB/c 25.3, a 67 week old Hgd-/- mouse treated with nitisinone. Schmorl's staining did not reveal any pigmented chondrons (arrowed) in the LTP of BALB/c Hgd-/- 25.3. Bar = 20µm.

The absence of pigmentation in another mouse treated with nitisinone highlighted the efficacy of the drug in preventing the deposition of pigment in the tibio-femoral joint. The chondrons in the joint appeared healthy and did not seem to be overly hypertrophic, especially in the LTP (Fig. 5.4). The lack of both cartilage degeneration and associated osteoarthropathy in the mice was encouraging and further demonstrated the efficacy of nitisinone to treat AKU.

5.3.1.1.3 BALB/c Hgd-/- 26.1 (♀) – 67 weeks

BALB/c Hgd-/- 26.1 (♀) displayed no signs of pigmentation throughout the knee joint. Chondrons in the ACC appeared relatively healthy and showed no signs of

ochronosis (Fig. 5.5). There did appear to be a small amount of SCB remodelling in the MTP (Fig. 5.5) and LFC (Fig.5.6). Cartilage damage and changes in bone are not uncommon to mice of old age, especially those on a BALB/c background as this strain is known to be associated with the onset of spontaneous OA [159].

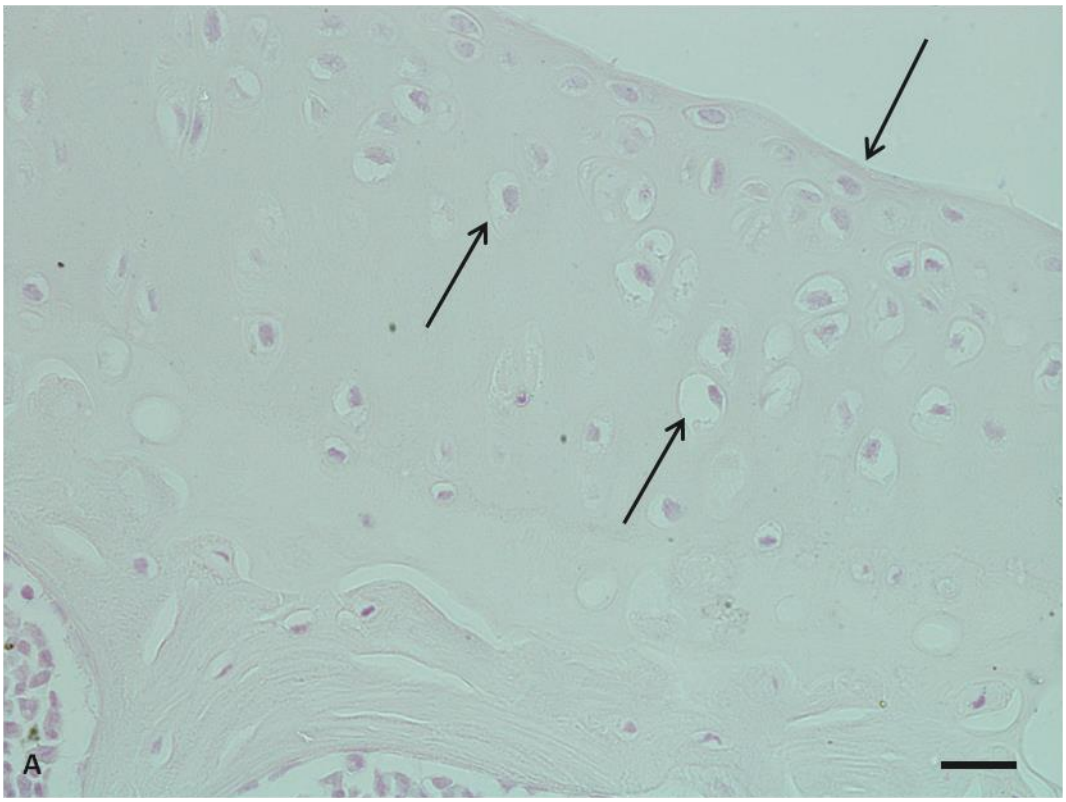

Figure 5.5 - Ochronotic pigmentation was not detectable in the medial tibial plateau of BALB/c 26.1, a 67 week old Hgd-/- mouse treated with nitisinone. Schmorl's staining did not reveal any pigmented chondrons (left arrows) in the MTP. Bar = 20µm.

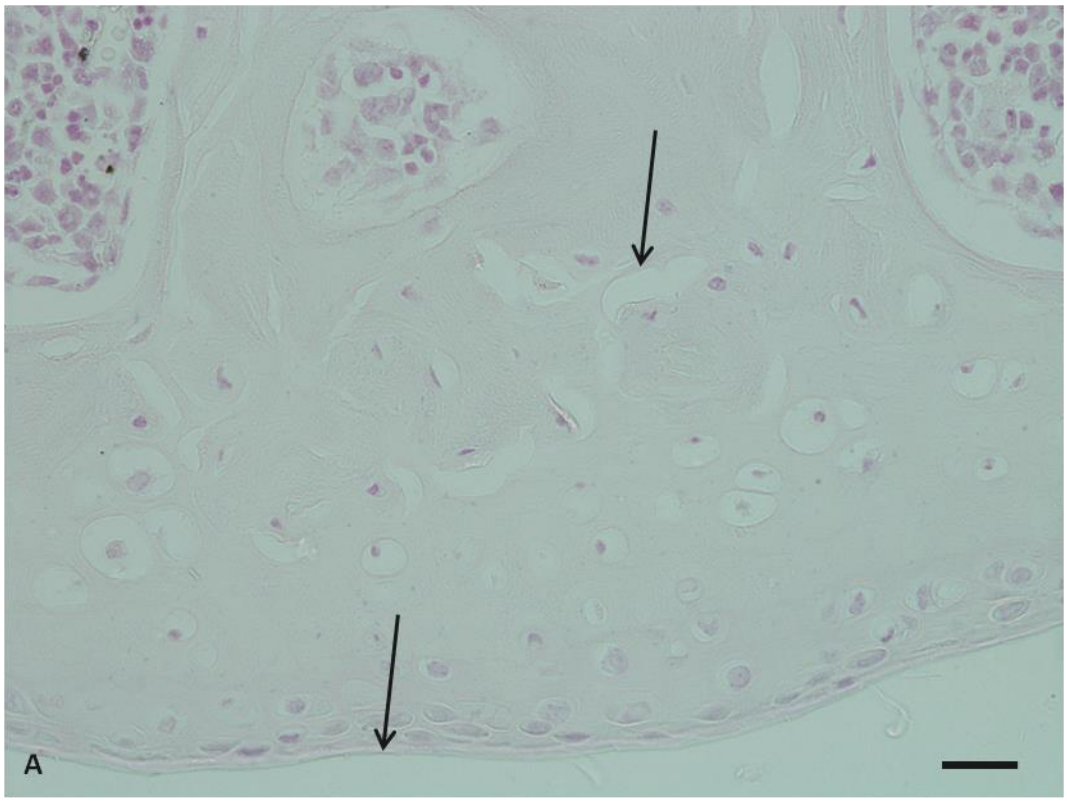

Figure 5.6 – Very minor fibrillation of the articular surface and subchondral bone remodelling in the lateral femoral condyle of BALB/c 26.1, a 67 week old Hgd-/- mouse treated with nitisinone. Very minor damage (left arrow) was seen on the articular surface of the LFC. Small amounts of SCB remodelling (right arrow) were located in the condyle which resulted in thinning of the ACC in some areas. Section stained with Schmorl's. Bar = 20µm.

Again, nitisinone prevented the deposition of ochronotic pigment in the chondrons and matrices in the cartilage. No blue staining, which is characteristic of pigmented chondrons, was observed in any areas of the joint. Signs of OA were present in the joint with cartilage degeneration and SCB remodelling both observed (Figs. 5.5 & 5.6).

5.3.1.1.4 BALB/c Hgd-/- 26.2 (♀) – 67 weeks

Like all previous mice described in the study, BALB/c Hgd-/- 26.2 (♀) contained no pigmented chondrons in any areas of the joint (Fig. 5.7). There did appear to be a very small amount of SCB remodelling taking place, most prominently in the LTP (Fig. 5.8). No cartilage degeneration was observed on any of the femoral condyles or along the TP.

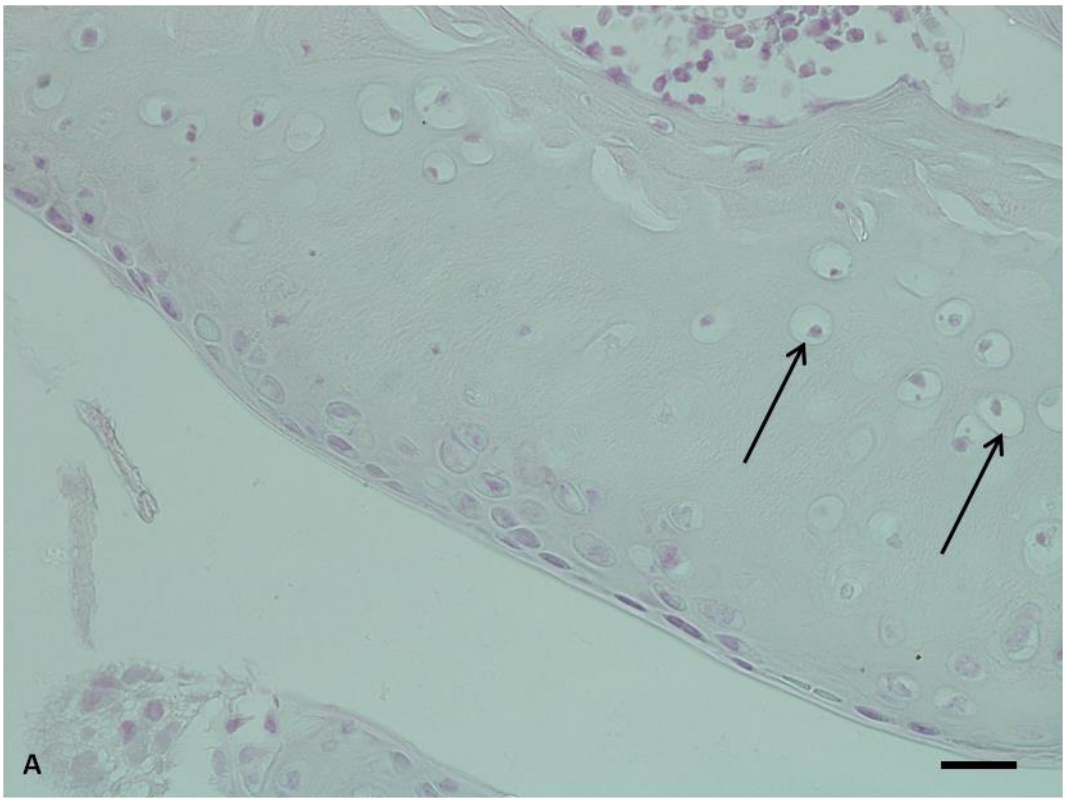

Figure 5.7 – Ochronotic pigmentation was not detectable in the medial femoral condyle of BALB/c 26.2, a 67 week old Hgd-/- mouse treated with nitisinone. Chondrons throughout the knee joint showed no signs of pigmentation. Two chondrons highlighted (arrowed) showed staining with the counter-stain NFR. Section stained with Schmorl's. Bar = 20µm.

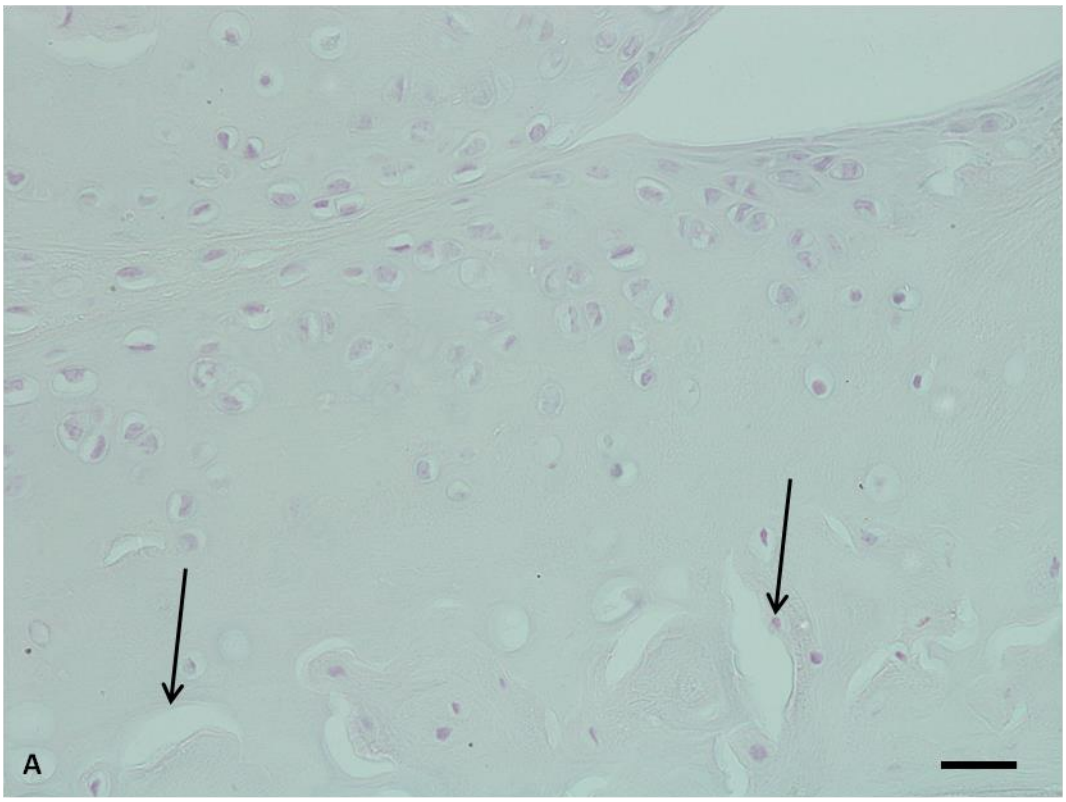

Figure 5.8 – Subchondral bone remodelling in the medial tibial plateau of BALB/c 26.2, a 67 week old Hgd-/- mouse treated with nitisinone. Small amounts of SCB remodelling were located in the MTP (arrowed). Chondrons above this area in the ACC showed no signs of pigmentation. Section stained with Schmorl's. Bar = 20µm.

Administration of nitisinone to BALB/c Hgd-/- 26.2 prevented pigmentation in the articular cartilage and the chondrons located within it. This was consistent with what had been seen previously in all of the BALB/c Hgd-/- mice administered nitisinone, regardless of whether they were culled halfway into the study or left until the end. Small amounts of SCB remodelling indicated the joint may have been becoming osteoarthritic however with no pigment deposited in the joint it was unlikely that the osteoarthropathy was associated with AKU. It is more likely to be related to the ageing of the mouse.

From the results shown it was clear that when given from the start of life, nitisinone prevented any deposition of ochronotic pigment throughout the whole knee joint. There were small signs of osteoarthropathy in a few of the mice but it is likely this was related to the ageing of the mice and not AKU. No adverse effects were reported which was encouraging as previous clinical trials with nitisinone, both in humans and rats, have seen tyrosine crystal formation and corneal lesions [53, 205]. These results show nitisinone to be an effective therapy in treating nitisinone when given for the whole of life and should be considered as a treatment for patients.

5.3.1.2 Control group

Of the sixteen mice in the control group, seven were culled halfway through the study and the remaining nine were kept until the end of the study. The results gained from the control group are similar to those of age matched samples included in the natural history study (Chapter 3) which was expected. They all showed signs of advanced pigmentation and associated osteoarthropathy.

5.3.1.2.1 BALB/c Hgd-/- 16.3 (♂) – 69 weeks

Large numbers of pigmented chondrons were scattered throughout the ACC of both femoral condyles and the TP. All pigmented chondrons were hypertrophic with the majority severely hypertrophic (Fig. 5.9). There was also damage to the articular surface of the LTP (Fig. 5.10) as well as osteophyte formation on the MTP.

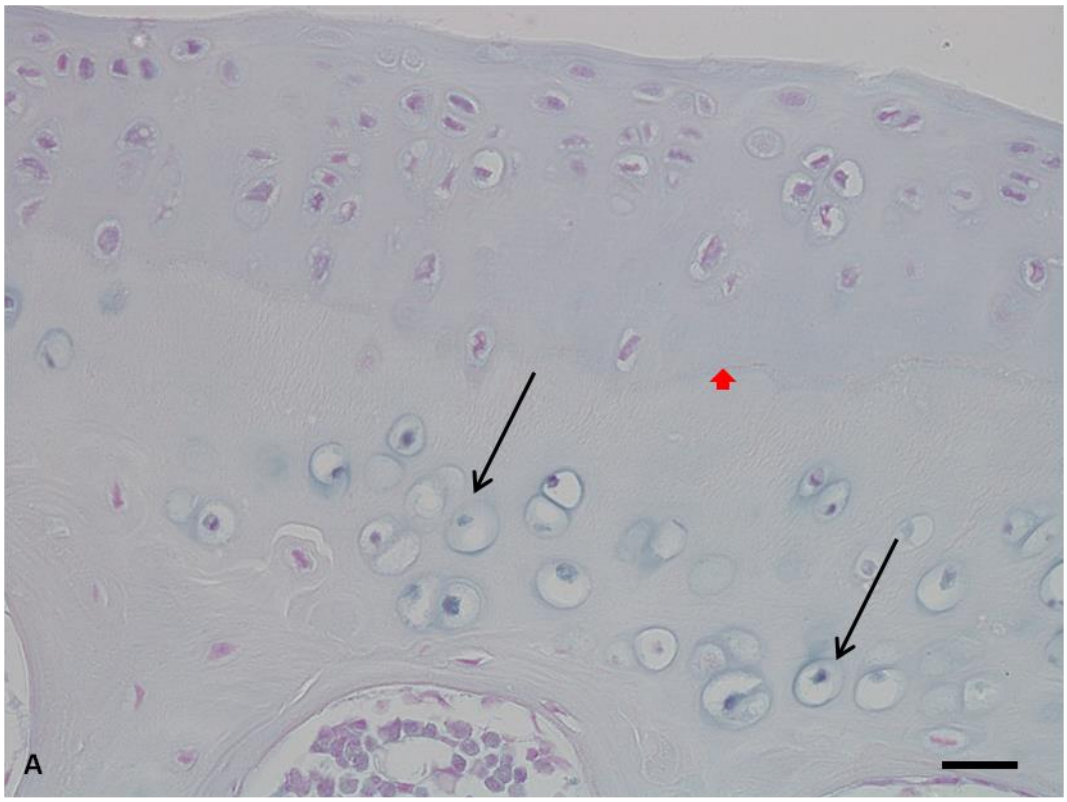

Figure 5.9 – Hypertrophic pigmented chondrons in the medial tibial plateau of BALB/c 16.3, a 69 week old Hgd-/- mouse not treated with nitisinone. Large numbers of hypertrophic pigmented chondrons were located in the ACC of the MTP (arrowed). The tidemark, which represents the boundary between calcified and uncalcified cartilage, is highlighted (red arrowhead). Section stained with Schmorl's. Bar = 20µm.

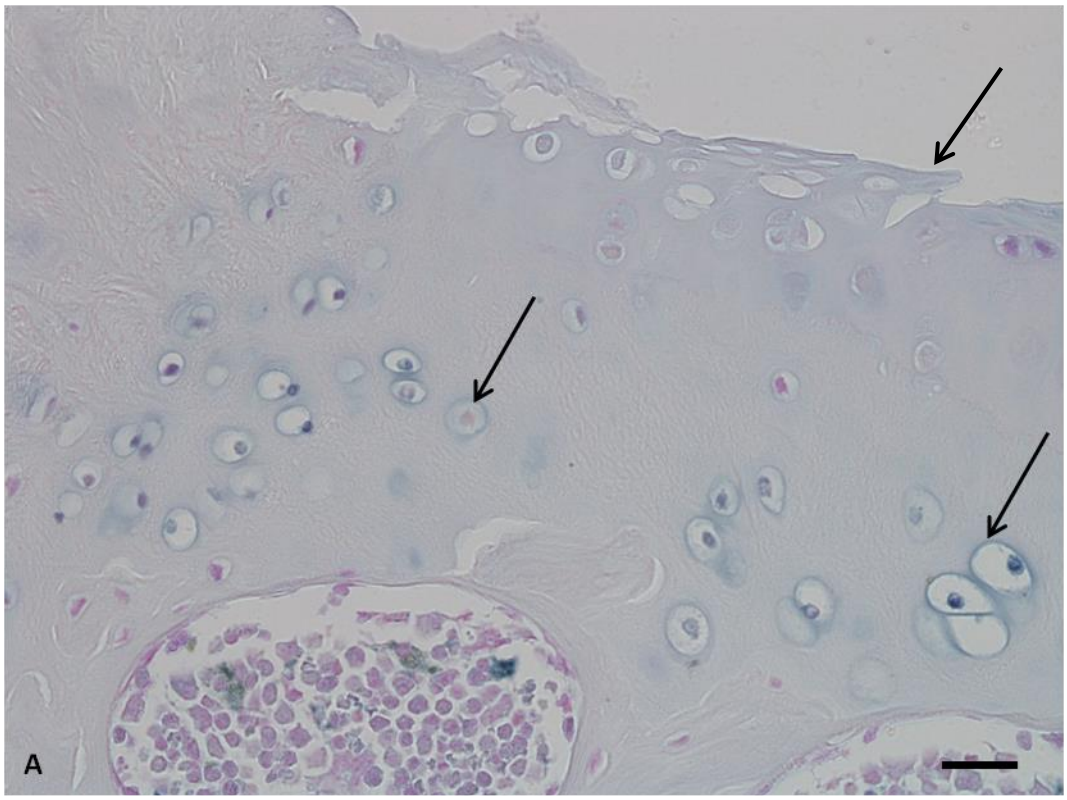

Figure 5.10 – Fibrillation on the articular surface of the lateral tibial plateau in BALB/c 16.3, a 69 week old Hgd-/- mouse not treated with nitisinone. Fibrillation of the articular surface and a minor vertical cleft were present on the LTP (top right arrow). A cluster of pigmented chondrons was seen deep in the ACC (bottom right arrow) while a chondron in the early stages of pigmentation, being only peri-pigmented, was located towards the ligamentous fibres in the intercondylar area of the tibia. Section stained with Schmorl's. Bar = 20µm.

BALB/c Hgd-/- 16.3 showed signs of severe ochronotic osteoarthropathy consistent with those seen in age-matched Hgd-/- mice in the natural history study. There were significant amounts of pigmentation throughout the knee joint and symptoms of OA including chondron hypertrophy, osteophyte formation and cartilage degeneration.

5.3.1.2.2 BALB/c Hgd-/- 18.1 (♀) – 69 weeks

BALB/c Hgd-/- 18.1 (♀) displayed severe signs of ochronotic osteoarthropathy. This was expected as all previous age-matched Hgd-/- mice had shown similar signs including large numbers of pigmented hypertrophic chondrons, cartilage degeneration and SCB remodelling. Dense areas of pigmentation were located towards the ligamentous fibres of the intercondylar area of the tibia (Fig. 5.11). Small amounts of SCB remodelling were also observed (Fig. 5.12).

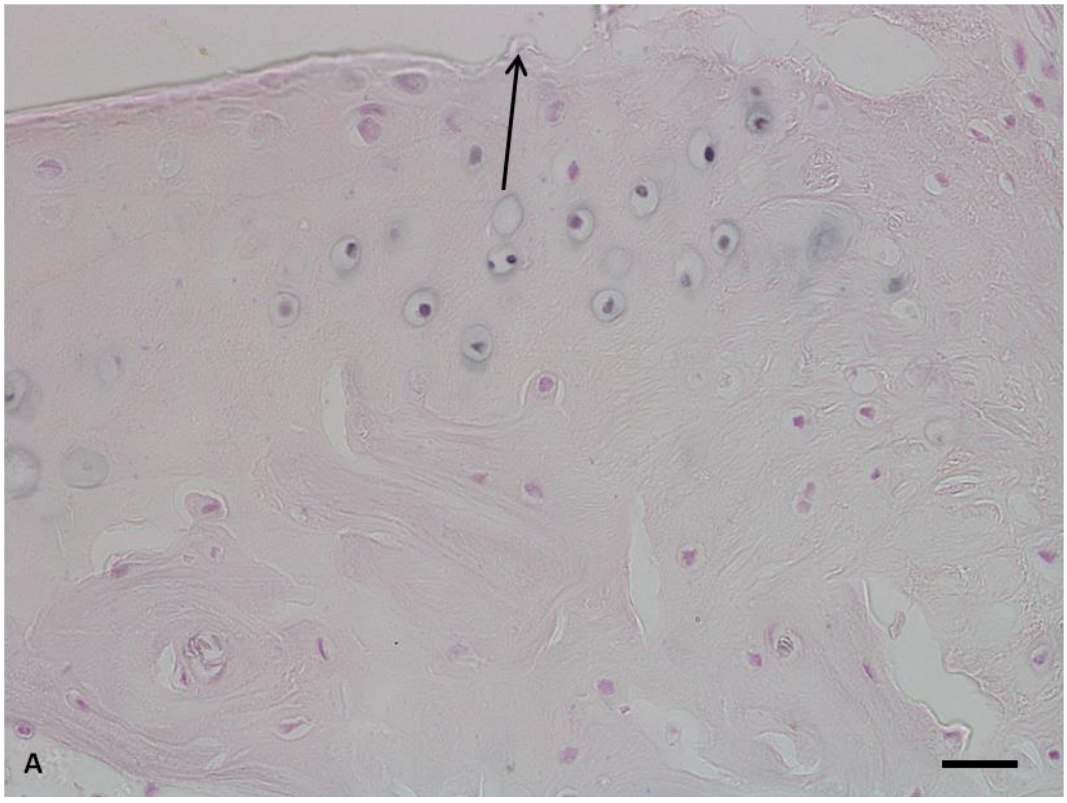

Figure 5.11 – Dense pigmentation in the intercondylar area of BALB/c 18.1, a 69 week old Hgd-/- mouse not treated with nitisinone. Pigmented chondrons were located at the intercondylar area of the tibia and highlight the stress placed upon this area of the joint. Minor fibrillation of the articular surface (arrowed) was also situated adjacent to this area. Section stained with Schmorl's. Bar = 20µm.

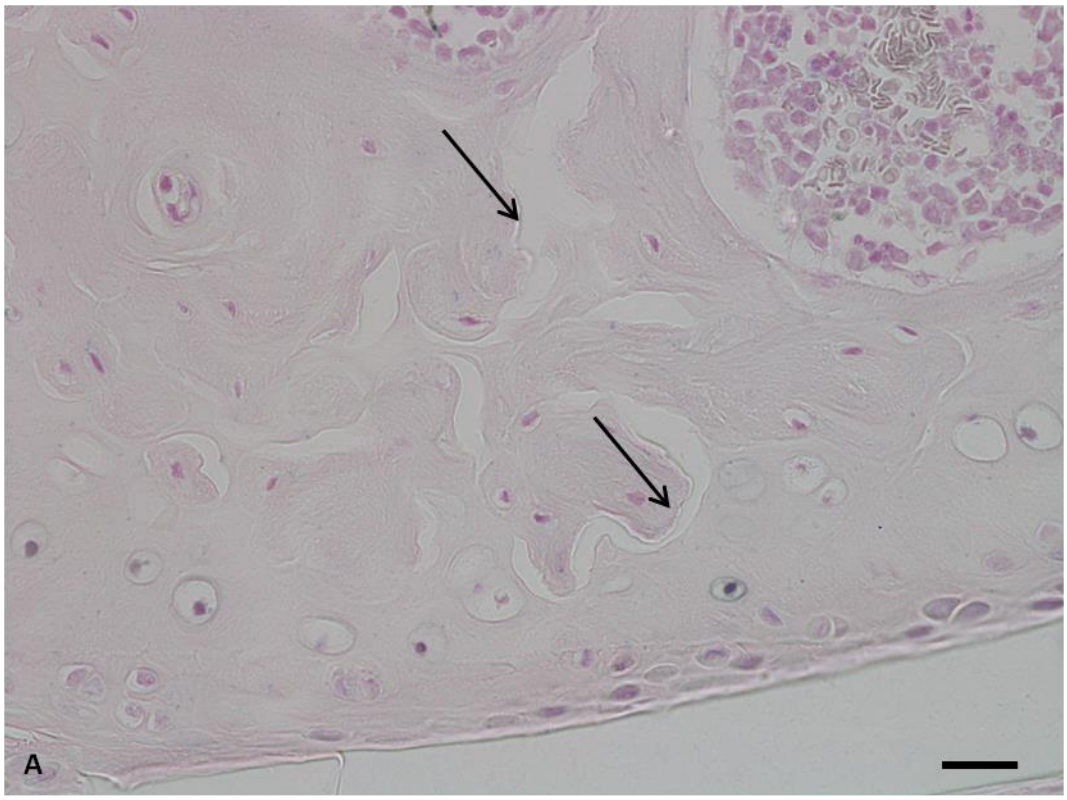

Figure 5.12 – Subchondral bone remodelling in the lateral femoral condyle of BALB/c 18.1, a 69 week old Hgd-/- mouse not treated with nitisinone. SCB resorption and remodelling (arrowed) were found in the LFC. This led to calcification and ossification of a significant portion of the ACC, resulting in thinning of this area. Section stained with Schmorl's. Bar = 20µm.

Both figures display the presence of pigmented chondrons in BALB/c Hgd-/- 18.1 and also show the severity of the associated osteoarthropathy in the knee joints. The thinning of the ACC and the resulting tidemark duplication and thinning of the HAC are all factors in the initiation and progression of ochronotic osteoarthropathy both in mice and in humans.

5.3.1.2.3 BALB/c Hgd-/- 18.2 (♀) – 69 weeks

BALB/c Hgd-/- 18.2 (♀) displayed large amounts of pigmented chondrons, especially in osteophytes located on the MFC (Fig. 5.13) and MTP (Fig. 5.14) respectively. Osteophyte formation has long been associated with OA and findings from the natural history study of Hgd-/- mice (Chapter 3) showed them to be present, especially in mice which had severe pigmentation.

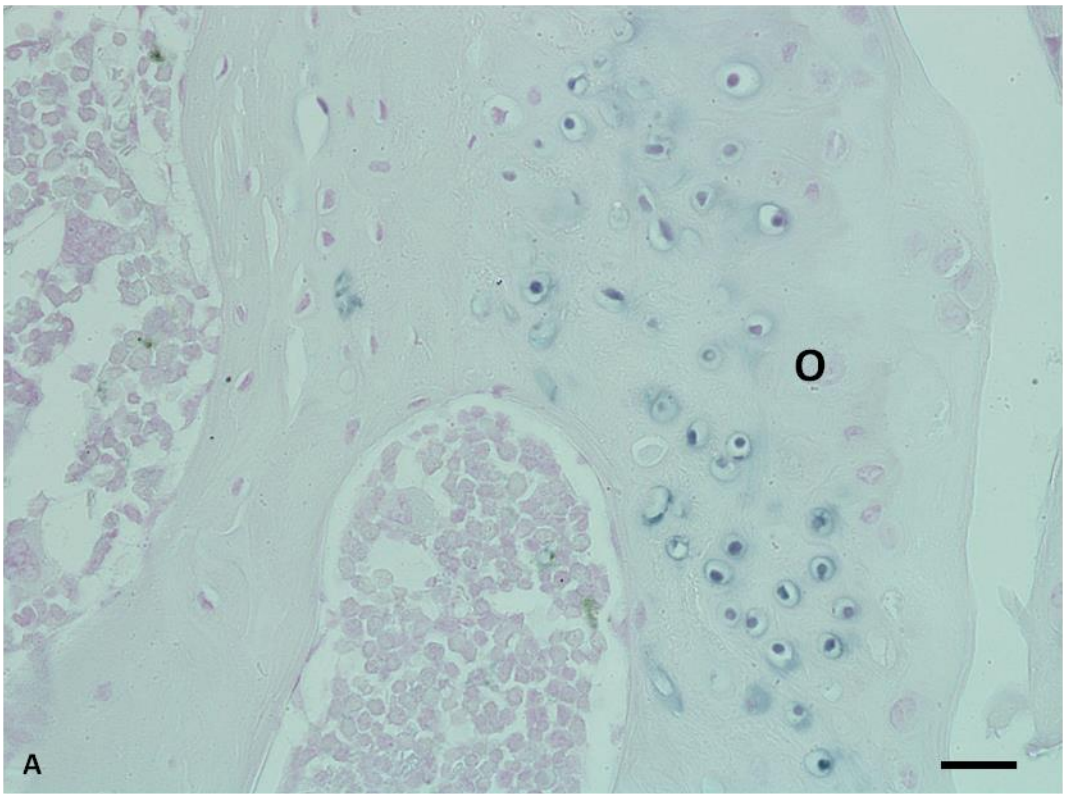

Figure 5.13 – A heavily pigmented osteophyte on the medial femoral condyle of BALB/c 18.2, a 69 week old Hgd-/- mouse not treated with nitisinone. An osteophyte (**O**) located on the MFC contained large numbers of pigmented chondrons. Section stained with Schmorl's. Bar = 20µm.

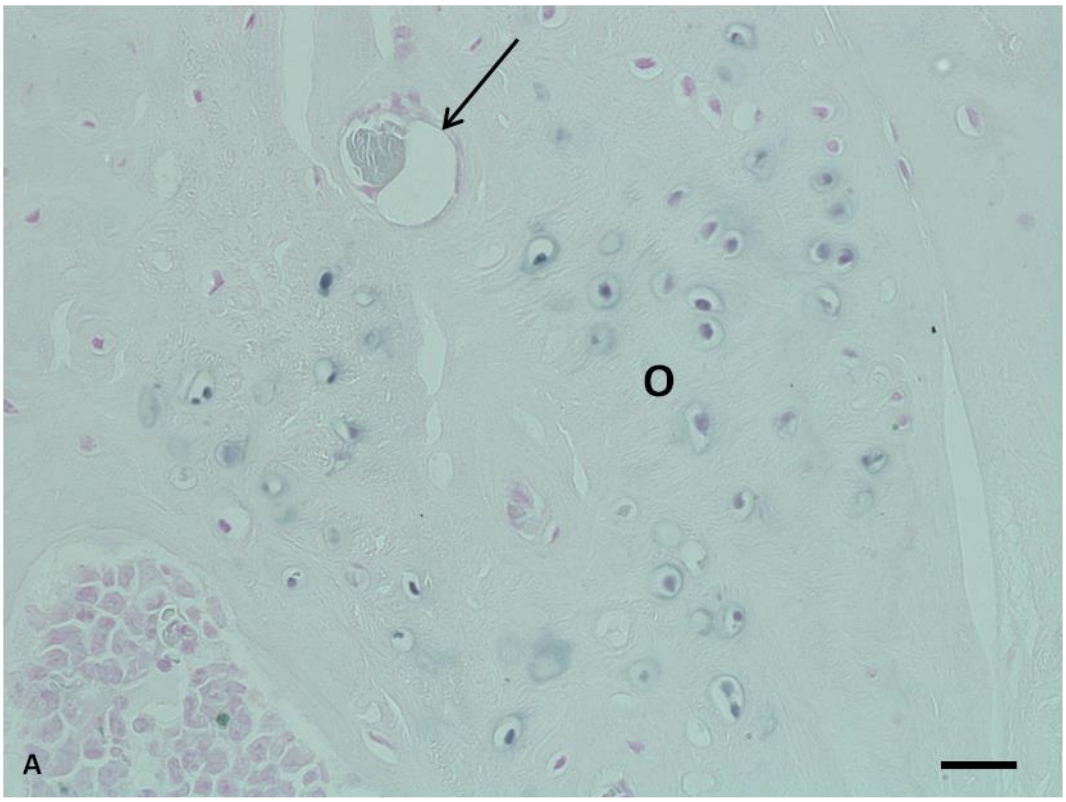

Figure 5.14 – A heavily pigmented osteophyte on the medial tibial plateau of BALB/c 18.2. An osteophyte (**O**) located on the MTP contained large numbers of pigmented chondrons. Ossification of the osteophyte is also highlighted (arrowed). Section stained with Schmorl's. Bar = 20µm.

Along with osteophyte formation and pigmentation, there was damage to the articular surface of the MFC. The results highlighted the significance of the administration of nitisinone as mice in the treated group displayed no pigmentation while the control group, including BALB/c Hgd-/- 18.2, showed very high levels of pigmentation.

5.3.1.2.4 BALB/c Hgd-/- 18.3 (♀) – 69 weeks

BALB/c Hgd-/- 18.3 (♀) was one of the most heavily pigmented mice in the control group and showed especially dense pigmentation towards the intercondylar area of the tibia (Fig. 5.15). This area regularly shows intense pigmentation which is probably linked to the sheer biomechanical stress this area undergoes. Large amounts of hypertrophic pigmented chondrons were located in the MFC. This area also showed some SCB resorption and remodelling (Fig. 5.16).

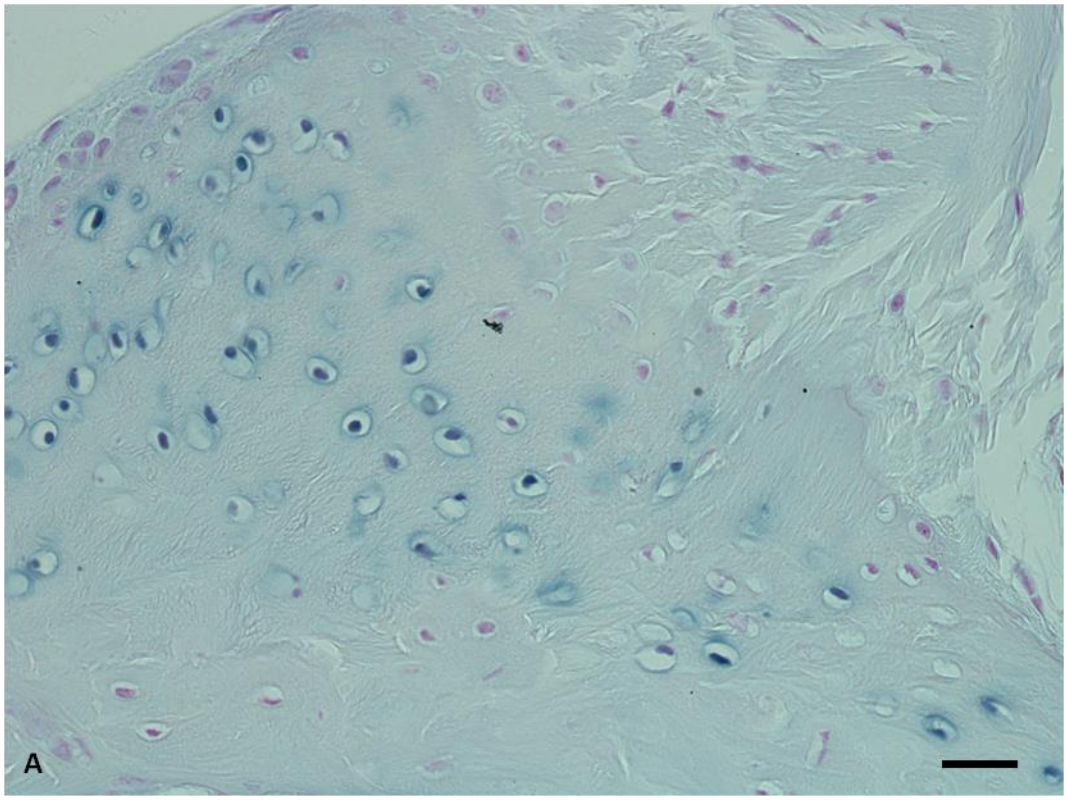

Figure 5.15 – Dense pigmentation of the intercondylar area of the tibia in BALB/c 18.3, a 69 week old Hgd-/- mouse not treated with nitisinone. Large amounts of pigmented chondrons were located towards the ligamentous fibres of the intercondylar area of the tibia; an area of high stress in the joint. Section stained with Schmorl's. Bar = 20µm.

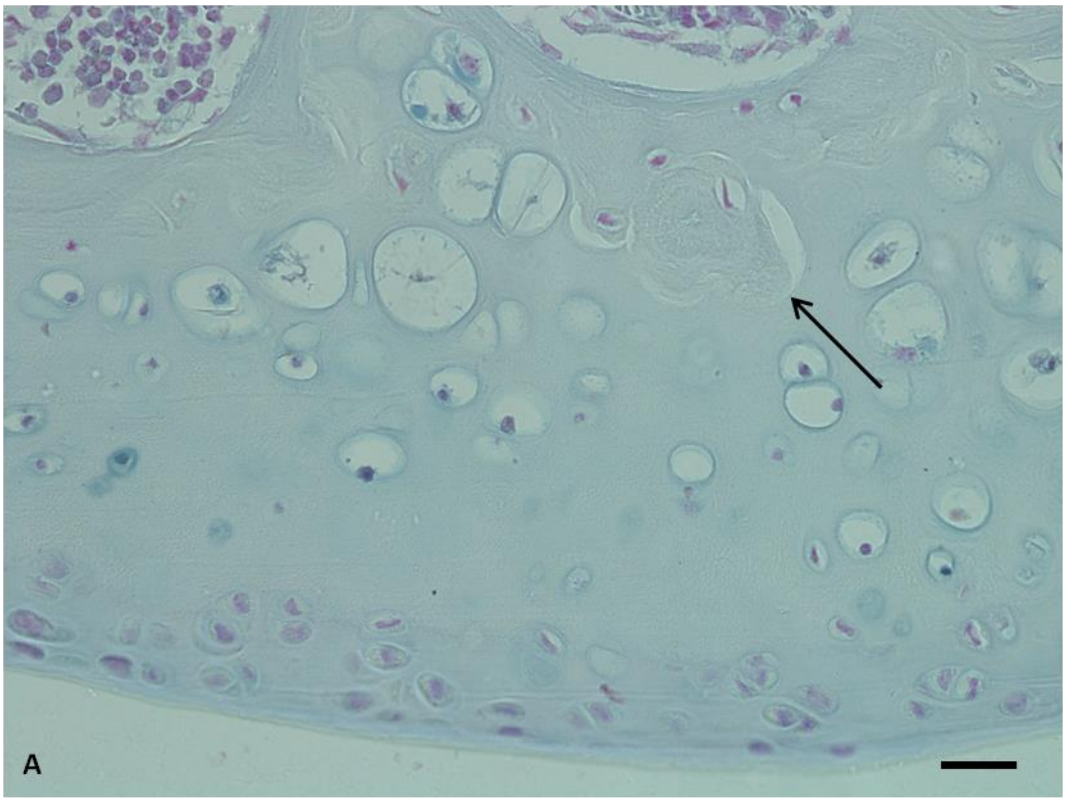

Figure 5.16 – Subchondral bone remodelling in the medial femoral condyle of BALB/c 18.3, a 69 week old Hgd-/- mouse not treated with nitisinone. A small amount of SCB resorption and remodelling (arrowed) was observed in the MFC which also contained large numbers of hypertrophic pigmented chondrons. Section stained with Schmorl's. Bar = 20µm.

The results gained from BALB/c Hgd-/- 18.3 are consistent with those seen in all of the mice in the control group and of those age-matched mice in the natural history study.

5.3.1.3 Quantification of pigmented chondrons (lifetime nitisinone study)

Pigmented chondron counts were made of the control and treated groups to emphasise the effect nitisinone had on the deposition of ochronotic pigment and to compare numbers against those obtained in the natural history study (Fig. 5.17). There was some variation between the number of pigmented chondrons in the

control group (lowest = 132, highest = 341) however this was in-line with what was seen in the natural history study (Chapter 3).

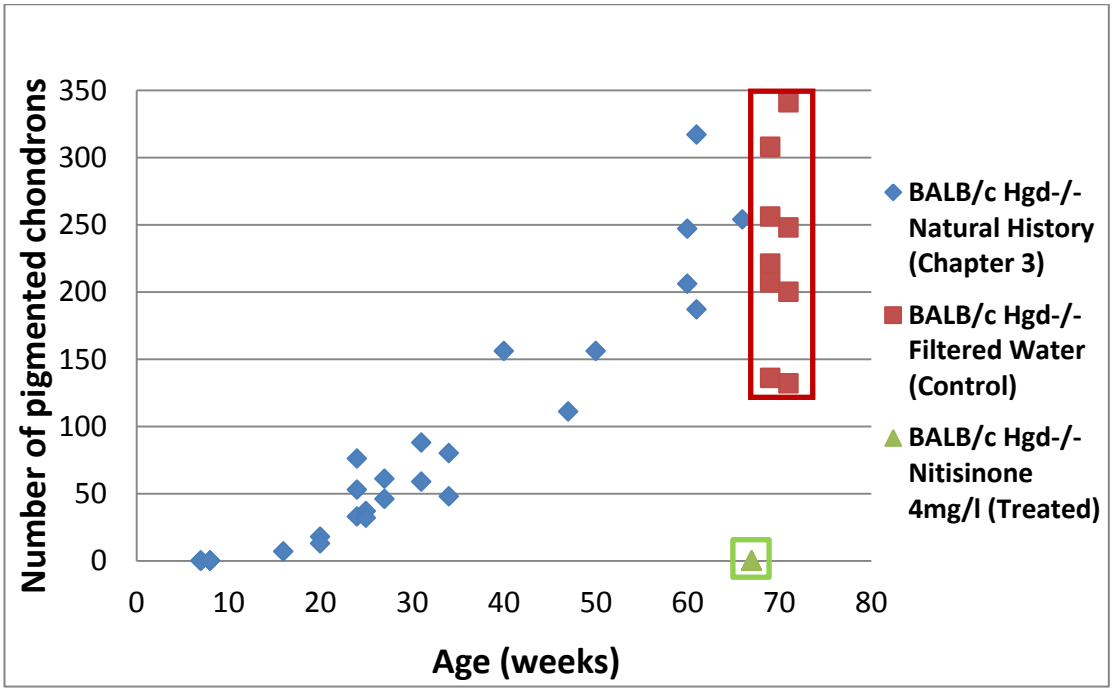

Figure 5.17 – The effect of lifetime nitisinone administration on the number of pigmented chondrons in BALB/c Hgd-/- mice. Scatter chart showing lifetime nitisinone administration prevented any chondrons from becoming pigmented. The control group showed levels of pigmentation comparable with those seen in the natural history study. Quantification of pigmented chondrons was performed on a single section from each mouse; this does not represent the total cell number in each mouse.

5.3.1.4 Plasma HGA levels (lifetime nitisinone study)

Lifetime HGA plasma levels were obtained from the control and treated groups to highlight the effect nitisinone has on these levels (Fig. 5.18). The statistical significance of treatment was examined by analysis of HGA concentrations at four time points: immediately prior to treatment at 8 weeks (mean (SE) 0.115±0.011 mM), and after treatment at 14 weeks (mean (±SE) 0.009±0.004 mM), 39 weeks

(mean (±SE) 0.011±0.002 mM) and 67 weeks (mean (±SE) 0.008±0.001 mM). A significant difference ($p<0.001$) was found between HGA concentrations before and after treatment at 8 and 14 weeks, respectively, with no further significant change observed throughout the study. After treatment with nitisinone there was an 88% drop of plasma HGA which was maintained for the duration of the study. Statistical analysis was performed using a two-tailed, two sample, unequal variance t test. Although a one-tailed test could have been used as it could have been expected that nitisinone would show a one way direction (suppression of plasma HGA, one-tailed) a two-tailed test was used to allow for greater statistical rigor. A two sample, unequal variance test was used as the two population variances were not assumed to be equal. Although the study started with similar numbers of BALB/c Hgd-/- mice in both the control and treated groups, some died before the end of the study, so the final population size of each group was different. The variance in the nitisinone treated BALB/c Hgd-/- mice is much smaller than the variance within untreated BALB/c Hgd-/- mice hence why an unequal variance t test was performed. Growth curves from both groups showed no significant difference between the mice in the control and treated groups (Fig. 5.19). This work was carried out by Dr. A. Preston.

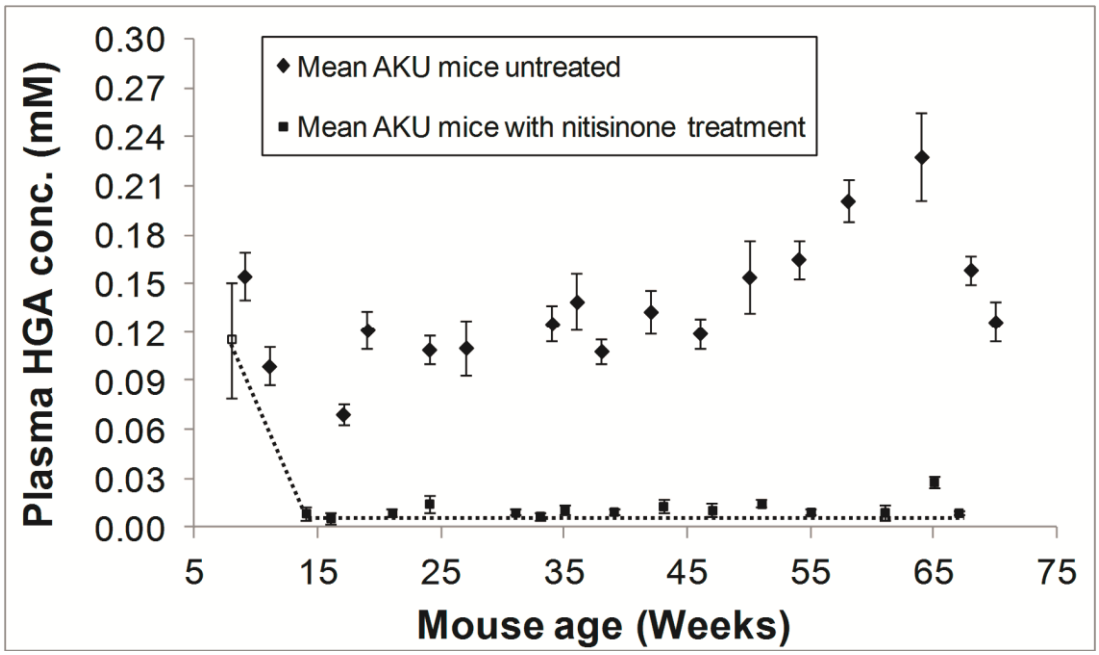

Figure 5.18 – The effect of lifetime nitisinone administration on plasma HGA levels in BALB/c Hgd-/- mice. Scatter chart showing lifetime treatment with nitisinone led to a significant reduction in plasma HGA levels. All measurements and data analysis performed by Dr. A. Preston.

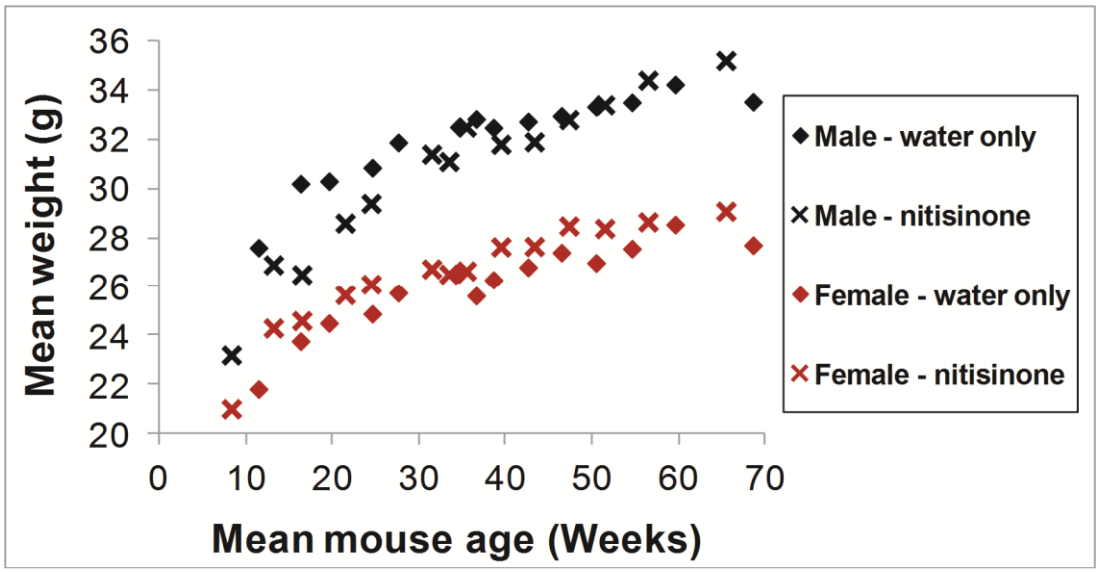

Figure 5.19 – Comparison of growth curves in BALB/c Hgd-/- mice with and without lifetime nitisinone treatment. Scatter chart showing lifetime treatment with nitisinone had no significant effect on the growth of both male and female Hgd-/- mice. All measurements and data analysis performed by Dr. A. Preston.

This study provided significant results about the effectiveness of nitisinone in preventing the initiation of ochronosis. Nitisinone maintained its efficacy over the mouse lifetime, and caused no obvious health or behavioural changes between the treated and control groups. The data collected provides evidence that early intervention with nitisinone in individuals with AKU will halt the pathogenesis of the disease which results in the devastating osteoarthropathy seen.

5.3.2 Mid-life treatment with nitisinone

A cohort of 8 BALB/c Hgd-/- mice (four male, four female) were provided with filtered water from 8 to 34 weeks of age. They were then provided with an ad libitum supply of water containing 4mg/l of nitisinone from 35 to 80 weeks of age. The control group of 8 BALB/c Hgd-/- mice (four male, four female) had no drug in their drinking water from 8 to 80 weeks of age.

5.3.2.1 Treated group

Of the eight mice treated with nitisinone mid-way through their lives, three were discovered to be deceased upon inspection of their cages at different time points during the study. Again, the deaths of these mice were not considered to be a consequence of nitisinone administration as death rates similar to these are often observed in long term animal studies. These mice were kept out of the study as they had started to undergo tissue necrosis before fixation therefore the results obtained from them could not be seen as consistent with the other mice in the study. All five of the mice that reached the endpoint of the study showed a significant reduction in terms of their overall number of pigmented chondrons present in the knee joint. What was immediately clear was that treatment with nitisinone did not reverse any previous pigment deposition; it only prevented further deposition of pigment throughout the joint.

5.3.2.1.1 BALB/c Hgd-/- 47.3 (♀) – 80 weeks

BALB/c Hgd-/- 47.3 (♀) displayed a large reduction in the amount of pigmented chondrons present in the ACC of the knee joint when compared to the control group (Fig. 5.30). Although pigmented chondrons could be seen in both the femoral condyles and along the TP there were significantly less of them than seen in untreated mice. Minor fibrillation of the articular surface of the MFC was observed (Fig. 5.21) and a large osteophyte could be seen on the MTP (Fig. 5.22).

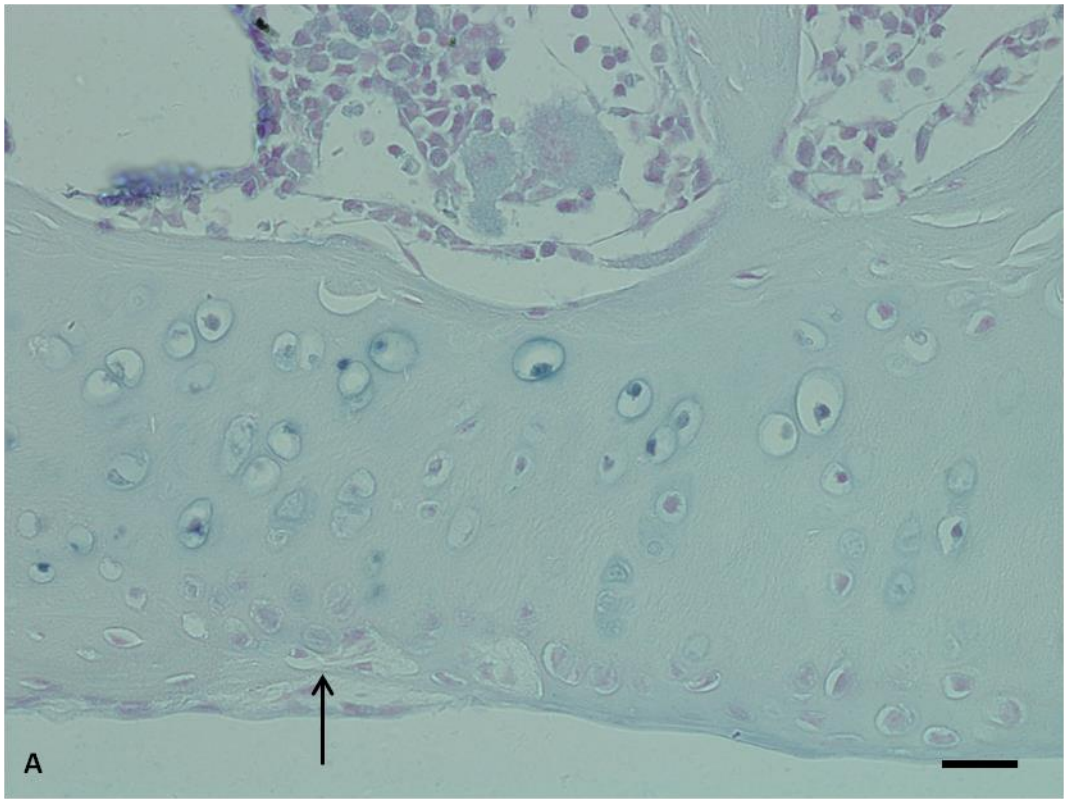

Figure 5.20 – Fibrillation on the articular surface of the medial femoral condyle of BALB/c 47.3, an 80 week old Hgd-/- mouse treated with nitisinone. A small amount of damage (arrowed) was observed on the articular surface of the MFC. Section stained with Schmorl's. Bar = 20µm.

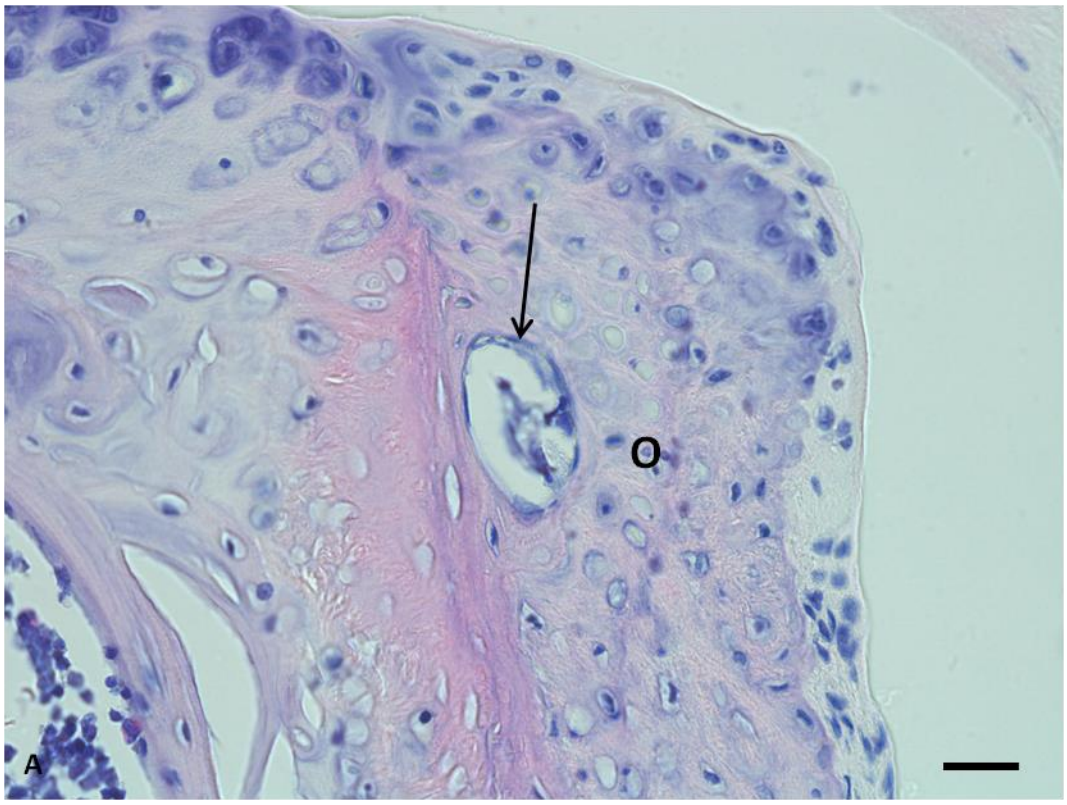

Figure 5.21 – Osteophyte formation on the medial tibial plateau of BALB/c 47.3, an 80 week old Hgd-/- mouse treated with nitisinone. A large fully formed osteophyte (**O**) was located on the MTP. Early signs of osteoarthritis are often prevalent on the medial aspects of joints. Section stained with H&E. Bar = 20µm.

Although there was a reduction in the number of pigmented chondrons in the ACC, the appearance of early osteoarthritic changes in the knee joint of BALB/c Hgd-/- 47.3 suggested that nitisinone may only be useful when given early on in life.

5.3.2.1.2 BALB/c Hgd-/- 48.1 (♂) – 80 weeks

There was a very large reduction in the number of pigmented chondrons present in BALB/c Hgd-/- 48.1 (♂) in comparison to the mice in the control group (Fig. 5.22 & 5.30). However, as seen previously in BALB/c Hgd-/- 47.3, there were also signs of osteoarthritic changes in the joint. There was complete erosion of the HAC on the MTP exposing the underlying layer of the ACC (Fig. 5.23). This type of damage is

associated with severe osteoarthropathy in joints and again shows that the effectiveness of nitisinone may only be seen when given at an earlier time point in life.

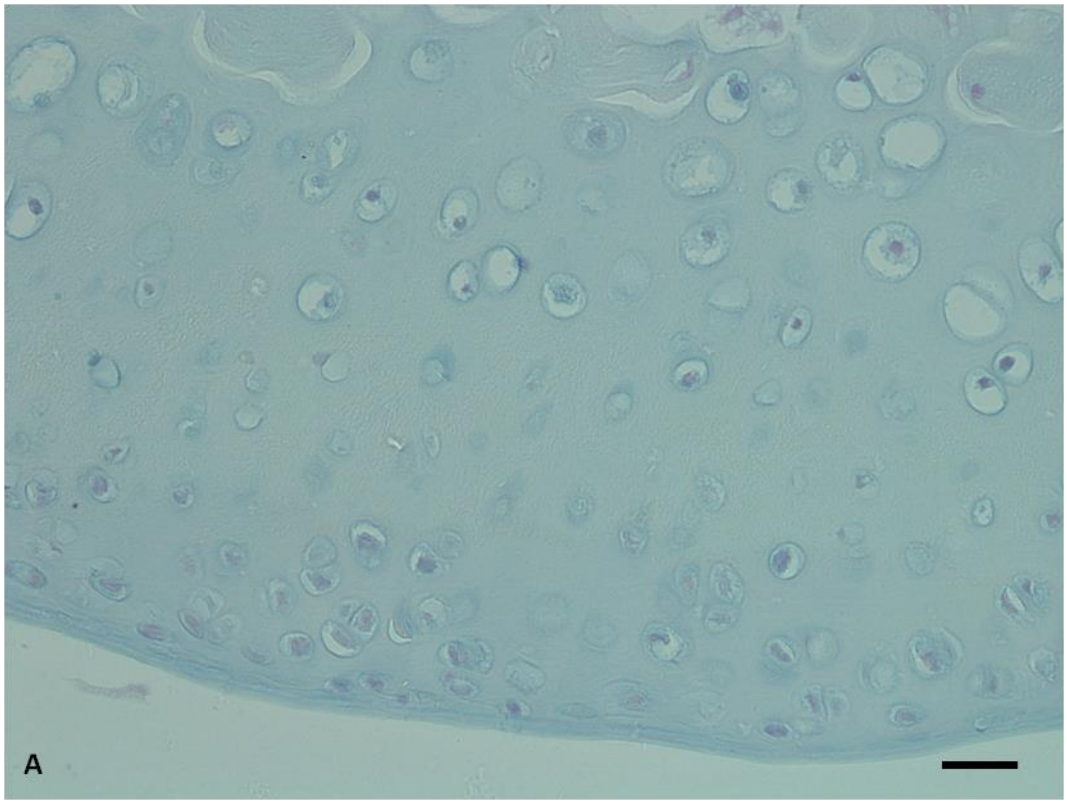

Figure 5.22 – Prevention of pigmentation in chondrons in the medial femoral condyle of BALB/c 48.1, an 80 week old Hgd-/- mouse treated with nitisinone. Nitisinone treatment significantly reduced the amount of pigmented chondrons that would normally be present in this area in Hgd-/- mice. Section stained with Schmorl's. Bar = 20µm.

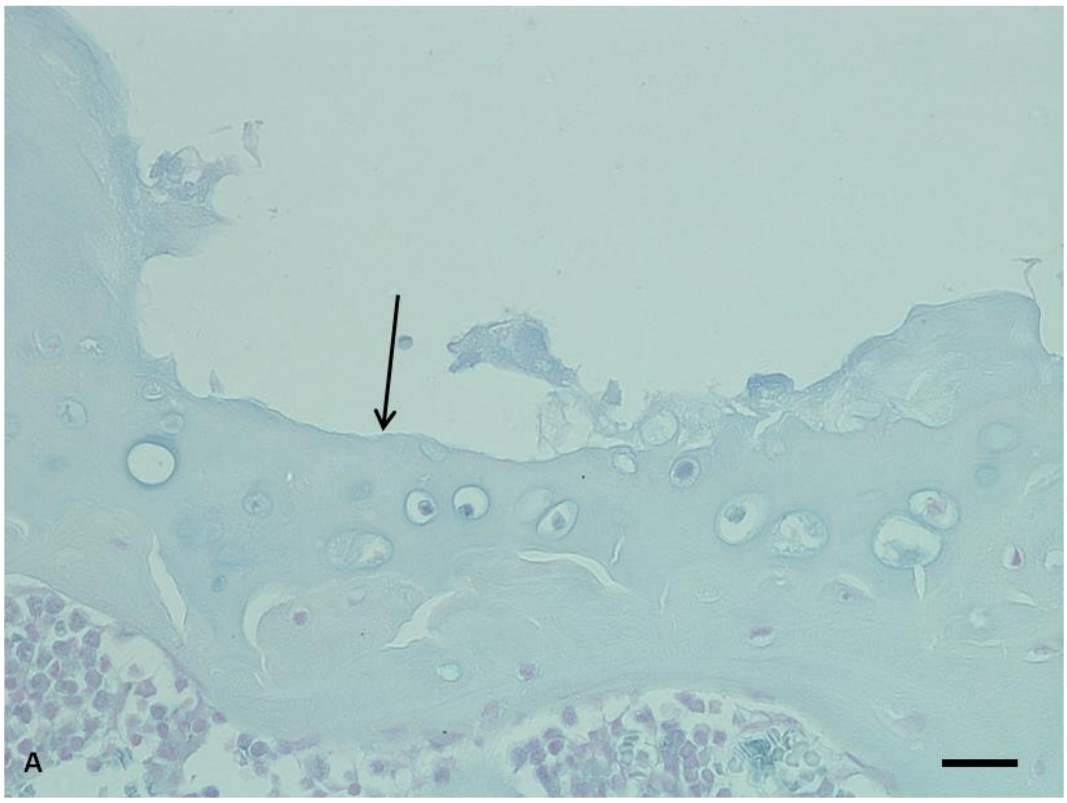

Figure 5.23 – Severe erosion of the hyaline articular cartilage on the medial tibial plateau of BALB/c 48.1, an 80 week old Hgd-/- mouse treated mid-life with nitisinone. Exposure of the ACC (arrowed) highlighted the severe osteoarthritic nature of the medial aspect of the knee joint in BALB/c Hgd-/- 48.1. Section stained with Schmorl's. Bar = 20µm.

5.3.2.1.3 BALB/c Hgd-/- 50.1 (♀) – 80 weeks

BALB/c Hgd-/- 50.1 (♀) displayed the highest number of pigmented chondrons from the treated group (Fig. 5.30). The total number was still lower than the lowest of the control group by 40-50 chondrons which is a reasonable amount. A large pigmented osteophyte was located on the MTP (Fig. 5.24); this seemed to be a trait with all of the mice in the treated group. Small areas of SCB remodelling and cartilage fibrillation could also be seen.

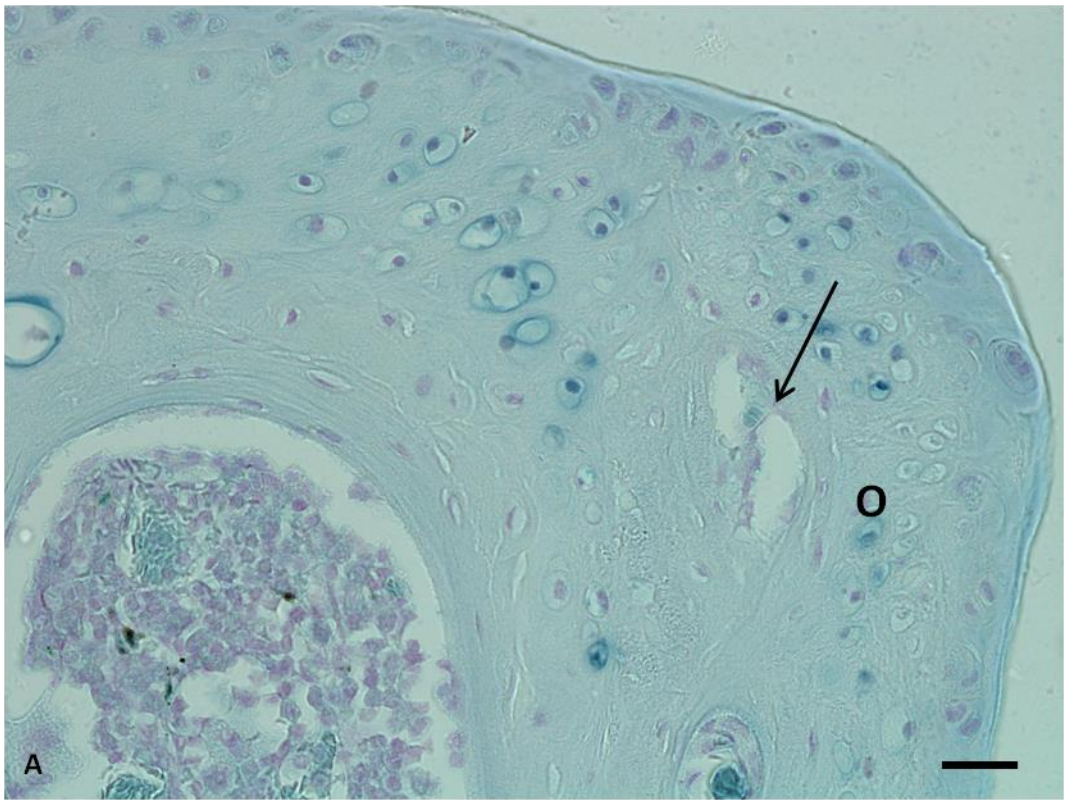

Figure 5.24 – A large osteophyte present on the medial tibial plateau of BALB/c 50.1, an 80 week old Hgd-/- mouse treated with nitisinone. An osteophyte (**O**) containing pigmented chondrons was located on the MTP of BALB/c Hgd-/- 50.1. Section stained with Schmorl's. Bar = 20µm.

5.3.2.2 Control group

Of the eight mice in the control group, six continued until the planned end of the study, while two others were found deceased upon inspection of their cages. The results gained from the control group are similar to those of age matched samples included in the natural history study (Chapter 3). They all showed signs of advanced pigmentation and associated osteoarthropathy.

5.3.2.2.1 BALB/c Hgd-/- 47.2 (♀) – 80 weeks

BALB/c Hgd-/- 47.2 (♀) showed a significant increase in the number of pigmented chondrons when compared to the mice in the treated group. Chondrons in the LTP were heavily pigmented and very hypertrophic (Fig. 5.25) indicating they were in the final stages of pigmentation and close to death. A large, pigmented osteophyte was located on the MTP (Fig. 5.26) which was indicative of the associated osteoarthropathy seen previously in age-matched Hgd-/- mice in the natural history study.

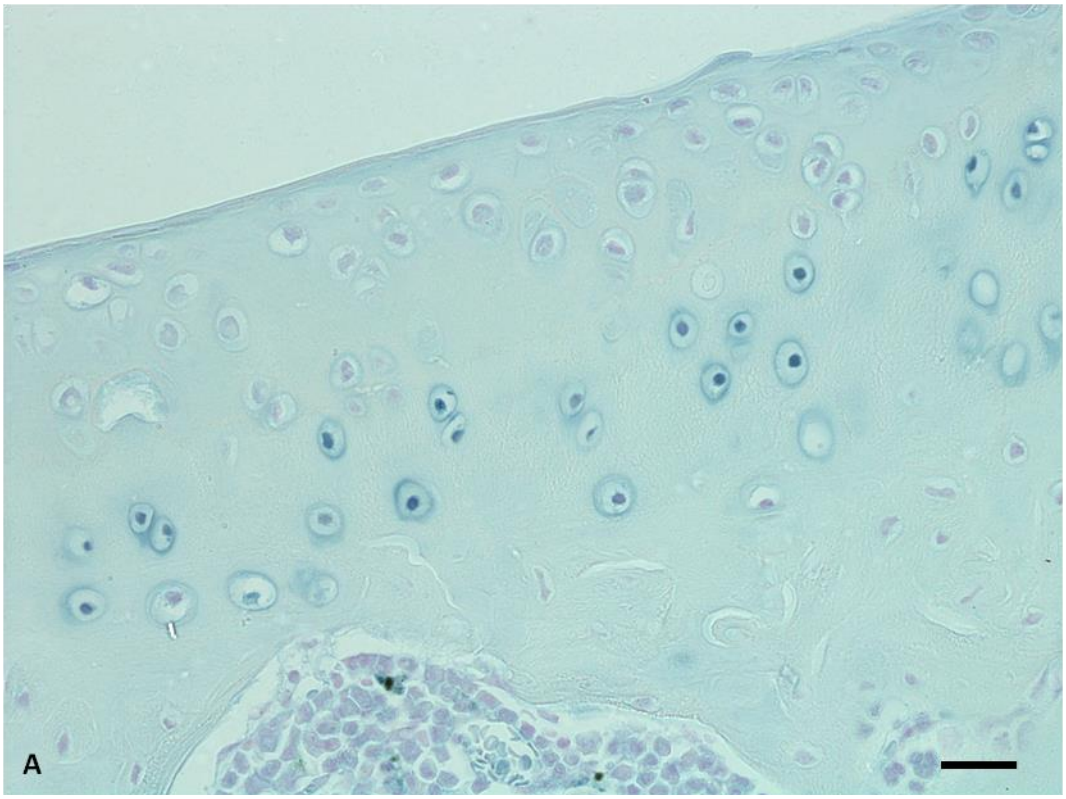

Figure 5.25 – Fully pyknotic chondrons in the lateral tibial plateau of BALB/c 47.2, an 80 week old Hgd-/- mouse not treated with nitisinone. Large numbers of pigmented pyknotic chondrons were located in the ACC of the LTP. Section stained with Schmorl's. Bar = 20µm.

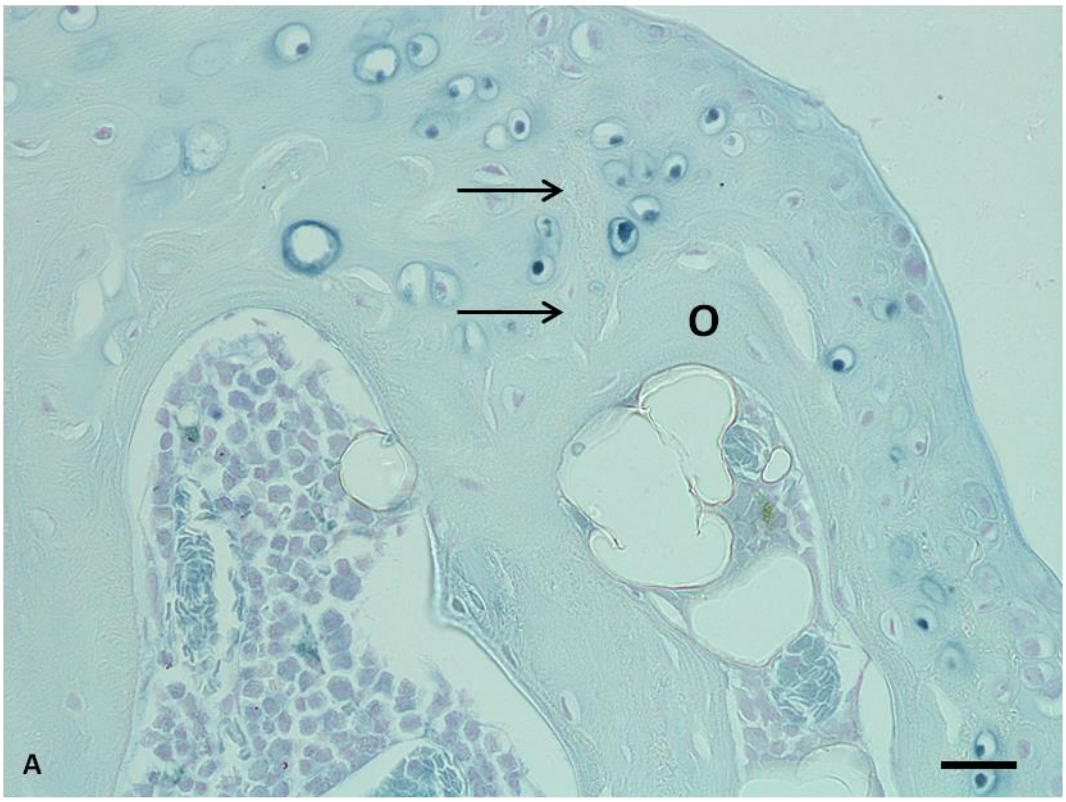

Figure 5.26 – A large, fully formed osteophyte located on the medial tibial plateau of BALB/c 47.2, an 80 week old Hgd-/- mouse not treated with nitisinone. A pigmented osteophyte was located on the MTP; formation of the osteophyte (**O**) is marked (arrows). Section stained with Schmorl's. Bar = 20µm.

5.3.2.2.2 BALB/c Hgd-/- 47.4 (♀) – 80 weeks

BALB/c Hgd-/- 47.4 (♀) displayed serious cartilage damage on the medial aspect of the knee joint. There was complete erosion of around 50% of the HAC on both the MFC and MTP leading to the exposure of the underlying ACC (Fig. 5.27). This was some of the most severe osteoarthropathy seen in any of the Hgd-/- mice examined, underlining how debilitating ochronosis and the associated OA can be without treatment. Large osteophytes were also located on both the MFC and MTP; the osteophyte on the MTP was very heavily pigmented (Fig. 5.28). The number of pigmented chondrons in the joint was much higher than in any of the treated mice.

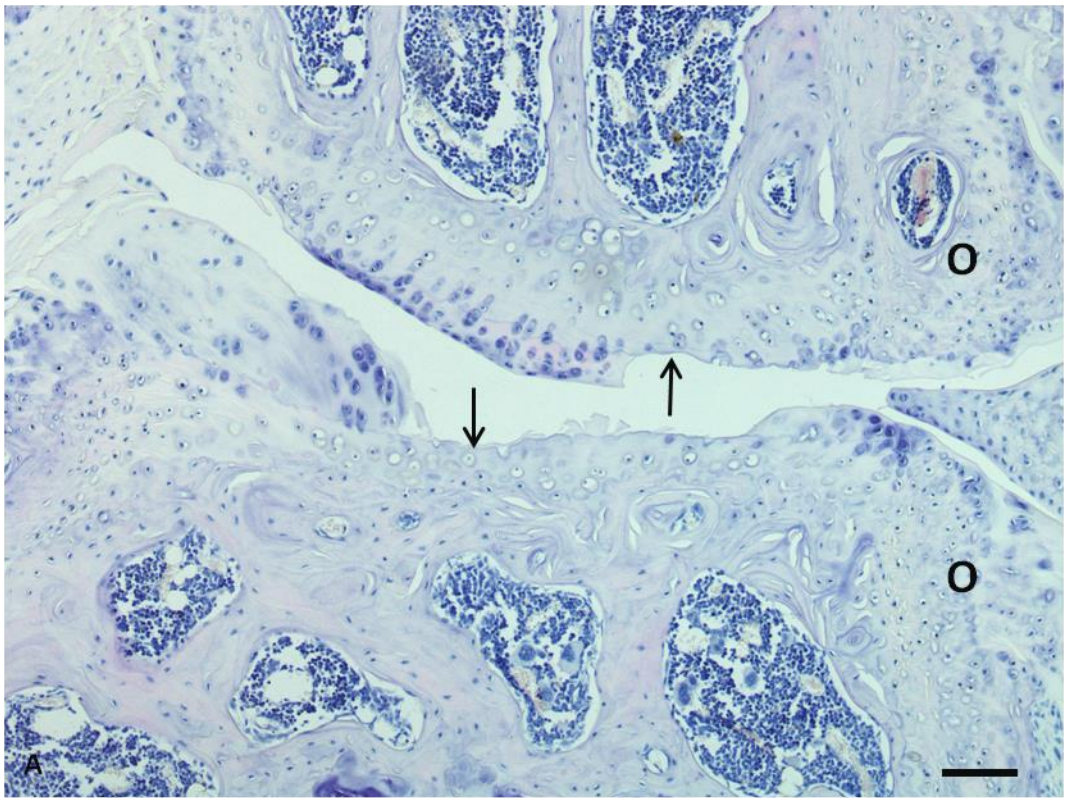

Figure 5.27 – Severe cartilage damage on the medial aspect of the knee joint in BALB/c 47.4, an 80 week old Hgd-/- mouse not treated with nitisinone. Erosion of the HAC (arrows) and osteophyte formation (**O**), both signs of severe osteoarthropathy, were present on the medial aspect of the knee joint. Section stained with H&E. Bar = 100µm.

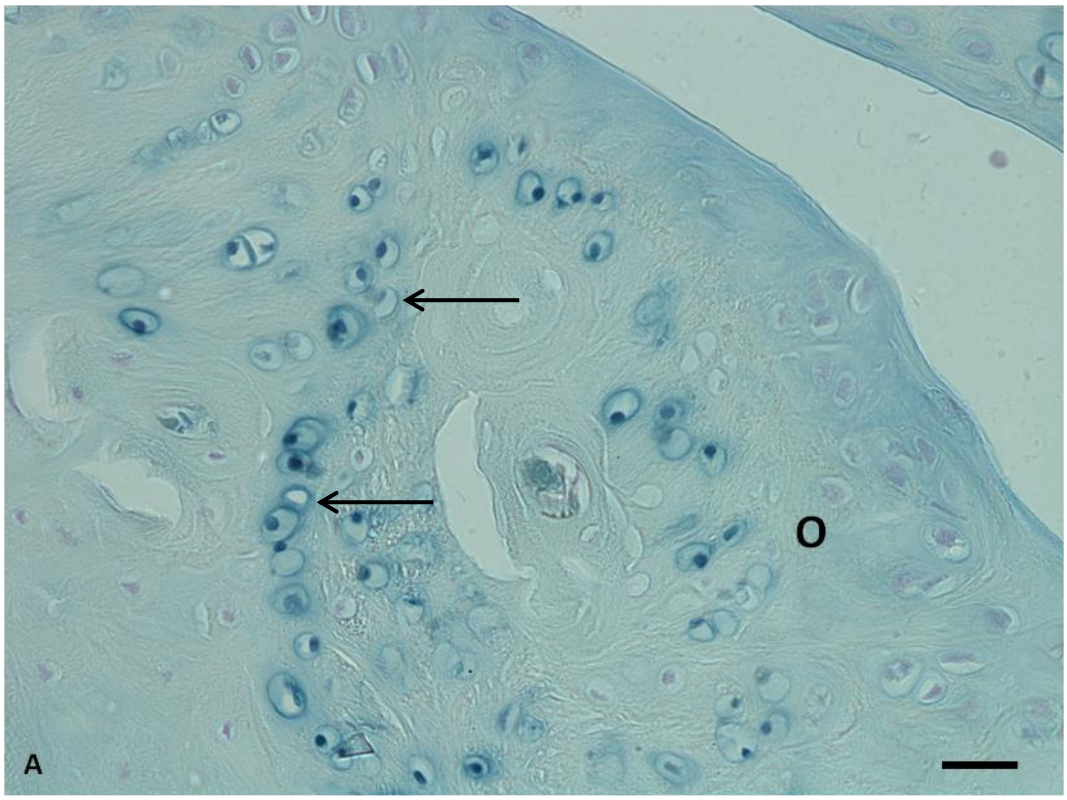

Figure 5.28 – Pigmentation of an osteophyte located on the medial tibial plateau in BALB/c 47.4, an 80 week old Hgd-/- mouse not treated with nitisinone. Pigmented chondrons were located in the osteophyte (**O**) and at the boundary of formation of the osteophyte (arrowed). Section stained with Schmorl's. Bar = 20µm.

5.2.2.2.3 BALB/c Hgd-/- 51.1 (♂) – 80 weeks

BALB/c Hgd-/- 51.1 (♂) had the lowest number of pigmented chondrons from the control group, yet this number was still higher than any of the treated group showing the effect of nitisinone in preventing any further pigment deposition. Along the LFC was the densest area of pigmentation (Fig. 5.29); all chondrons in this area were heavily pigmented and hypertrophic. There was no obvious major cartilage damage; some minor fibrillation of the articular surface on both the femur and tibia was seen but it was not severe.

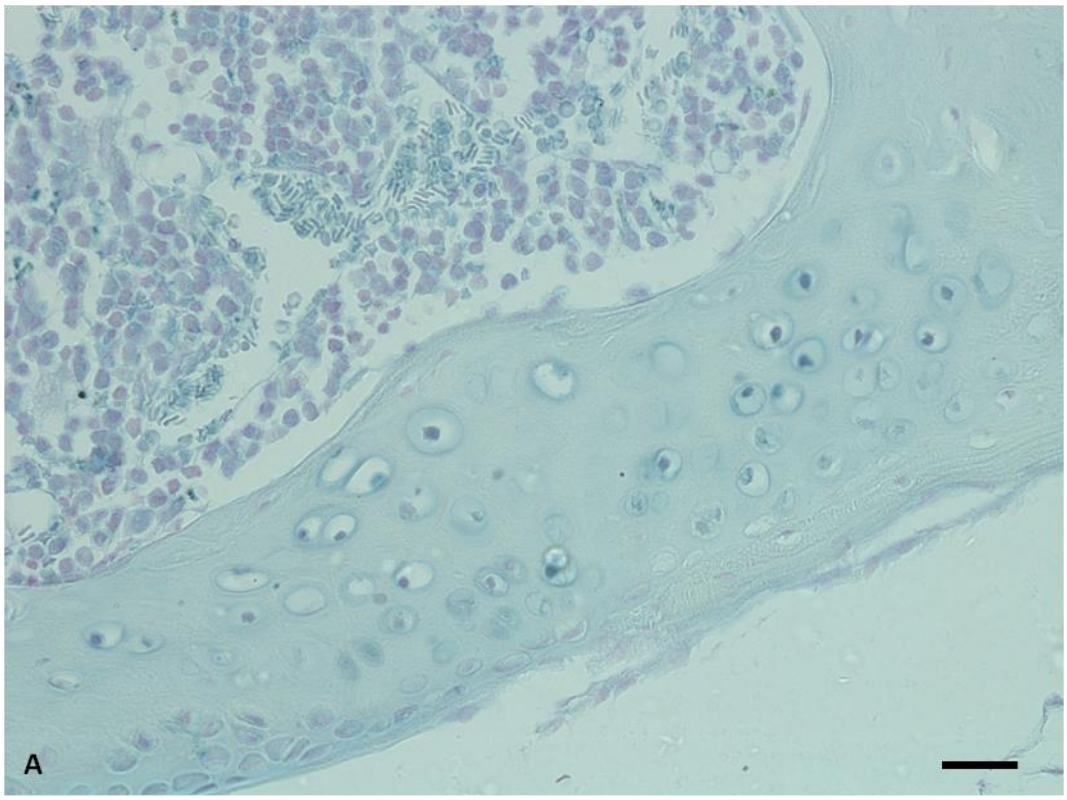

Figure 5.29 – Pigmentation of the lateral femoral condyle in BALB/c 51.1, an 80 week old Hgd-/- mouse not treated with nitisinone. A dense area of pigmented chondrons was located along the LFC. Section stained with Schmorl's. Bar = 20µm.

5.3.2.3 Quantification of pigmented chondrons (mid-life nitisinone study)

Pigmented chondrons were quantified in the control and treated groups to determine the effect nitisinone had on preventing further deposition of pigment in Hgd-/- mice (Fig. 5.30). There was some variation between the number of pigmented chondrons in the control group (lowest = 142, highest = 273) however this was in-line with what was seen in the natural history study (counts in Chapter 4) and was not excessive. It was clear from the scatter chart that treatment with nitisinone prevented HGA from becoming deposited in chondrons. The numbers of pigmented chondrons in the treated group were comparable to mice much younger and those still in the early stages of ochronosis.

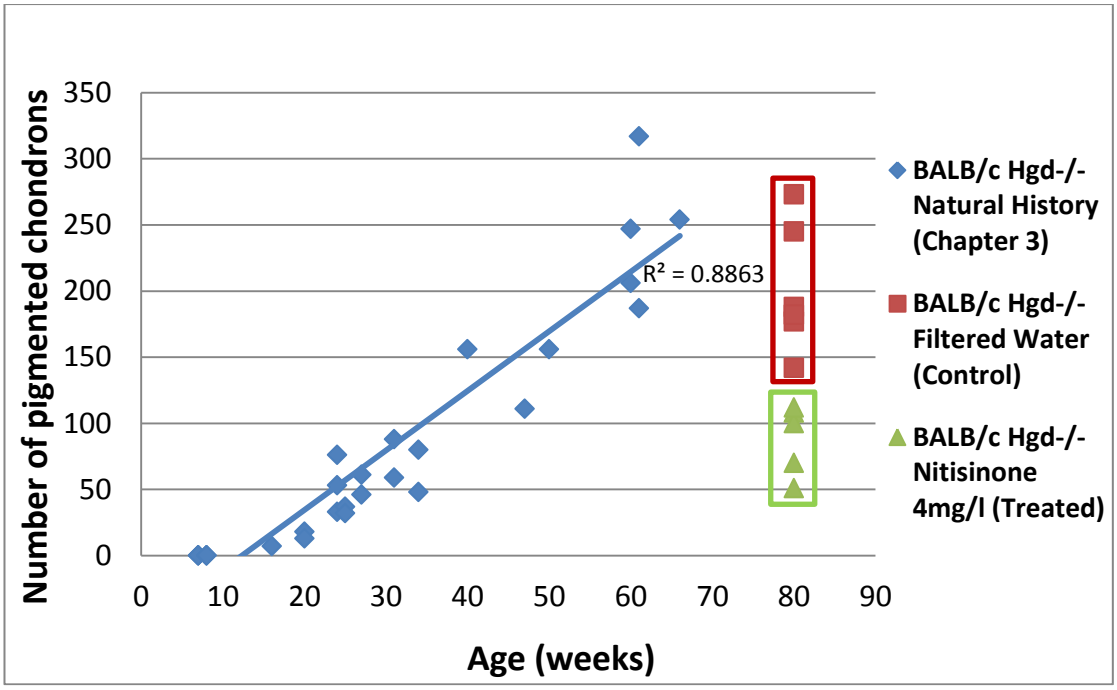

Figure 5.30 – The effect of nitisinone in BALB/c Hgd-/- mice when given after 34 weeks of age. Scatter chart showing that starting nitisinone treatment midway through life prevented further pigment deposition. The control group showed levels of pigmentation comparable with those seen in the natural history study. Quantification of pigmented chondrons was performed on a single section from each mouse; this does not represent the total cell number in each mouse.

An independent samples t-test was generated in order to compare the number of pigmented chondrons between the nitisinone treated and control Hgd-/- mice. A statistically significant difference was observed between the mean number of pigmented chondrons for the nitisinone treated Hgd-/- mice (88.2) and the control Hgd-/- mice groups (201.17) (p=0.001). In other words, the control Hgd-/- mice had a statistically significantly higher mean number of pigmented chondrocytes than the nitisinone treated Hgd-/- mice.

This study has shown that mid-life treatment with nitisinone can prevent further pigment deposition however it does not appear that it can reverse any pigmentation and/or damage already present in the knee joint. This is important as

it shows pigment deposition is probably not reversible and that joint damage caused by pigmentation will continue to proceed. It also highlights the need to treat patients with AKU as early as possible to prevent any ochronotic pigment from being laid down as once this occurs it appears inevitable that some form of osteoarthropathy will develop.

5.4 DISCUSSION

This Chapter described the evaluation of the efficacy of nitisinone as a treatment for the prevention of AKU in BALB/c Hgd-/- mice. Nitisinone was originally developed as a herbicide, but has been used in the treatment of HT-1 since the early 1990s [206]. It has also seen some success in the treatment of oculotaneous albinism [207] where elevation of plasma tyrosine, induced by nitisinone, stabilises the Tyr^{c-h} mutant protein resulting in the production of melanin and improving visual function. It is currently the first line of treatment for HT-1, replacing liver transplantation and has helped lead to a decrease in fatalities [50, 208]. Manning and colleagues when working with Fah-/-, Hgd+-/ mice, discovered that withdrawal of nitisinone, used to prevent liver failure resulting from HT-1, caused a small number of mice to undergo a spontaneous loss of heterozygosity and revert to the Hgd-/- genotype, becoming phenotypically AKU [125]. Taylor and colleagues [111] published data showing these mice to be a model of ochronosis. However due to the spontaneity of their formation and their associated renal pathology they were never considered as a practical experimental model of AKU. The murine model of AKU presented in this thesis is a consistent model of AKU that shows the same metabolic and cellular characteristics of AKU in humans. As this was the case it was decided to see if nitisinone, which had already been shown to reduce plasma HGA levels in humans [53], could prevent the progression of ochronosis in a model that reproduced the pathology seen in patients.

The first study analysed the effects of lifetime nitisinone administration on BALB/c Hgd-/- mice. The treated group were given a dose of 4mg/l of nitisinone; this was selected from HPLC studies which showed this to be the lowest dose which had an effect on HGA levels. Mice from both the control (filtered water) and treated groups were culled halfway through the study to determine the efficacy of nitisinone up to that point. Although no data from these mice was shown in this Chapter, the treated group showed no signs of ochronosis and/or pigmentation whilst the control group all contained pigmented chondrons in numbers similar to

those seen in age-matched Hgd-/- mice in the natural history study (Chapter 3). The remaining mice in both groups were left in the study and culled at a pre-determined end-point. All of the mice in the control group showed extensive pigmentation throughout the ACC in both the femur and tibia which was expected. There were slight variations in the number of pigmented chondrons between each mouse in the control group (Fig. 5.17) however this was no different from what was seen in BALB/c Hgd-/- mice in the natural history study (Chapter 3). The variations in the number of pigmented chondrons may be attributed to how active each individual mouse was on a daily basis. Repetitive and continuous mechanical loading of the knee joint is known to cause changes in the composition and organisation of the ECM, micro fracture of the underlying SCB and to accelerate cartilage degradation, [209-211] which has already been cited in this thesis as a possible mechanism for pigmentation initiation. Mice which are not as active as others are less likely to cause as much significant damage to their ECM and therefore it is reasonable to assume less chondrons in these mice will undergo the necessary cellular and extracellular changes required to become pigmented.

Signs of osteoarthropathy including cartilage fibrillations and osteophyte formation were observed in most of the control mice (Figs. 5.10, 5.12 & 5.14), again this was expected. It is possible these changes resulted from the deposition of pigment in the joint, as this is thought to alter the biomechanics of the joint leading to the development of OA. However some of these changes may simply be related to the advancing age of the mice. Quantifying the joint damage between control and treated groups, using the OARSI histopathology initiative [120], may help to determine if the damage observed was as a consequence of pigment deposition or ageing. The mice treated with nitisinone showed different pathology as no chondron pigmentation was observed throughout the knee joint (Fig. 5.17), although some cartilage damage was observed. The result is consistent with the findings obtained from Hgd-/- mice culled halfway through the lifetime study. Nitisinone efficacy was maintained during the mouse lifetime and there were no noticeable changes in the behaviour and health between the control and treated

groups. Nitisinone works by inhibiting the HPPD enzyme [212, 213] consequently preventing the formation of HGA. This step is critical in the treatment of AKU however it can result in abnormally high tyrosine levels therefore a low tyrosine diet is usually recommended when treating with nitisinone. Previous clinical trials in humans have reported adverse effects resulting from high tyrosine levels [53], whilst another study reported impaired cognitive function in some patients receiving nitisinone [214]. With no adverse effects reported in any of the mice it demonstrated that the right dosage of nitisinone can prevent any manifestation of ill effects. It is highly significant that the study was completed over the whole life as it provided vital data that would otherwise be unobtainable in other species or indeed AKU patients. The study of the natural history of ochronotic osteoarthropathy in Hgd-/- mice showed that pigment deposition begins at a very early age and continues to progress, to the point of severe osteoarthropathy. This data was used to determine the starting point for the treatment regime and also allowed for a study of the effects on the initiation, progression and prevention of AKU with long term nitisinone treatment. Determination of HGA levels in Hgd-/- mice also provided important data with regards to the efficacy of nitisinone. Lifetime plasma HGA levels measured in both groups showed an 88% drop in plasma HGA when Hgd-/- mice were treated with nitisinone (Fig. 5.18). Age-related loss of renal function normally occurs in humans [215] and mice [216]; therefore it is possible declining excretion may lead to rising plasma HGA levels which lead to the midlife observation of pathological, ochronotic changes. However, as the mean HGA plasma level remained broadly steady across the Hgd-/- mouse lifetime (Fig. 5.18), it suggested that decreasing kidney function did not initiate ochronosis. It appears from the data presented in this thesis that in AKU patients the midlife onset of ochronotic osteoarthropathy is the clinical manifestation of a pathological process beginning much earlier than when decline in kidney function occurs. The data gathered in this Chapter strongly suggests that early intervention with nitisinone will prevent the pathological process that leads to irreversible cartilage damage and joint destruction. It should be noted that although no adverse effects were reported in Hgd-/- mice, administration of nitisinone particularly from a very young age may have detrimental effects. Previous reports have suggested mental

impairment may develop as a result of 4-HPPD inhibition by nitisinone, as this results in tyrosinemia type III which is thought to be associated with neurological problems [52]. This is something that would have to be taken into account and monitored closely in clinical trials involving young AKU patients. The data from the lifetime nitisinone study should be of significant use for future clinical trials involving AKU and nitisinone as they offer evidence that nitisinone administration earlier in life provides beneficial effects by preventing the onset of ochronotic osteoarthropathy.

The second study detailed in this Chapter described the efficacy of nitisinone administration midway through life, again in BALB/c Hgd-/- mice. The treated group were given the same dose of nitisinone (4mg/l) as used in the lifetime study whilst the control group were again kept on filtered water. The control group showed signs consistent with severe ochronotic osteoarthropathy including large numbers of pigmented chondrons (Fig. 5.25), osteophyte formation and pigmentation (Fig. 5.26), and erosion of the HAC (Fig. 5.27). These mice presented with some of the most severe osteoarthropathy seen in Hgd-/- mice, yet a few of them had relatively low numbers of pigmented chondrons for their age. Variation between the numbers of pigmented chondrons in individual mice has been a consistent observation throughout all the studies described in this thesis, however some individual counts were particularly low. BALB/c Hgd-/- 51.1 (♂) had only 142 pigmented chondrons throughout its knee joint which is more akin to a Hgd-/- mouse aged 45 weeks, not 80 (Fig. 5.30). Again this may be linked to the inactivity of aged mice when compared to that of younger mice. Decreased renal function is probably not involved as steady levels of plasma HGA were maintained over the lifetime. The results obtained from the treated group were expected, at least in relation to the numbers of pigmented chondrons identified. All six mice in the treated group showed a significant drop in the number of pigmented chondrons in the ACC (Fig. 5.30). The numbers of pigmented chondrons in the treated mice were in a range that would be expected in mice aged between 25 and 38 weeks. The prevention of further pigment deposition when nitisinone treatment began

highlighted the efficacy of the compound. However nitisinone was only able to prevent further pigmentation of the cartilage and not reverse the effects of ochronosis which had taken place up to the point of administration. These results are important as they provide further evidence that nitisinone treatment should begin early in life to completely prevent any pigment deposition and the associated osteoarthropathy. Once pigment has been laid down in the ACC the pathological process resulting in severe osteoarthropathy appears to have already begun; treatment with nitisinone appears to do little to halt this process. Osteophytes (Figs. 5.21 & 5.24) were identified in several of the treated mice and severe cartilage erosion was also seen (Fig. 5.23). The presence of these osteoarthritic markers leads to the assumption that nitisinone can do little to prevent osteoarthropathy from setting in once the process has begun.

This Chapter demonstrated the first ever inhibition of ochronotic pigment with nitisinone. This result is an important advance in AKU research as it shows that nitisinone, whether given from the start of life or at a selected time point, prevents pigmentation in the articular cartilage of the tibio-femoral joint. The ability to study the effects of nitisinone in an AKU murine model provides data that otherwise would not be available. There is difficulty in obtaining data from human trials due to a number of factors including the length of the study, regular access to patients and most importantly in the case of AKU, the inability to analyse articulating joints histologically at selected time intervals. The studies described in this Chapter also provide very important data about how and when treatment should commence with nitisinone. The data suggest that nitisinone treatment should begin as early as possible in order to prevent the initiation of the pathological process which culminates in irreparable cartilage damage and severe ochronotic osteoarthropathy. The data collected from the trials described in this Chapter have been presented to the European Medicines Agency in support of the Suitability of Nitisinone in Alkaptonuria (SONIA) 1 and 2 clinical trials. Future clinical trials using nitisinone to treat AKU, including SONIA 2, would be well advised to include young patients who have yet to develop any joint arthropathies, to establish whether

cartilage damage and eventual joint destruction in humans can be delayed or prevented.

6. Surgical and chemical interventions in Hgd-/- mice

6.1 INTRODUCTION

The identification of ochronotic pigment in Hgd-/- mice (Chapter 3) has provided opportunities to investigate further whether interventions, both preventative and potentially damaging, can halt or accelerate pigmentation. The use of nitisinone as a therapeutic treatment for AKU has been described in Chapter 5 of this thesis and is shown to prevent pigmentation in Hgd-/- mice. This Chapter details the effectiveness of surgical and chemical intervention in increasing the amount of ochronotic pigment deposited in Hgd-/- mice.

DMM is a surgical technique developed by Glasson *et al* [118] which has been shown to induce mild to moderate OA in mice four weeks post-operatively (post-op), and moderate to severe OA eight weeks post-op. Early onset of severe OA is a recognized consequence of AKU [20], and micro damage resulting from repetitive mechanical loading is thought to be a factor in the initiation and progression of this ochronotic osteoarthropathy [36]. This Chapter details whether the damage caused by DMM surgery resulted in an increased number of pigmented chondrons in the ACC due to a possible association between microdamage and the initiation of ochronosis and OA.

HGA is the “culprit molecule”, the single most important factor in the pathogenesis of AKU. Elevated plasma levels of HGA are essential in the initiation and continued progression of ochronosis both in humans [9] and mice [217]. Other factors are also involved in the process of pigmentation leading to specific tissues becoming susceptible to pigment deposition. Although large amounts of HGA are excreted in urine, high levels remain in plasma which ultimately leads to the development of ochronotic osteoarthropathy. This Chapter details whether supplementing Hgd-/- mice with 5mM HGA increased plasma HGA levels even further, and led to an increase in the number of pigmented chondrons in Hgd-/- mice.

6.2 DESIGN OF STUDY

6.2.1 Surgical intervention

DMM surgery was performed on the left knee of six BALB/c Hgd-/- mice (three males, three females). All mice were aged between 48 and 52 weeks when the surgery was completed. Three of the mice were left for eight weeks post-op and three for twelve weeks post-op before being culled. Once the *in vivo* portion of the study had concluded both experimental (left) and contralateral control (right) knees were dissected out from the mice and stained with H&E and Schmorl's stain. One whole section of the entire tibio-femoral joint was quantified to identify any effect on the level of pigmentation between the experimental and contralateral control joints.

6.2.2 Chemical intervention

Water containing 5mM of HGA was given to a group of ten BL/6 Hgd-/- mice over their whole lifespan. A control group had access to normal drinking water in the same timeframe. Plasma HGA levels were measured and one whole section of the entire tibio-femoral joint was quantified to identify if any effect could be observed on the level of pigmentation.

6.3 RESULTS

6.3.1 Destabilization of the medial meniscus

6.3.1.1 Eight weeks post-op

6.3.1.1.1 BALB/c Hgd-/- 100.1 (♀) – 60 weeks

Signs of OA were discovered in both the medial and lateral aspects of the tibio-femoral joint in the experimental knee of BALB/c Hgd-/- 100.1 (♀). The photomicrograph below (Fig. 6.1) shows the formation of an osteophyte on the MTP, and the MM slightly out of place due to the transection of the MMTL (Fig. 6.1). There appeared to be no obvious cartilage degradation on either the MFC or the MTP, and only minor fibrillations on the LTP (Fig. 6.2) indicating the osteoarthritic changes in the joint were mild to moderate, not severe.

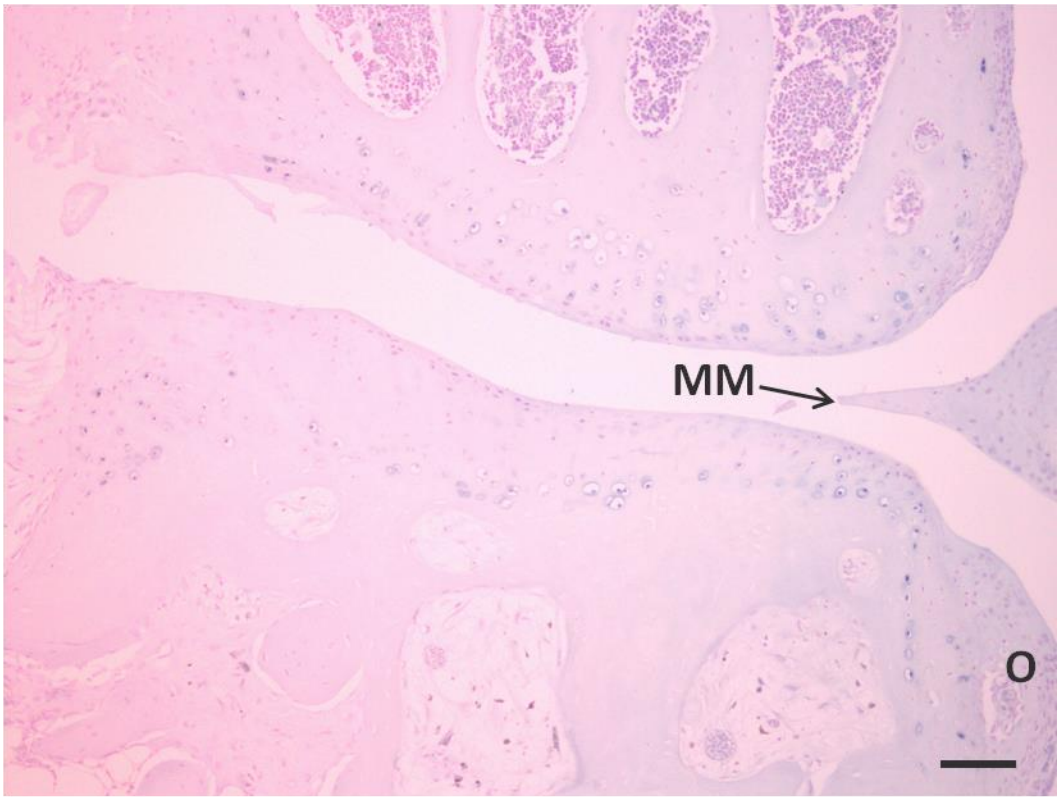

Figure 6.1 – Osteophyte formation on the medial tibial plateau of BALB/c 100.1, a 60 week old Hgd-/- mouse culled at 8 weeks post-op. Schmorl's staining showed significant amounts of pigmentation in the osteophyte (**O**) and MTP and MFC. Bar = 100µm.

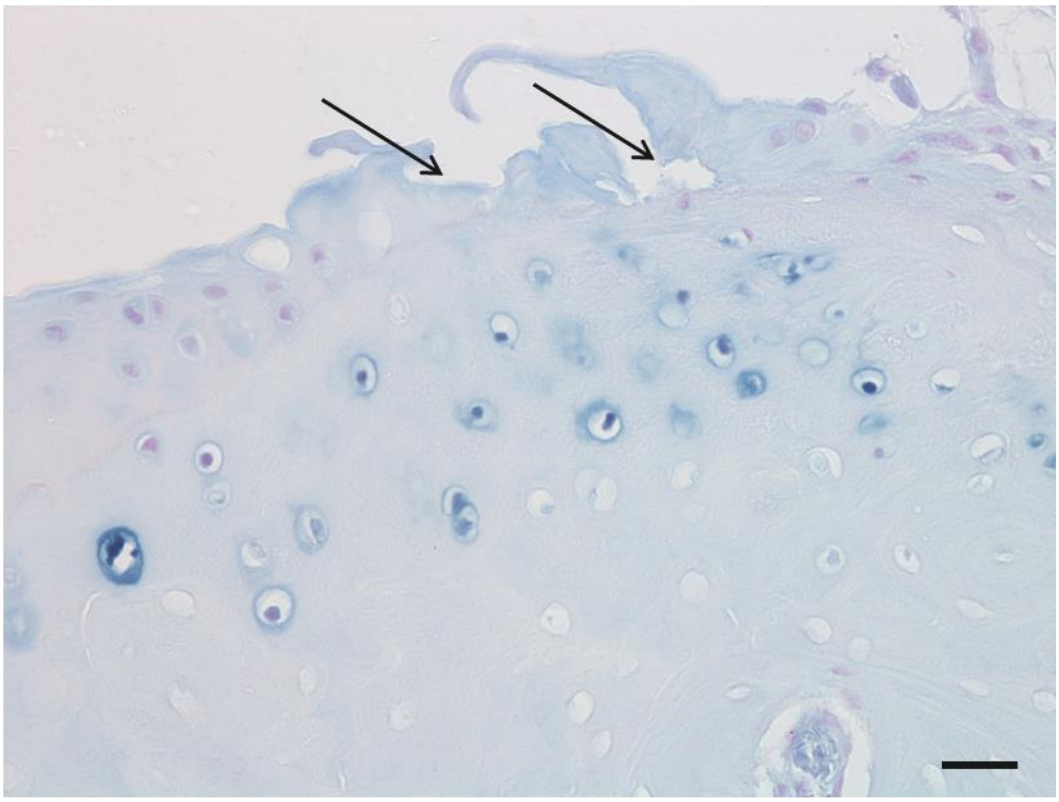

Figure 6.2 – Minor fibrillations on the lateral tibial plateau in the experimental knee of BALB/c 100.1, a 60 week old Hgd-/- mouse culled at 8 weeks post-op. Fibrillations were observed on the LTP and were consistent with mild to moderate OA (arrowed). Schmorl's staining also highlighted heavily pigmented chondrons in the ACC. Bar = 20μm.

Quantification of the pigmented chondrons showed numbers similar to those seen in Hgd-/- mice aged 48 weeks (data from Chapter 3) (Fig. 6.11). Variation in the number of pigmented chondrons was observed throughout the natural history study so these results are not unexpected. It does appear to show however, at least in this mouse, that DMM has not increased the amount of pigmentation present.

Analysis of the contralateral control showed very minor fibrillations on the LFC (Fig. 6.3). No other damage was observed throughout the rest of the joint, and no osteophytes or SCB sclerosis or remodelling was present. Quantification of the

pigmented chondrons revealed a higher number located in the control knee joint (183) in comparison to the experimental knee joint (110) (Fig. 6.11 & Table. 6.1). One possible explanation for this data is that the mouse placed more pressure on its control knee joint as constant loading of its experimental knee joint was too painful.

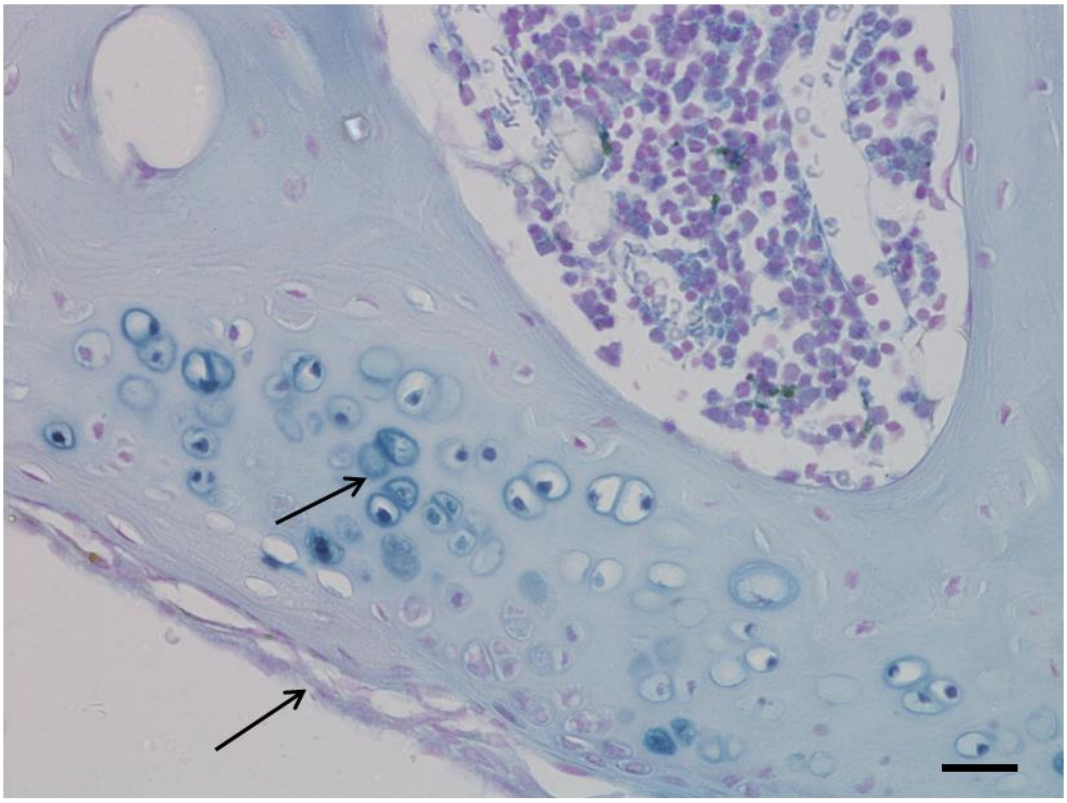

Figure 6.3 – Minor fibrillations on the lateral femoral condyle in the control knee of BALB/c 100.1, a 60 week old Hgd-/- mouse culled at 8 weeks post-op. Schmorl's staining showed fibrillations on the LFC consistent with very mild OA (right arrow). Heavily pigmented chondrons were present in large numbers in the ACC of the LFC (left arrow). Bar = 20µm.

6.3.1.1.2 BALB/c Hgd-/- 100.2 (♀) – 60 weeks

Obvious signs of OA were observed in the experimental tibio-femoral joint of BALB/c Hgd-/- 100.2 (♀). Small osteophytes were located on both the MFC and

MTP along with loss of surface lamina on both (Figs. 6.4 & 6.5). Fibrillations of the HAC were present on the MTP and there was also detachment of the HAC from the ACC in one area of the MTP (Fig. 6.4). These data suggest DMM surgery caused moderate to severe OA in the experimental knee joint.

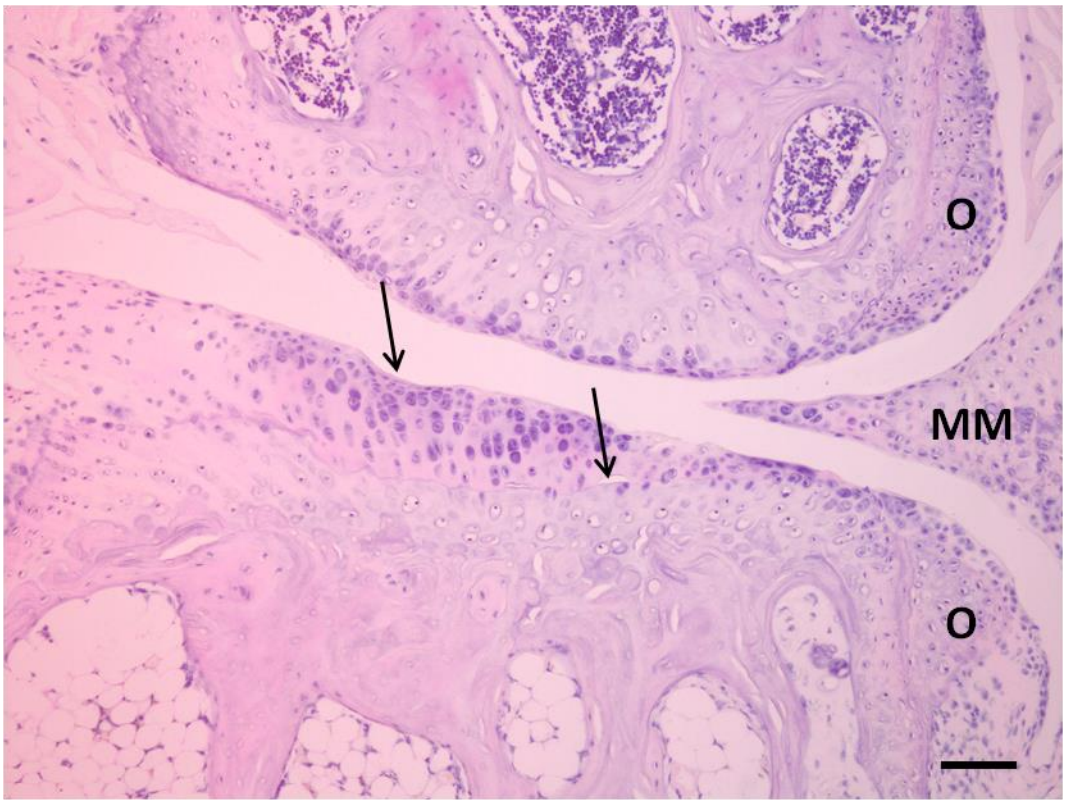

Figure 6.4 – Identification of osteophytes and hyaline articular cartilage damage in the experimental knee of BALB/c 100.2, a 60 week old Hgd-/- mouse culled at 8 weeks post-op. H&E staining revealed the presence of two small osteophytes (**O**) on the MTP and MFC. Loss of the surface lamina was located along the MTP (left arrow), while detachment of the HAC from the ACC was observed in a small area of the MTP (right arrow). Bar = 100µm.

Quantification of the pigmented chondrons showed numbers similar to those observed in Hgd-/- mice of around 56 weeks of age (data from Chapter 3) (Fig. 6.11). Again, similar to BALB/c Hgd-/- 100.1, this result was consistent with the level of variability observed in Hgd-/- mice in the natural history study. The result also

appeared to show that DMM surgery did not increase the amount of pigmented chondrons in Hgd-/- mice.

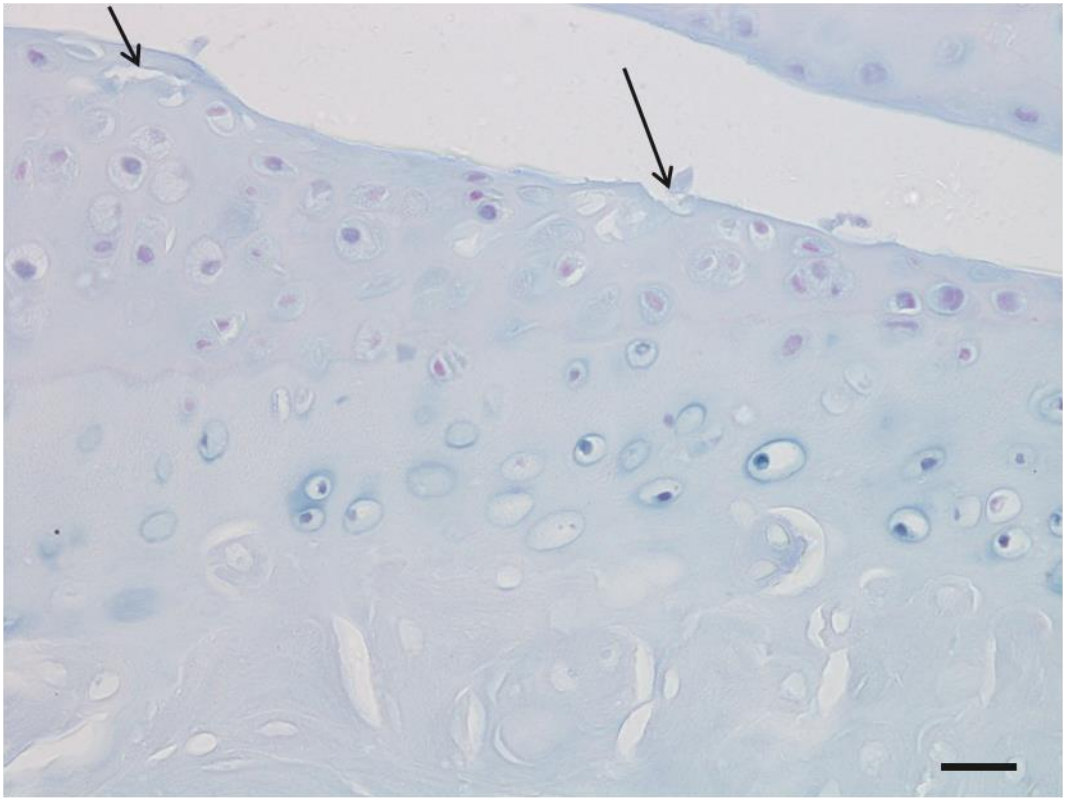

Figure 6.5 – Hyaline articular cartilage damage in the experimental knee of BALB/c 100.2, a 60 week old Hgd-/- mouse culled at 8 weeks post-op. Schmorl's staining of the MTP showed damage along the articular surface (arrowed) and the presence of hypertrophic heavily pigmented chondrons in the ACC. Bar = 20µm.

Analysis of the contralateral control showed minor damage along the articular surface on the MFC (Fig. 6.6). An osteophyte was located on the MFC (Fig. 6.6) however the rest of the knee joint showed no damage. Quantification of the pigmented chondrons revealed a lower number of pigmented chondrons (148) than the experimental knee joint (172) (Fig. 6.11 & Table. 6.1).

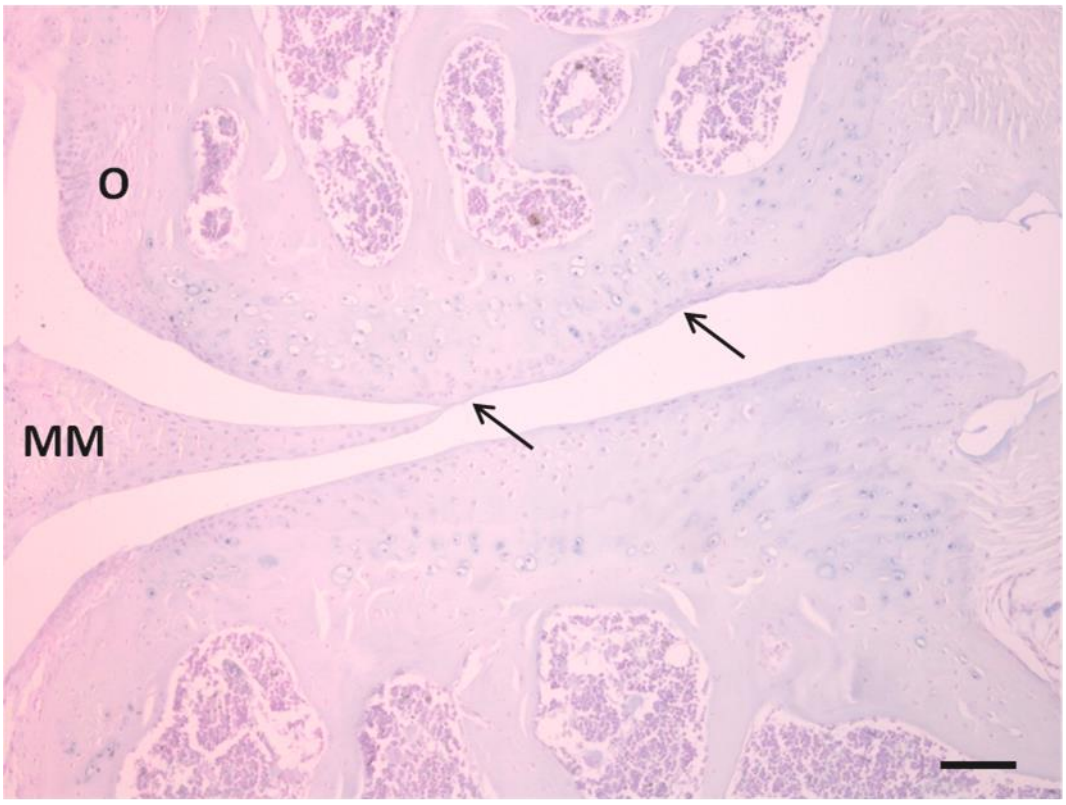

Figure 6.6 – Minor damage along the articular surface of the medial femoral condyle in the control knee of BALB/c 100.2, a 60 week old Hgd-/- mouse culled at 8 weeks post-op. Schmorl's staining showed minimal damage along the MFC with definite loss of the surface lamina (arrowed). Large numbers of pigmented chondrons were located throughout the ACC in both the MFC and MTP. Bar = 100µm.

6.3.1.1.3 BALB/c Hgd-/- 101.1 (♂) – 60 weeks

BALB/c Hgd-/- 101.1 (♂) displayed the most severe OA out of the three mice culled at eight weeks post-op. There was significant HAC erosion on the MTP exposing the underlying ACC (Fig. 6.7). A large ossified osteophyte was present on the MTP and significant damage was located along the articular surface of the MFC (Fig. 6.7). More severe damage was located on both the LFC and LTP. There appeared to be ≥90% of HAC eroded on the LFC and ≤50% eroded on the LTP, exposing the ACC underneath (Fig. 6.8).

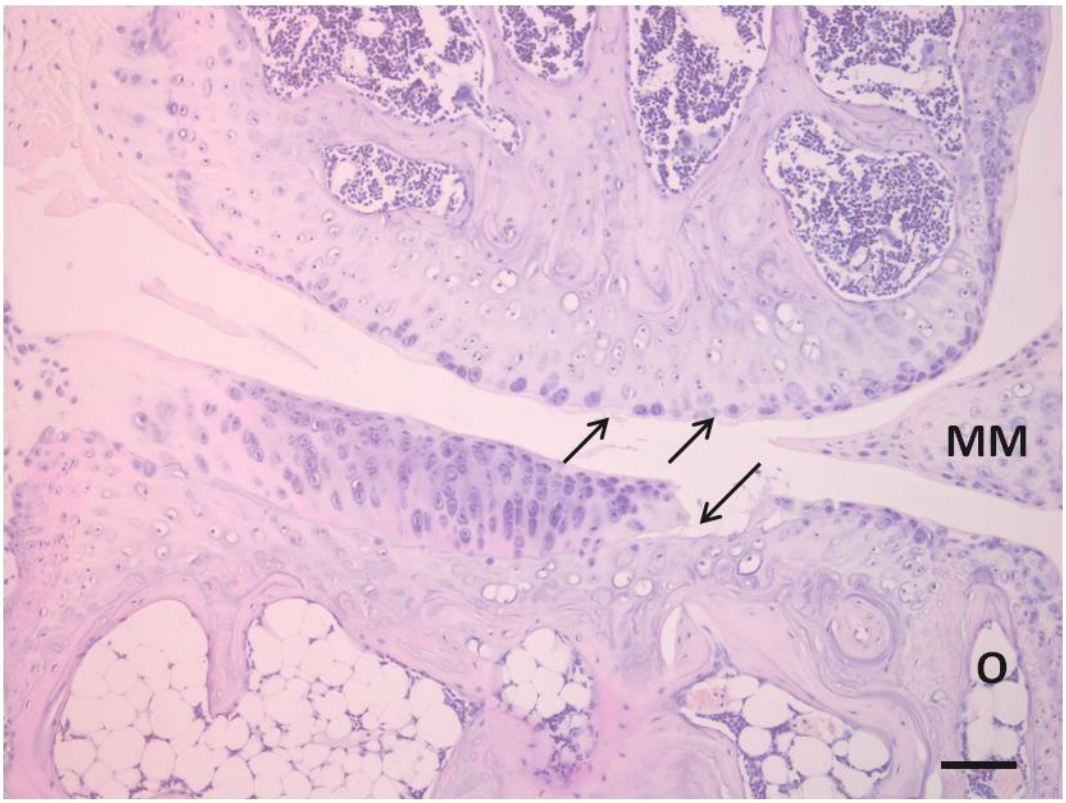

Figure 6.7 – Severe cartilage erosion on the medial tibial plateau, and partial erosion of the cartilage on the medial femoral condyle in the experimental knee of BALB/c 101.1, a 60 week old Hgd-/- mouse culled at 8 weeks post-op. H&E staining revealed a small but significant loss of HAC leading to the exposure of ACC on the MTP (right arrow). Loss of surface lamina and small amount of cartilage erosion were located on the MFC (left arrows). Bar = 100µm.

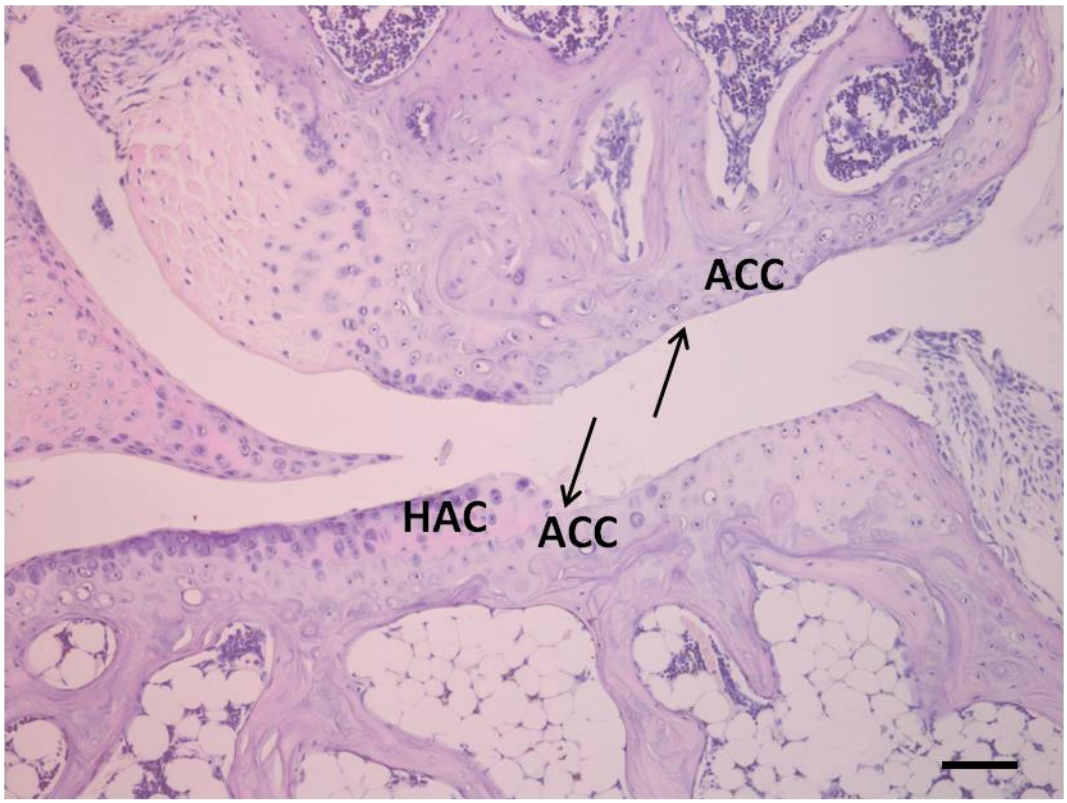

Figure 6.8 – Severe cartilage erosion on the lateral tibial plateau and lateral femoral condyle in the experimental knee of BALB/c 101.1, a 60 week old Hgd-/- mouse culled at 8 weeks post-op. H&E staining revealed extensive loss of HAC on both the LTP and LFC (arrowed). The severity of OA seen in the lateral aspect of this joint represents some of the most severe observed in any Hgd-/- mouse examined. Bar = 100µm.

Clusters of heavily pigmented chondrons were located adjacent to the damaged areas (Fig. 6.9). Quantification of the pigmented chondrons revealed numbers consistent with those seen in Hgd-/- mice aged 36-40 weeks (data from Chapter 3) (Fig. 6.11). Although variability is expected between individual mice, BALB/c Hgd-/- 101.1 having numbers similar to mice 20-24 weeks younger was slightly surprising.

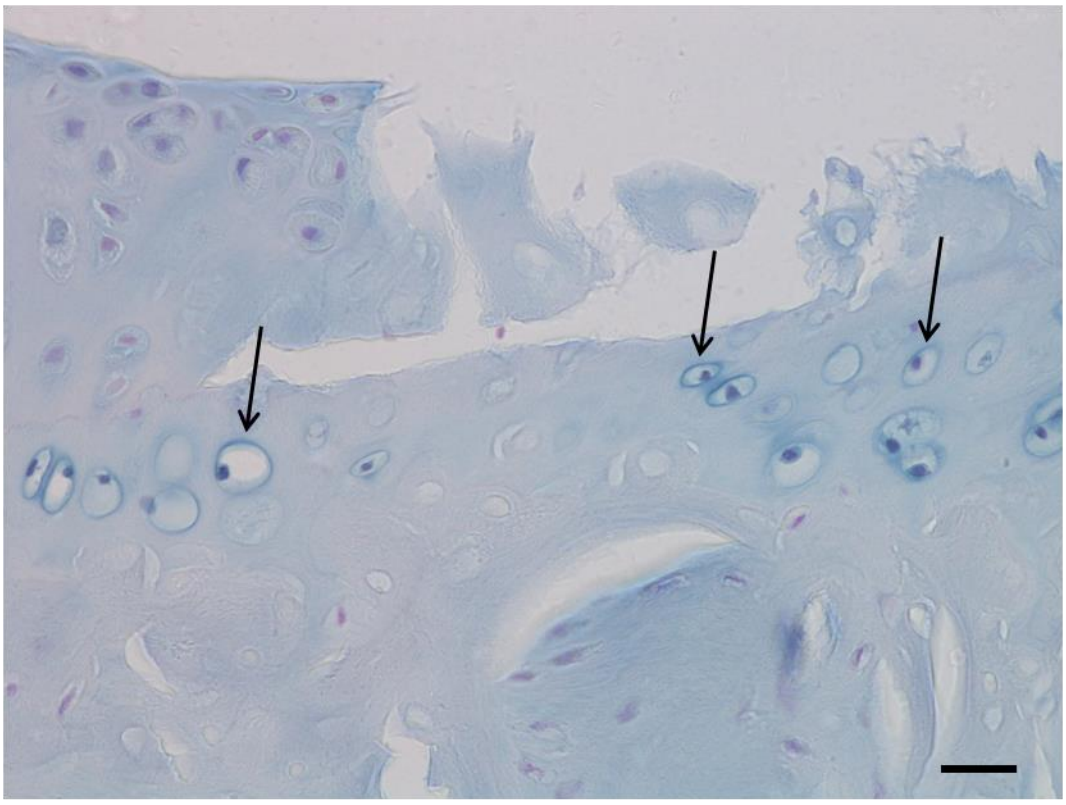

Figure 6.9 – Heavily pigmented chondrons located adjacent to cartilage erosion in the medial tibial plateau of the experimental knee of BALB/c 101.1, a 60 week old Hgd-/- mouse culled at 8 weeks post-op. Schmorl's staining showed pyknotic chondrons located close to the damaged area (arrowed). Bar = 20µm.

The contralateral control showed virtually no sign of OA, only very minor loss of the surface lamina was located along the MFC (Fig. 6.10). There were no signs of any cartilage loss or osteophyte formation throughout the rest of the knee joint. Quantification of pigmented chondrons revealed there to be a higher number in the control joint (151) to that observed in the experimental joint (109) (Fig. 6.11 & Table. 6.1). This was also seen in BALB/c Hgd-/- 100.1 which again appeared to imply that DMM surgery did not increase the number of pigmented chondrons present in the ACC.

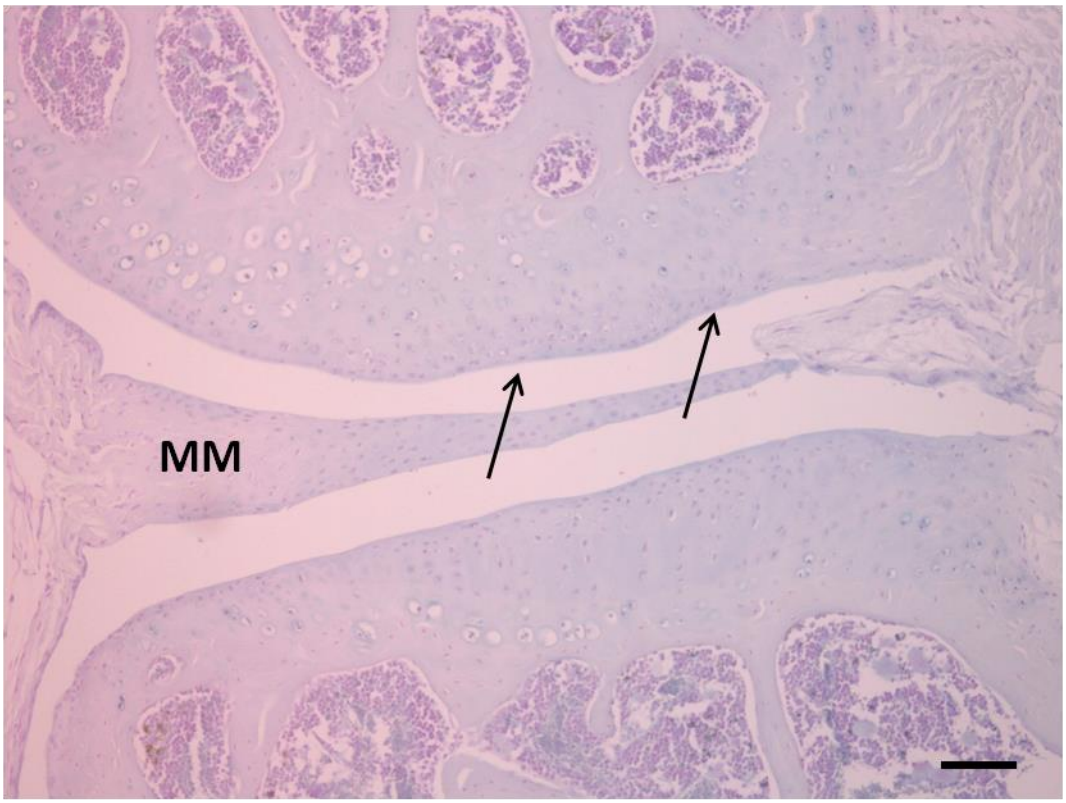

Figure 6.10 – Loss of surface lamina along the medial femoral condyle in the control knee of BALB/c 101.1, a 60 week old Hgd-/- mouse culled at 8 weeks post-op. Schmorl's staining showed a small loss of the surface lamina along the MFC. Large numbers of hypertrophic pigmented chondrons were located in the ACC of the MFC and MTP. Bar = 100µm.

6.3.1.1.4 Quantification of pigmented chondrons at eight weeks post-op

Pigmented chondrons in both the experimental and contralateral control tibio-femoral joints were quantified to determine if DMM surgery had had any effect on their numbers (Fig. 6.11). It is apparent from the data shown on the scatter chart that DMM surgery did not have the proposed effect of increasing the number of pigmented chondrons present in the ACC of BALB/c Hgd-/- mice.

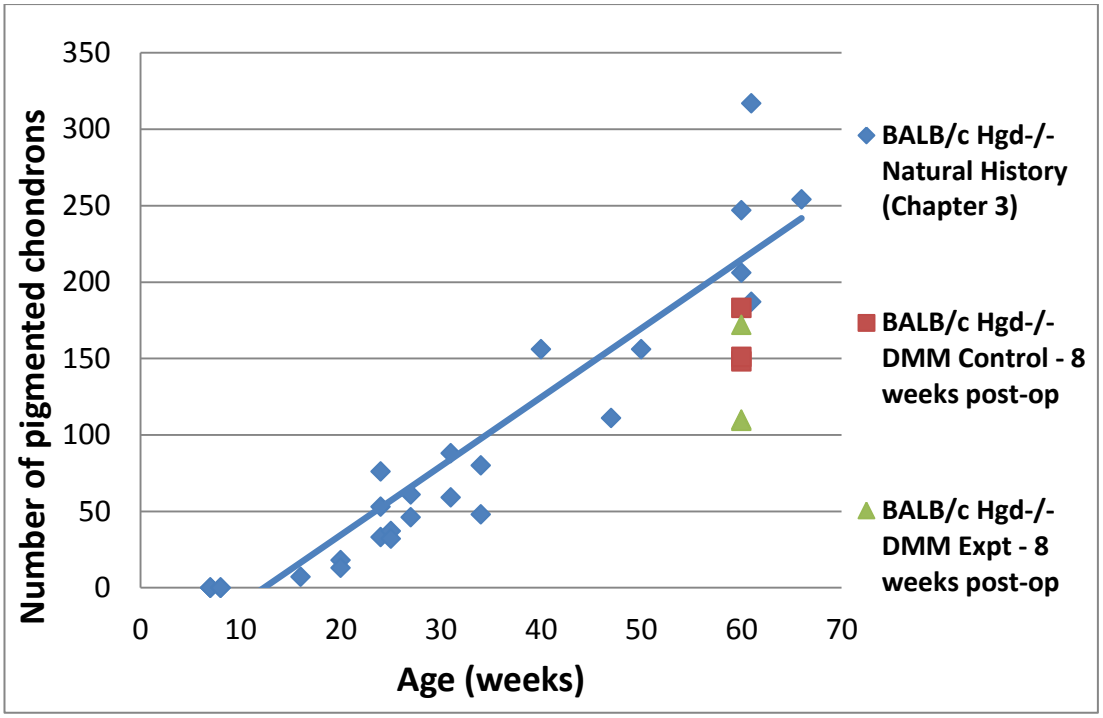

Figure 6.11 – The effect of DMM surgery, at eight weeks post-op, on the number of pigmented chondrons in BALB/c Hgd-/- mice. Scatter chart showing that DMM surgery did not appear to cause an increase in the number of pigmented chondrons in BALB/c Hgd-/- mice. Quantification of pigmented chondrons was performed on a single section from each mouse; this does not represent the total cell number in each mouse.

6.3.1.2 Twelve weeks post-op

6.3.1.2.1 BALB/c Hgd-/- 102.2 (♂) – 60 weeks

Signs of severe OA were observed on both the medial and lateral aspects of the experimental tibio-femoral joint in BALB/c Hgd-/- 102.2 (♂). Erosion of the HAC, exposing the underlying ACC was observed on ≥30% of the MTP (Fig. 6.12). A very large, fully ossified osteophyte was also located on the MTP while a small, developing osteophyte was located on the MFC (Fig. 6.12). Severe HAC erosion was observed on the LFC with ≤75% fully eroded exposing ACC (Fig. 6.13). Ossification of the LM was also seen (Fig. 6.13). Large clusters of heavily pigmented chondrons were located adjacent to the damaged area on the MTP (Fig. 6.14). This is consistent with the most severe OA observed in the mice at eight weeks post-op.

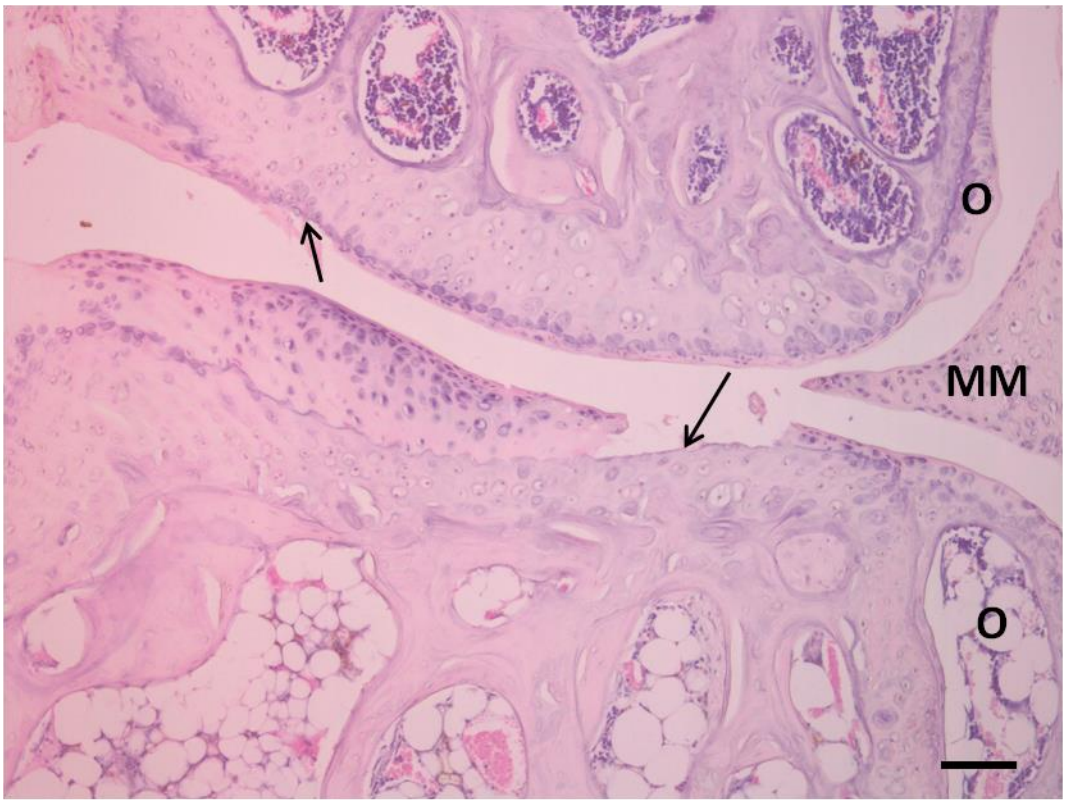

Figure 6.12 – Severe erosion of hyaline articular cartilage on the medial tibial plateau, and osteophyte formation in the experimental knee of BALB/c 102.2, a 60 week old Hgd-/- mouse culled at 12 weeks post-op. H&E staining showed loss of a significant portion of HAC along the MTP (right arrow) and fibrillations of HAC on the MFC (left arrow). Osteophytes (**O**) were located on both the MTP and MFC. Bar = 100µm.

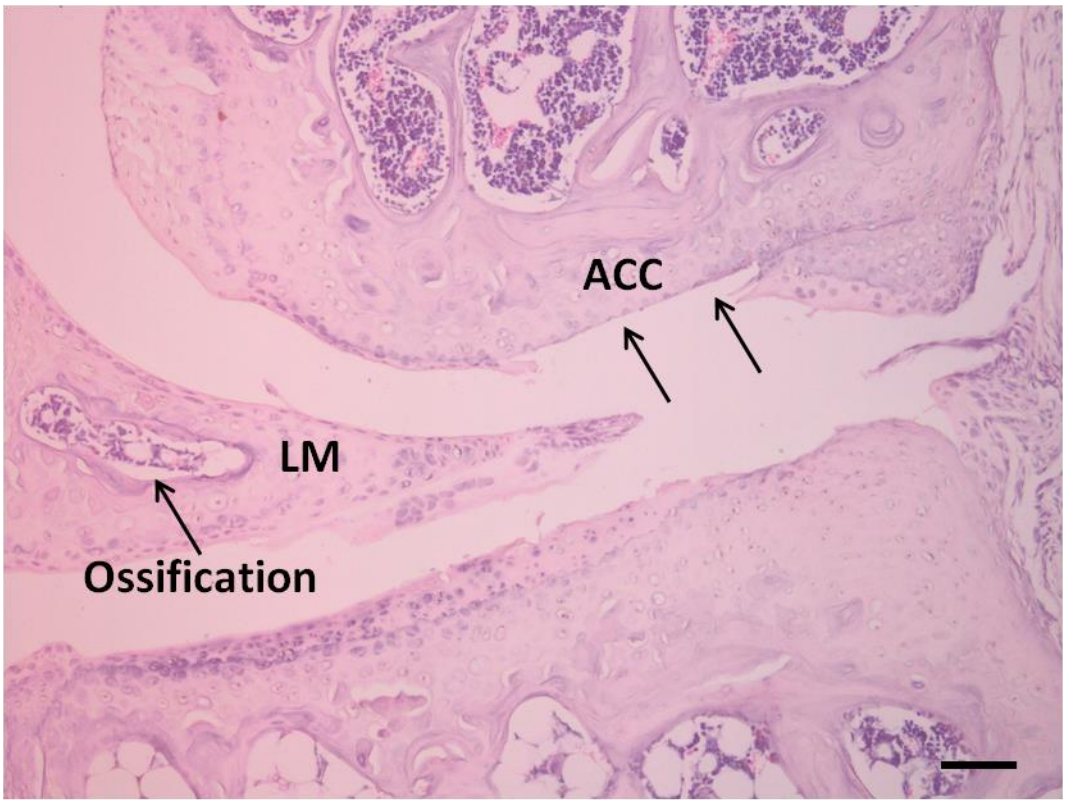

Figure 6.13 – Severe erosion of hyaline articular cartilage on the lateral femoral condyle, and ossification of the lateral menisci in the experimental knee of BALB/c 102.2, a 60 week old Hgd-/- mouse culled at 12 weeks post-op. H&E staining showed loss of a significant portion of the HAC along the LFC (right arrows) and ossification of the LM (left arrow). Bar = 100µm.

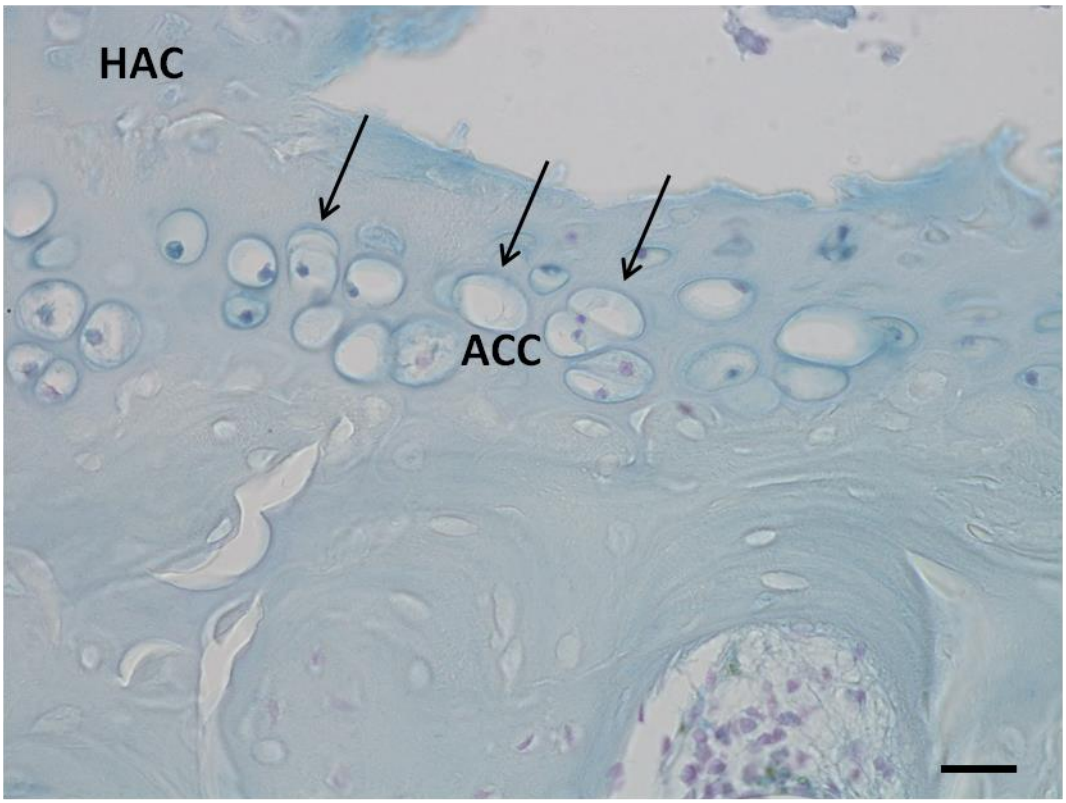

Figure 6.14 – Clustering of heavily pigmented chondrons adjacent to hyaline articular cartilage erosion in the medial tibial plateau of the experimental knee of BALB/c 102.2, a 60 week old Hgd-/- mouse culled at 12 weeks post-op. Schmorl's staining showed pyknotic chondrons adjacent to the damaged area of the MTP. Bar = 20µm.

Analysis of the contralateral control showed there to be very little damage. A small loss of surface lamina seen along the MTP was the only observed sign of cartilage degeneration. Large numbers of pigmented chondrons were present in the knee joint which was expected (Fig. 6.15). Quantification of both the experimental and control knee joints revealed there to be a higher number of pigmented chondrons in the experimental joint (156) than in the control joint (132) (Fig. 6.21 & Table. 6.1). These levels were in line with Hgd-/- mice aged 50 weeks, again highlighting the variability between individual mice.

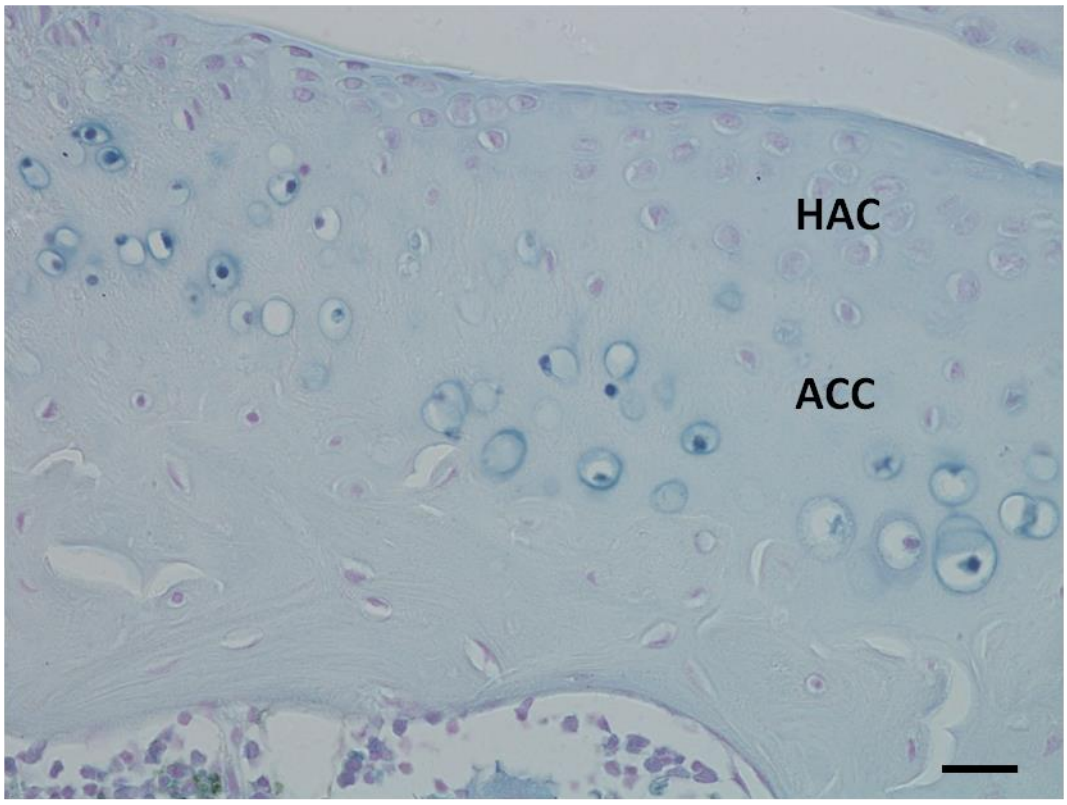

Figure 6.15 – Large numbers of pigmented chondrons in the medial tibial plateau of the control knee of BALB/c 102.2, a 60 week old Hgd-/- mouse culled at 12 weeks post-op. Schmorl's staining showed heavily pigmented chondrons throughout ACC of the MTP. Bar = 20µm.

6.3.1.2.2 BALB/c Hgd-/- 102.3 (♂) – 60 weeks

Signs of severe OA were present in the experimental tibio-femoral joint of BALB/c Hgd-/- 102.3 (♂), particularly on the medial aspect. Erosion of HAC was observed on ≥50% of the MTP and ≤50% on the MFC, exposing the ACC underneath (Fig. 6.16). A large ossified osteophyte was present on the MTP, and a small developing osteophyte was present on the MFC (Fig. 6.16). Fibrillations were seen along the articular surface of both the LTP and LFC (Fig. 6.17). The LM was also in the process of ossification (Fig. 6.17). Like previous mice in both DMM studies, pigmented chondrons were located adjacent to the areas of cartilage erosion on the MTP and MFC (Fig. 6.18).

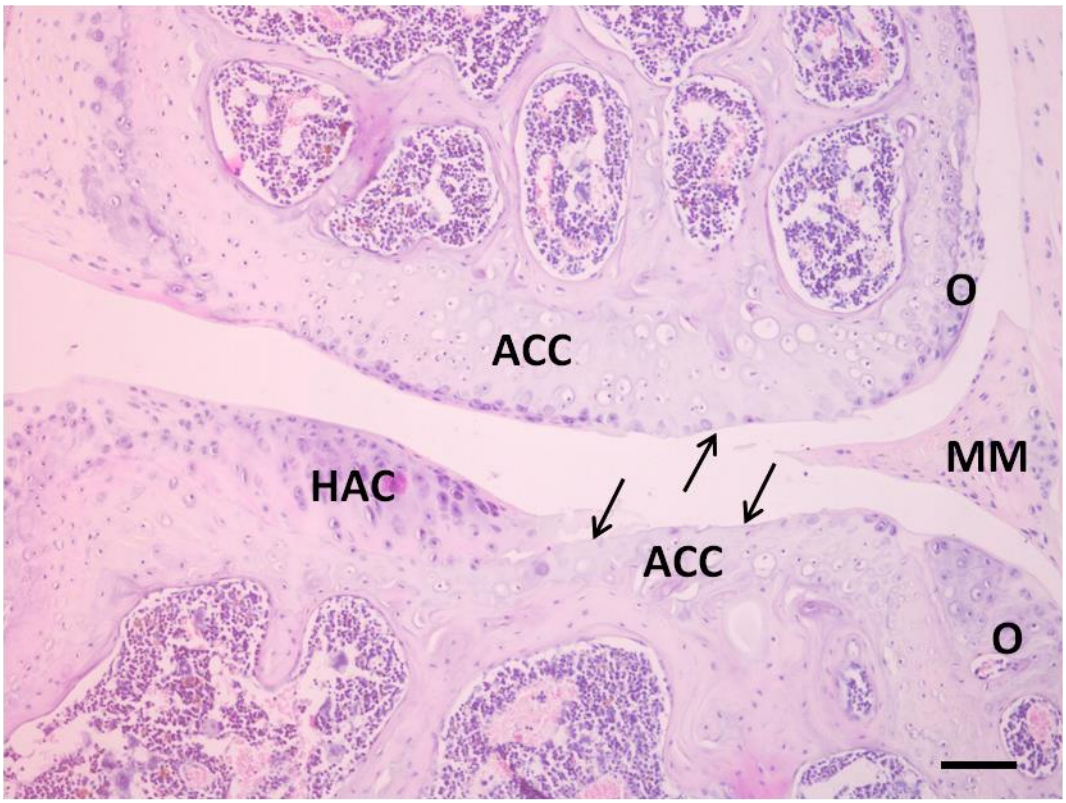

Figure 6.16 – Severe erosion of hyaline articular cartilage on the medial tibial plateau and medial femoral condyle in the experimental knee of BALB/c 102.3, a 60 week old Hgd-/- mouse culled at 12 weeks post-op. H&E staining showed loss of a significant portion of the HAC along both the MTP and MFC (arrowed). Osteophytes (**O**) were also seen on both the MTP and MFC. Bar = 100µm.

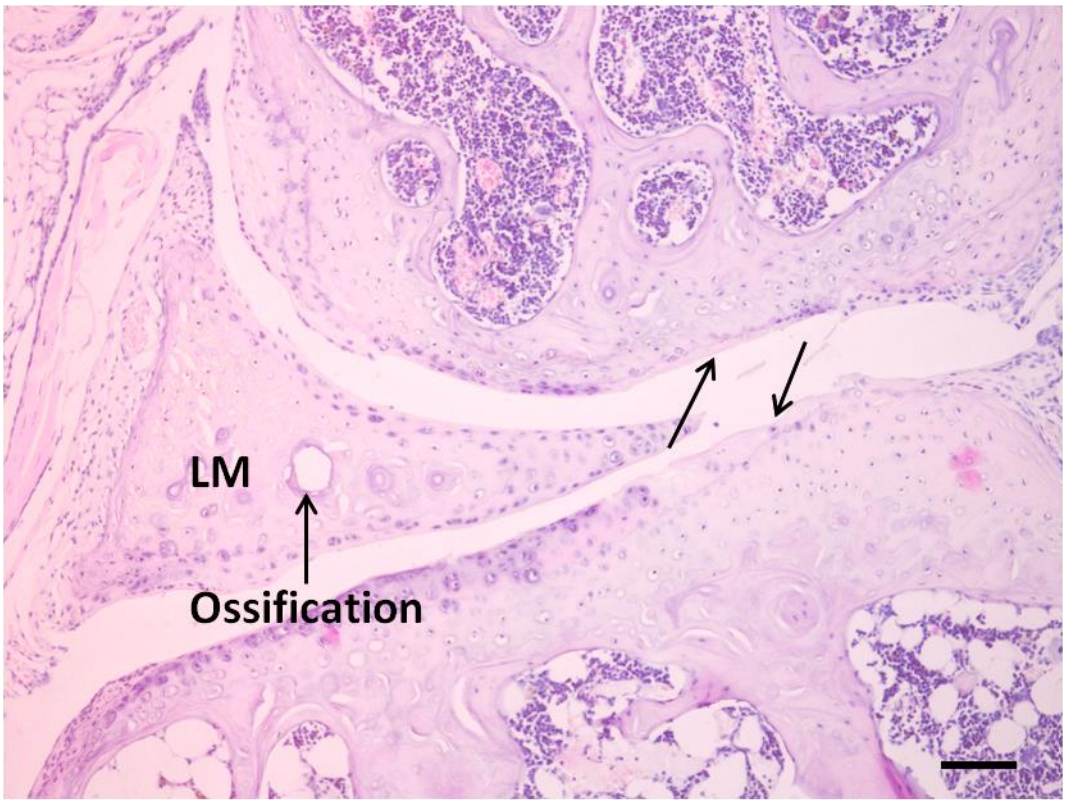

Figure 6.17 – Fibrillations along the hyaline articular cartilage on both the lateral tibial plateau and lateral femoral condyle in the experimental knee of BALB/c 102.3, a 60 week old Hgd-/- mouse culled at 12 weeks post-op. H&E staining showed fibrillation of the articular surface of both the LTP and LFC. The LM was also seen to be undergoing ossification. Bar = 100µm.

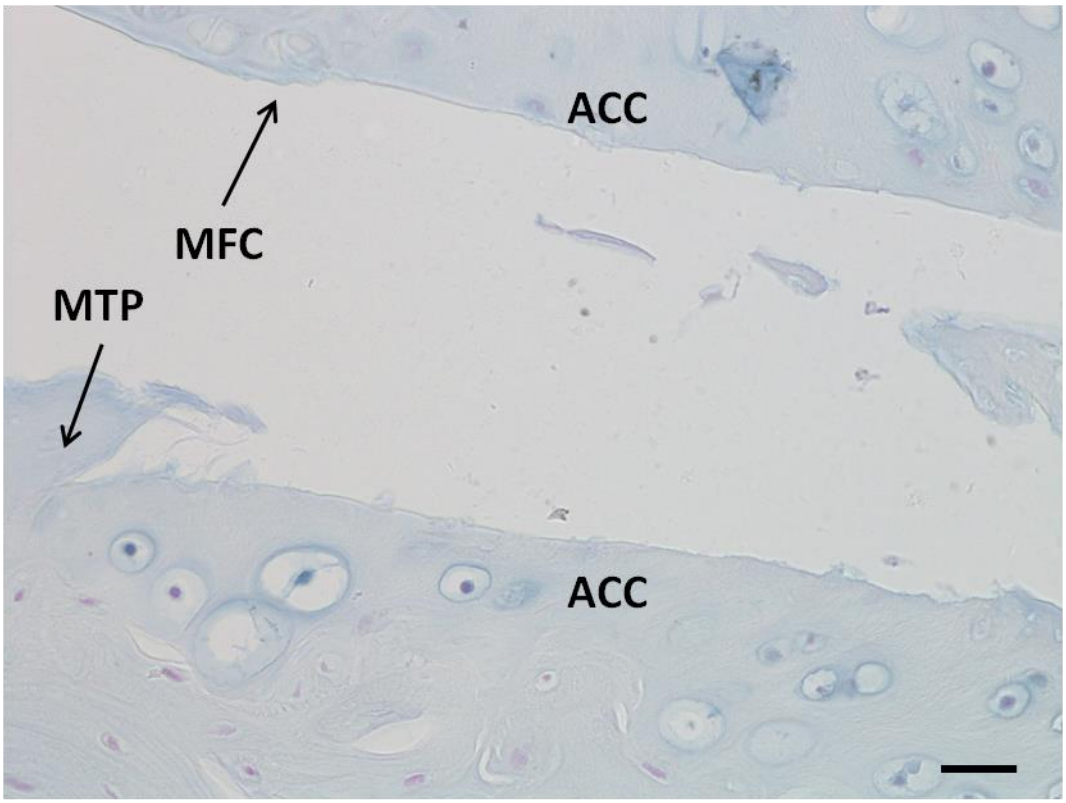

Figure 6.18 – Pigmented chondrons located at areas of damage in the medial aspect of the experimental knee of BALB/c 102.3, a 60 week old Hgd-/- mouse culled at 12 weeks post-op. Schmorl's staining showed heavily pigmented chondrons in the ACC located directly adjacent to areas of cartilage erosion on the MTP and MFC. Bar = 20µm.

Analysis of the contralateral control showed minimal damage, with ossification of the LM the only observed degeneration. Quantification of both the experimental and control knee joints revealed there to be a higher number of pigmented chondrons in the experimental joint (86) than the control joint (71) (Fig. 6.21 & Table. 6.1). These numbers were particularly low for a mouse aged 60 weeks, however this was only observed in one of the six mice used in the study therefore it appeared to be an anomaly.

6.3.1.2.3 BALB/c Hgd-/- 103.1 (♀) – 60 weeks

Signs of severe OA were observed in the experimental tibio-femoral joint of BALB/c Hgd-/- 103.1 (♀) with the most obvious being the detachment of ≥75% of the HAC from the underlying ACC (Fig. 6.19) on the MTP. Although the cartilage still appears to be in the correct position it can clearly be seen to be detached from ACC. Pigmented chondrons were located directly opposite the damaged area in ACC of the MTP (Fig. 6.20). The lateral aspect of the joint showed no signs of OA.

Figure 6.19 – Detachment of hyaline articular cartilage from articular calcified cartilage on the medial tibial plateau in the experimental knee of BALB/c 103.1, a 60 week old Hgd-/- mouse culled at 12 weeks post-op. H&E staining revealed detachment of a large area of the HAC from the ACC on the MTP (black arrows). There did appear to be a small area still attached to the ACC (red arrow) however most was completely free from the cartilage underneath. Bar = 100µm.

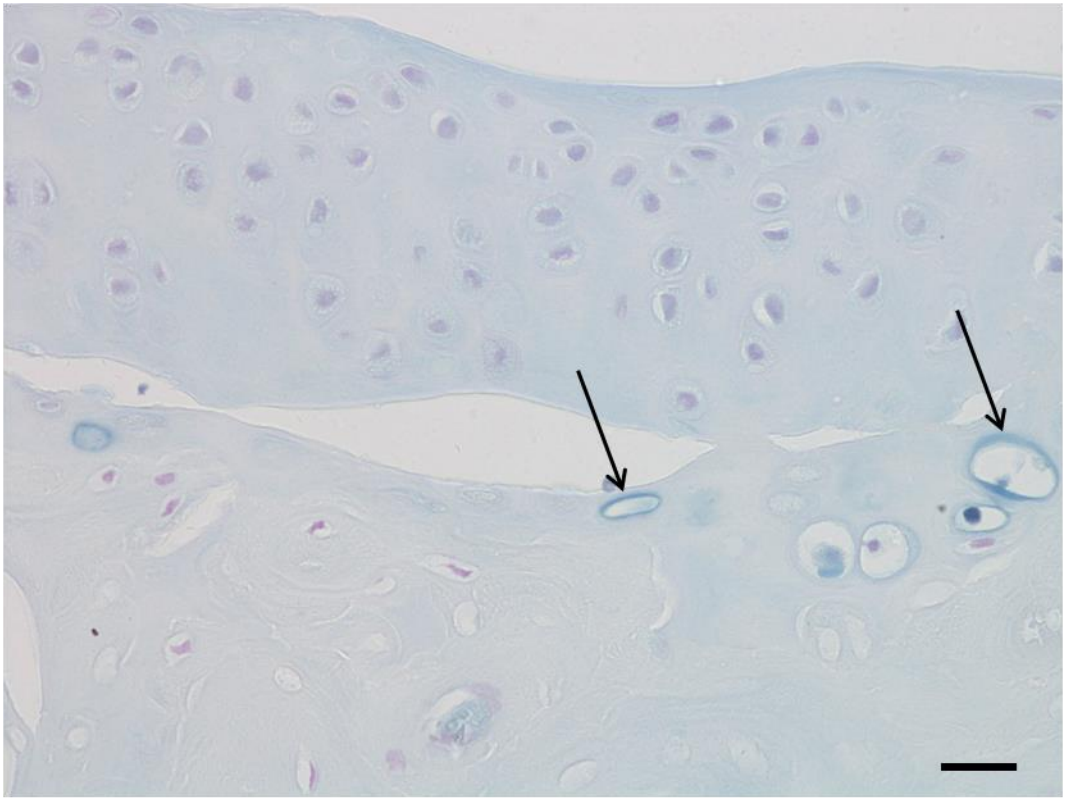

Figure 6.20 – Pigmented chondrons at the site of detachment on the medial tibial plateau in the experimental knee of BALB/c 103.1, a 60 week old Hgd-/- mouse culled at 12 weeks post-op. Schmorl's staining showed pigmented chondrons situated directly adjacent to the area of damage in the MTP. This was consistent with previous mice in the DMM study. Bar = 20µm.

Analysis of the contralateral control from BALB/c Hgd-/- 103.1 showed there to be minimal damage, with ossification of the LM the only observed degeneration. Quantification of both the experimental and control knee joints revealed there to be a higher number of pigmented chondrons in the experimental joint (151) than the control joint (130) (Fig. 6.21 & Table. 6.1). These numbers were consistent with what had been previously observed in the DMM study.

6.3.1.2.4 Quantification of pigmented chondrons at twelve weeks post-op

Pigmented chondrons in both the experimental and control tibio-femoral joints were quantified to determine if DMM surgery had had any effect on the number (Fig. 6.21). It was clear the data did not show an increase in pigmented chondrons present in the ACC of BALB/c Hgd-/- mice following surgery. Statistical analysis, performed using a paired t test, revealed no specific evidence of an increase in the number of pigmented chondrons in the experimental and contralateral control limbs (Table 6.1), both at 8 and 12 weeks post-op (P = 0.3872).

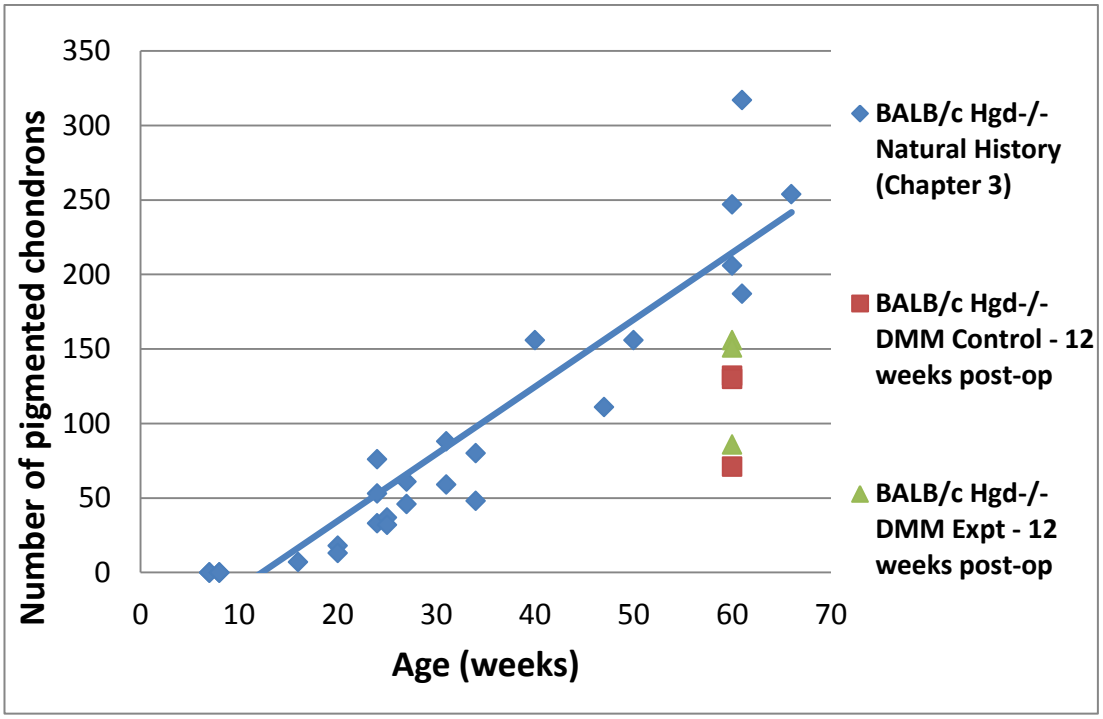

Figure 6.21 – The effect of DMM surgery, at twelve weeks post-op, on the number of pigmented chondrons in BALB/c Hgd-/- mice. Scatter chart showing that DMM surgery did not appear to cause an increase in the number of pigmented chondrons in BALB/c Hgd-/- mice. Quantification of pigmented chondrons was performed on a single section from each mouse; this does not represent the total cell number in each mouse.

6.3.1.3 Comparison of DMM Hgd-/- mice at eight and twelve weeks post-op

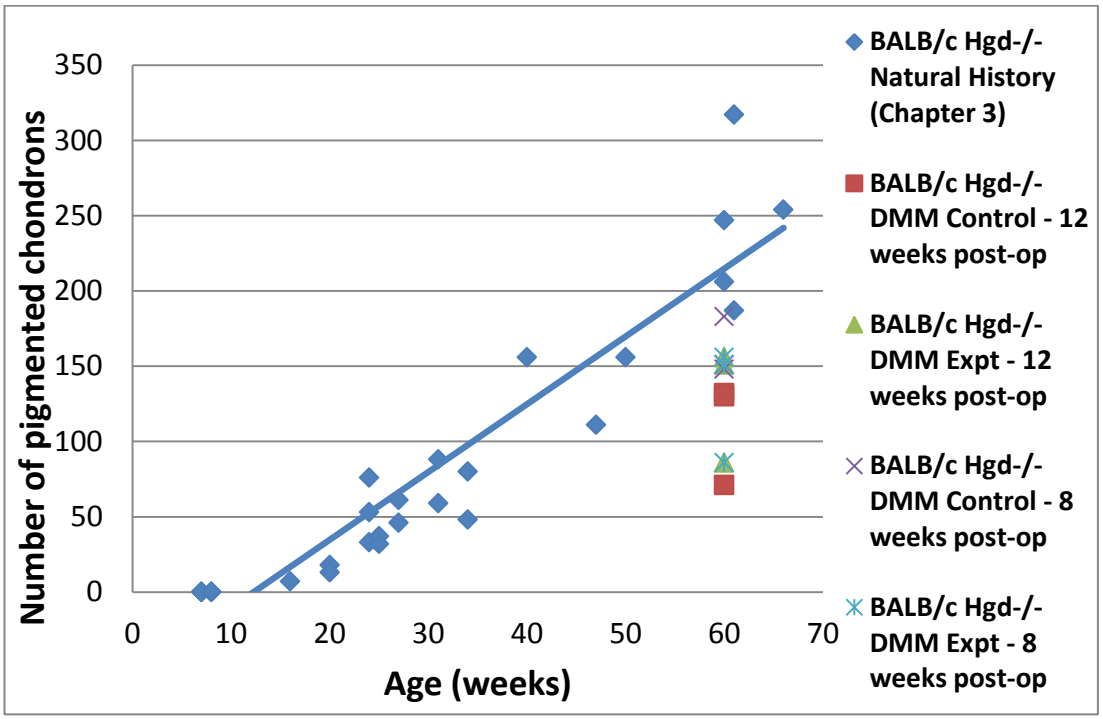

Figure 6.22 – A comparison of the effect of DMM surgery, at eight and twelve weeks post-op, on the number of pigmented chondrons in BALB/c Hgd-/- mice. Scatter chart showing that DMM surgery did not appear to cause an increase in the number of pigmented chondrons, both at eight and twelve weeks post-op, in BALB/c Hgd-/- mice. Quantification of pigmented chondrons was performed on a single section from each mouse; this does not represent the total cell number in each mouse.

BALB/c Hgd-/-	Pigmented chondrons – control limb (R)	Pigmented chondrons – experimental limb (L)
100.1 (♀)	183	110
100.2 (♀)	148	172
101.1 (♂)	151	109
102.2 (♂)	132	156
102.3 (♂)	71	86
103.1 (♀)	130	151
Mean	135.8333	130.6667
p	0.3872	

Table 6.1 – Quantification of pigmented chondrons in Hgd-/- DMM mice at eight and twelve weeks post-op. Animals highlighted in yellow are eight weeks post-op; animals highlighted in green are twelve weeks post-op.

Using the method described by the OARSI histopathology initiative for mice [120] both the experimental and contralateral control joints were scored to determine the severity of OA in the four quadrants (MTP, MFC, LTP, LFC). Statistical analysis, performed with a Wilcoxon signed-rank test, revealed a significant difference ($p=0.0273$) between the severity of OA in the experimental and contralateral control limbs (Tables. 6.2 & 6.3).

BALB/c Hgd-/-	Grading of OA changes – control limb (R)	Grading of OA changes – experimental limb (L)
100.1 (♀)	3	5
100.2 (♀)	2	7
101.1 (♂)	1	15
102.2 (♂)	1	15
102.3 (♂)	1	13
103.1 (♀)	1	9
Mean	1.5	10.6667
p	0.0273	

Table 6.2 – Cumulative grading scores of OA damage in Hgd-/- DMM mice at eight and twelve weeks post-op. Animals highlighted in yellow are eight weeks post-op; animals highlighted in green are twelve weeks post-op.

The results showed the highest severity of OA was located in the experimental tibio-femoral joints. There was a marked increase in the severity of OA at 12 weeks post-op however BALB/c 101.1 (8 weeks post-op) did show scores consistent with those observed at 12 weeks post-op. Another interesting observation was that three out of the six mice (100.1, 101.1, & 102.2) showed greater damage on the lateral aspect of the joint, rather than the medial aspect where the surgery was performed. As the medial portion of the joint is more prone to OA changes [218-220] the level of damage on the lateral aspect in these mice was somewhat surprising.

Scoring of the histological sections from the DMM study showed a higher severity of OA in males compared to females. This is consistent with previously reported literature where males have been shown to develop more OA than females in both DMM and collagenase induced models of OA [221, 222].

BALB/c (8 weeks post-op)	MTP	MFC	LTP	LFC	Total (MTP+MFC)	Total (LTP+LFC)	Cumulative Total
100.1 (L) 60wks (♀)	0	1	2	2	1	4	5
100.1 (R) 60wks	0	0	1	2	0	3	3
100.2 (L) 60wks (♀)	2	2	0	3	4	3	7
100.2 (R) 60wks	0	1	0	1	1	1	2
101.1 (L) 60wks (♂)	3	2	4	6	5	10	15
101.1 (R) 60wks	0	1	0	0	1	0	1
BALB/c (12 weeks post-op)	**MTP**	**MFC**	**LTP**	**LFC**	**Total (MTP+MFC)**	**Total (LTP+LFC)**	**Cumulative Total**
102.2 (L) 60wks (♂)	4	3	3	5	7	8	15
102.2 (R) 60wks	1	0	0	0	1	0	1
102.3 (L) 60wks (♂)	5	4	2	2	9	4	13
102.3 (R) 60wks	0	0	1	0	0	1	1
103.1 (L) 60wks (♀)	6	1	1	1	7	2	9
103.1 (R) 60wks	0	0	0	1	0	1	1

Table 6.3 – Histological scoring of osteoarthritic damage in DMM mice at eight and twelve weeks post-op. (L = experimental, R = control).

6.3.1.4 Retrospective power calculation

In retrospect it appeared that the DMM study was most likely underpowered and therefore did not provide accurate or reliable data. To prevent this from occurring in future studies a retrospective power calculation was carried out using the data from the BALB/c Hgd-/- natural history study (Chapter 3) as a guide.

6.3.1.4.1 8 weeks post-op

The mean number of pigmented chondrons in the BALB/c Hgd-/- DMM control group equalled 160.7, whilst the BALB/c Hgd-/- DMM experimental group equalled 130.3. The standard deviation of the difference between the two groups was equal to 49.54. These figures resulted in a power equal to 0.1029, meaning that a difference in the number of pigmented chondrons would be observed about 10% of the time. As a power of at least 80% is required for reliable data this shows the DMM study at 8 weeks post-op was underpowered. In case of any future studies, a total of 23 subjects would give an 80% chance of detecting the observed difference at a two-tailed significance level of 0.05.

6.3.1.4.2 12 weeks post-op

The mean number of pigmented chondrons in the BALB/c Hgd-/- DMM control group equalled 111, whilst the BALB/c Hgd-/- DMM experimental group equalled 131. The standard deviation of the difference between the two groups was equal to 4.58. These figures resulted in a power equal to 0.9416, meaning that a difference in the number of pigmented chondrons would be observed about 94% of the time. This data shows that the DMM study at 12 weeks post-op, even with only three subjects included, had more than enough power to detect the observed difference.

The use of animals in research is heavily regulated and there is a commitment to reduce the number used for scientific purposes. The 3Rs (Replacement, Reduction and Refinement) were introduced as a framework for humane animal research and are used to help develop alternative approaches which avoid the use of animals in scientific research. The use of power calculations is particularly relevant to the 3Rs (specifically Reduction) as it provides information on the numbers of mice needed per study to obtain reliable data. This helps to minimise the number of animals used in experiments, thereby reducing the overall number by avoiding unnecessary and excessive use of animals. Power calculations are a valuable contribution to the 3Rs as they help to provide maximal data from minimal animal use.

6.3.2 5mM HGA supplementation

6.3.2.1 Treated group

Ten BL/6 Hgd-/- mice were given water containing 5mM of HGA over their lifetime. The mice were culled between the ages of 51 and 74 weeks and then processed histologically to allow for quantification of pigmented chondrons. Plasma HGA levels were measured regularly throughout their lifespan. One mouse from the treated group, BL/6 Hgd-/- 41.2 (45 weeks), was not included in the data shown as it was culled due to ill health.

Photomicrographs from a small selection of mice in both the treated and control groups are shown. As the photomicrographs demonstrate the presence of pigmented chondrons in the joint, only a small number will be shown as they are similar to the photomicrographs contained in the natural history study (Chapter 3).

6.3.2.1.1 BL/6 Hgd-/- 52.2 (♂) – 51 weeks (5mM HGA supplementation for 40 weeks)

Schmorl's stain revealed a relatively low amount of pigmented chondrons throughout BL/6 Hgd-/- 52.2 (♂). Quantification of the chondrons showed the total amount to be lower than what would have been expected from a mouse aged 51 weeks (Fig. 6.28) not supplemented with HGA. There was no obvious cartilage damage on each of the four quadrants of the tibio-femoral joint however there was a small amount of vascularisation of the MFC. Large pigmented hypertrophic chondrons were located prominently in the MTP (Fig. 6.23) which was consistent with previous data.

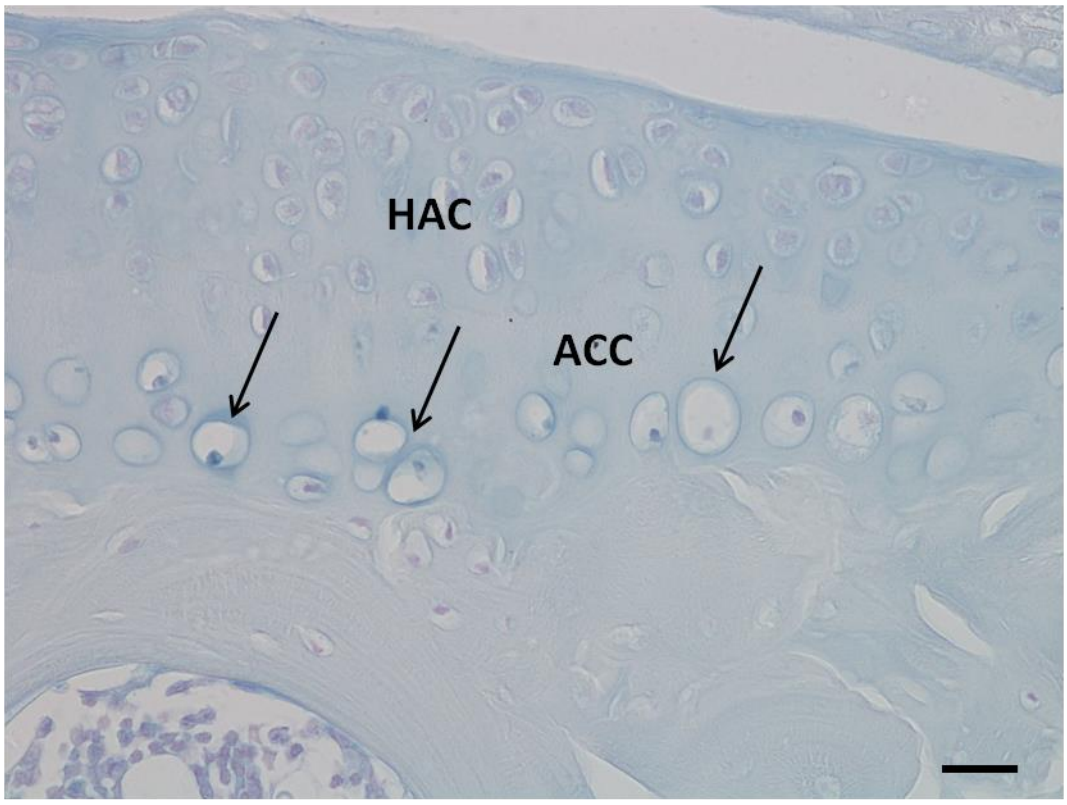

Figure 6.23 – Hypertrophic pigmented chondrons in the medial tibial plateau of BL/6 52.2, a 51 week old Hgd-/- mouse supplemented with 5mM HGA for 40 weeks. Large numbers of very hypertrophic chondrons (arrowed) were located in the MTP. Section stained with Schmorl's. Bar = 20µm.

6.3.2.1.2 BL/6 Hgd-/- 57.2 (♀) – 63 weeks (5mM HGA supplementation for 56 weeks)

BL/6 Hgd-/- 57.2 (♀) showed significant osteoarthritic changes on the MTP with fibrillations and loss of the surface lamina observed (Fig. 6.24). There also appeared to be detachment of the ACC from the underlying SCB bone (Fig. 6.24), highlighting the severity of OA in the mouse. Quantification of the pigmented chondrons showed the total amount to be comparable to mice of similar age not supplemented with HGA (Fig. 6.28).

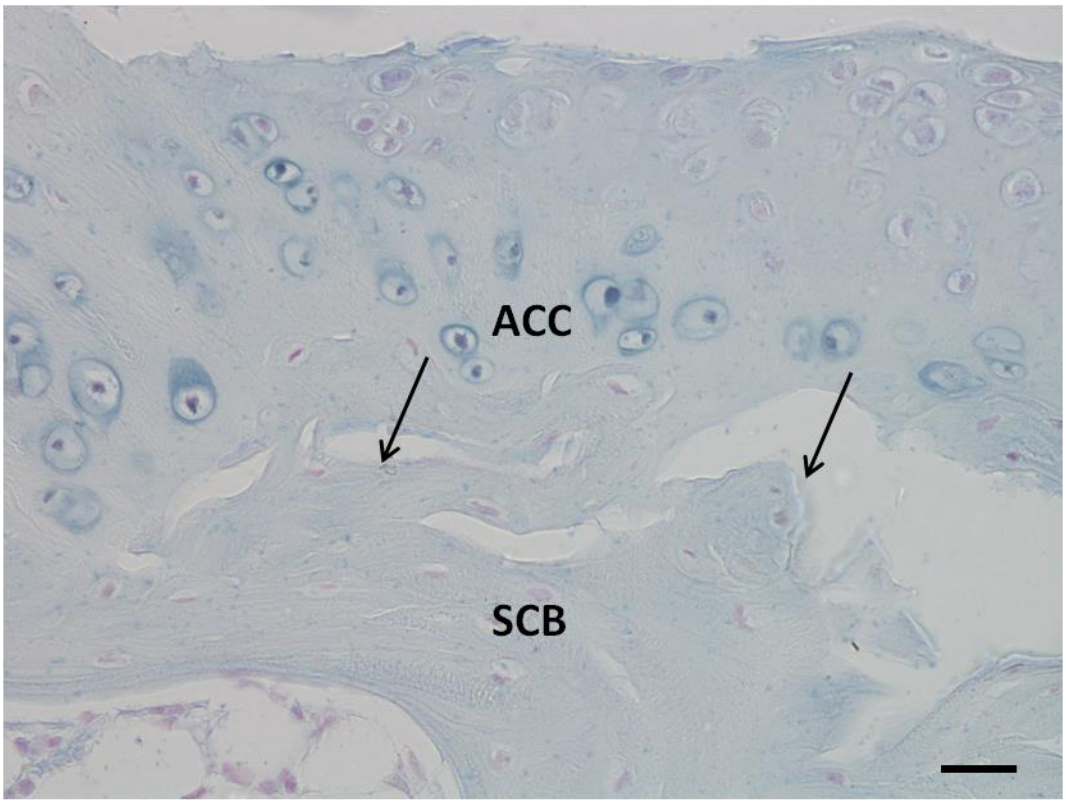

Figure 6.24 – Detachment of articular calcified cartilage from subchondral bone in BL/6 57.2, a 63 week old Hgd-/- mouse supplemented with 5mM HGA for 56 weeks. A substantial section of the ACC appeared to be removed from the SCB in the MTP. Section stained with Schmorl's. Bar = 20µm.

6.3.2.1.3 BL/6 Hgd-/- 31.2 (♂) – 74 weeks (5mM HGA supplementation for 56 weeks)

BL/6 Hgd-/- 31.2 (♂) showed very severe osteoarthritic changes on the medial aspect of the joint with complete erosion of the HAC on both the MFC and MTP (Fig. 6.25). Fibrillations and loss of surface lamina were also observed on both the LFC and LTP. Quantification of the pigmented chondrons showed numbers comparable to those seen in mice of similar ages (Fig. 6.28).

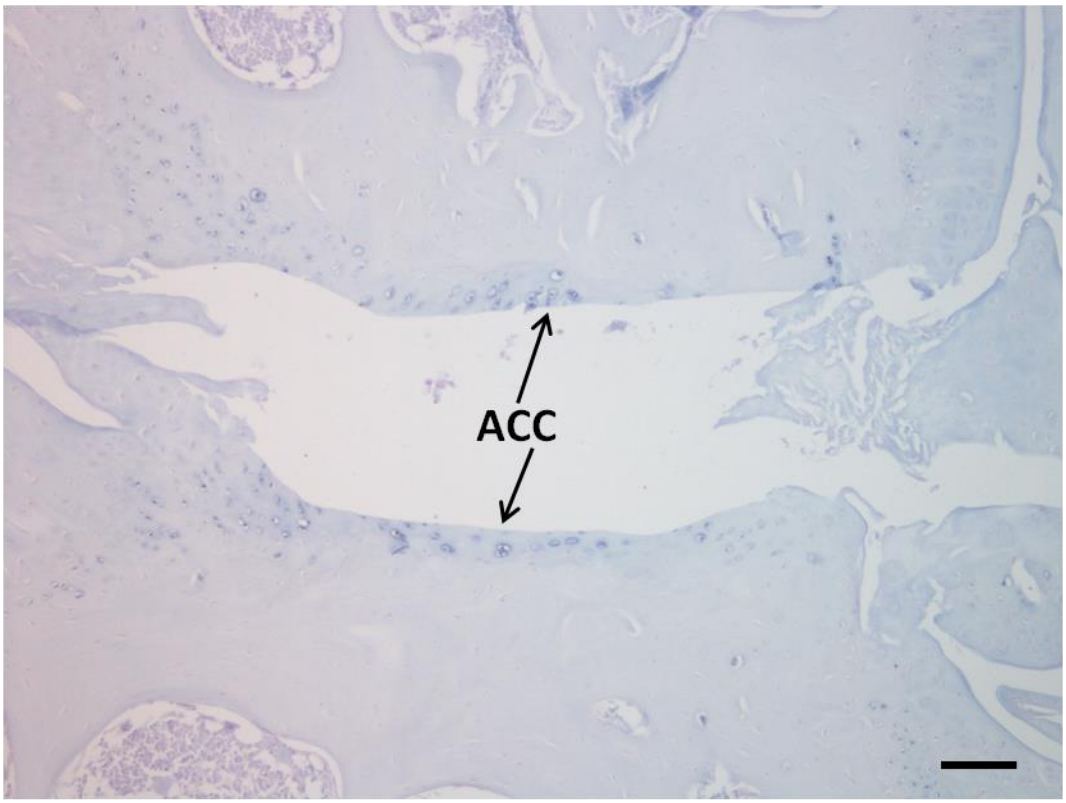

Figure 6.25 – Complete loss of hyaline articular cartilage in BL/6 31.2, a 74 week old Hgd-/- mouse supplemented with 5mM HGA for 56 weeks. The HAC had eroded completely exposing the underlying ACC. Section stained with Schmorl's. Bar = 100µm.

6.3.2.2 Control group

Ten BL/6 Hgd-/- mice were supplied with standard drinking water for their lifespan. The mice were culled between the ages of 63 and 72 weeks and then processed histologically to allow for quantification of pigmented chondrons. Plasma HGA levels were measured regularly throughout their lifespan. One mouse from the control group, BL/6 42.1 (64 weeks), was not included in the data shown as it was culled due to ill health.

6.3.2.2.1 BL/6 Hgd-/- 49.1 (♀) – 68 weeks

Areas of damage were observed throughout the tibio-femoral joint of BL/6 Hgd-/- 49.1 (♀), with fibrillations present on the MFC (Fig. 6.26) and the MTP. SCB remodelling was visible in the MFC (Fig. 6.26) and MTP. Small amounts of damage were located on the lateral aspect of the joint however the most significant damage was in the medial portion of the joint. Quantification of the pigmented chondrons showed numbers similar to those seen in mice of the same age (Fig. 6.28).

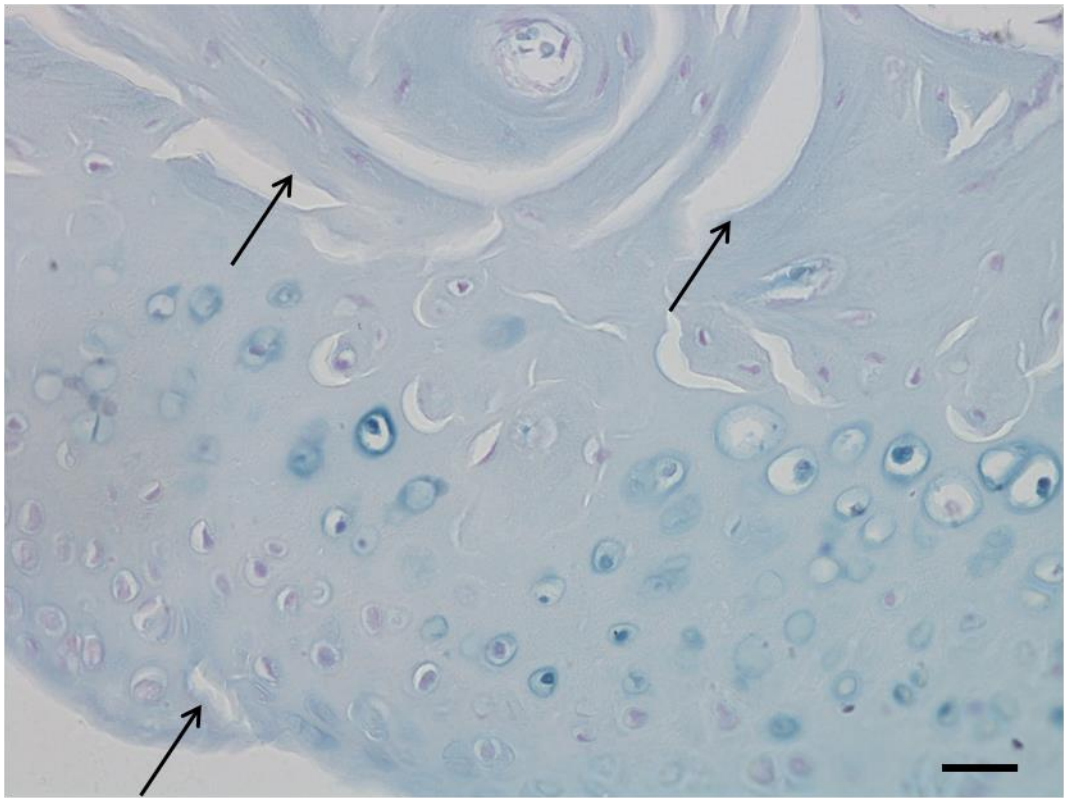

Figure 6.26 – Articular cartilage fibrillations and subchondral bone remodelling in BL/6 49.1, a 68 week old Hgd-/- mouse. A small fibrillation/cleft was located on the articular surface of the MFC (bottom arrow). Considerable amounts of SCB remodelling were also located in the condyle (top arrows). Section stained with Schmorl's. Bar = 20µm.

6.3.2.2.2 BL/6 Hgd-/- 42.2 (♂) – 70 weeks

Severe osteoarthritic changes were located on the MFC and MTP in BL/6 Hgd-/- 42.2 (♂) (Fig. 6.27). Similar to BL/6 Hgd-/- 31.2 (♂) in the treated group, there was complete erosion of HAC leading to the exposure of the underlying SCB (Fig. 6.27). The lateral portion of the joint did not show as extreme damage, only minor cartilage fibrillations and loss of surface lamina. Quantification of the pigmented chondrons in the joint showed numbers slightly higher than previously seen in mice of similar ages (Fig. 6.28).

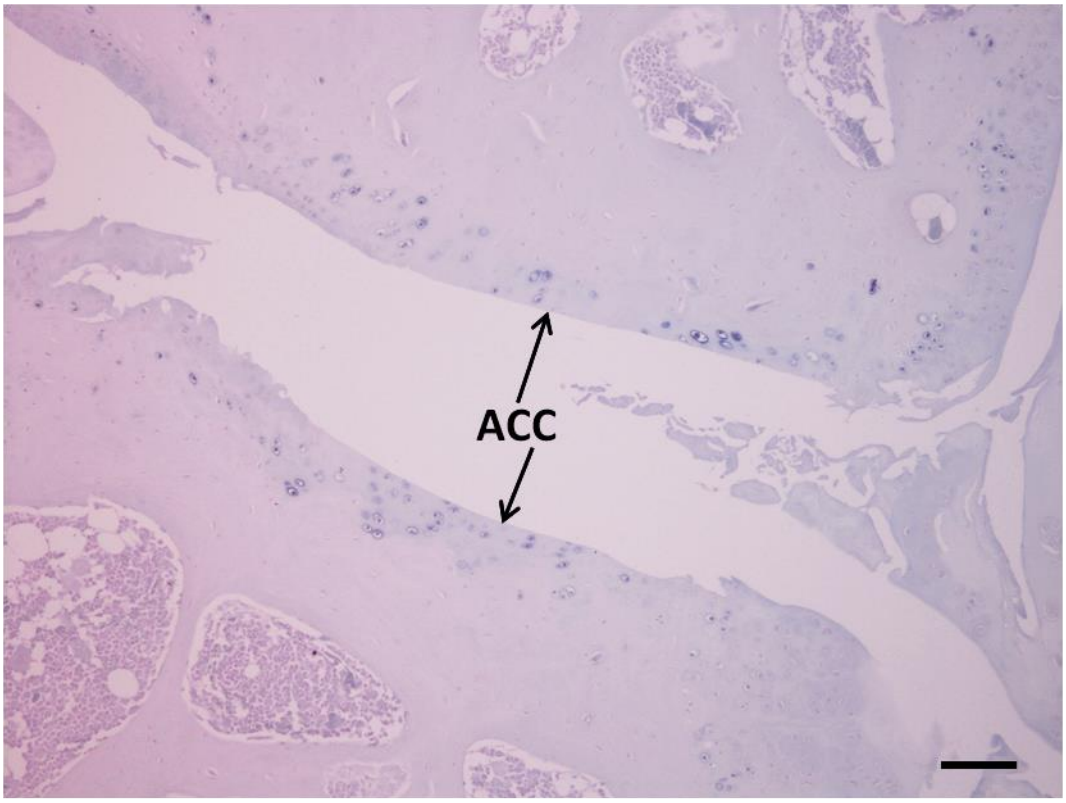

Figure 6.27 – Complete erosion of hyaline articular cartilage in BL/6 42.2, a 70 week old Hgd-/- mouse. The HAC had eroded completely exposing the underlying ACC. Section stained with Schmorl's. Bar = 100µm.

6.3.2.3 Quantification of pigmented chondrons

Pigmented chondrons in both the 5mM HGA treated group and the control group were quantified to demonstrate the effect, if any, of 5mM HGA supplementation on the number of pigmented chondrons in the tibio-femoral joints of Hgd-/- mice.

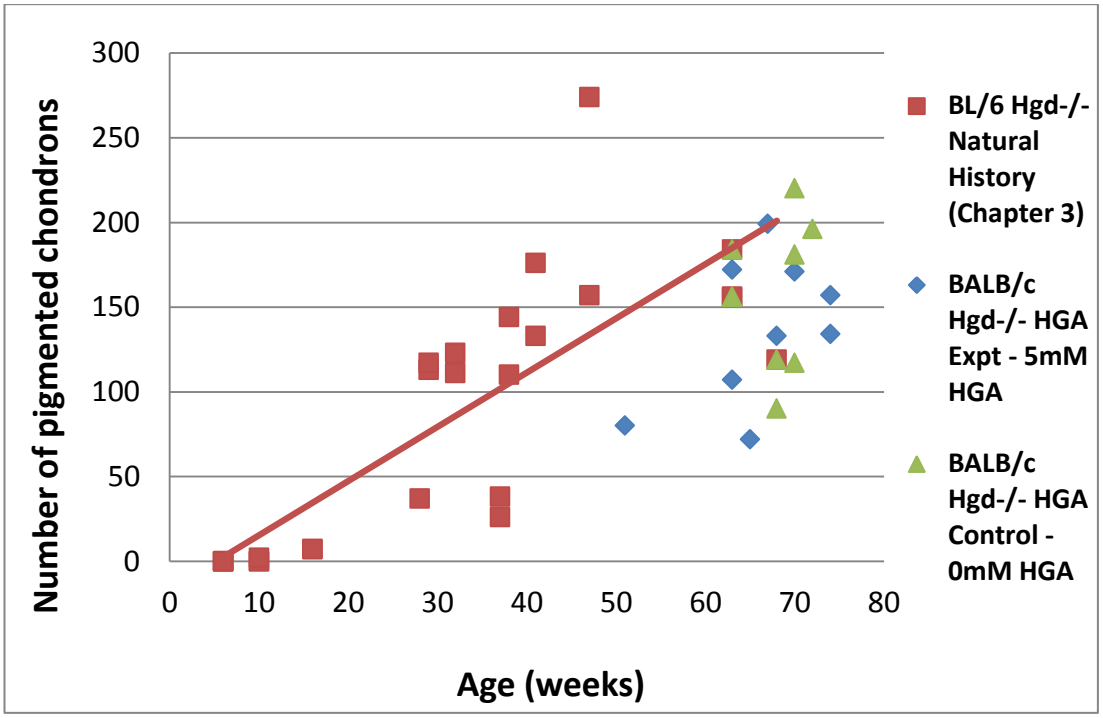

Figure 6.28 – The effect of 5mM HGA supplementation on the number of pigmented chondrons in BL/6 Hgd-/- mice. Scatter chart showing how HGA supplementation affects pigmentation levels in BL/6 Hgd-/- mice. Quantification of pigmented chondrons was performed on a single section from each mouse; this does not represent the total cell number in each mouse.

6.3.2.4 Plasma HGA levels (5mM HGA study)

Lifetime plasma HGA levels were collected from both the treated and control groups to identify if 5mM HGA supplementation increased plasma HGA when compared to control (non-supplemented) Hgd-/- mice (Fig. 6.29). The data showed no significant increase in the lifetime plasma HGA levels of the mice supplemented

with 5mM HGA. The levels of plasma HGA measured in both groups were consistent with those observed in control Hgd-/- mice in the nitisinone study (Fig. 5.18).

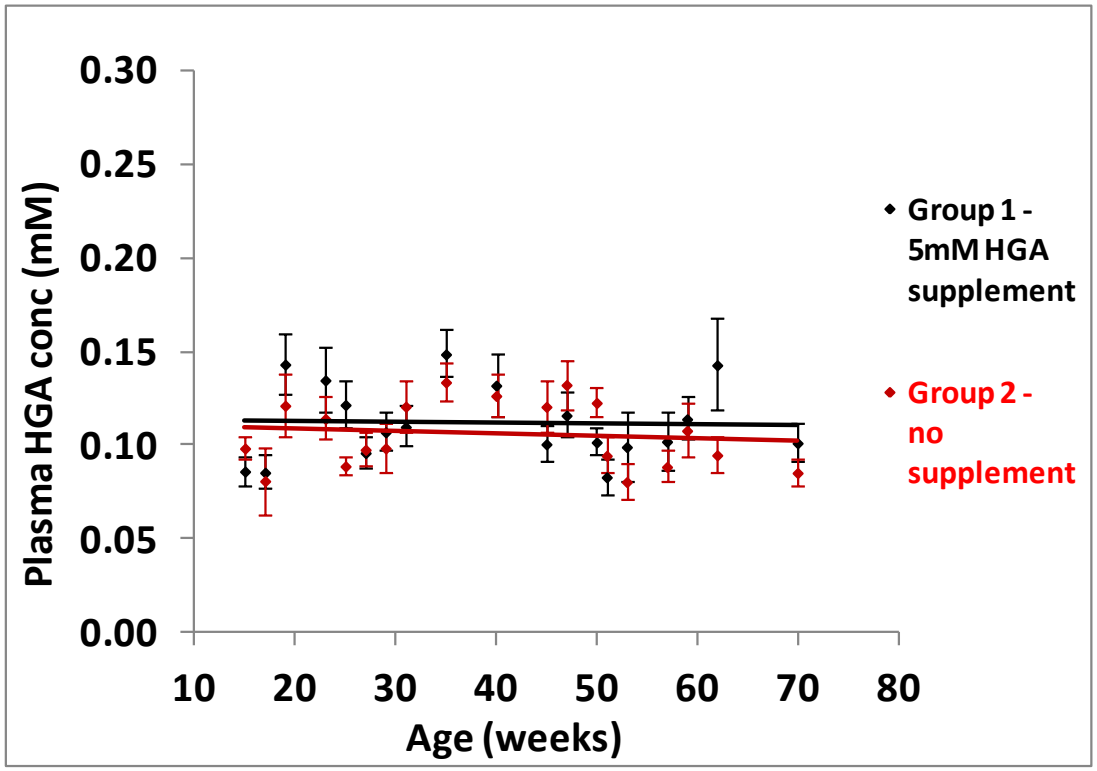

Figure 6.29 – The effect of 5mM HGA supplementation in BL/6 Hgd-/- mice. Scatter chart showing lifetime supplementation with additional 5mM HGA had no effect on plasma HGA levels. (All measurements and data analysis performed by Dr. A. Preston).

Both plasma HGA and chondron quantification data revealed no clear pattern of an increase in pigmented chondron numbers or plasma HGA in Hgd-/- mice supplemented with 5mM HGA. From the data obtained it appears that additional HGA in the diet did not cause an increase in pigment deposition.

6.4 DISCUSSION

This Chapter investigated whether DMM surgery or supplementation with HGA increased the amount of ochronotic pigment deposited in the calcified cartilage of BALB/c (DMM) and BL/6 (5mM HGA) Hgd-/- mice. [118]. The development of severe osteoarthropathy is closely associated with the progression of AKU in humans [24, 223]. Data from the natural history study of ochronotic osteoarthropathy in Hgd-/- mice (Chapter 3) showed mild, moderate and severe OA at different ages throughout their lifetime. There was variability between individual mice, both of different and similar ages, in relation to the number of pigmented chondrons present in the ACC, and the severity of cartilage damage in the tibio-femoral joint. Although a clear pattern did not emerge between these factors, it has been suggested that pigmentation is initiated following biomechanical damage at the ACC-SCB interface [36]. Changes in the biomechanical and structural properties of the ACC are also believed to lead to an increased deposition of ochronotic pigment [36], thus causing further cartilaginous destruction and resulting in increased OA severity. The mechanism appears to be similar to a positive feedback system as biomechanical damage leads to initial pigment deposition which then leads to further biomechanical damage and then an increase in pigment deposition. Data from Chapter 4 of this thesis identified a similar mechanism for the initiation of ochronotic pigment in Hgd-/- mice. With data from both human and murine studies showing an apparent association between biomechanical damage and pigmentation, DMM surgery was performed on Hgd-/- mice to identify if the damage caused by the procedure accelerated the rate of pigmentation, and/or increased the amount of pigment deposited. Correlation between these factors would provide evidence that biomechanical damage to the cartilage is a major cause of ochronotic osteoarthropathy in AKU.

The first three DMM Hgd-/- mice to be analysed in the study, BALB/c Hgd-/- 100.1 (♀), 100.2 (♀), and 101.1 (♂) were left for 8 weeks post-op. All three were aged 52 weeks when the surgery took place and age 60 weeks when culled. As expected

with Hgd-/- mice at 60 weeks, signs of OA were identified in the tibio-femoral joint. Osteophyte formation (Figs. 6.1 & 6.4) and articular surface fibrillations (Figs. 6.2 & 6.5) were observed to some extent in all of the mice, comparable to those seen in mice of a similar age in the natural history study (Figs. 3.10 – 3.13). However the use of DMM surgery did lead to very severe damage at 8 weeks post-op, located on the lateral portion of the experimental joint in BALB/c Hgd-/- 101.1 (Fig. 6.8). Although there was considerable cartilage erosion on the MTP (Fig. 6.7), both the LTP and LFC displayed significantly more erosion, with ≥90% of HAC on the LFC eroded. As expected the experimental joint showed increased osteoarthritic changes compared to the contralateral control, in all of the mice at 8 weeks post-op (Table. 6.3). What was surprising was the amount of damage inflicted on the lateral portion of the experimental joint in BALB/c Hgd-/- 100.1 and 101.1, with both showing more OA lesions on the LTP and LFC than the MTP and MFC (Table. 6.3). Loading of the tibio-femoral joint is known to be greater on the medial compartment with forces approximately 2.5 times greater than those on the lateral compartment [224], leading to a greater prevalence of medial lesions in OA [225]. Therefore it seems unexpected that there are more lateral lesions in two of the three mice at 8 weeks post-op, considering the DMM procedure is designed to cause maximal damage on the medial compartment. Research by Lapveteläinen *et al* [226], in which mice containing a mutation in the type II procollagen gene were provided with a running wheel, showed there to be an increase in the severity of OA in the LTP and LFC, when compared to the MTP and MFC. They state that this is likely due to structural abnormalities in the collagen network of the matrix, and uneven loading across the tibio-femoral joint. Although Hgd-/- mice do not contain this mutation, deposition of ochronotic pigment is thought to disrupt the composition and organisation of the collagenous matrix. Therefore it is reasonable to suggest that this phenomenon along with uneven loading of the experimental knee joint led to increased OA severity on the lateral aspect of the joint. It is possible that displacement of the MM caused uneven loading of the tibio-femoral joint in these two mice, leading to a disproportionate amount of pressure to be placed upon the lateral compartment of the joint, and increasing the severity of OA.

BALB/c Hgd-/- 102.2 (♂), 102.3 (♂), and 103.1 (♀), left for 12 weeks post-op, showed increased OA severity in comparison with the mice culled 8 weeks post-op. Like these mice, the three culled 12 weeks post-op were also aged 60 weeks. What was immediately obvious was the severity of OA in the experimental joints compared to the contralateral controls, which showed very little, if any damage (Fig. 6.15). Both BALB/c Hgd-/- 102.2 and 102.3 showed severe erosion of HAC exposing the underlying ACC, along with the large fully ossified osteophytes on the MTP (Figs. 6.12 & 6.16). Smaller osteophytes were located on the MFC in both mice while ossification of the LM was also observed (Figs. 6.13 & 6.17). Detachment of ≥75% of the HAC on the MTP was visible in BALB/c 103.1 (Fig. 6.19), highlighting the severity of OA in the mouse. Although damage was located on the lateral compartment in all of the mice, in only one (BALB/c 102.2) was it more severe than that observed in the medial portion of the joint (Table. 6.3). The observation of increased OA severity on the MTP and MFC, in two of the three mice, is consistent with the data reported by Glasson *et al* in the original study [118].

The apparent association between biomechanical damage, and the initiation and progression of ochronotic pigmentation has been previously documented [36, 227]. NMR studies have also shown there to be disorder in the collagen network in ochronotic tissue [39], thus affecting its biomechanical properties. Along with inducing moderate to severe OA in Hgd-/- mice, DMM was performed to identify if the presence of significant damage in the joint led an increase in the amount of pigment deposited in the articular cartilage, therefore highlighting a possible link between damage and pigment deposition. Results from both 8 weeks (Fig. 6.11), and 12 weeks (Fig. 6.21) post-op showed no statistically significant increase in the total number of pigmented chondrons in Hgd-/- mice. In two of the three of the mice examined at 8 weeks post-op there was actually a greater number of pigmented chondrons in the contralateral control than the experimental tibio-femoral joint (Fig. 6.11). At 12 weeks post-op the opposite effect was observed with a greater number of pigmented chondrons in the experimental tibio-femoral joint (Fig. 6.21). This was interesting as the mice at 12 weeks post-op also showed

increased OA severity in their experimental limb (Table. 6.1). However as the data shows (Fig. 6.22) no statistically significant increase in pigmented chondron numbers from 8 weeks post-op to 12 weeks post-op was observed. As mechanical damage is thought to be involved in the initiation and progression of pigmentation it is unclear why there was no significant increase in the number of pigmented chondrons. It is possible inter-individual variability contributed to the low number of pigmented chondrons in BALB/c Hgd-/- 100.1 and 101.1, which both displayed higher numbers of pigmented chondrons in the contralateral control limb. Although plasma levels of HGA in Hgd-/- mice remain steady across their lifetime there is variability with regards to the number of pigmented chondrons in Hgd-/- mice of the same age, as seen in Chapter 3 of this thesis. It is likely other factors are involved in the reduction of pigmented chondrons in these mice including catabolic factors expressed by damaged/abnormal chondrocytes however further analysis of an increased number of DMM Hgd-/- mice may reveal this data to be no more than an anomaly. There is little doubt changes resulting from biomechanical damage do play a role in the pathogenesis of AKU however, how much they are involved is still not fully understood.

In the event of future DMM studies there are a number of improvements which could be made to ensure the data collected is reliable. Both non-surgical and sham controls should be included in any future studies as they provide important information. Using a sham control ensures that the effects observed in the experimental mice are as a result of the surgical procedure and no other factor(s). Although the contralateral limb was used as a non-surgical control in the DMM study it is possible this limb was placed under increased mechanical loading as a result of the mice refraining from placing weight on the surgically operated limb, possibly resulting in the development of OA in the control limb. This highlights the need to use a non-surgical control group. Following DMM surgery the mice were single housed to prevent any aggressive behaviour occurring between individuals. As each mouse had a surgical wound it was decided single housing would be best to prevent any problems post-surgery such as nibbling of the sutures, by other mice.

Once the wound was healed the mice were housed together with same sex siblings. This must be done to stop any fighting between the mice, especially when dealing with male mice. It has been reported in some studies that group housing does not appear to have any detrimental effects on the mice post-surgery, however it may be that the rough and tumble nature of mice housed together could possibly exacerbate the development of OA in some models of DMM. This would have to be carefully monitored against the mice in both the sham and control groups. In the event of any future DMM studies it may be best to house the mice together as they would be housed in groups of 3 or 4 pre-surgery, and monitor carefully for any problems with the healing of the skin incision. To determine the number of mice needed in each group (controls and experimental), a power calculation can be used as this will provide the maximum number of mice required to observe an effect. Power calculations are very helpful as they prevent the unnecessary use of animals in experiments; this helps to reduce the number of mice used which is in line with the 3Rs. In retrospect it may have been better to use young mice in the study as aged mice are more likely to develop spontaneous OA whilst also having high numbers of pigmented chondrons. As the aim of the DMM experiment was to determine if damage to the joint initiated pigmentation, using young animals which have yet to develop joint damage or pigmentation may have been the best strategy. Using the OARSI histopathology initiative for mice [120] the severity of OA induced by DMM can be assessed. This method provides a system to score the four quadrants of the tibio-femoral joint and determine the severity of OA throughout. A Kruskal-Wallis test can be used to determine if any statistically significant differences are present between the severity and amount of OA in the experimental and control groups whilst an independent samples t-test can be generated to compare the number of pigmented chondrons between the experimental and control groups.

Supplementing the drinking water of Hgd-/- mice, with 5mM HGA, was also used as a possible method to increase the amount of ochronotic pigment deposited. Two groups, one containing mice supplemented with 5mM HGA and the other

containing mice with no HGA in their drinking water were analysed to see whether supplementation with HGA increased the number of pigmented chondrons and/or their plasma HGA levels. Histological analysis revealed little differences between the treated and control groups with mice from both groups showing severe OA lesions (Figs. 6.27 & 6.28) in the tibio-femoral joint. Quantification of the pigmented chondrons did not show a considerable difference in the number between both groups (Fig. 6.28). The highest number of pigmented chondrons was actually seen in one of the control mice suggesting supplementation with 5mM HGA had no effect on pigment deposition. Lifetime plasma HGA levels (Fig. 6.29) also revealed no significant difference between the treated and control groups. Some variation was seen over the lifetime however this was in line with that normally seen in Hgd-/- mice (Fig. 5.18). Quantification of pigmented chondrons and analysis of plasma HGA levels showed supplementation with additional HGA did not increase the amount of pigment deposited in Hgd-/- mice, nor did it increase the circulating levels of HGA. Although some HGA remains in the plasma the majority is excreted in the urine, therefore it seems likely that any additional HGA is simply excreted and is never converted to ochronotic pigment. It is clear that this level of HGA supplementation does not have an effect on the amount of pigment present in plasma or deposited in Hgd-/- mice.

7. Ultrastructural analysis of cartilage in Hgd-/- and wild type mice

7.1 INTRODUCTION

This Chapter presents in depth ultrastructural analysis of murine cartilage from both BALB/c Hgd-/- and WT mice. There has been little research performed on the ultrastructure of murine cartilage using TEM as it is known to be difficult to obtain high quality sections. Silberberg and colleagues [228, 229] performed TEM analysis on the femoral heads of mice of various ages but little attention was paid to the ACC in their studies. Ultrastructural analysis using scanning electron microscopy (SEM), such as the study by Hughes *et al* [230] have shown in detail the orientation of chondrocytes, and collagen fibres in the territorial and interterritorial matrices of murine HAC but have also neglected the ultrastructure of the ACC.

The structure, ultrastructure and function of the HAC and SCB have been the subject of much investigation and their potential involvement in the pathogenesis of OA has been widely recognised [84, 100, 231, 232]. However much less attention has been focussed on the ACC and its significance in the development of OA has been largely ignored [233]. The ultrastructure and cell biology of the ACC is poorly described which often causes its role in OA to be overlooked.

This Chapter highlights the differences between the HAC and ACC and the chondrocytes that reside in each zone. Analysis of both Hgd-/- and WT mice revealed the appearance of concentric lamellae structures surrounding hypertrophic chondrocytes located in the ACC. Extensive literature searches revealed this was a novel finding in mice. These concentric lamellae were more prevalent in Hgd-/- mice and further analysis revealed other structural differences between Hgd-/- and WT mice which may help us understand the progression of ochronotic osteoarthropathy.

7.2 DESIGN OF STUDY

Young and aged BALB/c Hgd-/- mice and aged WT mice, ranging from 7.8 to 69 weeks, were culled and their tissues harvested. Following fixation and decalcification small sections from the top of the MFC containing HAC, ACC and a small amount of SCB, were taken and processed for TEM analysis.

Detailed ultrastructural analysis of the HAC and ACC were carried out to identify if any changes had occurred which could help further understand the relationship between AKU and the onset of severe osteoarthropathy.

7.3 RESULTS

7.3.1 Ultrastructural analysis of cartilage and chondrons in BALB/c Hgd-/- mice

Detailed TEM photomicrographs from an area of the MFC highlighted the ultrastructure of HAC and ACC and the cells and collagenous matrices contained within them (Figs. 7.1 & 7.2).

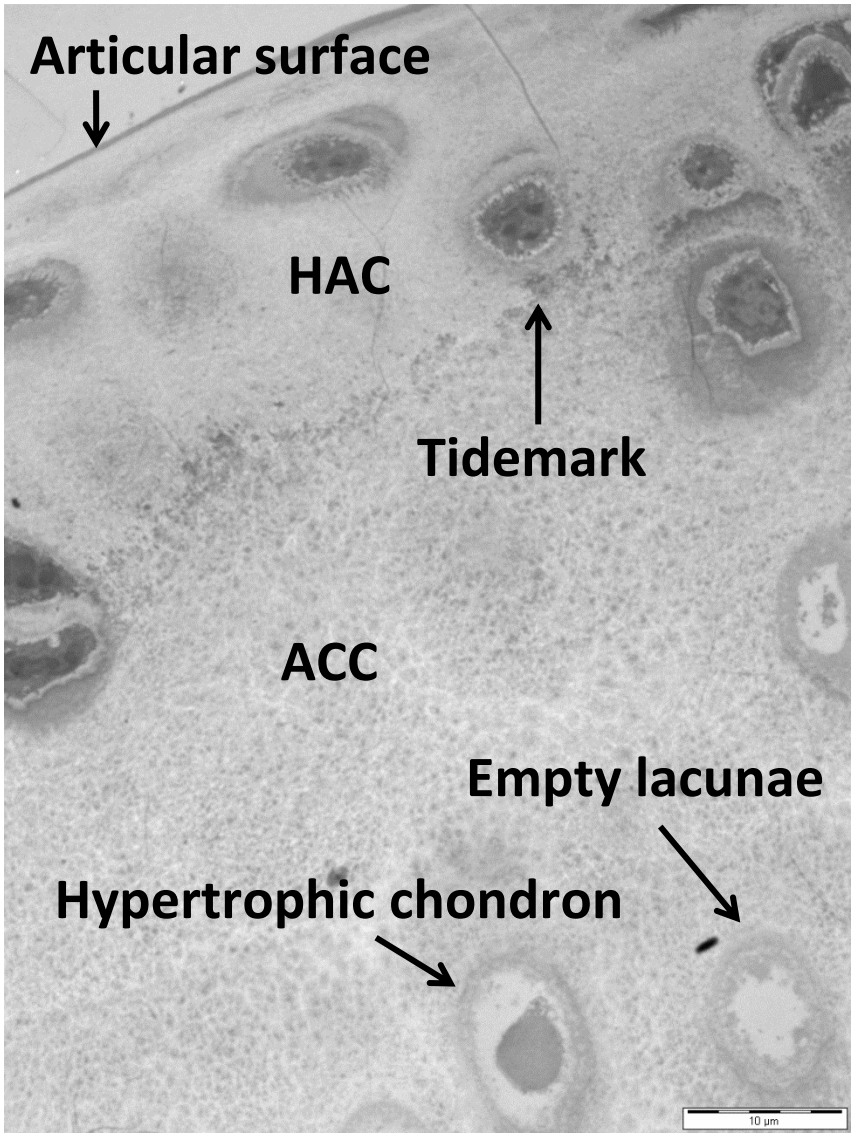

Figure 7.1 – TEM photomicrograph of an area of the medial femoral condyle from BALB/c 145.3, a 53 week old Hgd-/- mouse. Calcified and uncalcified regions of cartilage and the boundary (tidemark) separating them are highlighted. Tissue fixed in glutaraldehyde (x1250). Bar = 10µm.

The tidemark, which is labelled in the above figure (Fig. 7.1), is reported to be a composition of several different molecules including alkaline phosphatase [234], adenosine triphosphate [235], and apoptotic bodies from chondrocytes [236]. The inclusion of these constituents ensures that even though the tissue has been decalcified, the tidemark still remains.

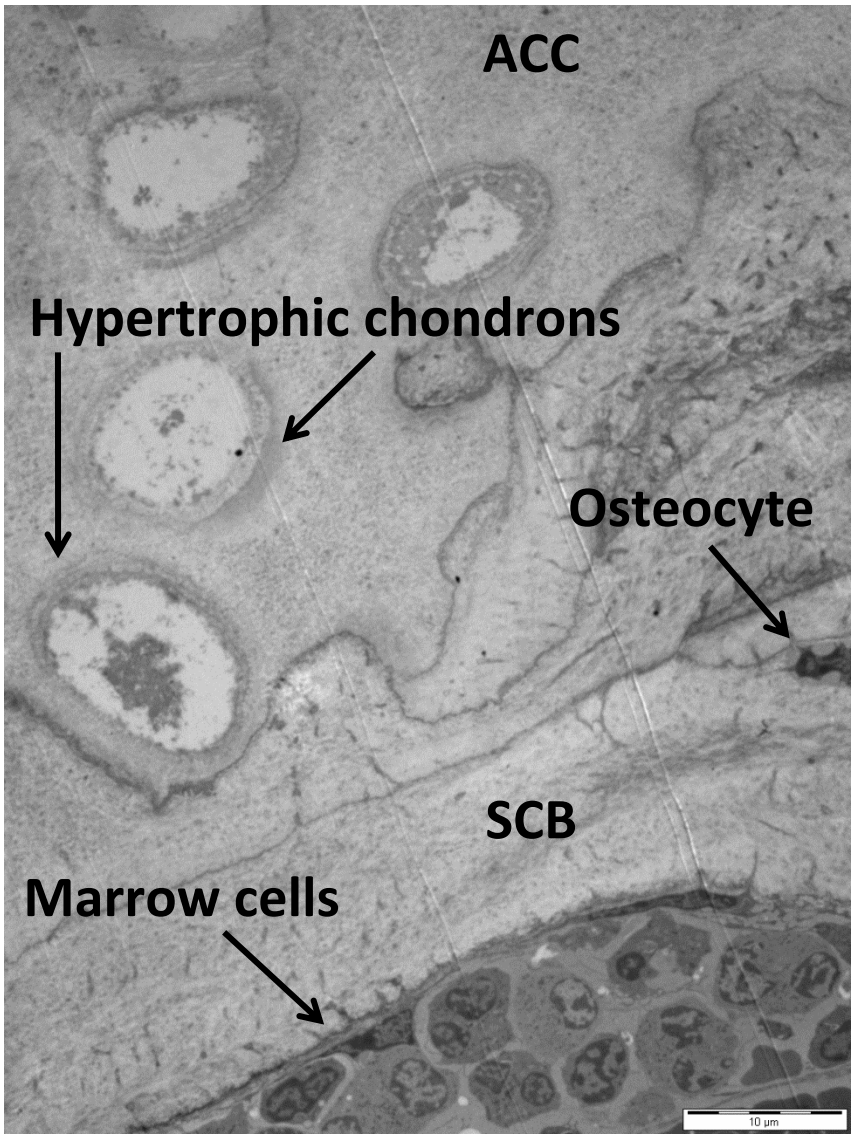

Figure 7.2 – TEM photomicrograph of an area of the medial femoral condyle from BALB/c 145.3, a 53 week old Hgd-/- mouse. Detailed structures including the calcified cartilage and SCB and the cells within them are highlighted. Tissue fixed in glutaraldehyde (x1250). Bar = 10µm.

The following images highlight the different phenotypes of chondrons located in the HAC and ACC of the MFC. As discussed in Chapters 3 & 4, hypertrophic pigmented chondrons were localised to the ACC. Chondrons located in the HAC, which did not pigment, were much smaller and flatter in comparison to those located in the ACC.

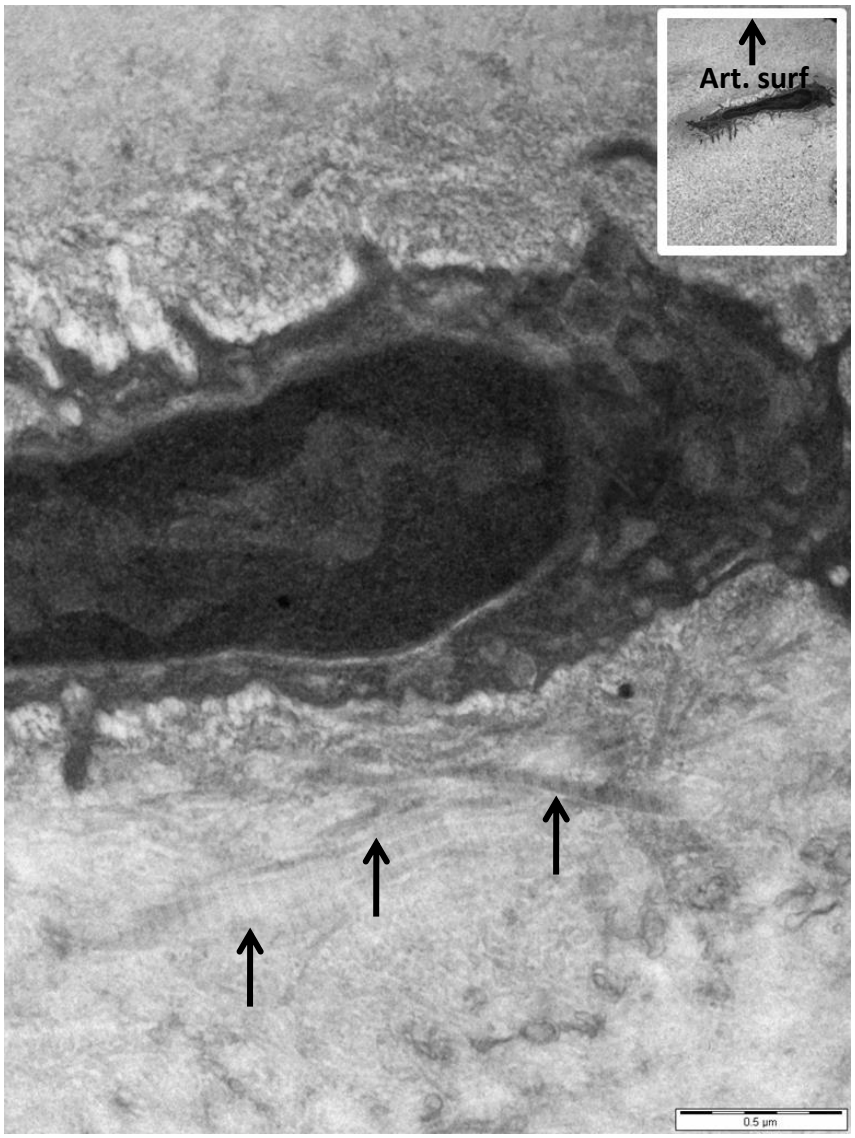

Figure 7.3 – TEM photomicrograph of a flattened chondron located in the superficial zone of the hyaline articular cartilage from BALB/c 145.3, a 53 week old Hgd-/- mouse. Individual collagen fibres located in the PCM of the chondron (arrowed) are highlighted. (x26,500). Inset: TEM image showing the location of the chondron in HAC. Tissue fixed in glutaraldehyde (x8250). Bar = 0.5 µm.

Chondrons located in the superficial zone lay parallel to the articular surface and were small in size (Fig.7.3). The next zone of cartilage, the middle zone, contained chondrons which were similar to those located in the superficial zone, but were larger in size, and appeared more rounded.

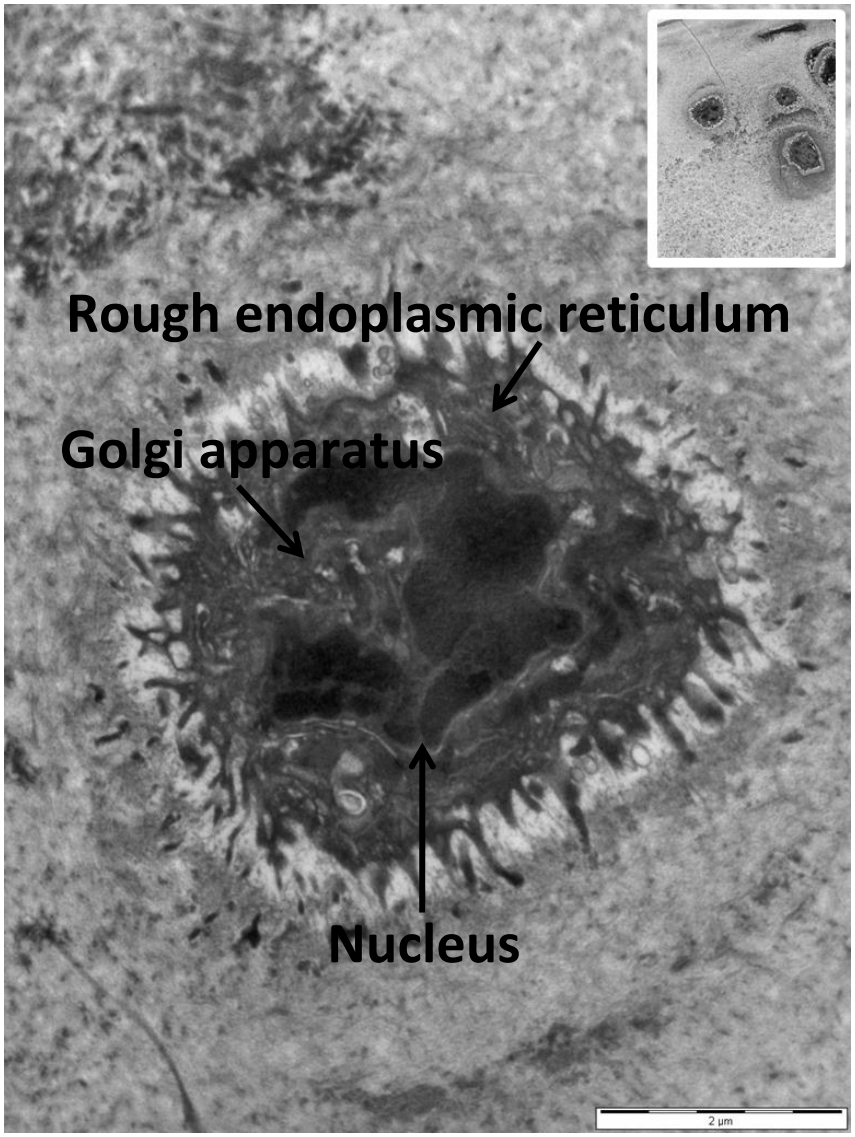

Figure 7.4 – TEM photomicrograph of a chondron located in the deep zone of the hyaline articular cartilage of BALB/c 145.3, a 53 week old Hgd-/- mouse. Ultrastructure of the chondron is detailed, highlighting specific structures within the cell. (x9900). Bar = 2µm. Inset: TEM photomicrograph showing the location of the chondron in the HAC. Tissue fixed in glutaraldehyde (x2500).

Chondrons located in the deep zone were large in size and had a rounded appearance (Fig. 7.4). These chondrons lay perpendicular to the articular surface as did the collagen fibres in the surrounding matrices. All chondrons present in the HAC appeared healthy suggesting they were metabolically active and involved in the turnover of the cartilaginous matrix. The next zone of cartilage, ACC, differs from HAC due to the presence of calcium in the matrix.

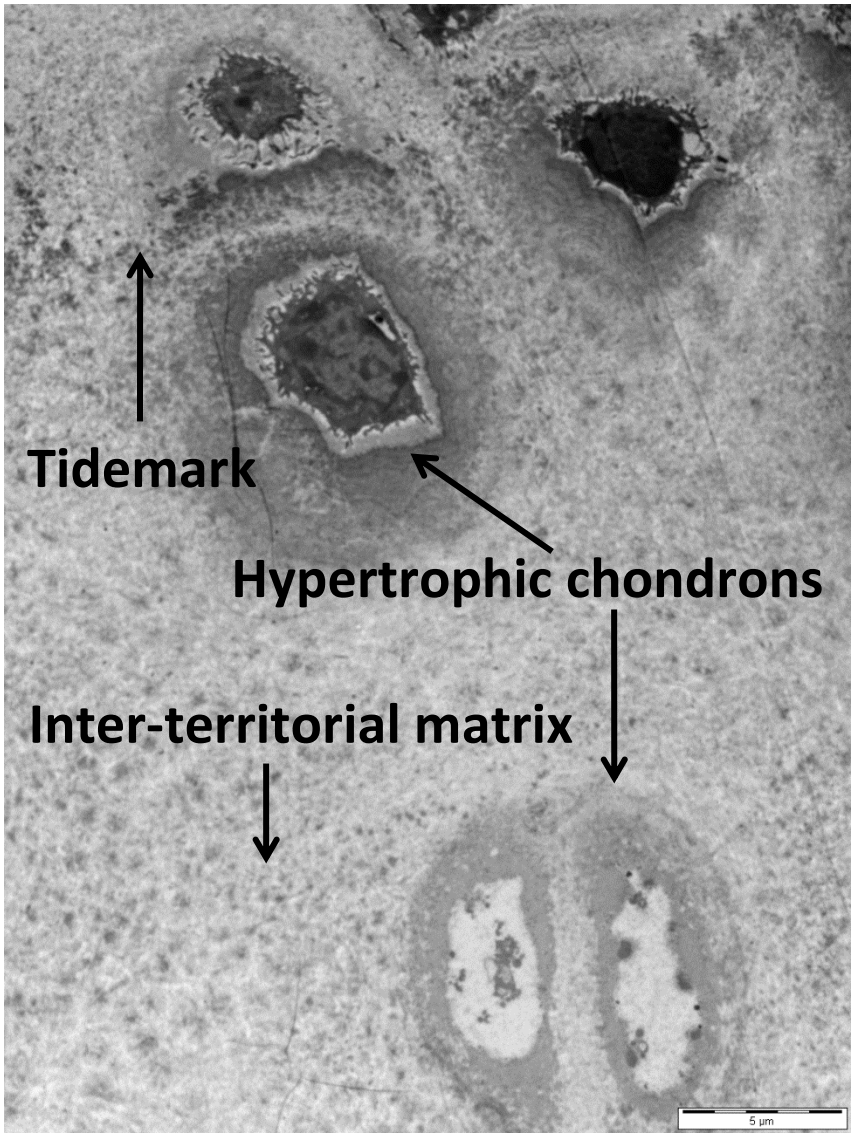

Figure 7.5 – TEM photomicrograph of healthy chondrons located in the articular calcified cartilage of BALB/c 145.3, a 53 week old Hgd-/- mouse. Both chondrons highlighted appeared healthy as opposed to the second set of chondrons located deep in the calcified cartilage. Tissue fixed in glutaraldehyde (x2500). Bar = 5µm.

Although the majority of the chondrons located in the calcified cartilage were hypertrophic, a small number located directly adjacent to the tidemark were not and appeared healthy (Fig. 7.5). What was apparent from looking at the chondrons was the appearance of concentric lamellar structures around the chondrons. The lamellae initially looked as if they formed part of the PCM but upon further observation it was clear that they reached out into areas of the TM. Further analysis revealed the presence of the lamellae around the large majority of chondrons in the ACC; this will be shown in detail in the next part of this chapter.

As the chondrons progressed deeper into the ACC, close to the boundary with the SCB, they became increasingly hypertrophic and chondroptotic. Patchy condensing of nuclear chromatin, increasing amounts of rough endoplasmic reticulum (rER) and cellular disintegration (Figs 7.6 & 7.7), which are hallmarks of chondroptosis [237], were observed in all of the aged mice.

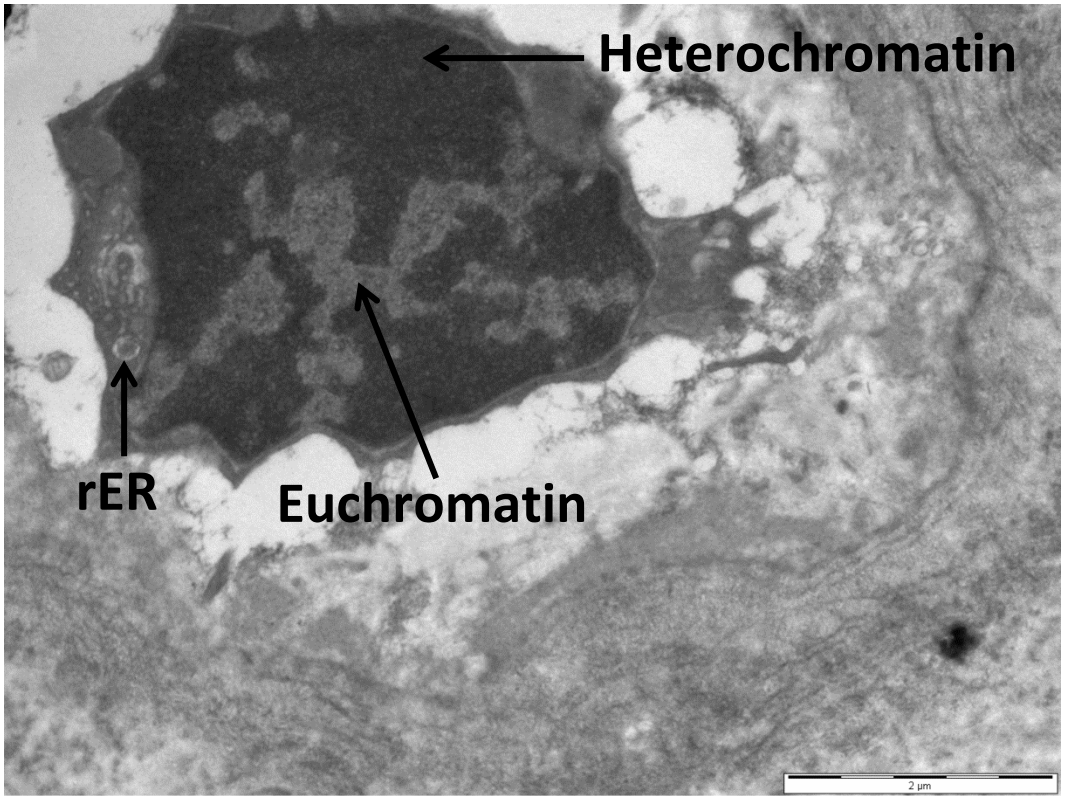

Figure 7.6 – TEM photomicrograph of a hypertrophic chondron in the articular calcified cartilage of BALB/c 145.3, a 53 week old Hgd-/- mouse, displaying signs of chondroptosis. Patchy condensation of both heterochromatin and euchromatin and cell disintegration indicated the cell was in the process of chondroptosis. Tissue fixed in glutaraldehyde (x11,500). Bar = 2µm.

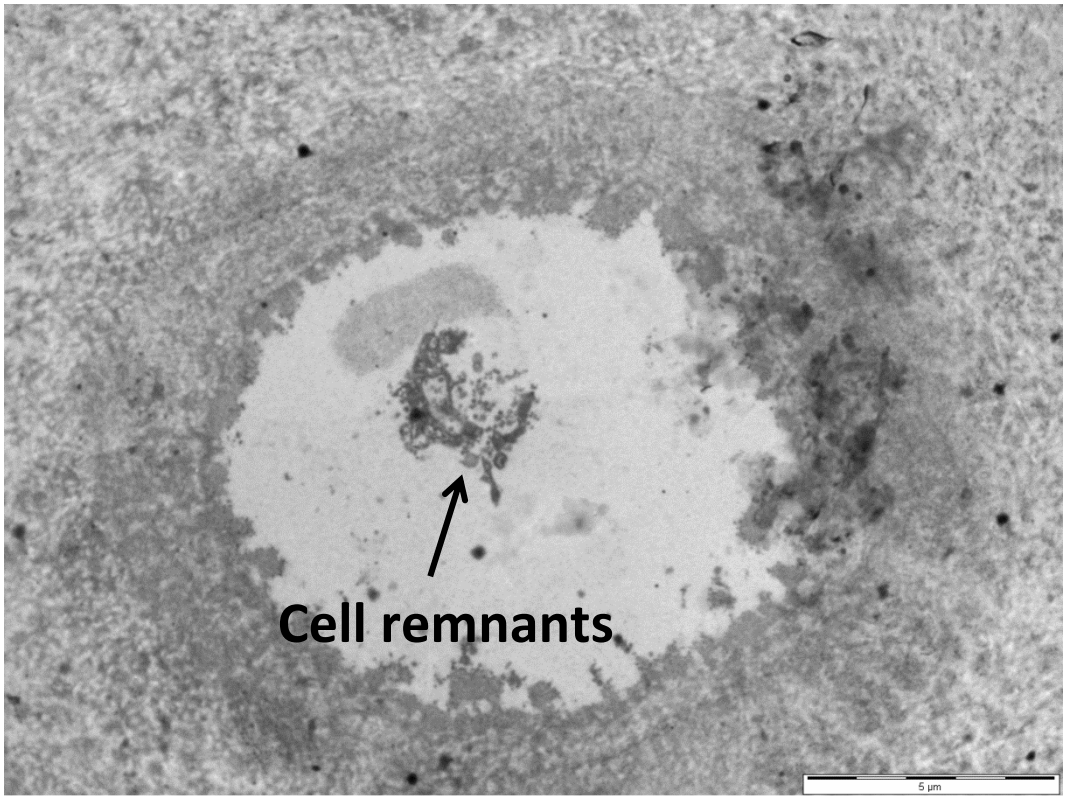

Figure 7.7 – TEM photomicrograph of end stage chondroptosis. The chondron, which was located deep in the ACC, had undergone complete chondroptosis with only remnants of the cell left behind. Section taken from BALB/c Hgd-/- 138.3, a 56 week old Hgd-/- mouse. Tissue fixed in glutaraldehyde (x4200). Bar = 5µm.

7.3.2 Identification of concentric lamellae in the articular calcified cartilage of BALB/c Hgd-/- and wild type mice

7.3.2.1 Hgd-/- mice

During the initial study which highlighted the different regions of cartilage and the chondrons present in them, a distinct pattern of concentric circles or lamellae was observed around chondrons located in the ACC. These lamellae encircled both viable chondrons located towards the mineralisation front (Fig. 7.8) and hypertrophic and necrotic chondrons which were located deep in the ACC, close to the boundary with the SCB (Fig. 7.9).

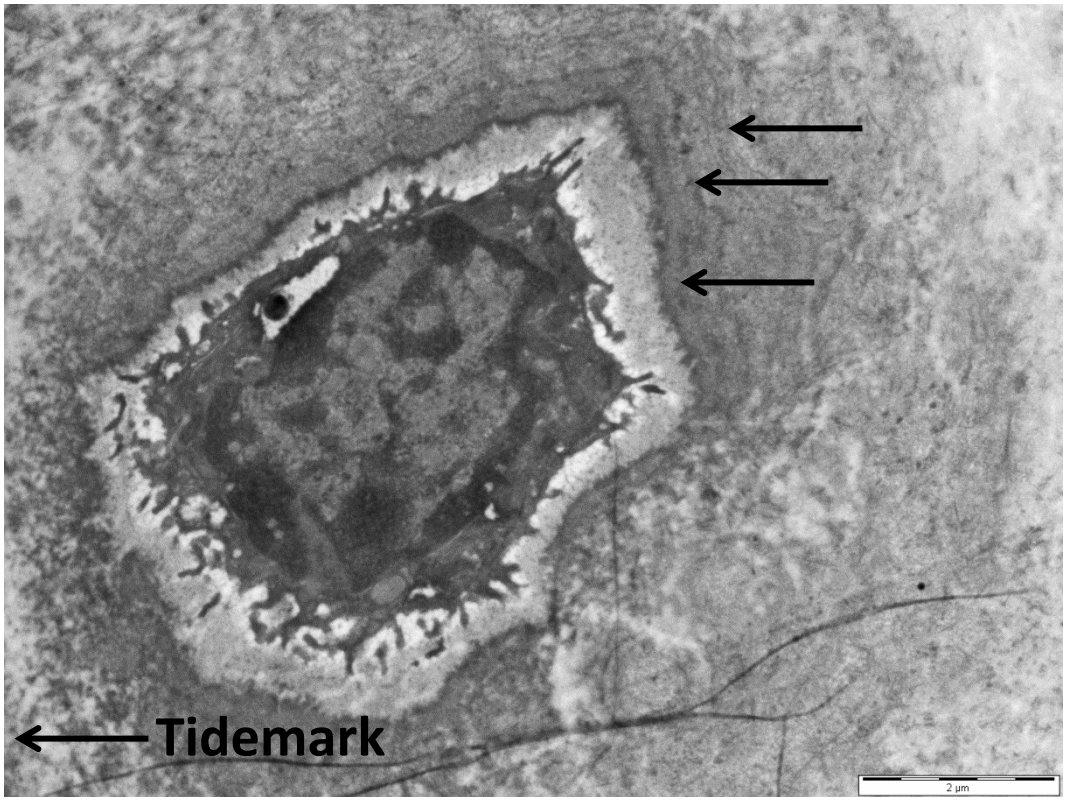

Figure 7.8 – TEM photomicrograph highlighting the identification of concentric lamellae. The chondron, which was located adjacent to the tidemark, was surrounded by lamellae (arrowed) in what appeared to be a periodic-like manner. Image taken from BALB/c Hgd-/- 145.3, a 54.4 week old Hgd-/ mouse. Tissue fixed in glutaraldehyde (x8200). Bar = 2µm.

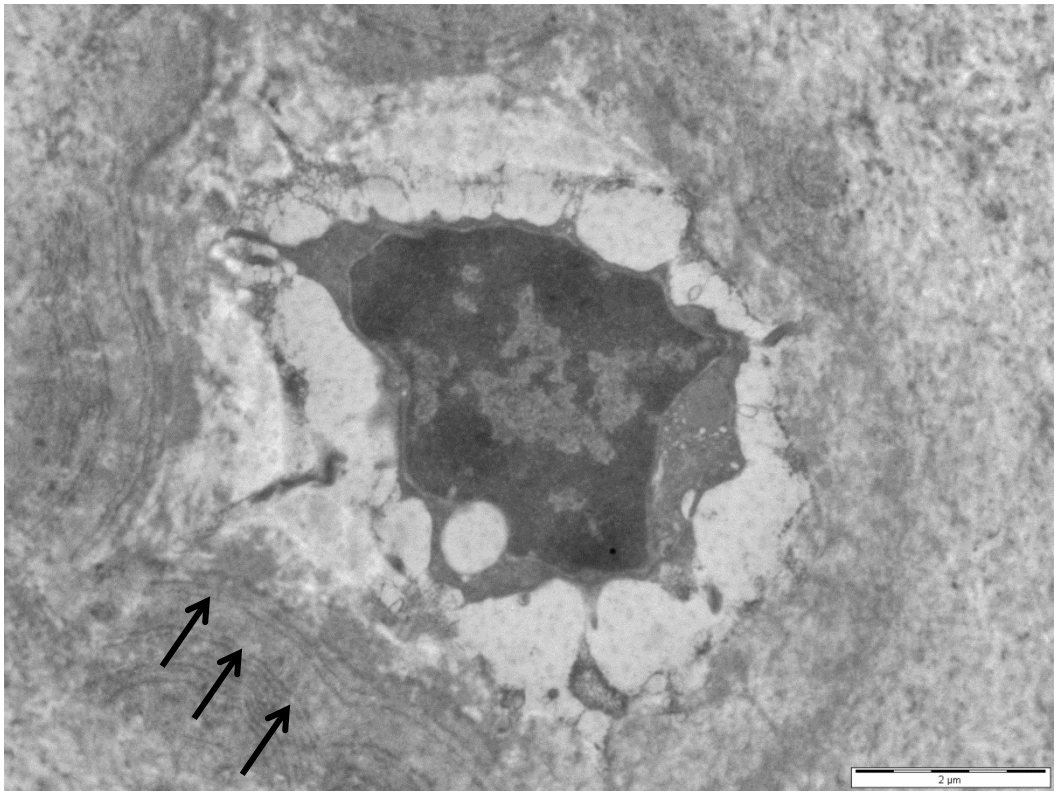

Figure 7.9 – TEM photomicrograph of concentric lamellae surrounding a chondron deep in the articular calcified cartilage. Concentric lamellae were seen surrounding the cell (arrowed) in a periodic manner, identical to what was seen in the chondron at the mineralisation front (Fig. 7.8). Image taken from BALB/c Hgd-/- 145.3, a 54.4 week old Hgd-/ mouse. Tissue fixed in glutaraldehyde (x8200). Bar = 2µm.

The number of lamellae and the distance between each one appeared to vary with individual chondrons. It is interesting to note that the lamellae surround both viable and hypertrophic chondrons suggesting that their formation is not linked to any apoptotic processes.

Chondrons that were located towards the mineralisation front appeared to be partially engulfed by the lamellae (Fig. 7.10), before progressing deeper into the ACC (Fig. 7.11). Stages of this progression were identified in all Hgd-/- mice.

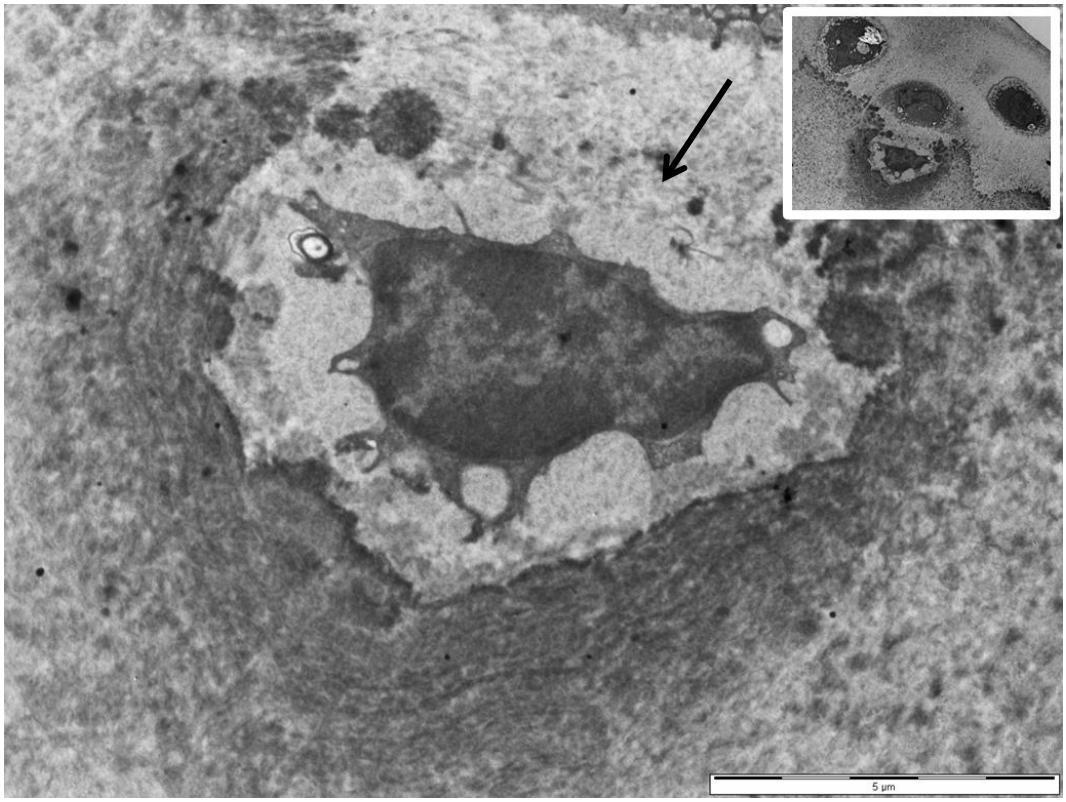

Figure 7.10 – TEM photomicrograph of a chondron located at the mineralisation front partially engulfed by concentric lamellae. The chondron appeared to be partially engulfed by concentric lamella, while not fully immersed in the ACC. Image taken from BALB/c Hgd-/- 61.3, a 60 week old Hgd-/- mouse. (x6000). Bar = 5µm. Inset: Location of the chondron in the ACC showing apparent 'opening' of the tidemark (arrowed) allowing the chondron to be engulfed by the concentric lamellae in the ACC. Tissue fixed in PBFS (x2500).

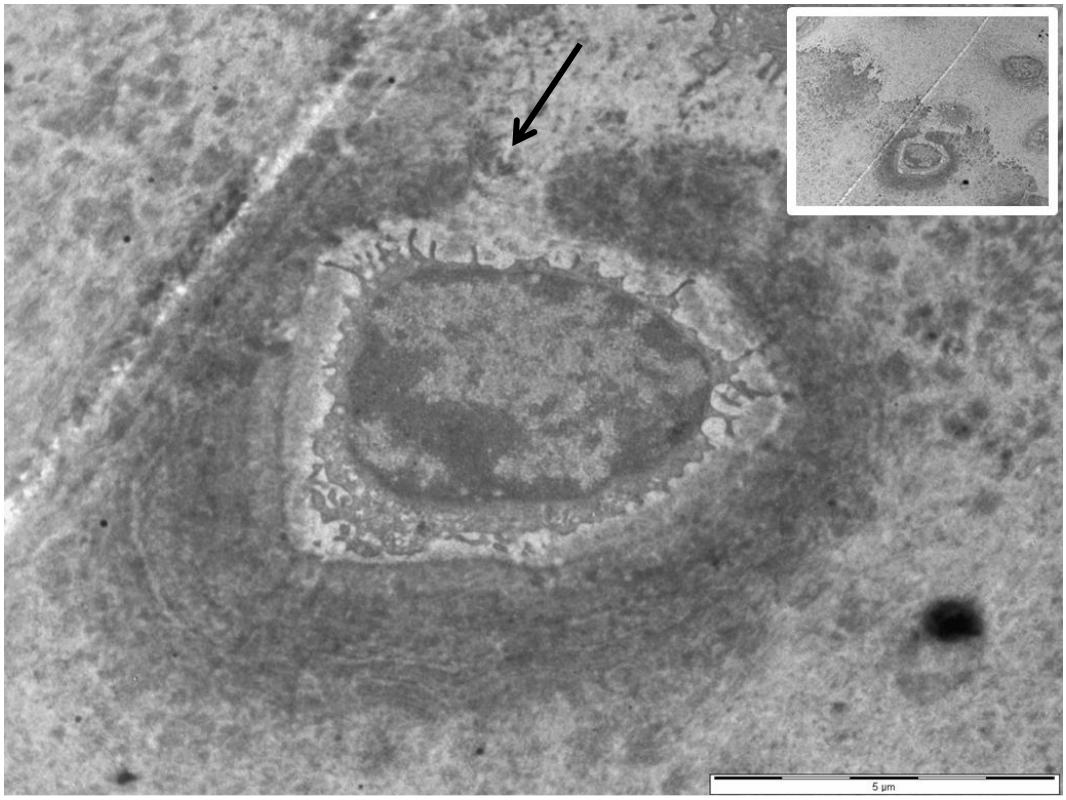

Figure 7.11 – TEM photomicrograph of a chondron located at the mineralisation front progressing deeper into the articular calcified cartilage. The chondron was almost completely encircled by lamellae as it progressed deeper into the calcified cartilage. Image taken from BALB/c Hgd-/- 61.3, a 60 week old Hgd-/- mouse. (x6000). Bar = 5µm. Inset: Location of chondron in the ACC showing apparent 'closing' of the tidemark (arrowed) once the chondron had been completely engulfed by the concentric lamellae and is embedded in the ACC. Tissue fixed in PBFS (x2500).

Figures 7.10 and 7.11 appeared to an apparent 'opening' and 'closing' of the tidemark as the chondron(s) become partially, and then completely engulfed by the concentric lamellae once embedded in ACC. This process is most probably linked to increased calcification of the cartilage matrix as the lamellae appeared to be laid down in association with the advancing tidemark; these processes are known to be linked, especially in the pathogenesis of OA.

As the chondrons progressed deeper into the ACC the lamellae became more defined and appeared to increase in number in a proportion of the chondrons (Fig. 7.12). Hypertrophy is a common feature of chondrons in the ACC so this may account for the changes seen deeper in ACC. Alkaline phosphatase is released during hypertrophy and is known to contribute to calcification of the surrounding matrices so it may be the release of alkaline phosphatase is involved in the formation of the lamellae.

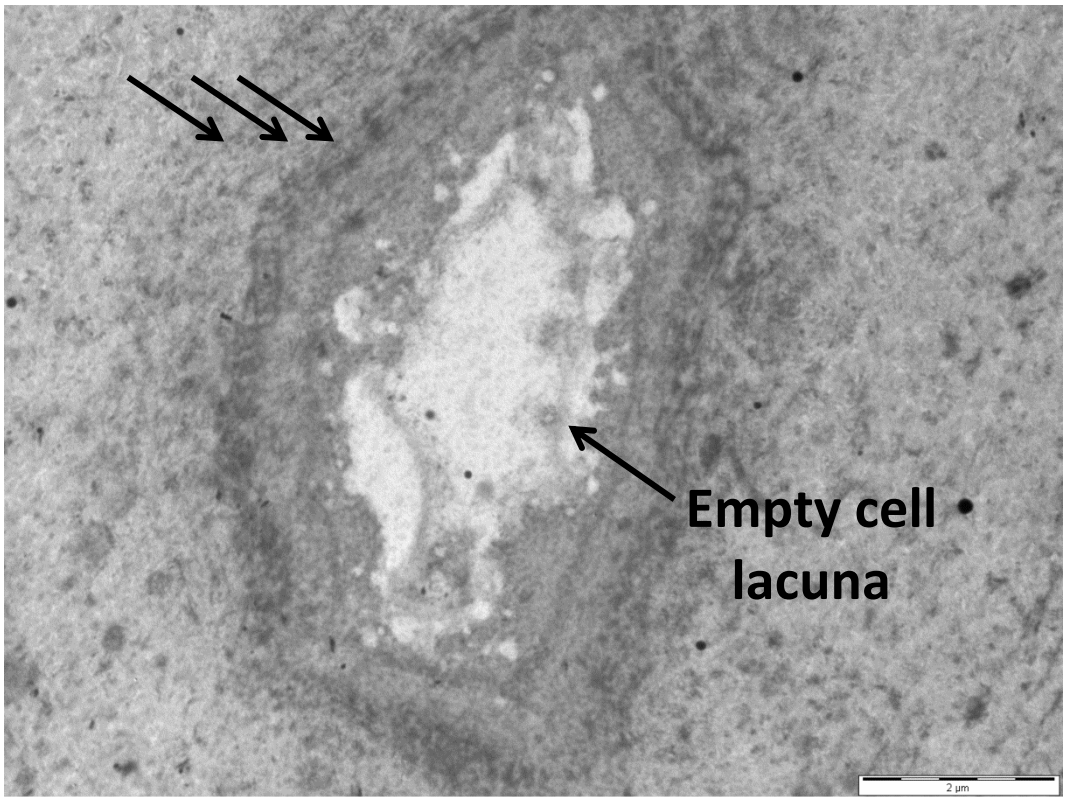

Figure 7.12 – TEM photomicrograph of a chondron located deep in the articular calcified cartilage with clearly defined concentric lamellae. The chondron appeared completely engulfed by lamellae (arrows) which were more defined than lamellae surrounding chondrons at the mineralisation front. Image taken from BALB/c Hgd-/- 61.4, a 60 week old Hgd-/- mouse. Tissue fixed in glutaraldehyde (x8200). Bar = 2µm.

As the lamellae became more defined it became easier to quantify them. This allowed us to show whether the amount of them increased or decreased with age and whether their size changed with age. Ten samples were subjected to quantitative analysis, however most were from aged mice. Only two out of the ten samples were from young mice (6.5 and 7.8 weeks), the rest were from mice aged 53 weeks or older (included one WT). Although this limited the scope of the study, it was still possible to draw initial conclusions from the data obtained.

Preliminary analysis of all the samples appeared to show that there was an increase in the number of lamella present in aged mice. BALB/c Hgd-/- 132.1 (♀, 6.5 weeks) and BALB/c Hgd-/- 131.1 (♂, 7.8 weeks) both showed a decreasing trend in lamellae width and quantity (Fig. 7.13), in comparison to aged Hgd-/- mice (Figs. 7.14 & 7.15).

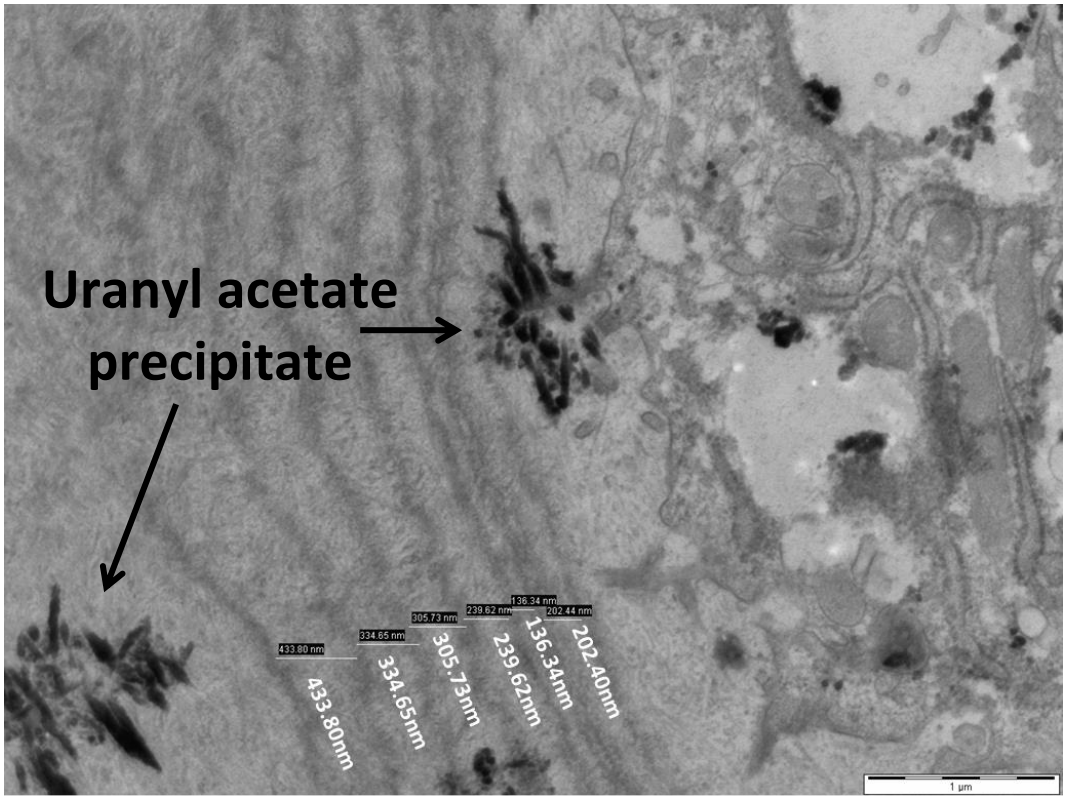

Figure 7.13 – TEM photomicrograph of a chondron, from BALB/c 131.1, a 7.8 week old Hgd-/- mouse, surrounded by lamellae. Measurements of the lamellae showed, apart from the first lamellae, an increase in width as they progressed further from the cell. UA precipitate has been labelled to make clear it is not shards of ochronotic pigment. Tissue fixed in glutaraldehyde (x16,500). Bar = 1µm.

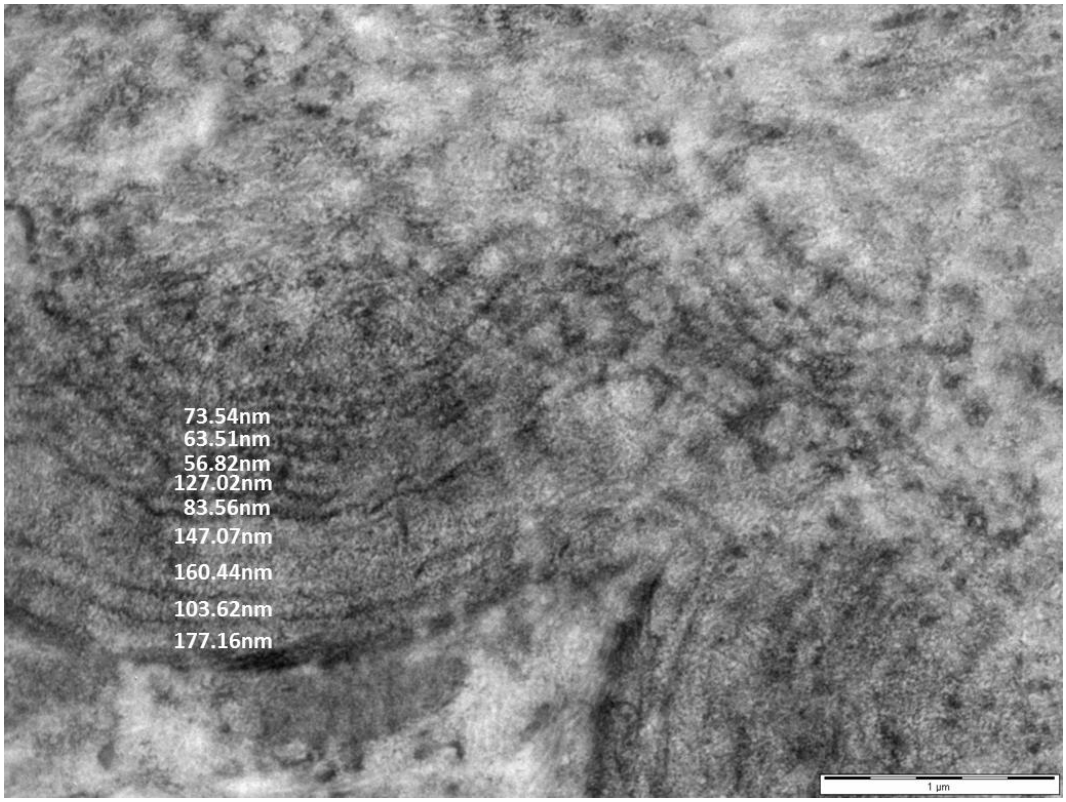

Figure 7.14 – TEM photomicrograph of a chondron, from BALB/c 145.3, a 53 week old BALB/c Hgd-/- mouse, surrounded by a large number of lamellae. The number of lamellae surrounding the chondron increased in comparison to the young Hgd-/- mouse (Fig. 7.13), with several appearing narrower than what was seen in the young BALB/c Hgd-/- mice (Fig. 7.13). Tissue fixed in glutaraldehyde (x26,500). Bar = 1µm.

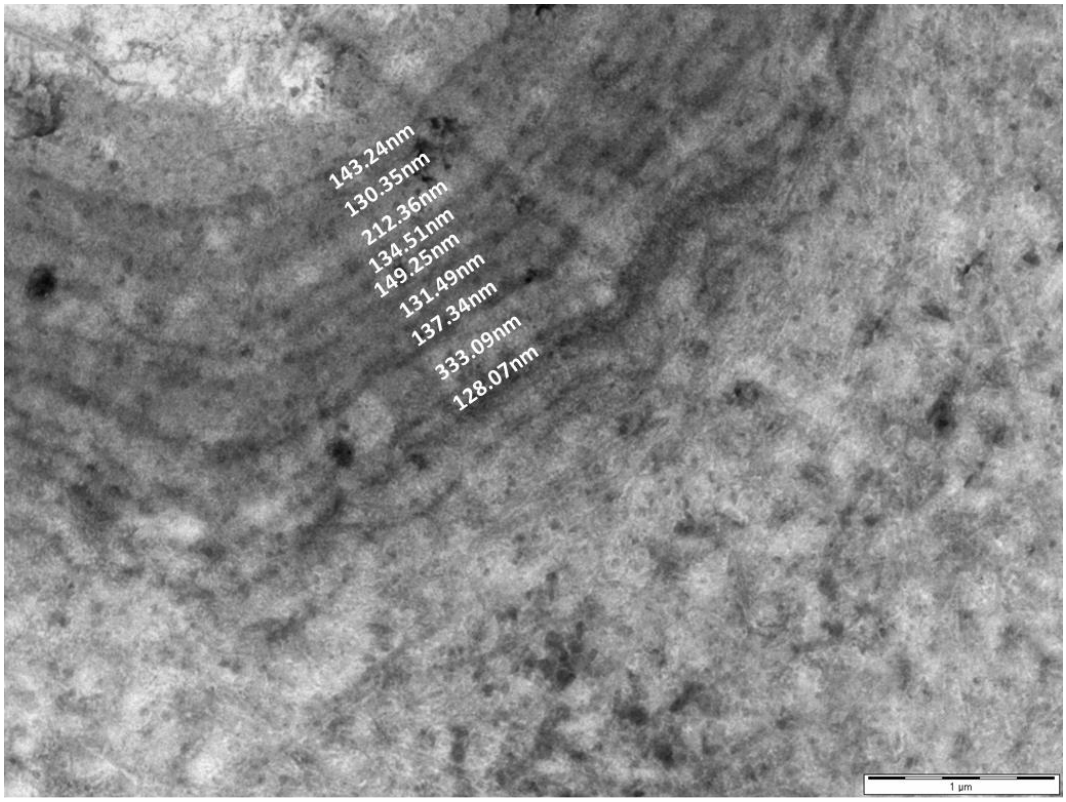

Figure 7.15 – TEM photomicrograph of a chondron, from BALB/c 59.3, a 61 week old BALB/c Hgd-/- mouse, surrounded by a large number of lamellae. Measurements of the lamellae found the majority to be narrower than younger Hgd-/- mice (Fig. 7.13). This is consistent with what was found in another aged Hgd-/- mouse (Fig. 7.14). Tissue fixed in PBFS (x16,500). Bar = 1µm.

Figures 7.14 and 7.15 showed an increase in the amount of lamellae in aged mice. What also appeared to be apparent from the images is that the widths of the majority of the lamellae become narrower as they become more frequent and the mice become older. From the data obtained there appeared to be an initial trend of a decrease in width of the lamellae throughout the samples analysed. In younger mice (Fig. 7.13) the lamellae were fewer and thicker than what was seen in the aged mice.

Further analysis of the lamellae revealed details about their composition. Most of the high powered photomicrographs shed little detail about what comprised the lamellae but a small number did show the presence of collagen fibres in the lamellae of aged mice (Figs 7.16 & 7.17).

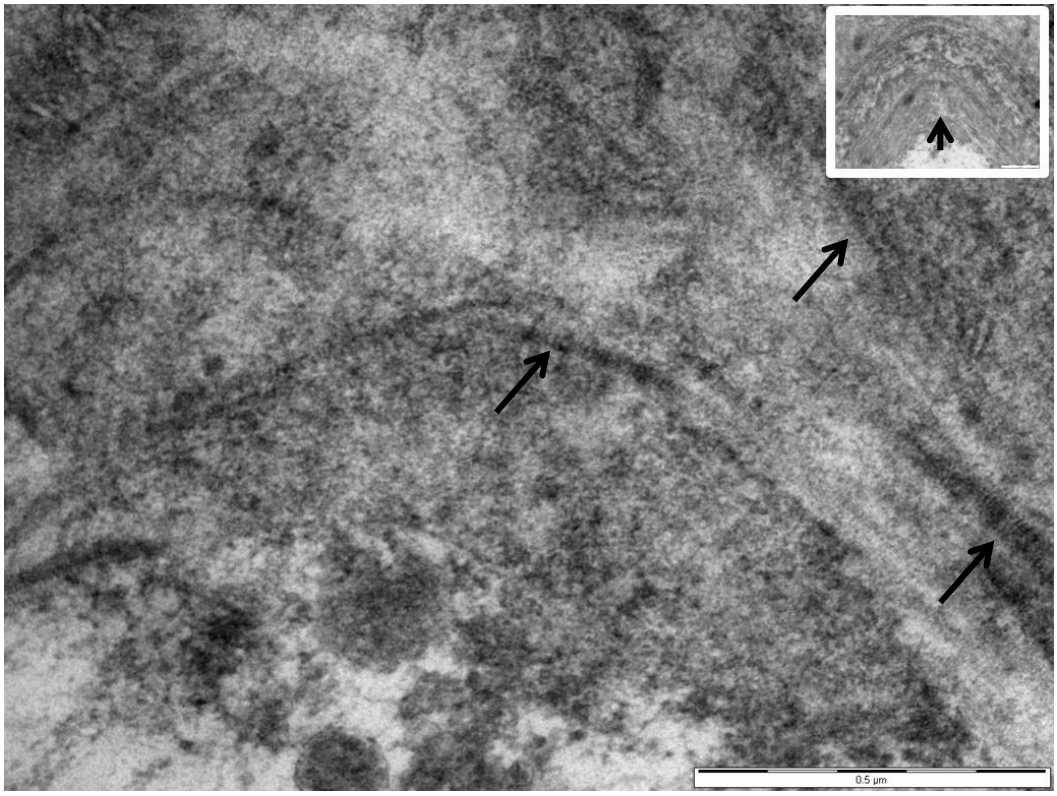

Figure 7.16 – TEM photomicrograph of collagen fibres in lamellae. Collagen fibres were identified in the lamellae of BALB/c 138.3, a 56 week old Hgd-/- mouse (arrows). Periodic banding can be seen along the fibre(s) which is distinctive of collagen. Bar = 0.5µm. Inset: Low power image highlighting the location of the collagen fibres in the lamellae. Tissue fixed in glutaraldehyde (x60,000). Inset bar = 1µm.

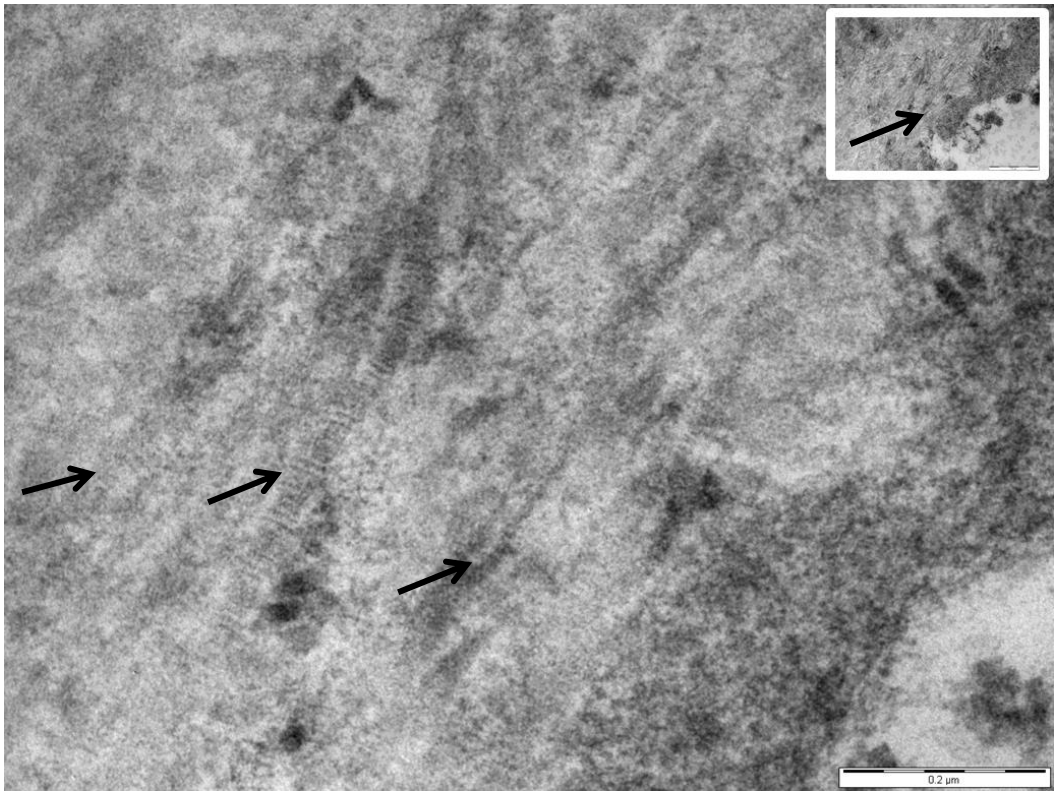

Figure 7.17 – TEM photomicrograph of collagen fibres in lamellae II. Collagen fibres were identified in the lamellae of a chondron deep in the ACC BALB/c 61.4, a 60 week old Hgd-/- mouse. Again, periodic banding can be seen along the fibre(s) which is distinctive of collagen. Bar = 0.2µm. Inset: Low power image highlighting the location of the collagen fibres in the lamellae. Tissue fixed in PBFS (x87,000). Inset bar = 0.5µm.

7.3.2.2 Wild type mice

Following the discovery of concentric lamellae around chondrons in the ACC of BALB/c Hgd-/- mice, WT mice were analysed to see if chondrons in the ACC of these mice displayed the same or similar features.

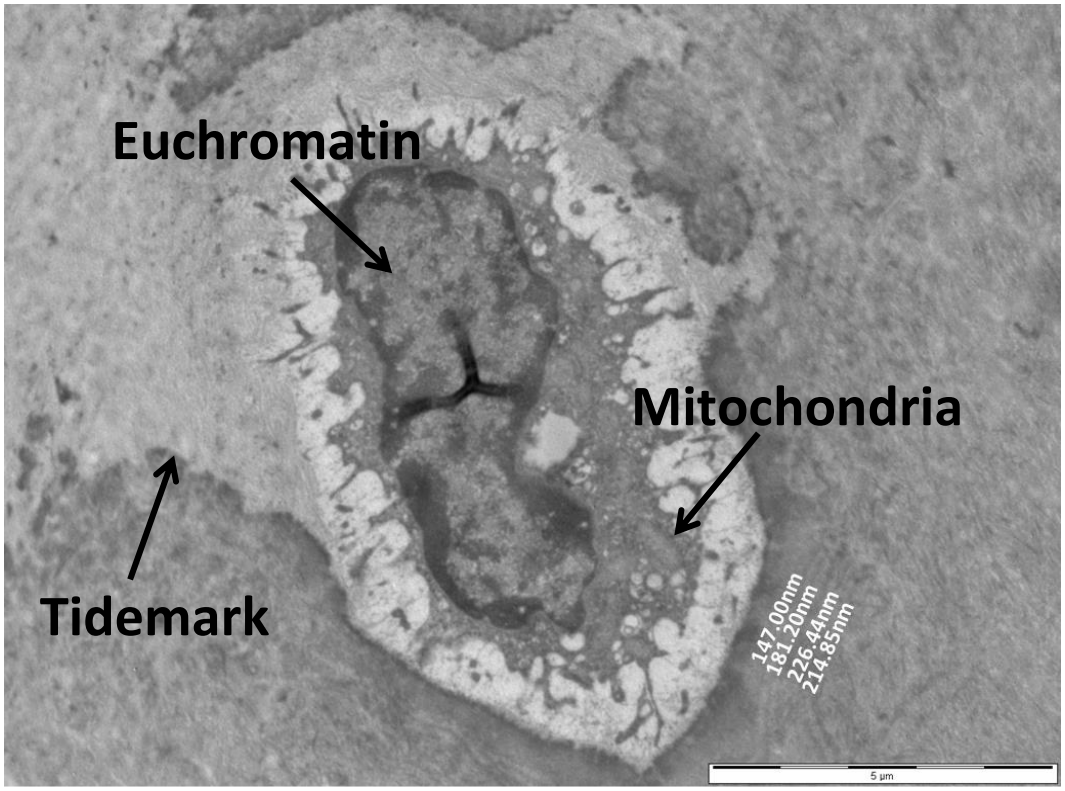

Figure 7.18 – TEM photomicrograph highlighting structures and lamellae widths in a 69 week old wild type mouse. The lamella values appeared to be very similar to what was seen in aged BALB/c Hgd-/- mice (Figs. 7.14 & 7.15). Although not as many lamella were identified when compared to the aged Hgd-/- mice, the comparable values of the lamella widths is important. Tissue fixed in PBFS (x6000). Bar = 5µm.

Figure 7.18 showed the presence of concentric lamellae in the ACC of WT mice. The chondron and its surrounding lamellae depicted in the figure were almost identical to what was seen in the aged Hgd-/- mice (Figs. 7.10 & 7.11). Again, similar to what was observed in the Hgd-/- mice, there appeared to be an 'opening' of the tidemark

leading to the chondron being engulfed by lamellae in the ACC. Although the lamellae were present in WT mice, only a small number of chondrons appeared to be engulfed by them in comparison to the Hgd-/- mice. The number of lamellae surrounding the chondrons also appeared to decrease in WT mice. The width of the lamellae seemed to be consistent with Hgd-/- mice of similar age (Fig. 7.15), which appears to confirm that an increase in the age of the mice leads to a decrease in the width of the lamellae present in the cartilage.

7.4 DISCUSSION

The first part of this Chapter detailed the ultrastructure of the HAC and ACC, as well as the underlying SCB of BALB/c Hgd-/- mice. These mice are a model of experimental OA as well as a model of AKU due to the osteoarthritic phenotype they show including cartilage degeneration, SCB remodelling and increasing amounts of calcification. As this was the case, there was a desire to see if changes in the cartilage ultrastructure could be identified and how these changes can help in understanding the role played, especially by the ACC in the initiation and progression of OA.

TEM photomicrographs taken from aged BALB/c Hgd-/- mice depicted the location and orientation of chondrons in both areas of the articular cartilage. Chondrons located in the superficial zone of the HAC appeared flattened and lay parallel towards the articular surface (Fig. 7.3), as did the surrounding collagen fibres in the PCM. These chondrons appeared active and healthy suggesting they were unaffected by the associated osteoarthropathy. Chondrons located in the middle and deep zones were larger in size and had a more rounded appearance (Fig. 7.4). These chondrons lay perpendicular to the articular surface as did the collagen fibres in the surrounding matrices. Again these chondrons appeared to be active and healthy. They showed no signs of hypertrophy and/or chondroptosis, nor did they appear to be pigmented. The orientation and location of the chondrons and collagen fibres in mice have been studied in detail by Hughes and colleagues [230] and the findings from the Hgd-/- mice are consistent with what they report.

Analysis of the ACC in Hgd-/- mice revealed the presence of concentric lamellae around the majority of chondrons scattered throughout this zone of cartilage. The lamellae were also present around chondrons in the ACC of WT mice but to a much lesser extent. Extensive literature searches revealed that these lamellae were a novel finding in the ACC. The structures may be related to the lamellae detected

using SEM by Hirotani et al [238], who proposed the existence of a lamellar system around chondrocytes in the deep zone of the articular cartilage in patients with secondary OA. It must be noted however that these were found only in the HAC and not in the ACC. No definitive reasoning is given by Hirotani *et al* [238] as to why they believe a lamellae system appears in the cartilage, although it is suggested it may be as a result of shrinkage from tissue preparation, and with no other literature describing this phenomenon, the mechanism behind their formation is not clearly understood. There is evidence, both from the work described in this chapter and the results gained by Hirotani that the lamellae are related to the pathogenesis of OA. The lamellae appeared around both viable chondrons towards the tidemark, which appeared to be partially engulfed by lamellae, and to a much higher degree around hypertrophic chondrons located deep in the ACC (Figs. 7.8 & 7.9). The fact they appear much more regularly around hypertrophic chondrons may be significant as to the origins of their formation. Hypertrophic chondrons express type X collagen [144, 179], and release increased levels of alkaline phosphatase [239] leading to cartilage calcification [143, 240]. Cartilage calcification has been associated with both ageing of tissues [241, 242] and OA pathogenesis [164, 240]. Calcification of cartilage associated with OA pathogenesis leads to thinning of HAC [243] and thickening of ACC [83], and can be identified by advancement of the tidemark [244, 245]. Thinning of the ACC can also occur during OA if the rate of subchondral remodelling is quicker than the rate of tidemark advancement [246]. Cartilage degeneration and SCB changes are hallmark features of OA. The lamellae identified in the ACC appeared to be laid down in association with the advancing tidemark which would indicate they are formed during cartilage calcification. Viable chondrons at the mineralisation front could be seen to be partially engulfed by the lamellae (Figs. 7.10 & 7.11). This suggests that chondrons in the HAC which are close to the tidemark are engulfed by ACC and the lamellae are then laid down during calcification of the cartilage.

The mechanisms behind the formation of the lamellae are at present unknown and have proven difficult to establish from the data collected for this chapter. However

as they may be linked to calcification it is possible their formation is related to one or more of the mechanisms and/or signalling molecules involved in cartilage calcification. Increased levels of IL-1 have been associated with increased levels of cartilage calcification [247], as have increased levels of insulin-like growth factors [248]. Although levels of these cytokines have yet to be determined in Hgd-/- mice it is probable they are sufficiently high enough to be a significant cause of calcification and are a factor in the formation of lamellae. Collagen is a major component of articular cartilage and it has been suggested that it can promote calcium pyrophosphate dihydrate (CPPD) deposition as collagen fibrils have been shown to be nucleators of CPPD [249], which along with basic calcium phosphate (BCP) are generated in OA cartilage [250]. Collagen can also bind different growth factors as well as interact with matrix proteins that regulate hydroxyapatite, both of which can affect cartilage calcification [248]. It is reasonable to assume that collagen plays a significant role in lamellae formation as not only can it directly influence calcification of the cartilaginous matrix, it was identified in the lamellae in a number of the Hgd-/- mice examined (Figs. 7.19 & 7.20). Although difficult to distinguish, individual collagen fibrils could be seen in portions of the lamellae. The complete structure of the lamellae could not be entirely identified but collagen fibres were clearly present thus highlighting collagen controlled calcification as a contributor to lamellae formation. Matrix vesicles which contain apatite crystals in OA cartilage are known to be involved in the calcification process [164]. Although they play a role in cartilage calcification and are almost certain to be involved in lamellae formation, as are both BCP and CPPD, decalcification of the tissue prior to processing will have removed any trace of them so it is difficult to determine what their actual role is.

The lamellae appeared in both aged and young, and Hgd-/- and WT mice. Although the presence of the lamellae in WT mice may seem surprising, as their formation is associated with increased levels of calcification, it can be explained by taking into account the age of the mice. All of the WT mice examined were over 69 weeks of age; both cartilage degeneration and small amounts of calcification are linked with

ageing [251] therefore some lamellae formation is not unexpected. Hgd-/- mice showed around an 80-90% increase in the number of chondrons engulfed by the lamellae in comparison with WT mice highlighting the apparent association between them and AKU. The greater abundance of lamellae in Hgd-/- mice, which are a model of OA, show that they may have a role in the pathogenesis of OA. To confirm this, more samples from BALB/c Hgd-/- and WT mine need to be examined to identify the number of chondrons associated with lamellae formation. The comparison between young and aged mice can only be made in reference to Hgd-/- mice as no young WT mice were examined for the study. Lamellae were present in young Hgd-/- mice (Fig. 7.13) suggesting that cartilage calcification and OA initiation begins at a young age in OA mice. There were fewer individual lamellae surrounding the chondrons in young Hgd-/- mice and they appeared thicker than those seen in aged Hgd-/- mice. As the mice increased in age the lamellae became thinner and more frequent around the chondrons. This correlates with the increased calcification and cartilage thinning seen in aged mice. Increased calcification which is associated with OA progression [233] appears to be linked to increasing amounts of lamellae formation around chondrons in ACC of aged Hgd-/- mice.

Although it is possible the lamellae may be involved in the development and progression of OA, they may also form as a result of ageing. Lamellae were present in both young and aged Hgd-/- mice; the number of lamellae around chondrocytes increased in aged Hgd-/- mice. The lamellae were also identified in an aged WT mouse which showed very little cartilage degeneration, suggesting that their formation, at least in this mouse, may have been related to ageing. Increasing the number of mice examined, over a wide range of ages, should help determine whether the lamellae are linked to either the development of OA or the process of ageing.

No ochronotic pigment was observed ultrastructurally in any of the samples analysed. During dissection of the tissues no pigmentation could be observed

macroscopically as opposed to human ochronotic joints when it is routinely observed [20, 252, 253]. The lack of macroscopic pigmentation is certainly a factor in the absence of identifiable ultrastructural pigmentation in Hgd-/- mice. Taylor *et al* [28] identified ochronotic pigment ultrastructurally in the ligamentous capsule, however Di Franco and colleagues noted that it may be almost impossible to identify pigment granules in calcified cartilage due to the presence of calcification nodules [37]. It is clear work needs to be done on refining the method of identifying pigment ultrastructurally.

The development of early, severe OA is associated with the progression of AKU [36] and it has been previously shown in Chapter 3 of this thesis that Hgd-/- mice show many similar signs of OA to those seen in AKU patients. Analysis of both Hgd-/- and WT mice revealed the appearance of novel concentric lamellae like structures surrounding hypertrophic chondrons in the ACC. Their possible association with mineralisation and advancement of the tidemark, and their greater abundance in OA indicate that the formation of these lamellae might be important in the pathogenesis of OA, since thinning of articular cartilage due to advancing mineralisation is reported to be a characteristic of joints undergoing OA. Further work on identifying the underlying mechanism(s) by how the lamellae are formed should provide a better understanding of the function and regulation of the ACC, and its role in the initiation and progression of OA.

8. General Discussion

Over one hundred years have passed since Sir Archibald Garrod described AKU as the first 'inborn error of metabolism' [1]. Around 50 years after Garrod made his initial observations on AKU, La Du and colleagues established that the defect in AKU was limited to the HGD enzyme [254], and that there was a link between arthritis and AKU [255]. Fernandez-Canon and colleagues, nearly 20 years ago, established that AKU results from a defect in the HGD gene [54, 56]. More recently there has been important discoveries relating to the pathogenesis of the disorder [9, 20], and the mechanism of ochronotic osteoarthropathy [28, 36, 183]. Whilst significant improvements have been made in understanding factors contributing to AKU there has been less progress made in preventing the disease, with no effective treatment currently available to AKU patients. Nitisinone has been shown to reduce plasma HGA levels in a clinical setting [53] however no results have been obtained to show whether prevented pigmented deposition in tissues. The lack of current treatment options available can be linked to the fact that a murine model of AKU showing pathology similar to humans, had prior to this thesis, never been reported. Studies on Hgd-/- mice by Montagutelli showed increased plasma levels of HGA but no ochronotic lesions in the tissues examined [110]. A more complex model of AKU was reported in mice containing an HT-1 mutation (Fah-/-) combined with Hgd heterozygosity [111], however this model was not considered practical as it relied on a spontaneous mutation. This thesis presents novel data, describing in detail the identification and progression of ochronotic osteoarthropathy in Hgd-/- mice, whilst also showing the progression of pigmentation in chondrons at different stages. It also discusses the efficacy of nitisinone as a therapeutic treatment for AKU, the use of surgical and chemical intervention to attempt modulate pigment deposition, and the discovery of concentric lamellae around hypertrophic chondrons in OA and WT mice.

The data presented in Chapter 3 represented the first time that ochronotic pigmentation and its associated osteoarthropathy, had been identified in Hgd-/- mice. As discussed in Chapter 3 it was originally thought Hgd-/- mice did not develop ochronotic lesions, even though they had abnormally high levels of plasma

HGA. Several reasons were given as to why this may have been the case including the short lifespan of mice, their ability to produce ascorbic acid endogenously [110], and possible low circulating levels of HGA. It was apparent from the data presented in Chapter 3 that none of these hypotheses were correct, and in fact Hgd-/- mice generally have higher circulating HGA than people with AKU and develop ochronotic osteoarthropathy over their life span. Although another mouse model of ochronosis has been described [111], the complexity of the genetic makeup of the model made it an unattractive and impractical model to study AKU. The importance of observing ochronotic osteoarthropathy in Hgd-/- cannot be underestimated as it, for the first time, provided an insight into the pathogenesis of AKU throughout the entire lifespan. Histological observations showed that pigment deposition began very early on in life, it was first detected at 15.7 and 10.4 weeks in BALB/c and BL/6 Hgd-/- mice respectively, and became progressively worse with increasing age. Both BALB/c and BL/6 strains of Hgd-/- mice showed an increase in pigmented chondrons with age, highlighting the progression of AKU. Once pigmentation had reached a certain stage, osteoarthritic changes in the tibio-femoral joint were noticeable. Cartilage erosion, osteophyte formation, tidemark duplication, and SCB remodelling were all observed in the knee joints of a high proportion of Hgd-/- mice. The appearance of osteoarthritic changes in Hgd-/- mice further highlighted the pathological similarities between the murine and human model of AKU. Whilst the mice never reached the stage of 'blanket' pigmentation, as seen in advanced human ochronosis, they did show very similar signs of pigmentation initiation and progression. Analysis of tissue from Hgd-/- mice at an early age showed initial pigment deposition occurred at the pericellular level of chondrons in calcified cartilage, similar to that reported in humans [36]. Data from Chapter 4 of this thesis, and Preston *et al* [217] suggests that pigment deposition may initiate following compositional and organisational changes in the collagen network. Studies have shown that the matrix of ochronotic tissue is disordered at the atomic level [39], however it is unknown whether this leads to pigment deposition or is a consequence of pigmentation. Intracellular pigmentation, consistent with ochronosis in humans, was observed in Hgd-/- mice and most likely resulted from an increased amount of pigment deposition following initial transformation of the

pericellular environment. End stage ochronosis resulting in 'blanket' and macroscopic pigmentation of articular cartilage often seen in human tissues samples was not observed in Hgd-/- mice. As discussed in Chapter 3 it is possible this is linked to the short murine lifespan, and reduced joint loading due to the quadrupedal nature of mice. It was clear from the data collected that BALB/c and BL/6 Hgd-/- mice developed ochronosis, and that the deposition of ochronotic pigment at a very early age in the mice showed that AKU, though presenting as painful syndrome in mid-life, is the result of a lifelong pathological process.

The progression of ochronosis in Hgd-/- mice appeared to be associated with the development of mild to severe osteoarthropathy in the tibio-femoral joint. Studies of human AKU tissue have shown that the early onset of severe osteoarthropathy is linked to the progression of ochronosis [256-258]. Analysis of both Hgd-/- and WT mice appeared to show that the most severe signs of OA were linked with AKU. There were very few signs of cartilage degeneration in any of the WT mice analysed. In comparison, the majority of Hgd-/- mice, from around 30-40 weeks onwards, showed some form of osteoarthritic change in the knee joint. The most frequent markers of OA in Hgd-/- mice were osteophyte formation and tidemark duplication, both of which are heavily involved in OA initiation and progression [259, 260]. Pigmented chondrons were identified in all osteophytes, providing further evidence that cartilage becomes susceptible to pigmentation at a relatively early stage of development. The extreme OA phenotype observed in advanced human ochronosis [36], resulting in complete resorption of the SCB plate, was not seen in Hgd-/- mice however this was not surprising as the mice did not show such advanced stages of pigmentation.

The data presented in Chapter 3 detailed the importance of the ACC and SCB in the development of ochronotic osteoarthropathy. The significance of SCB involvement in the pathogenesis of OA has been widely discussed [84, 126, 261-263], yet the involvement of the ACC in the initiation and progression of OA has often been

overlooked. ACC plays an important role in the distribution of load from HAC to SCB [264], both of which are heavily involved in OA, suggesting it also has a significant, yet undetermined role in OA pathogenesis. ACC certainly plays a key role in the initiation and progression of ochronotic osteoarthropathy, particularly in Hgd-/- mice where pigmentation is localized to mineralized cartilage. It is still unclear why pigmentation initiates in the ACC, and how the pigment actually moves to the sites of deposition in cartilage. Chondrocytes receive nutrients through diffusion therefore it may be that HGA diffuses through to the cartilage and chondrocytes from the synovial fluid surrounding the joints, before polymerizing and depositing in the cells. Another possible route is diffusion of HGA across the SCB-ACC interface. The SCB is vascularized therefore HGA may accumulate in the vessels of the SCB and diffuse across the SCB-ACC interface before becoming deposited as a polymerized pigment in chondrons. The primary binding site for ochronotic pigment appears to be associated with collagen, yet collagen fibres are located throughout the matrices of both the HAC and ACC. This suggests other factors in the ACC mediate the process of pigmentation. Chondrocytes in the ACC differ from those located in the HAC as they express a hypertrophic phenotype. These chondrocytes release factors which actively degrade the surrounding matrices thus altering the biomechanical properties of the cartilage. This altered state of biomechanics may lead to initial deposition in the PCM of chondrocytes in the ACC and then proliferation of chondron pigmentation following further biomechanical changes of the matrices. As chondrocytes in the ACC are surrounded by a calcified matrix it is surprising they survive as the level of nutrients they receive must be extremely low. It is possible this low level of nutrients leads to altered chondrocyte function, and an increased rate of chondrocyte death compared to the cells in the HAC. The altered function of chondrocytes in ACC may result in them becoming susceptible to pigment deposition. Collagen fibres are the most probable binding site for ochronotic pigment in particular types VI and X, both of which are located in the PCM of chondrons. Type X collagen is found in the PCM of hypertrophic chondrons yet it is also located throughout the ACC, and type VI collagen is also found in the PCM of chondrons in the HAC therefore the question remains, why does pigmentation initiate, and stay localized, in chondrons in the ACC? Proteomic and

metabolomic analyses may help provide some answers with regards to the make-up of cells at certain stages of pigmentation, however ultrastructural analysis of pigmented and non-pigmented chondrons in the ACC and HAC may provide the best opportunity to uncover the reasons behind this phenomenon. AKU presents with symptoms consistent with early onset, severe OA [36, 265, 266], resulting from pigment deposition and subsequent biomechanical changes in the ACC, demonstrating further the apparent involvement of the ACC in OA pathogenesis.

A single pigmented chondrocyte was located in the EP of the tibia of both BALB/c Hgd-/- 61.3 (♀) and 61.4 (♀) (Figs. 3.10 & 3.11). Although pigmented chondrocytes were located throughout the tibio-femoral joint the presence of a single pigmented cell in the EP of just two mice appeared peculiar. Chondrocytes in the EP express a number of different phenotypes as they are involved in endochondral ossification, and also synthesize a number of different collagens and proteoglycans. There is scarce literature on the EP in adult mice, most is focussed on its role in bone development, however Chambers *et al* reported that the EP remains open in aged mice and the embedded chondrocytes remain viable and actively synthesize type II collagen and aggrecan [142]. The authors also stated the chondrocytes no longer synthesized type X collagen indicating the EP was not in a stage of active hypertrophy. It has been shown previously that ochronotic pigment binds preferentially to collagen fibres [28] so it is possible that pigment deposition in these two chondrocytes is due to the presence of collagen fibres which the cells synthesize. However as all of the cells in the EP synthesize collagen it is unclear why only these two cells pigmented. There are likely to be other factors involved which alter chondrocyte activity and function, and may have resulted in these cells becoming pigmented. Immunostaining for factors which alter chondrocyte function, including TNF-α and IL-1 which are both inflammatory cytokines may help determine if factors other than mechanical damage lead to pigment deposition.

It is impossible to fully understand the pathogenesis of AKU, or any other disorder without knowledge of the mechanism behind its initiation and progression. Taylor and colleagues [36] have previously suggested a possible mechanism for AKU initiation and progression in human tissue, however the work discussed in Chapter 4 is the first time a staging of chondron pigmentation has been suggested in Hgd-/- mice. Histological analysis of the tibio-femoral joint showed pigmentation initially began in the PCM of hypertrophic chondrons in the ACC before progressing intracellularly, identical to what Taylor *et al* observed in human AKU tissue. The results appeared to indicate that a change had occurred in the PCM of Hgd-/- mice, possibly in its composition and/or organisation, prior to pigment deposition. The mechanical properties of the PCM are known to alter in disease states [180, 267] which fits in with the hypothesis proposed. It would be interesting to measure the Young's modulus of cartilage from both Hgd-/- and WT mice to determine how much biomechanical alteration had occurred from pigment deposition. Recent work by Taylor *et al* [183] showed that ochronotic cartilage is much stiffer than both normal and OA cartilage highlighting further the possible role of mechanical damage in the progression of AKU. It is unclear whether the changes resulting in pigment deposition, both mechanical and age related, also occur in non-AKU tissues. Therefore it is possible that in the case of ochronosis HGA acts as a marker of tissue damage. *In vitro* incubation of OA tissue with varying concentrations of HGA may help elucidate whether this hypothesis is correct. Administration of HGA to other murine models of OA, as well as WT mice, may also help elucidate whether HGA is a marker of mechanical and age related degenerative changes in tissues. If the theory that tissues need to undergo mechanical damage or ageing to make them susceptible to pigmentation is correct, the detection of ochronosis in Hgd-/- mice, so early in their life, provides one of the earliest signs of ageing observed.

Further similarities between the pathogenesis of AKU in mice and humans were reported in Chapter 4 with the identification of pigmentation in several other articulating joints. Although the tibio-femoral joint is severely affected in humans, ochronosis is also present in other tissues, particularly load-bearing joints.

Pigmented chondrons were located in the femoral head, calcaneus, and humerus epicondyles, all of which are heavily pigmented in humans. The majority of chondrons in all tissues were heavily pigmented, however a small proportion of lightly stained cells were located in the femoral head indicating the proposed mechanism of pigmentation applied to all ochronotic tissue. The three joints examined were obtained from a 65 week old, heavily pigmented, mouse therefore it is imperative that the same joints are examined from each mouse in the natural history study to determine whether they undergo the same age related decline as the tibio-femoral joint.

No practical treatment option is currently available to AKU sufferers, and as a result AKU patients are forced to suffer severe pain prior to joint replacement surgery. The identification of pigmentation in Hgd-/- mice has provided a model, with pathology very similar to AKU in humans, to test therapeutics to treat AKU. In Chapter 5 of this thesis, nitisinone; originally developed as a herbicide and subsequently used in the treatment of HT-1, was administered to Hgd-/- mice to determine its efficacy in treating AKU. Nitisinone, previously trialled as a possible treatment for AKU [53], was administered to the mice for their entire lifespan, and mid-way through their life. Both studies were undertaken to determine if nitisinone prevented pigmentation and if so, when treatment should commence. Whole life treatment with nitisinone was shown to prevent any pigment deposition in the mice, this being the first time nitisinone had been shown to stop pigmentation. There was no evidence from the mid-life intervention study that nitisinone therapy could reverse previously laid down pigment as had been suggested anecdotally by patients and physicians. The results collected from the studies clearly showed that nitisinone is an effective treatment for AKU. The data from Chapter 5 was included as part of a successful clinical trial application, which has recently started, to use nitisinone in the treatment of AKU. This shows the availability and practicality of the AKU mouse model is important as it provides a practical model of AKU in which treatments can be tested. Research is currently being carried out using antisense

therapy, gene therapy, and enzyme replacement therapy as other possible treatments for AKU.

Chapter 6 detailed the use of surgical and chemical intervention to attempt to accelerate the rate of pigment deposition. It was hypothesised that DMM surgery and HGA supplementation could significantly decrease the time required for Hgd-/- mice to develop severe ochronotic osteoarthropathy, due to increased mechanical damage and an increased amount of circulating HGA. Results from the DMM study showed no statistically significant increase between the number of pigmented chondrons in the experimental and contralateral control limbs. Although moderate to severe OA was observed in all of the mice, the results showed an apparent lack of correlation between joint damage and the number of pigmented chondrons in two of the six mice in the study. Both of these mice, BALB/c Hgd-/- 100.1 and 101.1, were culled at 8 weeks post-op yet they showed extensive signs of OA particularly BALB/c Hgd-/- 101.1 who displayed severe OA in the experimental limb. As mechanical damage is thought to be involved in the initiation and progression of pigmentation it is unclear why two of the mice displayed lower number of pigmented chondrons in the experimental limb. It is possible inter-individual variability at least contributes to the reduction in pigmented chondron numbers. Although the plasma levels of HGA in Hgd-/- mice remain steady across their lifetime there is variability with regards to the number of pigmented chondrons in Hgd-/- mice of the same age, as seen in Chapter 3 of this thesis. This may have played a role in the low pigmented chondron numbers observed in the experimental limbs of BALB/c Hgd-/- 100.1 and 101.1. It is likely other factors are involved in the reduction of pigmented chondrons in these mice including catabolic factors expressed by damaged/abnormal chondrocytes however further analysis of an increased number of DMM Hgd-/- mice may reveal this data to be no more than an anomaly. Supplementation with 5mM HGA also showed no significant difference in the number of pigmented chondrons between the experimental and control groups; the highest pigmented chondron count was actually observed in a control mouse. Plasma levels of HGA were also shown not to have increased. It appears

that the additional HGA given to the mice is simply excreted and therefore is never converted to ochronotic pigment. The inability to accelerate the rate of pigment deposition and to increase the amount of pigment deposited highlights possible protective pathways in Hgd-/- mice which may affect the pathogenesis of ochronotic osteoarthropathy.

Although pigmentation was identified histologically, TEM examination of the ACC from Hgd-/- mice (Chapter 7) provided no clear evidence of ochronotic pigment at the ultrastructural level. Taylor *et al* [28] had previously showed ochronotic pigment to bind preferentially to collagen fibres in the matrices of the ACC. It has been suggested in this thesis that changes occur in the collagen network of the PCM of pigmented chondrons, rendering them susceptible to pigmentation. Using TEM it was thought these changes, and the pigment deposited following them may be identified, however this was not the case. Although frustrating, the inability to identify ochronotic pigment at the ultrastructural level may be related to the lack of macroscopic pigmentation. Human tissue samples analysed using TEM were at an advanced stage of the disease and showed macroscopic pigmentation, clearly demonstrating the large amount of pigment deposited. This stage of pigmentation was never observed in Hgd-/- mice which may have accounted for the inability to identify pigmentation on the ultrastructural level. Further work is required on Hgd-/- mice of all ages to determine if changes in the collagen network of the matrices, which may lead to the initiation of pigmentation, can be identified. Initially the primary objective for TEM analysis of Hgd-/- mice was identification of ochronotic pigment however this was unsuccessful. Despite the failure to identify ochronotic pigment at the ultrastructural level, high resolution TEM revealed the presence of previously undescribed microanatomical concentric lamellae. The lamellae were located around both healthy and apoptotic chondrons in the ACC of Hgd-/- mice initially, and then were subsequently found in WT mice. Extensive literature searches revealed this to be a novel discovery in mice, however Hirotani *et al* [238] described a similar findings in the femoral heads of patients with secondary OA. The lamellae were more abundant in Hgd-/- mice, particularly around severely

hypertrophic chondrons, suggesting a possible link between their formation and the pathogenesis of OA. There was some evidence that appeared to show the lamellae were laid down were advancement of the tidemark and increased mineralisation of the cartilage, both of which are associated with OA. Further work is required to determine the periodicity of the lamellae and the mechanism behind their formation. Immunohistochemical analysis of the ACC from both Hgd-/- and WT mice, to determine how much type X collagen is present, may help elucidate if increased cartilage calcification is related to the formation of the lamellae. Measuring levels of IL-1 and insulin-like growth factors, both of which are also involved in cartilage calcification, may also help determine if the lamellae are formed through increased calcification. The lamellae, although a possible indicator of the development of OA, may also be a consequence of ageing. They were identified in both young and aged Hgd-/- mice with their frequency increasing significantly in the aged mice. The lamellae were also identified in an aged WT mouse which showed very little cartilage degeneration, suggesting that their formation at least in this mouse may have been related to ageing. Increasing the amount of samples examined at the ultrastructural level will help provide a clearer picture of whether the lamellae are linked to either the development of OA or the process of ageing.

In summary the studies reported in this thesis present novel findings on the identification of pigmentation, and the pathogenesis of ochronotic osteoarthropathy in Hgd-/- mice. The prevention of ochronotic pigmentation, using the drug nitisinone, was also reported for the first time highlighting the effectiveness of the Hgd-/- mouse model. The results reported provide new information on the initiation and progression of ochronosis, the mechanisms involved, and the use of a potential therapeutic to prevent pigment deposition.

REFERENCES

1. Garrod AE: **The incidence of alkaptonuria: A study in chemical individuality. 1902 [classical article]**. *The Yale Journal of Biology & Medicine* 2002, **75**(4):221-231.
2. Garrod AE, Clarke JW: **A new case of alkaptonuria**. *The Biochemical Journal* 1907, **2**(5-6):217-220.
3. Lee SL, Stenn FF: **Characterization of mummy bone ochronotic pigment**. *The Journal of the American Medical Association* 1978, **240**(2):136-138.
4. Stenn FF, Milgram JW, Lee SL *et al*: **Biochemical identification of homogentisic acid pigment in an ochronotic egyptian mummy**. *Science* 1977, **197**(4303):566-568.
5. Gaines JJ, Jr.: **The pathology of alkaptonuric ochronosis**. *Human Pathology* 1989, **20**(1):40-46.
6. Virchow RL: **Rudolph Virchow on ochronosis**. *Arthritis & Rheumatism* 1966, **9**(1):66-71.
7. Garrod AE, Hele TS: **The uniformity of the homogentisic acid excretion in alkaptonuria**. *The Journal of Physiology* 1905, **33**(3):198-205.
8. Garrod A: **The croonian lectures on inborn errors of metabolism**. *The Lancet* 1908, **172**(4427):1-7.
9. Phornphutkul C, Introne WJ, Perry MB *et al*: **Natural history of alkaptonuria**. *The New England Journal of Medicine* 2002, **347**(26):2111-2121.
10. Milch RA: **Studies of alcaptonuria: Inheritance of 47 cases in eight highly inter-related dominican kindreds**. *American Journal of Human Genetics* 1960, **12**(1):76-85.
11. Zatkova A, de Bernabe DB, Polakova H *et al*: **High frequency of alkaptonuria in Slovakia: evidence for the appearance of multiple mutations in HGO involving different mutational hot spots**. *American Journal of Human Genetics* 2000, **67**(5):1333-1339.
12. Al-Sbou M, Mwafi N: **Nine cases of alkaptonuria in one family in southern Jordan**. *Rheumatology International* 2012, **32**(3):621-625.

13. Al-Sbou M, Mwafi N, Lubad MA: **Identification of forty cases with alkaptonuria in one village in Jordan**. *Rheumatology International* 2012, **32**(12):3737-3740.

14. Al-sbou M: **Novel mutations in the homogentisate 1,2 dioxygenase gene identified in Jordanian patients with alkaptonuria**. *Rheumatology International* 2012, **32**(6):1741-1746.

15. Zatkova A, Polakova H, Micutkova L *et al*: **Novel mutations in the homogentisate-1,2-dioxygenase gene identified in Slovak patients with alkaptonuria**. *Journal of Medical Genetics* 2000, **37**(7):539-542.

16. Zatkova A, Sedlackova T, Radvansky J *et al*: **Identification of 11 novel homogentisate 1,2 dioxygenase variants in alkaptonuria patients and establishment of a novel LOVD-based HGD mutation database**. *Journal of Inherited Metabolic Disease Reports* 2012, **4**:55-65.

17. Peker E, Yonden Z, Sogut S: **From darkening urine to early diagnosis of alkaptonuria**. *Indian Journal of Dermatology, Venereology & Leprology* 2008, **74**(6):700.

18. Bory C, Boulieu R, Chantin C *et al*: **Homogentisic acid determined in biological fluids by HPLC**. *Clinical Chemistry* 1989, **35**(2):321-322.

19. Bory C, Boulieu R, Chantin C *et al*: **Diagnosis of alcaptonuria: rapid analysis of homogentisic acid by HPLC**. *Clinica Chimica Acta; International Journal of Clinical Chemistry* 1990, **189**(1):7-11.

20. Helliwell TR, Gallagher JA, Ranganath L: **Alkaptonuria--a review of surgical and autopsy pathology**. *Histopathology* 2008, **53**(5):503-512.

21. Karimzadeh H, Mohtasham N, Karimifar M *et al*: **A case of ochronosis with gout and Monckeberg arteries**. *Rheumatology International* 2009, **29**(12):1507-1510.

22. Merola JF, Meehan S, Walters RF *et al*: **Exogenous ochronosis**. *Dermatology Online Journal* 2008, **14**(10).

23. Merolla G, Dave A, Pegreffi F *et al*: **Shoulder arthroplasty in alkaptonuric arthropathy: A clinical case report and literature review**. *Musculoskeletal Surgery* 2012, **96**(1):93-99.

24. Ventura-Ríos L, Hernández-Díaz C, Gutiérrez-Pérez L *et al*: **Ochronotic arthropathy as a paradigm of metabolically induced degenerative joint disease. A case-based review**. *Clinical Rheumatology* 2014:1-7.

25. Cebesoy O, Isik M, Subasi M *et al*: **Total hip replacement for an ochronotic patient: A technical trick**. *The American Journal of Case Reports* 2014, **15**:27-30.

26. Ozmanevra R, Guran O, Karatosun V *et al*: **Total knee arthroplasty in ochronosis: A case report and critical review of the literature**. *Joint Diseases & Related Surgery* 2013, **24**(3):169-172.

27. Manoj Kumar RV, Rajasekaran S: **Spontaneous tendon ruptures in alkaptonuria**. *Journal of Bone & Joint Surgery, British Volume* 2003, **85-B**(6):883-886.

28. Taylor AM, Wlodarski B, Prior IA *et al*: **Ultrastructural examination of tissue in a patient with alkaptonuric arthropathy reveals a distinct pattern of binding of ochronotic pigment**. *Rheumatology* 2010, **49**(7):1412-1414.

29. Parambil JG, Daniels CE, Zehr KJ *et al*: **Alkaptonuria diagnosed by flexible bronchoscopy**. *CHEST Journal* 2005, **128**(5):3678-3680.

30. Fisher AA, Davis MW: **Alkaptonuric ochronosis with aortic valve and joint replacements and femoral fracture: A case report and literature review**. *Clinical Medicine & Research* 2004, **2**(4):209-215.

31. Hannoush H, Introne WJ, Chen MY *et al*: **Aortic stenosis and vascular calcifications in alkaptonuria**. *Molecular Genetics & Metabolism* 2012, **105**(2):198-202.

32. Concistrè G, Fiorani B, Ranocchi F *et al*: **Black aorta in a patient with alkaptonuria (ochronosis)**. *Journal of Cardiovascular Medicine* 2011, **12**(6):444-445.

33. Taylor AM, Batchelor TJP, Adams VL *et al*: **Ochronosis and calcification in the mediastinal mass of a patient with alkaptonuria**. *Journal of Clinical Pathology* 2011, **64**(10):935-936.

34. Lagier R, Steiger U: **Hip arthropathy in ochronosis: anatomical and radiological study**. *Skeletal Radiology* 1980, **5**(2):91-98.

35. O'Brien WM, La Du BN *et al*: **Biochemical, pathologic and clinical aspects of alcaptonuria, ochronosis and ochronotic arthropathy: Review of world literature (1584–1962)**. *The American Journal of Medicine* 1963, **34**(6):813-838.

36. Taylor AM, Boyde A, Wilson PJ *et al*: **The role of calcified cartilage and subchondral bone in the initiation and progression of ochronotic arthropathy in alkaptonuria**. *Arthritis & Rheumatism* 2011, **63**(12):3887-3896.

37. Di Franco M, Coari G, Bonucci E: **A morphological study of bone and articular cartilage in ochronosis**. *Virchows Archiv : An International Journal of Pathology* 2000, **436**(1):74-81.

38. Melis M, Onori P, Aliberti G *et al*: **Ochronotic arthropathy: Structural and ultrastructural features**. *Ultrastructural Pathology* 1994, **18**(5):467-471.

39. Chow WY, Taylor AM, Reid DG *et al*: **Collagen atomic scale molecular disorder in ochronotic cartilage from an alkaptonuria patient, observed by solid state NMR**. *Journal of Inherited Metabolic Disease* 2011, **34**(6):1137-1140.

40. Sealock RR, Silberstein HE: **The control of experimental alcaptonuria by means of vitamin C**. *Science* 1939, **90**(2344):517.

41. Zannoni VG, Lomtevas N, Goldfinger S: **Oxidation of homogentisic acid to ochronotic pigment in connective tissue**. *Biochimica et Biophysica Acta* 1969, **177**(1):94-105.

42. Forslind K, Wollheim FA, Akesson B *et al*: **Alkaptonuria and ochronosis in three siblings. Ascorbic acid treatment monitored by urinary HGA excretion**. *Clinical & Experimental Rheumatology* 1988, **6**(3):289-292.

43. Mayatepek E, Kallas K, Anninos A *et al*: **Effects of ascorbic acid and low-protein diet in alkaptonuria**. *European Journal of Pediatrics* 1998, **157**(10):867-868.

44. de Haas V, Carbasius Weber EC, de Klerk JBC *et al*: **The success of dietary protein restriction in alkaptonuria patients is age-dependent**. *Journal of Inherited Metabolic Disease* 1998, **21**(8):791-798.

45. Angelini C, Semplicini C: **Enzyme replacement therapy for pompe disease**. *Current Neurology & Neuroscience Reports* 2012, **12**(1):70-75.

46. Gungor D, Kruijshaar M, Plug I *et al*: **Impact of enzyme replacement therapy on survival in adults with pompe disease: Results from a prospective international observational study**. *Orphanet Journal of Rare Diseases* 2013, **8**(1):49.

47. Hamdan MA, Almalik MH, Mirghani HM: **Early administration of enzyme replacement therapy for Pompe disease: Short-term follow-up results**. *Journal of Inherited Metabolic Disease* 2008, **31**(2):431-436.

48. Schulz A, Ort O, Beyer P *et al*: **SC-0051, a 2-benzoyl-cyclohexane-1,3-dione bleaching herbicide, is a potent inhibitor of the enzyme p-hydroxyphenylpyruvate dioxygenase**. *Federation of European Biochemical Societies Letters* 1993, **318**(2):162-166.

49. McKiernan PJ: **Nitisinone in the treatment of hereditary tyrosinaemia type 1**. *Drugs* 2006, **66**(6):743-750.

50. McKiernan PJ: **Nitisinone for the treatment of hereditary tyrosinemia type I**. *Expert Opinion on Orphan Drugs* 2013, **1**(6):491-497.

51. Suzuki Y, Oda K, Yoshikawa Y *et al*: **A novel therapeutic trial of homogentisic aciduria in a murine model of alkaptonuria**. *Journal of Human Genetics* 1999, **44**(2):79-84.

52. Suwannarat P, O'Brien K, Perry MB : **Use of nitisinone in patients with alkaptonuria**. *Metabolism: Clinical & Experimental* 2005, **54**(6):719-728.

53. Introne WJ, Perry MB, Troendle J *et al*: **A 3-year randomized therapeutic trial of nitisinone in alkaptonuria**. *Molecular Genetics & Metabolism* 2011, **103**(4):307-314.

54. Granadino B, Beltran-Valero de Bernabe D, Fernandez-Canon JM *et al*: **The human homogentisate 1,2-dioxygenase (HGO) gene**. *Genomics* 1997, **43**(2):115-122.

55. Vilboux T, Kayser M, Introne W *et al*: **Mutation spectrum of homogentisic acid oxidase (HGD) in alkaptonuria**. *Human Mutation* 2009, **30**(12):1611-1619.

56. Fernandez-Canon JM, Granadino B, Beltran-Valero de Bernabe D *et al*: **The molecular basis of alkaptonuria**. *Nature Genetics* 1996, **14**(1):19-24.

57. Titus GP, Mueller HA, Burgner J *et al*: **Crystal structure of human homogentisate dioxygenase**. *Nature Structural Biology* 2000, **7**(7):542-546.

58. Zatkova A: **An update on molecular genetics of alkaptonuria (AKU)**. *Journal of Inherited Metabolic Disease* 2011, **34**(6):1127-1136.

59. Martin JP, Jr., Batkoff B: **Homogentisic acid autoxidation and oxygen radical generation: implications for the etiology of alkaptonuric arthritis**. *Free Radical Biology & Medicine* 1987, **3**(4):241-250.

60. Kotob SI, Coon SL, Quintero EJ *et al*: **Homogentisic acid is the primary precursor of melanin synthesis in vibrio cholerae, a hyphomonas strain, and shewanella colwelliana**. *Applied & Environmental Microbiology* 1995, **61**(4):1620-1622.

61. Coon SL, Kotob S, Jarvis BB *et al*: **Homogentisic acid is the product of MelA, which mediates melanogenesis in the marine bacterium shewanella colwelliana D**. *Applied & Environmental Microbiology* 1994, **60**(8):3006-3010.

62. Yabuuchi E, Ohyama A: **Characterization of "pyomelanin" producing strains of pseudomonas aeruginosa**. *International Journal of Systematic Bacteriology* 1972, **22**(2):53-64.

63. Alexopoulos LG, Setton LA, Guilak F: **The biomechanical role of the chondrocyte pericellular matrix in articular cartilage**. *Acta Biomaterialia* 2005, **1**(3):317-325.

64. Otero M, Goldring MB: **Cells of the synovium in rheumatoid arthritis. Chondrocytes**. *Arthritis Research & Therapy* 2007, **9**(5):220.

65. Swann DA, Radin EL: **The molecular basis of articular lubrication. I. Purification and properties of a lubricating fraction from bovine synovial fluid**. *The Journal of Biological Chemistry* 1972, **247**(24):8069-8073.

66. Kempson GE, Muir H, Pollard C *et al*: **The tensile properties of the cartilage of human femoral condyles related to the content of collagen and glycosaminoglycans**. *Biochimica et Biophysica Acta* 1973, **297**(2):456-472.

67. Redler IMD, Mow VCPD, Zimny MLPD *et al*: **The ultrastructure and biomechanical significance of the tidemark of articular cartilage**. *Clinical Orthopaedics & Related Research October* 1975, **112**:357-362.

68. Kirsch T, von der Mark K: **Isolation of human type X collagen and immunolocalization in fetal human cartilage**. *European Journal of Biochemistry* 1991, **196**(3):575-580.

69. Poole CA, Flint MH, Beaumont BW: **Morphological and functional interrelationships of articular cartilage matrices**. *Journal of Anatomy* 1984, **138 (Pt 1)**:113-138.

70. Poole CA, Ayad S, Schofield JR: **Chondrons from articular cartilage: I. Immunolocalization of type VI collagen in the pericellular capsule of isolated canine tibial chondrons**. *Journal of Cell Science* 1988, **90 (Pt 4)**:635-643.

71. Poole CA, Glant TT, Schofield JR: **Chondrons from articular cartilage. (IV). Immunolocalization of proteoglycan epitopes in isolated canine tibial chondrons**. *The Journal of Histochemistry & Cytochemistry: Official Journal of the Histochemistry Society* 1991, **39**(9):1175-1187.

72. Poole CA, Wotton SF, Duance VC: **Localization of type IX collagen in chondrons isolated from porcine articular cartilage and rat chondrosarcoma**. *The Histochemical Journal* 1988, **20**(10):567-574.

73. Poole CA, Flint MH, Beaumont BW: **Chondrons in cartilage: Ultrastructural analysis of the pericellular microenvironment in adult human articular cartilages**. *Journal of Orthopaedic Research: Official Publication of the Orthopaedic Research Society* 1987, **5**(4):509-522.

74. Liacini A, Sylvester J, Qing Li W *et al*: **Induction of matrix metalloproteinase-13 gene expression by TNF-α is mediated by MAP kinases, AP-1, and NF-κB transcription factors in articular chondrocytes**. *Experimental Cell Research* 2003, **288**(1):208-217.

75. de Isla NG, Stoltz JF: **In vitro inhibition of IL-1β catabolic effects on cartilage: A mechanism involved on diacerein anti-OA properties**. *Biorheology* 2008, **45**(3):433-438.

76. Gordon MK, Hahn RA: **Collagens**. *Cell & Tissue Research* 2010, **339**(1):247-257.

77. Gelse K, Poschl E, Aigner T: **Collagens--structure, function, and biosynthesis**. *Advanced Drug Delivery Reviews* 2003, **55**(12):1531-1546.

78. Porter S, Clark IM, Kevorkian L *et al*: **The ADAMTS metalloproteinases**. *The Biochemical Journal* 2005, **386**(Pt 1):15-27.

79. Hopkins DR, Keles S, Greenspan DS: **The bone morphogenetic protein 1/Tolloid-like metalloproteinases**. *Matrix Biology* 2007, **26**(7):508-523.

80. Hulmes DJS: **Collagen Diversity, Synthesis and Assembly**. *Collagen,* Springer US; 2008: 15-47.

81. You L, Temiyasathit S, Lee P *et al*: **Osteocytes as mechanosensors in the inhibition of bone resorption due to mechanical loading**. *Bone* 2008, **42**(1):172-179.

82. Bonewald LF, Johnson ML: **Osteocytes, mechanosensing and Wnt signaling**. *Bone* 2008, **42**(4):606-615.

83. Burr DB: **The importance of subchondral bone in the progression of osteoarthritis**. *The Journal of Rheumatology* 2004, **70**:77-80.

84. Goldring MB, Goldring SR: **Articular cartilage and subchondral bone in the pathogenesis of osteoarthritis**. *Annals of the New York Academy of Sciences* 2010, **1192**:230-237.

85. Kwan Tat S, Lajeunesse D, Pelletier J-P *et al*: **Targeting subchondral bone for treating osteoarthritis: What is the evidence?** *Best Practice & Research Clinical Rheumatology* 2010, **24**(1):51-70.

86. Castaneda S, Roman-Blas JA, Largo R *et al*: **Subchondral bone as a key target for osteoarthritis treatment**. *Biochemical Pharmacology* 2012, **83**(3):315-323.

87. Arden N, Nevitt MC: **Osteoarthritis: Epidemiology**. *Best Practice & Research Clinical Rheumatology* 2006, **20**(1):3-25.

88. Zhang Y, Jordan JM: **Epidemiology of osteoarthritis**. *Clinics in Geriatric Medicine* 2010, **26**(3):355-369.

89. Buckwalter JA, Anderson DD, Brown TD *et al*: **The roles of mechanical stresses in the pathogenesis of osteoarthritis: Implications for treatment of joint injuries**. *Cartilage* 2013, **4**(4):286-294.

90. Griffin TM, Guilak F: **The role of mechanical loading in the onset and progression of osteoarthritis**. *Exercise & Sport Sciences Reviews* 2005, **33**(4):195-200.

91. Sun HB: **Mechanical loading, cartilage degradation, and arthritis**. *Annals of the New York Academy of Sciences* 2010, **1211**(1):37-50.

92. Knudson W, Casey B, Nishida Y *et al*: **Hyaluronan oligosaccharides perturb cartilage matrix homeostasis and induce chondrocytic chondrolysis**. *Arthritis & Rheumatism* 2000, **43**(5):1165-1174.

93. Hamamura K, Zhang P, Zhao L *et al*: **Knee loading reduces MMP13 activity in the mouse cartilage**. *BioMed Central Musculoskeletal Disorders* 2013, **14**:312.

94. Zhang P, Sun Q, Turner CH *et al*: **Knee loading accelerates bone healing in mice**. *Journal of Bone & Mineral Research: The Official Journal of the American Society for Bone & Mineral Research* 2007, **22**(12):1979-1987.

95. Goldring SR: **Alterations in periarticular bone and cross talk between subchondral bone and articular cartilage in osteoarthritis**. *Therapeutic Advances in Musculoskeletal Disease* 2012, **4**(4):249-258.

96. Radin EL, Rose RM: **Role of subchondral bone in the initiation and progression of cartilage damage**. *Clinical Orthopaedics & Related Research* 1986(213):34-40.

97. Walsh DA, Bonnet CS, Turner EL *et al*: **Angiogenesis in the synovium and at the osteochondral junction in osteoarthritis**. *Osteoarthritis & Cartilage* 2007, **15**(7):743-751.

98. Felson DT, Lawrence RC, Dieppe PA *et al*: **Osteoarthritis: New insights. Part 1: The disease and its risk factors**. *Annals of Internal Medicine* 2000, **133**(8):635-646.

99. Loeser RF: **Systemic and local regulation of articular cartilage metabolism: Where does leptin fit in the puzzle?** *Arthritis & Rheumatism* 2003, **48**(11):3009-3012.

100. Roman-Blas J, Castaneda S, Largo R *et al*: **Subchondral bone remodelling and osteoarthritis**. *Arthritis Research & Therapy* 2012, **14**(Suppl 2):A6.

101. Hackam DG, Redelmeier DA: **Translation of research evidence from animals to humans**. *The Journal of the American Medical Assoication* 2006, **296**(14):1731-1732.

102. Perel P, Roberts I, Sena E *et al*: **Comparison of treatment effects between animal experiments and clinical trials: Systematic review**. *British Medical Journal* 2007, **334**(7586):197.

103. Florey H: **Early experiences with penicillin therapy**. *Connecticut State Medical Journal* 1947, **11**(1):5.

104. Florey HW: **Penicillin; its development for medical uses**. *Proceedings of the Royal Institution of Great Britain* 1946, **33**(150 Pt 1):23-30.

105. Costantini F, Lacy E: **Introduction of a rabbit beta-globin gene into the mouse germ line**. *Nature* 1981, **294**(5836):92-94.

106. Jaenisch R, Mintz B: **Simian virus 40 DNA sequences in DNA of healthy adult mice derived from preimplantation blastocysts injected with viral DNA**. *Proceedings of the National Academy of Sciences* 1974, **71**(4):1250-1254.

107. Johnson EH, Miller RL: **Alkaptonuria in a cynomolgus monkey (Macaca fascicularis)**. *Journal of Medical Primatology* 1993, **22**(7-8):428-430.

108. Keeling ME, McClure HM, Kibler RF: **Alkaptonuria in an orangutan (Pongo pygmaeus)**. *American Journal of Physical Anthropology* 1973, **38**(2):435-438.

109. Moran TJ, Yunis EJ: **Studies on ochronosis. 2. Effects of injection of homogentisic acid and ochronotic pigment in experimental animals**. *The American Journal of Pathology* 1962, **40**:359-369.

110. Montagutelli X, Lalouette A, Coude M *et al*: **aku, a mutation of the mouse homologous to human alkaptonuria, maps to chromosome 16**. *Genomics* 1994, **19**(1):9-11.

111. Taylor AM, Preston AJ, Paulk NK *et al*: **Ochronosis in a murine model of alkaptonuria is synonymous to that in the human condition**. *Osteoarthritis & Cartilage* 2012, **20**(8):880-886.

112. Mason RM, Chambers MG, Flannelly J *et al*: **The STR/ort mouse and its use as a model of osteoarthritis**. *Osteoarthritis & Cartilage* 2001, **9**(2):85-91.

113. Wilhelmi G, Faust R: **Suitability of the C57 black mouse as an experimental animal for the study of skeletal changes due to ageing, with special reference to osteo-arthrosis and its response to tribenoside**. *Pharmacology* 1976, **14**(4):289-296.

114. Sahebjam S, Khokha R, Mort JS: **Increased collagen and aggrecan degradation with age in the joints of Timp3(-/-) mice**. *Arthritis & Rheumatism* 2007, **56**(3):905-909.

115. Neuhold LA, Killar L, Zhao W *et al*: **Postnatal expression in hyaline cartilage of constitutively active human collagenase-3 (MMP-13) induces osteoarthritis in mice**. *The Journal of Clinical Investigation* 2001, **107**(1):35-44.

116. Valverde-Franco G, Binette JS, Li W *et al*: **Defects in articular cartilage metabolism and early arthritis in fibroblast growth factor receptor 3 deficient mice**. *Human Molecular Genetics* 2006, **15**(11):1783-1792.

117. Kamekura S, Hoshi K, Shimoaka T *et al*: **Osteoarthritis development in novel experimental mouse models induced by knee joint instability**. *Osteoarthritis & Cartilage* 2005, **13**(7):632-641.

118. Glasson SS, Blanchet TJ, Morris EA: **The surgical destabilization of the medial meniscus (DMM) model of osteoarthritis in the 129/SvEv mouse**. *Osteoarthritis & Cartilage* 2007, **15**(9):1061-1069.

119. Manning K, Fernandez-Canon JM, Montagutelli X *et al*: **Identification of the mutation in the alkaptonuria mouse model. Mutations in brief no. 216. Online**. *Human Mutation* 1999, **13**(2):171.

120. Glasson SS, Chambers MG, Van Den Berg WB *et al*: **The OARSI histopathology initiative – recommendations for histological assessments of osteoarthritis in the mouse**. *Osteoarthritis & Cartilage* 2010, **18, Supplement 3**(0):S17-S23.

121. Bancroft JD, Stevens A, Stevens A: **Theory and practice of histological techniques**: Churchill Livingstone; 1982.

122. Tinti L, Taylor AM, Santucci A *et al*: **Development of an in vitro model to investigate joint ochronosis in alkaptonuria**. *Rheumatology* 2011, **50**(2):271-277.

123. Russell WL: **X-ray-induced mutations in mice**. *Cold Spring Harbor Symposia on Quantitative Biology* 1951, **16**:327-336.

124. Thomas JW, LaMantia C, Magnuson T: **X-ray-induced mutations in mouse embryonic stem cells**. *Proceedings of the National Academy of Sciences* 1998, **95**(3):1114-1119.

125. Manning K, Al-Dhalimy M, Finegold M *et al*: **In vivo suppressor mutations correct a murine model of hereditary tyrosinemia type I**. *Proceedings of the National Academy of Sciences* 1999, **96**(21):11928-11933.

126. Goldring SR: **Role of bone in osteoarthritis pathogenesis**. *The Medical Clinics of North America* 2009, **93**(1):25-35, xv.

127. Pedersen HE: **The ossicles of the semilunar cartilages of rodents**. *The Anatomical Record* 1949, **105**(1):1-9.

128. Van Breuseghem I, Geusens E, Pans S *et al*: **The meniscal ossicle revisited**. *Journal Belge de Radiologie-Belgisch Tijdschrift voor Radiologi : Organe de la Societe Royale Belge de Radiologie* 2003, **86**(5):276-277.

129. Guilak F, Alexopoulos LG, Upton ML *et al*: **The pericellular matrix as a transducer of biomechanical and biochemical signals in articular cartilage**. *Annals of the New York Academy of Sciences* 2006, **1068**:498-512.

130. Meyer EG, Baumer TG, Slade JM *et al*: **Tibiofemoral contact pressures and osteochondral microtrauma during anterior cruciate ligament rupture due to excessive compressive loading and internal torque of the human knee**. *The American Journal of Sports Medicine* 2008, **36**(10):1966-1977.

131. van der Kraan PM, Blaney Davidson EN, van den Berg WB: **Bone morphogenetic proteins and articular cartilage: To serve and protect or a wolf in sheep clothing's?** *Osteoarthritis & Cartilage* 2010, **18**(6):735-741.

132. Wang X, Manner PA, Horner A *et al*: **Regulation of MMP-13 expression by RUNX2 and FGF2 in osteoarthritic cartilage**. *Osteoarthritis & Cartilage* 2004, **12**(12):963-973.

133. Chia SL, Sawaji Y, Burleigh A *et al*: **Fibroblast growth factor 2 is an intrinsic chondroprotective agent that suppresses ADAMTS-5 and delays cartilage degradation in murine osteoarthritis**. *Arthritis & Rheumatism* 2009, **60**(7):2019-2027.

134. Sawaji Y, Hynes J, Vincent T *et al*: **Fibroblast growth factor 2 inhibits induction of aggrecanase activity in human articular cartilage**. *Arthritis & Rheumatism* 2008, **58**(11):3498-3509.

135. Bank RA, Soudry M, Maroudas A *et al*: **The increased swelling and instantaneous deformation of osteoarthritic cartilage is highly correlated with collagen degradation**. *Arthritis & Rheumatism* 2000, **43**(10):2202-2210.

136. Heinegard D: **Proteoglycans and more--from molecules to biology**. *International Journal of Experimental Pathology* 2009, **90**(6):575-586.

137. Heinegard D, Saxne T: **The role of the cartilage matrix in osteoarthritis**. *Nature Reviews Rheumatology* 2011, **7**(1):50-56.

138. Glasson SS, Askew R, Sheppard B *et al*: **Deletion of active ADAMTS5 prevents cartilage degradation in a murine model of osteoarthritis**. *Nature* 2005, **434**(7033):644-648.

139. Stanton H, Rogerson FM, East CJ *et al*: **ADAMTS5 is the major aggrecanase in mouse cartilage in vivo and in vitro**. *Nature* 2005, **434**(7033):648-652.

140. Benjamin M, Toumi H, Ralphs JR *et al*: **Where tendons and ligaments meet bone: attachment sites ('entheses') in relation to exercise and/or mechanical load**. *Journal of Anatomy* 2006, **208**(4):471-490.

141. Benjamin M, Hillen B: **Mechanical influences on cells, tissues and organs - 'mechanical morphogenesis'**. *European Journal of Morphology* 2003, **41**(1):3-7.

142. Chambers MG, Kuffner T, Cowan SK *et al*: **Expression of collagen and aggrecan genes in normal and osteoarthritic murine knee joints**. *Osteoarthritis & Cartilage* 2002, **10**(1):51-61.

143. Chen-An P, Andreassen KV, Henriksen K *et al*: **Investigation of chondrocyte hypertrophy and cartilage calcification in a full-depth articular cartilage explants model**. *Rheumatology International* 2013, **33**(2):401-411.

144. van der Kraan PM, van den Berg WB: **Chondrocyte hypertrophy and osteoarthritis: Role in initiation and progression of cartilage degeneration?** *Osteoarthritis & Cartilage* 2012, **20**(3):223-232.

145. Aigner T, Reichenberger E, Bertling W *et al*: **Type X collagen expression in osteoarthritic and rheumatoid articular cartilage**. *Virchows Archiv B, Cell Pathology including Molecular Pathology* 1993, **63**(4):205-211.

146. Pfander D, Swoboda B, Kirsch T: **Expression of early and late differentiation markers (proliferating cell nuclear antigen, syndecan-3, annexin VI, and alkaline phosphatase) by human osteoarthritic chondrocytes**. *The American Journal of Pathology* 2001, **159**(5):1777-1783.

147. Fawns HT, Landells JW: **Histochemical studies of rheumatic conditions. I. Observations on the fine structures of the matrix of normal bone and cartilage**. *Annals of the Rheumatic Diseases* 1953, **12**(2):105-113.

148. Lane LB, Bullough PG: **Age-related changes in the thickness of the calcified zone and the number of tidemarks in adult human articular cartilage**. *The Journal of Bone & Joint Surgery British Volume* 1980, **62**(3):372-375.

149. Oettmeier R, Abendroth K, Oettmeier S: **Analyses of the tidemark on human femoral heads. II. Tidemark changes in osteoarthrosis--a histological and histomorphometric study in non-decalcified preparations**. *Acta Morphologica Hungarica* 1989, **37**(3-4):169-180.

150. McNulty MA, Loeser RF, Davey C *et al*: **A Comprehensive Histological Assessment of Osteoarthritis Lesions in Mice**. *Cartilage* 2011, **2**(4):354-363.

151. Bateman JF, Rowley L, Belluoccio D *et al*: **Transcriptomics of wild-type mice and mice lacking ADAMTS-5 activity identifies genes involved in osteoarthritis initiation and cartilage destruction**. *Arthritis & Rheumatism* 2013, **65**(6):1547-1560.

152. van der Kraan PM, van den Berg WB: **Osteophytes: relevance and biology**. *Osteoarthritis & Cartilage* 2007, **15**(3):237-244.

153. Orzincolo C, Castaldi G, Scutellari PN *et al*: **Ochronotic arthropathy in alkaptonuria. Radiological manifestations and physiopathological signs**. *La Radiologia Medica* 1988, **75**(5):476-481.

154. Jebaraj I, Chacko BR, Chiramel GK *et al*: **A simplified staging system based on the radiological findings in different stages of ochronotic spondyloarthropathy**. *The Indian Journal of Radiology & Imaging* 2013, **23**(1):101-105.

155. Pottenger LA, Phillips FM, Draganich LF: **The effect of marginal osteophytes on reduction of varus-valgus instability in osteoarthritic knees**. *Arthritis & Rheumatism* 1990, **33**(6):853-858.

156. Goldring MB, Goldring SR: **Osteoarthritis**. *Journal of Cellular Physiology* 2007, **213**(3):626-634.

157. Menon IA, Persad SD, Haberman HF *et al*: **Characterization of the pigment from homogentisic acid and urine and tissue from an alkaptonuria patient**. *Biochemistry & Cell Biology* 1991, **69**(4):269-273.

158. Schmaler-Ripcke J, Sugareva V, Gebhardt P *et al*: **Production of pyomelanin, a second type of melanin, via the tyrosine degradation pathway in aspergillus fumigatus**. *Applied & Environmental Microbiology* 2009, **75**(2):493-503.

159. Stoop R, van der Kraan PM, Buma P *et al*: **Type II collagen degradation in spontaneous osteoarthritis in C57Bl/6 and BALB/c mice**. *Arthritis & Rheumatism* 1999, **42**(11):2381-2389.

160. Poole AR, Kobayashi M, Yasuda T *et al*: **Type II collagen degradation and its regulation in articular cartilage in osteoarthritis**. *Annals of the Rheumatic Diseases* 2002, **61 Suppl 2**:ii78-81.

161. Khan IM, Palmer EA, Archer CW: **Fibroblast growth factor-2 induced chondrocyte cluster formation in experimentally wounded articular cartilage is blocked by soluble Jagged-1**. *Osteoarthritis & Cartilage* 2010, **18**(2):208-219.

162. Clark AL, Votta BJ, Kumar S *et al*: **Chondroprotective role of the osmotically sensitive ion channel transient receptor potential vanilloid 4: Age- and sex-dependent progression of osteoarthritis in Trpv4-deficient mice**. *Arthritis & Rheumatism* 2010, **62**(10):2973-2983.

163. Cheung HS, Sallis JD, Demadis KD *et al*: **Phosphocitrate blocks calcification-induced articular joint degeneration in a guinea pig model**. *Arthritis & Rheumatism* 2006, **54**(8):2452-2461.

164. Ea HK, Nguyen C, Bazin D *et al*: **Articular cartilage calcification in osteoarthritis: Insights into crystal-induced stress**. *Arthritis & Rheumatism* 2011, **63**(1):10-18.

165. Caleb Ríos J, Reyes A, Esquivel H *et al*: **Aortic stenosis and coronary artery disease in alkaptonuria. Case report**. *Revista Española de Cardiología (English Version)* 2010, **63**(09):1105-1106.

166. Vavuranakis M, Triantafillidi H, Stefanadis C *et al*: **Aortic stenosis and coronary artery disease caused by alkaptonuria, a rare genetic metabolic syndrome**. *Cardiology* 1998, **90**(4):302-304.

167. Hangaishi M, Taguchi J, Ikari Y *et al*: **Aortic valve stenosis in alkaptonuria**. *Circulation* 1998, **98**(11):1148-1149.

168. Smith JW: **Ochronosis of the sclera and cornea complicating alkaptonuria: Review of the literature and report of four cases**. *The Journal of the American Medical Association* 1942, **120**(16):1282-1288.

169. Carlson DM, Helgeson MK, Hiett JA: **Ocular ochronosis from alkaptonuria**. *Journal of the American Optometric Association* 1991, **62**(11):854-856.

170. Srsen S: **Dark pigmentation of ear cerumen in alkaptonuria**. *The Lancet* 1978, **2**(8089):577.

171. Tharini G, Ravindran V, Hema N *et al*: **Alkaptonuria**. *Indian Journal of Dermatology* 2011, **56**(2):194-196.

172. Yoo JH, Yang BK, Son BK: **Meniscal ossicle: A case report**. *The Knee* 2007, **14**(6):493-496.

173. Dieppe P: **Developments in osteoarthritis**. *Rheumatology* 2011, **50**(2):245-247.

174. Lee GM, Loeser RF: **Interactions of the chondrocyte with its pericellular matrix**. *European Cells & Materials* 1998, **8**:135-149.

175. SundarRaj N, Fite D, Ledbetter S *et al*: **Perlecan is a component of cartilage matrix and promotes chondrocyte attachment**. *Journal of Cell Science* 1995, **108 (Pt 7)**:2663-2672.

176. Miosge N, Flachsbart K, Goetz W *et al*: **Light and electron microscopical immunohistochemical localization of the small proteoglycan core proteins decorin and biglycan in human knee joint cartilage**. *The Histochemical Journal* 1994, **26**(12):939-945.

177. Poole AR, Rosenberg LC, Reiner A *et al*: **Contents and distributions of the proteoglycans decorin and biglycan in normal and osteoarthritic human articular cartilage**. *Journal of Orthopaedic Research: Official Publication of the Orthopaedic Research Society* 1996, **14**(5):681-689.

178. Poole CA: **Articular cartilage chondrons: Form, function and failure**. *Journal of Anatomy* 1997, **191 (Pt 1)**:1-13.

179. von der Mark K, Kirsch T, Nerlich A *et al*: **Type X collagen synthesis in human osteoarthritic cartilage. Indication of chondrocyte hypertrophy**. *Arthritis & Rheumatism* 1992, **35**(7):806-811.

180. Alexopoulos LG, Haider MA, Vail TP *et al*: **Alterations in the mechanical properties of the human chondrocyte pericellular matrix with osteoarthritis**. *Journal of Biomechanical Engineering* 2003, **125**(3):323-333.

181. Poole CA, Flint MH, Beaumont BW: **Chondrons extracted from canine tibial cartilage: Preliminary report on their isolation and structure**. *Journal of Orthopaedic Research: Official Publication of the Orthopaedic Research Society* 1988, **6**(3):408-419.

182. Lee GM, Poole CA, Kelley SS *et al*: **Isolated chondrons: A viable alternative for studies of chondrocyte metabolism in vitro**. *Osteoarthritis & Cartilage* 1997, **5**(4):261-274.

183. Taylor AM, Hsueh MF, Ranganath LR *et al*: **Analysis of cartilage biomarkers of turnover and aging in the osteoarthropathy of alkaptonuria**. *Osteoarthritis & Cartilage* 2011, **19**:S80.

184. Tinti L, Spreafico A, Chellini F *et al*: **A novel ex vivo organotypic culture model of alkaptonuria-ochronosis**. *Clinical & Experimental Rheumatology* 2011, **29**(4):693-696.

185. Martin JA, Buckwalter JA: **Post-traumatic osteoarthritis: The role of stress induced chondrocyte damage**. *Biorheology* 2006, **43**(3-4):517-521.

186. Yudoh K, Nguyen v T, Nakamura H *et al*: **Potential involvement of oxidative stress in cartilage senescence and development of osteoarthritis: Oxidative stress induces chondrocyte telomere instability and downregulation of chondrocyte function**. *Arthritis Research & Therapy* 2005, **7**(2):R380-391.

187. Ewers BJ, Dvoracek-Driksna D, Orth MW *et al*: **The extent of matrix damage and chondrocyte death in mechanically traumatized articular cartilage explants depends on rate of loading**. *Journal of Orthopaedic Research* 2001, **19**(5):779-784.

188. Martin JA, Brown TD, Heiner AD *et al*: **Chondrocyte senescence, joint loading and osteoarthritis**. *Clinical Orthopaedics & Related Research* 2004(427 Suppl):S96-103.

189. Martin JA, Klingelhutz AJ, Moussavi-Harami F *et al*: **Effects of oxidative damage and telomerase activity on human articular cartilage chondrocyte senescence**. *The Journals of Gerontology Series A, Biological Sciences & Medical Sciences* 2004, **59**(4):324-337.

190. Taylor AM, Boyde A, Davidson JS *et al*: **Identification of trabecular excrescences, novel microanatomical structures, present in bone in osteoarthropathies**. *European Cells & Materials* 2012, **23**:300-308; discussion 308-309.

191. Hiraku Y, Yamasaki M, Kawanishi S: **Oxidative DNA damage induced by homogentisic acid, a tyrosine metabolite**. *Federation of the European Biochemical Societies Letters* 1998, **432**(1-2):13-16.

192. Brandl A, Hartmann A, Bechmann V *et al*: **Oxidative stress induces senescence in chondrocytes**. *Journal of Orthopaedic Research* 2011, **29**(7):1114-1120.

193. Braconi D, Laschi M, Taylor AM *et al*: **Proteomic and redox-proteomic evaluation of homogentisic acid and ascorbic acid effects on human articular chondrocytes**. *Journal of Cellular Biochemistry* 2010, **111**(4):922-932.

194. Hamada T, Yamamoto T, Shida J-i *et al*: **Subchondral insufficiency fracture of the femoral head in a patient with alkaptonuria**. *Skeletal Radiology* 2013:1-4.

195. Eyre D: **Collagen of articular cartilage**. *Arthritis Research* 2002, **4**(1):30-35.

196. Zhang Y, Wang F, Tan H *et al*: **Analysis of the mineral composition of the human calcified cartilage zone**. *International Journal of Medical Sciences* 2012, **9**(5):353-360.

197. Zizak I, Roschger P, Paris O *et al*: **Characteristics of mineral particles in the human bone/cartilage interface**. *Journal of Structural Biology* 2003, **141**(3):208-217.

198. Alexopoulos LG, Youn I, Bonaldo P *et al*: **Developmental and osteoarthritic changes in Col6a1-knockout mice: Biomechanics of type VI collagen in the cartilage pericellular matrix**. *Arthritis & Rheumatism* 2009, **60**(3):771-779.

199. Chang J, Poole CA: **Sequestration of type VI collagen in the pericellular microenvironment of adult chrondrocytes cultured in agarose**. *Osteoarthritis & Cartilage* 1996, **4**(4):275-285.

200. Wu JJ, Eyre DR, Slayter HS: **Type VI collagen of the intervertebral disc. Biochemical and electron-microscopic characterization of the native protein**. *The Biochemical Journal* 1987, **248**(2):373-381.

201. Duer MJ, Fria i T, Murray RC *et al*: **The mineral phase of calcified cartilage: Its molecular structure and interface with the organic matrix**. *Biophysical Journal* 2009, **96**(8):3372-3378.

202. Stephens M, Kwan AP, Bayliss MT *et al*: **Human articular surface chondrocytes initiate alkaline phosphatase and type X collagen synthesis in suspension culture**. *Journal of Cell Science* 1992, **103 (Pt 4)**:1111-1116.

203. van der Kraan PM, Vitters EL, Meijers THM *et al*: **Collagen type I antisense and collagen type IIA messenger RNA is expressed in adult murine articular cartilage**. *Osteoarthritis & Cartilage* 1998, **6**(6):417-426.

204. Underhill C, Andrews P, Zhang L: **Hypertrophic chondrocytes are surrounded by a condensed layer of hyaluronan**. *European Cells & Materials* 1998, **8**:63-71.

205. Lock EA, Gaskin P, Ellis MK *et al*: **Tissue distribution of 2-(2-nitro-4-trifluoromethylbenzoyl)cyclohexane-1-3-dione (NTBC): Effect on enzymes involved in tyrosine catabolism and relevance to ocular toxicity in the rat**. *Toxicology & Applied Pharmacology* 1996, **141**(2):439-447.

206. Lindstedt S, Holme E, Lock EA *et al*: **Treatment of hereditary tyrosinaemia type I by inhibition of 4-hydroxyphenylpyruvate dioxygenase**. *The Lancet* 1992, **340**(8823):813-817.

207. Onojafe IF, Adams DR, Simeonov DR *et al*: **Nitisinone improves eye and skin pigmentation defects in a mouse model of oculocutaneous albinism**. *The Journal of Clinical Investigation* 2011, **121**(10):3914-3923.

208. Larochelle J, Alvarez F, Bussières J-F *et al*: **Effect of nitisinone (NTBC) treatment on the clinical course of hepatorenal tyrosinemia in Québec**. *Molecular Genetics & Metabolism* 2012, **107**(1–2):49-54.

209. Horisberger M, Fortuna R, Valderrabano V *et al*: **Long-term repetitive mechanical loading of the knee joint by in vivo muscle stimulation accelerates cartilage degeneration and increases chondrocyte death in a rabbit model**. *Clinical Biomechanics* 2013, **28**(5):536-543.

210. Nagura T, Dyrby CO, Alexander EJ *et al*: **Mechanical loads at the knee joint during deep flexion**. *Journal of Orthopaedic Research: Official Publication of the Orthopaedic Research Society* 2002, **20**(4):881-886.

211. Wilson W, van Rietbergen B, van Donkelaar CC *et al*: **Pathways of load-induced cartilage damage causing cartilage degeneration in the knee after meniscectomy**. *Journal of Biomechanics* 2003, **36**(6):845-851.

212. Lock EA, Ellis MK, Gaskin P *et al*: **From toxicological problem to therapeutic use: The discovery of the mode of action of 2-(2-nitro-4-trifluoromethylbenzoyl)-1,3-cyclohexanedione (NTBC), its toxicology and development as a drug**. *Journal of Inherited Metabolic Disease* 1998, **21**(5):498-506.

213. Kavana M, Moran GR: **Interaction of (4-Hydroxyphenyl)pyruvate Dioxygenase with the Specific Inhibitor 2-[2-Nitro-4-(trifluoromethyl)benzoyl]-1,3-cyclohexanedione**. *Biochemistry* 2003, **42**(34):10238-10245.

214. Bendadi F, de Koning TJ, Visser G *et al*: **Impaired cognitive functioning in patients with tyrosinemia type I receiving nitisinone**. *The Journal of Pediatrics* 2014, **164**(2):398-401.

215. Weinstein JR, Anderson S: **The aging kidney: Physiological changes**. *Advances in Chronic Kidney Disease* 2010, **17**(4):302-307.

216. Urbieta-Caceres VH, Syed FA, Lin J *et al*: **Age-dependent renal cortical microvascular loss in female mice**. *American Journal of Physiology Endocrinology & Metabolism* 2012, **302**(8):E979-986.

217. Preston AJ, Keenan CM, Sutherland H *et al*: **Ochronotic osteoarthropathy in a mouse model of alkaptonuria, and its inhibition by nitisinone**. *Annals of the Rheumatic Diseases* 2014, **73**(1):284-289.

218. Ahlback S: **Osteoarthrosis of the knee. A radiographic investigation**. *Acta Radiologica: Diagnosis* 1968:Suppl 277:277-272.

219. Jones RK, Chapman GJ, Findlow AH *et al*: **A new approach to prevention of knee osteoarthritis: Reducing medial load in the contralateral knee**. *The Journal of Rheumatology* 2013, **40**(3):309-315.

220. Hu K, Xu L, Cao L *et al*: **Pathogenesis of osteoarthritis-like changes in the joints of mice deficient in type IX collagen**. *Arthritis & Rheumatism* 2006, **54**(9):2891-2900.

221. van Osch GJVM, van der Kraan PM, Vitters EL *et al*: **Induction of osteoarthritis by intra-articular injection of collagenase in mice. Strain and sex related differences**. *Osteoarthritis & Cartilage* 1993, **1**(3):171-177.

222. Ma HL, Blanchet TJ, Peluso D *et al*: **Osteoarthritis severity is sex dependent in a surgical mouse model**. *Osteoarthritis & Cartilage* 2007, **15**(6):695-700.

223. Holzer LA, Leithner A, Gruber G: **Ochronosis of the hip joint**. *The Journal of Rheumatology* 2013, **40**(4):535.

224. Schipplein OD, Andriacchi TP: **Interaction between active and passive knee stabilizers during level walking**. *Journal of Orthopaedic Research* 1991, **9**(1):113-119.

225. Thomas RH, Resnick D, Alazraki NP *et al*: **Compartmental Evaluation of Osteoarthritis of the Knee**. *Radiology* 1975, **116**(3):585-594.

226. Lapvetelainen T, Hyttinen MM, Saamanen AM *et al*: **Lifelong voluntary joint loading increases osteoarthritis in mice housing a deletion mutation in type II procollagen gene, and slightly also in non-transgenic mice**. *Annals of the Rheumatic Diseases* 2002, **61**(9):810-817.

227. Eberle P, Mohr W, Claes L: **Biomechanical studies on the pathogenesis of ochronotic arthropathy**. *Zeitschrift fur Rheumatologie* 1984, **43**(5):249-252.

228. Silberberg R, Silberberg M, Vogel A *et al*: **Ultrastructure of articular cartilage of mice of various ages**. *The American Journal of Anatomy* 1961, **109**:251-275.

229. Silberberg R, Silbereberg M, Feir D: **Life cycle of articular cartilage cells: An electron microscope study of the hip joint of the mouse**. *The American Journal of Anatomy* 1964, **114**:17-47.

230. Hughes LC, Archer CW, ap Gwynn I: **The ultrastructure of mouse articular cartilage: Collagen orientation and implications for tissue functionality. A polarised light and scanning electron microscope study and review**. *European Cells & Materials* 2005, **9**:68-84.

231. Buckwalter JA, Mankin HJ: **Articular cartilage: Degeneration and osteoarthritis, repair, regeneration, and transplantation**. *Instructional Course Lectures* 1998, **47**:487-504.

232. Sandell LJ, Aigner T: **Articular cartilage and changes in arthritis. An introduction: Cell biology of osteoarthritis**. *Arthritis Research* 2001, **3**(2):107-113.

233. Oegema TR, Jr., Carpenter RJ, Hofmeister F *et al*: **The interaction of the zone of calcified cartilage and subchondral bone in osteoarthritis**. *Microscopy Research & Technique* 1997, **37**(4):324-332.

234. Dmitrovsky E, Lane LB, Bullough PG: **The characterization of the tidemark in human articular cartilage**. *Metabolic Bone Disease & Related Research* 1978, **1**(2):115-118.

235. Havelka S, Horn V, Spohrova D *et al*: **The calcified-noncalcified cartilage interface: The tidemark**. *Acta Biologica Hungarica* 1984, **35**(2-4):271-279.

236. Simkin PA: **Consider the tidemark**. *The Journal of Rheumatology* 2012, **39**(5):890-892.

237. Roach HI, Aigner T, Kouri JB: **Chondroptosis: a variant of apoptotic cell death in chondrocytes?** *Apoptosis: An International Journal on Programmed Cell Death* 2004, **9**(3):265-277.

238. Hirotani H, Ito T: **Scanning electron microscopy of the articular surfaces of the hip joint disorders**. *Anatomischer Anzeiger* 1975, **138**(1-2):29-38.

239. Miao D, Scutt A: **Histochemical localization of alkaline phosphatase activity in decalcified bone and cartilage**. *Journal of Histochemistry & Cytochemistry* 2002, **50**(3):333-340.

240. Fuerst M, Bertrand J, Lammers L *et al*: **Calcification of articular cartilage in human osteoarthritis**. *Arthritis & Rheumatism* 2009, **60**(9):2694-2703.

241. Mitsuyama H, Healey RM, Terkeltaub RA *et al*: **Calcification of human articular knee cartilage is primarily an effect of aging rather than osteoarthritis**. *Osteoarthritis & Cartilage* 2007, **15**(5):559-565.

242. Karpouzas G, Terkeltaub R: **New developments in the pathogenesis of articular cartilage calcification**. *Current Rheumatology Reports* 1999, **1**(2):121-127.

243. Bennett LD, Buckland-Wright JC: **Meniscal and articular cartilage changes in knee osteoarthritis: A cross-sectional double-contrast macroradiographic study**. *Rheumatology* 2002, **41**(8):917-923.

244. O'Connor KM: **Unweighting accelerates tidemark advancement in articular cartilage at the knee joint of rats**. *Journal of Bone & Mineral Research* 1997, **12**(4):580-589.

245. Revell PA, Pirie C, Amir G *et al*: **Metabolic activity in the calcified zone of cartilage: Observations on tetracycline labelled articular cartilage in human osteoarthritic hips**. *Rheumatology International* 1990, **10**(4):143-147.

246. Burr DB: **Anatomy and physiology of the mineralized tissues: role in the pathogenesis of osteoarthrosis**. *Osteoarthritis & Cartilage* 2004, **12 Suppl A**:S20-30.

247. Johnson K, Hashimoto S, Lotz M *et al*: **Interleukin-1 induces pro-mineralizing activity of cartilage tissue transglutaminase and factor XIIIa**. *The American Journal of Pathology* 2001, **159**(1):149-163.

248. Boskey AL: **Pathogenesis of cartilage calcification: Mechanisms of crystal deposition in cartilage**. *Current Rheumatology Reports* 2002, **4**(3):245-251.

249. Mandel GS, Halverson PB, Rathburn M *et al*: **Calcium pyrophosphate crystal deposition: A kinetic study using a type I collagen gel model**. *Scanning Microscopy* 1990, **4**(1):175-179; discussion 179-180.

250. Howell DS: **Articular cartilage calcification and matrix vesicles**. *Current Rheumatology Reports* 2002, **4**(3):265-269.

251. Martin JA, Buckwalter JA: **Aging, articular cartilage chondrocyte senescence and osteoarthritis**. *Biogerontology* 2002, **3**(5):257-264.

252. Abimbola O, Hall G, Zuckerman JD: **Degenerative arthritis of the knee secondary to ochronosis**. *Bulletin of the NYU hospital for Joint Diseases* 2011, **69**(4):331-334.

253. Sag AA, Silbergleit R, Olson RE *et al*: **T1 hyperintense disc in alkaptonuria**. *Spine* 2012, **37**(21):E1361-1363.

254. La Du BN, Zannoni VG, Laster L *et al*: **The nature of the defect in tyrosine metabolism in alcaptonuria**. *The Journal of Biological Chemistry* 1958, **230**(1):251-260.

255. La Du BN, Seegmiller JE, Laster L *et al*: **Alcaptonuria and ochronotic arthritis**. *Bulletin on the Rheumatic Diseases* 1958, **8**(9):163-164.

256. Zhao B, Chen B, Shao D *et al*: **Osteoarthritis? Ochronotic arthritis!** *Knee Surgery, Sports Traumatology, Arthroscopy* 2009, **17**(7):778-781.

257. Araki K, Sudo A, Hasegawa M *et al*: **Devastating ochronotic arthropathy with successful bilateral hip and knee arthroplasties**. *Journal of Clinical Rheumatology: Practical Reports on Rheumatic & Musculoskeletal Diseases* 2009, **15**(3):138-140.

258. Yilmaz A, Egilmez E: **Knee arthroplasty for ochronotic arthropathy**. *The Journal of Knee Surgery* 2002, **15**(4):231-233.

259. Hashimoto S, Creighton-Achermann L, Takahashi K *et al*: **Development and regulation of osteophyte formation during experimental osteoarthritis**. *Osteoarthritis & Cartilage* 2002, **10**(3):180-187.

260. Pritzker KP, Gay S, Jimenez SA *et al*: **Osteoarthritis cartilage histopathology: grading and staging**. *Osteoarthritis & Cartilage* 2006, **14**(1):13-29.

261. Karsdal MA, Leeming DJ, Dam EB *et al*: **Should subchondral bone turnover be targeted when treating osteoarthritis?** *Osteoarthritis & Cartilage* 2008, **16**(6):638-646.

262. Felson DT, Neogi T: **Osteoarthritis: Is it a disease of cartilage or of bone?** *Arthritis & Rheumatism* 2004, **50**(2):341-344.

263. Karsdal MA, Bay-Jensen AC, Lories RJ *et al*: **The coupling of bone and cartilage turnover in osteoarthritis: Opportunities for bone antiresorptives and anabolics as potential treatments?** *Annals of the Rheumatic Diseases* 2014, **73**(2):336-348.

264. Ferguson VL, Bushby AJ, Boyde A: **Nanomechanical properties and mineral concentration in articular calcified cartilage and subchondral bone**. *Journal of Anatomy* 2003, **203**(2):191-202.

265. Balint G, Szebenyi B: **Hereditary disorders mimicking and/or causing premature osteoarthritis**. *Bailliere's Best Practice & Research Clinical Rheumatology* 2000, **14**(2):219-250.

266. Lagier R: **Ochronotic arthropathy, an approach to osteoarthritis bone remodelling**. *Rheumatology International* 2006, **26**(6):561-564.

267. Vincent TL: **Targeting mechanotransduction pathways in osteoarthritis: A focus on the pericellular matrix**. *Current Opinion in Pharmacology* 2013, **13**(3):449-454.

Appendix A: Pigmented chondron counts

BALB/c Hgd-/-	Age (weeks)	Number of pigmented chondrons	BALB/c Hgd-/-	Age (weeks)	Number of pigmented chondrons
132.1	6.5	0	**86.2**	25.2	32
132.2	6.5	0	**99.1**	27.4	61
132.3	6.5	0	**99.2**	27.4	46
129.2	7.8	0	**92.1**	30.9	88
131.1	7.8	0	**92.2**	30.9	59
131.2	7.8	0	**91.1**	34.4	80
93.2	15.7	7	**91.2**	34.4	48
94.1	15.7	7	**86.3**	40.4	156
120.1	19.6	18	**55.1**	47.4	156
120.2	19.6	13	**54.3**	49.6	111
106.1	23.5	76	**61.3**	60	206
106.2	23.5	53	**61.4**	60	247
106.3	23.5	33	**59.2**	61.3	317
86.1	25.2	37	**59.3**	61.3	187
			50.3	65.7	254

Table 1 – Pigmented chondron counts from BALB/c Hgd-/- mice natural history study (Chapter 3).

BL/6 Hgd-/-	Age (weeks)	Number of pigmented chondrons	BL/6 Hgd-/-	Age (weeks)	Number of pigmented chondrons
166.2	6.1	0	**101.3**	29.1	113
166.3	6.1	0	**102.3**	29.1	117
161.3	6.1	0	**98.3**	31.7	111
161.4	6.1	0	**99.4**	31.7	123
161.1	10.4	0	**94.1**	37.8	110
161.2	10.4	0	**95.1**	37.8	144
162.1	10.4	0	**82.1**	41.3	133
162.2	10.4	5	**83.1**	41.3	176
98.4	16.1	7	**66.3**	46.5	274
99.3	16.1	7	**67.1**	46.5	157
71.2	27.8	26	**62.3**	62.6	184
72.1	27.8	37	**49.2**	68.3	90
			35.1	71.7	156

Table 2 – Pigmented chondron counts from BL/6 Hgd-/- mice natural history study (Chapter 3).

BALB/c Hgd-/-	Age (weeks)	Number of pigmented chondrons	BALB/c Hgd-/-	Age (weeks)	Number of pigmented chondrons
16.3	69	221	**23.3**	67	0
18.1	69	136	**24.4**	67	0
18.2	69	207	**25.1**	67	0
18.3	69	256	**25.2**	67	0
22.1	69	308	**25.3**	67	0
13.3	71	200	**26.1**	67	0
14.1	71	248	**26.2**	67	0
14.2	71	341			
15.1	71	132			

Table 3 – Pigmented chondron counts from BALB/c Hgd-/- mice nitisinone whole-life study (Chapter 5). (Left side no nitisinone / Right side whole-life nitisinone).

BALB/c Hgd-/-	Age (weeks)	Number of pigmented chondrons	BALB/c Hgd-/-	Age (weeks)	Number of pigmented chondrons
47.2	80	273	**45.1**	80	108
47.4	80	245	**47.3**	80	100
48.2	80	177	**48.1**	80	70
49.3	80	188	**49.4**	80	51
50.2	80	182	**50.1**	80	112
51.1	80	142			

Table 4 – Pigmented chondron counts from BALB/c Hgd-/- mice nitisinone mid-life study (Chapter 5). (Left side no nitisinone / Right side mid-life nitisinone).

Appendix B: Publications

Keenan CM*, Preston AJ*, Sutherland H, Wilson PJ, Psarelli EE, Cox TF, Ranganath LR, Jarvis JC, Gallagher JA. Nitisinone arrests but does not reverse ochronosis in alkaptonuric mice. *Journal of Inherited Metabolic Disease, 2015, In press* (*Co-first authors).

Preston AJ*, **Keenan CM***, Sutherland H, Wilson PJ, Wlodarski B, Taylor AM, Williams DP, Ranganath LR, Gallagher JA, Jarvis JC. Ochronotic osteoarthropathy in a mouse model of Alkaptonuria and its inhibition by nitisinone. *Annals of Rheumatic Disease, 2014, **73**:284-289* (*Co-first authors).

Taylor AM, Preston A, Paulk NK, Sutherland H, **Keenan CM**, Wilson PJ, Wlodarski B, Grompe M, Ranganath LR, Gallagher JA, Jarvis JC. Ochronosis in a murine model of Alkaptonuria is synonymous to that in the human condition. *Osteoarthritis & Cartilage, 2012, 20(8):880-6.*